Joint Institute for Nuclear Research
Frank Laboratory of Neutron Physics

Annual Report 2006

FRANK LABORATORY OF NEUTRON PHYSICS OF THE JOINT INSTITUTE FOR NUCLEAR RESEARCH

The Joint Institute for Nuclear Research (JINR) is an international centre for experimental and theoretical investigations in the fields of elementary particle physics, nuclear and neutron physics, condensed matter research and related topics.

The JINR structure is determined by the fact that it is governed internationally and has many research specializations. Current scientific and financial affairs of the Institute's Laboratories, common services as well as the work of specialized departments are guided by the Institute Directorate.

The Frank Laboratory of Neutron Physics is one of the eight JINR Laboratories. It was established in 1956, soon after the foundation of JINR.

In 1960 a principally new source of neutrons - the IBR fast pulsed reactor of periodic operation - was created at FLNP under the leadership of Prof. D.I.Blokhintsev (11.01.1908 - 24.01.1979). The birth of this reactor gave rise to a new direction in the development of research neutron sources.

An extended scientific program with this reactor was initiated under the leadership of Nobel Prize Winner and Laboratory Director Prof. I.M.Frank (23.10.1908 - 22.06.1990) and Deputy Director Prof. F.L.Shapiro (06.04.1915 - 30.01.1973). Since 1960, a whole family of unique pulsed neutron sources for nuclear physics and condensed matter physics has been developed and constructed. The latest in the family, the IBR-2 high flux pulsed reactor, was commissioned in February 1984. The Laboratory was named after Prof. I.M.Frank in 1992. In the same year, in JINR the I.M.Frank Prize for Neutron Physics was established.

At present, the scientific activity of the Laboratory focuses on two fields of physics, namely nuclear physics and condensed matter physics. The first involves investigations of the neutron as an elementary particle and studies of compound states in neutron induced reactions. The second investigates pressing problems in the physics and chemistry of solid states, surfaces and liquids, and in molecular biology. Applied investigations are also carried out using nuclear physics methods.

PREFACE

We would like to offer the readers the report on the scientific activity of the Frank Laboratory of Neutron Physics for 2006. The first part presents a brief review of the experimental and theoretical results achieved in the main scientific directions – condensed matter physics, neutron nuclear physics and applied research. The second part includes the reports on the operation of the IBR-2 pulsed reactor and realization of the IREN project. The third part is concerned with the development and creation of elements of neutron spectrometers for condensed matter investigations. The fourth part presents the experimental reports that cover the main scientific directions in greater detail. The list of publications for 2006 completes the report.

In 2006 the IBR-2 reactor operated ~ 2250 hours for physical experiments. The main results of the IBR-2 modernization in 2006:

The main task of the year – manufacturing of fuel assemblies (FA) for the IBR-2M reactor – has been successfully fulfilled. In July, 2006 the license for manufacturing FA in JINR was obtained, and on 12.07.2006 the first FA was made in the presence of a special commission. On 16.11.2006 the work was completed: 89 FA were manufactured, which provided an initial charge of the new reactor (63 FA) and burn up margin of about ~ 40 %.

In JINR Experimental Workshops: The manufacturing of rolling shielding was completed, its check assembly and tests were carried out. The control systems of the reactor were manufactured (emergency system units, compensating regulators, manual regulator).

Automated Safety Control System (ASCS) of IBR-2M: The prototype model of ASCS (SNIIP-SYSTEMATOM) was manufactured and tested at the IBR-2 reactor. In SNIIP-SYSTEMATOM the work on standard ASCS (including a new control panel) was started. In the Institute of Electronic Control Machines (INEUM) the work to develop a system to control technological parameters was continued. In JINR EW a prototype model of compensating device (CD) drive was manufactured, work on a prototype model of emergency shutdown system drive is in progress.

Complex of moderators for IBR-2M. In December, 2006, the manufacturing of CHF-700/15 in “Heliymash”; detail design of moderators for 3 directions: beams 2-3, beams 4-6, beams 7-11 (NIKIET); design of technological part (SSDI); detail design of cryogenic pipeline and intermediate heat exchanger (Heliymash) were completed. In FLNP the calculations and experimental work on transportation of frozen C_9H_{12} pellets were performed; design documentation on pellet generator was worked out.

Program of works at the IBR-2 reactor in the temporary shutdown mode (2007-2010). The program of works at the IBR-2 reactor during temporary shutdown as well as the schedule of works on modernization of IBR-2 in this period were developed, agreed upon and approved.

IREN Project. The main tasks of the Frank Laboratory of Neutron Physics and the Laboratory of Particle Physics in 2006 were the completion of disassembling of the IBR-30 reactor and the assembling of the available equipment of the first stage of the LUE-200 linac.

Decommissioning of IBR-30. In accordance with the approved working schedule of the decommissioning the following works were carried out: «Report on Nuclear and Radiation Safety Assessment of the Research Pulsed Reactor IBR-30 in 2005» was prepared and submitted to Rostehnadzor of RF; all equipment from the reactor hall except for beam shutters, which would be used for the first stage of IREN, was dismantled and moved to building 117/b; All rooms of building 43 adjacent to the reactor hall were cleared; the decontamination and preparation of the reactor hall to repair were carried out.

Works on the LUE-200 linac. The theoretical substantiation of the possibility to obtain required parameters of an electron beam at the first stage of the linac was completed. The MK1 klystron modulator was assembled at the regular place and adjusted. The modulator and pulsed transformer for the electron gun were mounted at the regular place. Test assembling of the SHF-path of the first section was carried out. The power frame of the vacuum pump system of the LUE-200 first section was fully equipped. Test assembling was carried out. Test assembling and certification of the buncher coil were carried out. In building 43 the focusing solenoid of the first accelerating section was mounted with geodetic tie. The electron gun was assembled at the regular place. The pipeline laying-out of water supply for the water-cooling and thermostabilization system of LUE-200 was completed.

At the IBR-2 neutron spectrometers a number of experiments were carried out in currently central research directions.

In addition to the complex manganese oxides (manganites), whose main peculiarity is the effect of colossal magnetoresistance, growing interest is being shown in the complex cobalt oxides (cobaltites) of the $Ln_{1-x}M_xCoO_3$ type, where Ln – lanthanide, M – alkaline-earth element. From the scientific point of view, cobaltites are of interest due to strong correlations between lattice, charge, spin and orbital degrees of freedom. And from the viewpoint of practice cobalt oxides are of importance since they are used as electrodes in current power supplies. The peculiarities of phase transitions in cobaltites are connected with the imbalance

between the intra-atomic Hund energy and the energy of crystal field corresponding to the configuration of octahedrons of CoO_6. As a result, the Co^{3+} ion may be in three different spin states: low-spin (LS, $t_{2g}^6e_g^0$), intermediate (IS, $t_{2g}^5e_g^1$) and high-spin (HS, $t_{2g}^4e_g^2$) state.

At the IBR-2 reactor the investigations of atomic and magnetic structure of cobaltites were carried out (including experiments at high external pressures). At the HRFD diffractometer the composition of $Pr_{0.5}Sr_{0.5}CoO_3$ was studied, in which several magneto-structural phase transitions had been observed earlier. The diffraction spectra were measured in a wide range of temperatures (10 – 780 K) mainly in the mode of sample heating. In this range two phase transitions ($T_1 \approx 120$ K and $T_2 \approx 300$ K) were detected, in the course of which magnetic and crystal structures of the sample change. On heating the symmetry sequentially varies from triclinic to rhombic and then to rhombohedral one. The transitions are greatly spread over temperature, and between 120 K and 300 K the phases coexist (Fig.1). The magnetic measurements confirm that the structural transition at 300 K coincides with the Curie ferromagnetic point. The nature of the magnetic transition at 120 K remains unknown so far.

At the DN-12 diffractometer the investigation of the crystal and magnetic structure of hexagonal frustrated manganites $RMnO_3$ (R=Y, Lu) was performed at high pressures of up to 6 GPa. The obtained experimental data, along with the results of the previous investigations of other hexagonal manganites, made it possible to relate the symmetry of triangular AFM state with the parameter of distortion of triangular lattice *s* formed by Mn and O atoms. The obtained generalized magnetic phase diagram allows one to explain the observed changes of the symmetry of magnetic state at chemical substitution (change in the ion radius R of the element) and on application of high pressure due to variation of *s*.

Undulation forces of lipid membranes. Membranes belong to the so-called random fluctuating surfaces, which include a wide class of objects: from biomembranes to strings in the modern field theory trying to describe all fundamental interactions from a single viewpoint. This accounts for close attention of modern theoretical physics to biomembranes and, in particular, to lipid membranes. The establishment of the law and an initial estimate of the universal constant of interactions of such objects made by W. Helfrich in 1978 became a significant result in the statistical physics of random surfaces. His estimate gave the value of the universal constant $3\pi^2/128$. To appreciate the significance of the obtained result it may be safely said that this law is as important for the physics of random surfaces as the perfect gas laws for the point particle physics.

In 1986-89 C.R. Safinya et al. using the analysis of the shape of diffraction peaks from amphiphilic multilayers obtained at X-ray high-resolution diffractometers on synchrotron X-ray sources, interpreted the results of their experiments as complete quantitative verification of the results of the undulation force theory including the distance dependence of the force and the constant value $3\pi^2/128$. That was a triumph of W. Helfrich's concept. But as the further advancement of research in this field showed, it was a short-time triumph. Several groups, including theoretical physicists concerned with the quantum field theory, independently of one another and using different theoretical methods succeeded in obtaining an exact value of the universal constant of these interactions. Their results coincided, but the obtained value (close to $3\pi^2/256$) was twice as large as the experimental value. Such contradiction of theoretical and experimental results has received the name "enigmatic" and actually meant severe crisis in this field. In the work carried out with the participation of the FLNP physicists, new approaches to study intermembrane interactions and to determine the universal constant based on the investigation of temperature dependence of intermembrane interactions by means of complementary use of small-angle thermal neutron scattering and high-resolution diffraction on a synchrotron source have been developed. In particular, the value of the constant $3\pi^2/256$ has been obtained that coincides with the theoretical predictions. It also has been shown that the transition from multilamellar to unilamellar membranes proceeds in accordance with a two-state model. In addition, for the first time the true significance of undulation forces has been demonstrated – they really make a considerable contribution into the balance of intermembrane interactions, and what is more, become dominating at intermembrane distances larger than 20.5 Å.

In 2006 a number of experiments were carried out and some interesting results were obtained in the field of nuclear physics. The work to manufacture a full-scale facility to measure a neutron-neutron cross-section on the YAGUAR reactor was completed. First calibration measurements on rare gases with the well-known cross-sections were carried out. The data from the experiment carried out at the reactor in ILL (Grenoble) to observe a change in the neutron energy at passing through accelerated matter were processed. The existence of the effect follows from the validity of the equivalence principle and detailed neutron-optical calculations. The change in the neutron energy detected in the experiment is of the order of 2×10^{-10} eV, which is at the record level of accuracy attainable at the present state of the art. The experiment aimed at checking the efficiency of control over the polarization of thermal

and epithermal neutrons using a radio-frequency field was carried out on beam H8 of the KENS pulsed neutron source (KEK, Japan). The polarization of neutrons and analysis of their polarization were performed by the devices on the basis of polarized ^{3}He with optical pumping developed by the KEK-FLNP JINR collaboration in 2003-2005. The experimental results agree well with the calculations and have demonstrated high efficiency of the proposed method. The developed technique will be used to control neutron polarization in the experiment to verify T-invariance in interaction of polarized neutrons with polarized nuclei. The experiment is planned to be carried out on the JSNS source, which is under construction at present. In the framework of experiments to search for neutral currents in nucleon-nucleon interactions and to determine weak π-meson coupling constant, in collaboration with PNPI, ILL and TU Munich on beam PF1B of cold polarized neutrons (ILL, Grenoble) a "zero" experiment was performed to determine the background asymmetry for a series of measurements of P-odd asymmetry in the reaction ^{6}Li(n,α)^{3}H.

Within the collaboration Jyväskylä-Darmstadt-Dubna-Gatchina in JYFL (Finland) a series of experiments to study fission using two mosaics of semiconductor detectors was carried out. In the first experiment angular and mass-energy correlations of fission fragments in the reaction ^{238}U + ^{4}He (40 MeV) were investigated. The angular resolution of the facility made possible a direct search for the ternary collinear decay events. A number of effects, which could give indirect evidence to the existence of exotic fission modes, were discovered. In the second experiment a precision measurement of energy distributions of α-particles and nuclei of ^{6}He emitted in the process of ^{252}Cf ternary spontaneous fission was performed. A significant deviation of spectra from the Gaussian shape was observed in a low-energy region.

In the framework of collaboration with ISR RAS the specialists from FLNP and LRB performed calculations of angular dependence of efficiency of the Lunar Exploration Neutron Detector (LEND) (one of the instruments of the NASA Lunar Reconnaissance Orbiter 2008) intended to map the flux of neutrons from the lunar surface to search for evidence of water ice and provide measurements of the space radiation environment which can be useful for future human exploration. Also, experimental calibrations of the laboratory prototype of the instrument were carried out.

In the framework of the International Program «Atmospheric Heavy Metal Deposition in Europe – Estimations Based on Moss Analysis» a series of works that involved simultaneous collection of samples in 2005–2006 in a number of regions in Central Russia, Southern Urals, Belarus, Bulgaria, Slovakia, Poland, Romania, Serbia, Macedonia, Croatia

and Greece for multielement activation analysis at the IBR-2 reactor was completed. The results of the analysis on 13 elements: Al, As, Cd, Cr, Cu, Fe, Hg, Ni, Pb, Sb, Ti, V and Zn will be submitted to the European Atlas of Atmospheric Heavy Metal Deposition. Similar studies were carried out in Mongolia and Vietnam. The results of the analysis of moss-biomonitors from biosphere reserves (Prioksko-Terrasny and Voronezh biosphere reserves) obtained in collaboration with the Institute of Global Climate and Ecology (Moscow) are of particular interest.

In conclusion, it might be well to point out that great interest is being expressed by the JINR Member States in the work in the field of neutron investigations. It is also significant that in the last few years a lot of young people have come to the Laboratory. All these facts confirm that the Laboratory continues to develop successfully and dynamically, carrying out investigations in the interests of the JINR Member States.

04.04.2007 ***A.V.Belushkin***

Director

ПРЕДИСЛОВИЕ

Вашему вниманию предлагается отчёт о научной деятельности Лаборатории нейтронной физики им. И.М. Франка за 2006 год. В первой части представлен краткий обзор экспериментальных и теоретических результатов исследований, достигнутых по основным научным направлениям – физике конденсированных сред, нейтронной ядерной физике и прикладным исследованиям. Вторая часть включает отчёты о работе импульсного реактора ИБР-2 и реализации проекта ИРЕН. Третья часть посвящена разработке и созданию элементов нейтронных спектрометров для исследований конденсированных сред. В четвёртой части представлены экспериментальные отчеты, которые более подробно освещают основные направления исследований. Завершает отчёт список публикаций за 2006 год.

В 2006 г. реактор ИБР-2 отработал на физический эксперимент ~ 2250 часов. Основные результаты по модернизации ИБР-2 в 2006 г.:

Главная задача года – изготовление тепловыделяющих сборок (ТВС) для реактора ИБР-2М. В июле 2006 г. была получена лицензия на изготовление ТВС в ОИЯИ, а 12.07.2006 г. собрана первая ТВС в присутствии специальной комиссии. 16.11.2006 г. работа была завершена: изготовлено 89 ТВС, что обеспечивает стартовую загрузку нового реактора (63 ТВС) и запас на выгорание около 40 %.

В Опытном производстве (ОП) ОИЯИ. Завершено изготовление откатных защит, проведена их контрольная сборка и испытания; Изготовлены органы регулирования реактора (блоки аварийной защиты, компенсирующие регуляторы, ручной регулятор).

Автоматизированная система управления защиты (АСУЗ) ИБР-2М. Завершен опытный образец АСУЗ (СНИИП-СИСТЕМАТОМ), проводятся его испытания на реакторе ИБР-2. В СНИИП-СИСТЕМАТОМ начаты работы по штатной АСУЗ, включая новый пульт управления. В Институте электронных управляющих машин (ИНЭУМ) продолжались работы по созданию системы контроля технологических параметров. В ОП ОИЯИ изготовлен опытный образец привода компенсирующего органа (КО), ведется работа над опытным образцом привода аварийной защиты.

Комплекс замедлителей ИБР-2М. В декабре 2006 г. завершены: изготовление КГУ-700/15 в «Гелиймаше»; технический проект собственно замедлителей для 3-х направлений: 2-3 пучки, 4-6 пучки, 7-11 пучки (НИКИЭТ); проект технологической части (ГСПИ); рабочий проект криогенных трубопроводов и промежуточных теплообменников (Гелиймаш). В ЛНФ выполнены расчетные и экспериментальные работы по транспортировке шариков из

замороженного мезитилена C_9H_{12}, разработана конструкторская документация на генератор шариков.

Программа работ на реакторе ИБР-2 в режиме временного останова (2007-2010 годы»). Разработана, согласована и утверждена программа работ на ИБР-2, а также график работ по модернизации ИБР-2 в период временного останова.

Проект ИРЕН. Главными задачами Лаборатории нейтронной физики и Лаборатории физики частиц в 2006 году являлось завершение демонтажа реактора ИБР-30 и монтаж имеющегося оборудования первой очереди ускорителя ЛУЭ-200.

Вывод из эксплуатации ИБР-30. В соответствии с утвержденным планом-графиком вывода из эксплуатации, были выполнены следующие работы: подготовлен и представлен в гостехнадзор РФ «Отчет по оценке состояния ядерной и радиационной безопасности импульсного исследовательского реактора (ИИР) ИБР-30 в 2006 году; демонтировано и транспортировано в здание 117/6 все оборудование из зала реактора за исключением шиберов пучков, которые будут использованы для первой очереди ИРЕН; освобождены все смежные с залом реактора помещения здания 43; проведена дезактивация и подготовка зала реактора к ремонту.

Работы по ускорителю ЛУЭ-200. Завершено теоретическое обоснование возможности получения нужных параметров пучка электронов в 1-ой очереди ускорителя. Смонтирован на штатном месте и налажен модулятор клистрона МК1. Смонтирован на штатном месте модулятор и импульсный трансформатор для электронной пушки. Проведена контрольная сборка СВЧ-тракта первой секции. Укомплектована стойка питания системы вакуумных насосов первой секции ЛУЭ-200. Проведена контрольная сборка. Произведена контрольная сборка и паспортизация катушки группирователя. В здании 43 произведен монтаж с геодезической привязкой фокусирующего соленоида первой ускоряющей секции. Смонтирована на штатном месте электронная пушка. До конца года будет завершена прокладка трассы водоснабжения для системы водоохлаждения и термостабилизации ЛУЭ-200.

На нейтронных спектрометрах ИБР-2 выполнен ряд экспериментов по актуальным научным направлениям.

Вслед за сложными оксидами марганца (манганитами), основной особенностью которых является эффект колоссального магнитного сопротивления, растущий интерес проявляется к сложным оксидам кобальта (кобальтитам) типа $Ln_{1-x}M_xCoO_3$, где Ln – лантанид, M – щелочноземельный элемент. С научной точки зрения кобальтиты интересны сильными корреляциями между решеточными, зарядовыми, спиновыми и орбитальными

степенями свободы. Оксиды кобальта важны для практики в связи с их использованием в качестве электродов в источниках тока. Особенности фазовых переходов в кобальтитах связаны с нарушением баланса между внутриатомной энергией Хунда и энергией кристаллического поля, связанной с конфигурацией октаэдров CoO_6. В результате, ион Co^{3+} может находиться в трех разных спиновых состояниях: низкоспиновом (LS, $t_{2g}^6e_g^0$), промежуточном (IS, $t_{2g}^5e_g^1$) высокоспиновом (HS, $t_{2g}^4e_g^2$).

На реакторе ИБР-2 проведены исследования атомной и магнитной структуры кобальтитов, в том числе при высоких внешних давлениях. На дифрактометре ФДВР изучался состав $Pr_{0.5}Sr_{0.5}CoO_3$, в котором ранее наблюдались несколько магнито-структурных фазовых переходов. Дифракционные спектры были измерены в широком диапазоне температур (10 – 780 K), в основном в режиме нагрева образца. В этом диапазоне обнаружены два фазовых перехода ($T_1 \approx 120$ K и $T_2 \approx 300$ K), в ходе которых изменяются магнитная и кристаллическая структуры образца. При нагревании симметрия последовательно повышается от триклинной до ромбической и затем до ромбоэдрической. Переходы сильно размыты по температуре а между 120 K и 300 K фазы сосуществуют. Магнитные измерения подтверждают, что структурный переход при 300 K совпадает с ферромагнитной точкой Кюри. Природа магнитного перехода при 120 K пока остается неизвестной.

На дифрактометре ДН-12 проведено исследование кристаллической и магнитной структуры гексагональных фрустрированных манганитов $RMnO_3$ (R=Y, Lu) при высоких давлениях до 6 ГПа. Полученные экспериментальные данные, вместе с результатами предыдущих исследований других гексагональных манганитов, позволили установить взаимосвязь между симметрией треугольного АФМ состояния с параметром искажения треугольной решетки *s*, образованной атомами Mn и O. Полученная обобщенная магнитная фазовая диаграмма позволяет объяснить наблюдаемые изменения симметрии магнитного состояния при химическом замещении (изменении ионного радиуса R элемента) и приложении высокого давления за счет вариации *s*.

Ондуляционные силы липидных мембран. Мембраны относятся к так называемым случайным флуктуирующим поверхностям, к которым принадлежит широкий класс объектов: от биомембран до струн в современной теории поля, пытающейся описывать с единой точки зрения все фундаментальные взаимодействия. Это является одной из причин внимания современной теоретической физики к биомембранам и, в частности, к липидным мембранам. Значительным результатом статистической физики случайных поверхностей было установление в 1978 году В. Хельфрихом закона и оценка универсальной константы взаимодействия таких объектов. Его оценка дала значение константы $3\pi^2/128$. Отмечая

значимость полученного результата, можно сказать, что этот закон играет такую же роль в физике случайных поверхностей, как и закон идеального газа в физике точечных частиц. В 1986-89 годах С. Сафинья и др., используя анализ формы дифракционных пиков от мультислойных амфифильных мультислоев, измеренных на ренгеновских дифрактометрах высокого разрешения на синхротронных источниках рентгеновского излучения, интерпретировали результаты своих экспериментов как полное количественное подтверждение результатов теории ондуляционных сил, включая зависимость силы от расстояния и константу $3\pi^2/128$. Это было триумфом концепции В. Хельфриха. Но как показало дальнейшее развитие исследований в этой области, это был временный триумф. Несколько групп, в том числе физики-теоретики, работающие в области квантовой теории поля, независимо друг от друга и используя различные теоретические методы, сумели получить точное значение универсальной константы этих взаимодействий. Их результаты совпали, но полученное значение, близкое к $3\pi^2/256$, в два раза отличается от экспериментального значения. Такое противоречие теоретических и экспериментальных результатов получило название “загадочного” и фактически означало глубокий кризис в данной области. В работе, выполненной с участием физиков ЛНФ, были развиты новые подходы для исследования межмембранных взаимодействий и определения универсальной константы, основанные на исследовании температурной зависимости межмембранных взаимодействий с помощью комплементарного использования малоуглового рассеяния тепловых нейтронов и дифракции высокого разрешения на синхротронном источнике. В частности, получено значение константы взаимодействия равное $3\pi^2/256$, совпадающее с теоретически предсказанным. Показано также, что переход от мультислойных к одиночным мембранам происходит в соответствии с теоретически предсказанной моделью двух состояний. Кроме того, впервые показано, какова истинная величина ондуляционных сил - они действительно вносят значительный вклад в баланс межмембранных взаимодействий и, более того, эти силы становятся доминирующими на расстояниях больше 20 Å.

В 2006 г. был выполнен ряд работ и получены интересные результаты в области ядерной физики. Были завершены работы по изготовлению полномасштабной установки для измерения сечения рассеяния нейтрона на нейтроне на реакторе ЯГУАР. Выполнены первые калибровочные измерения на инертных газах с хорошо известным сечением.

Обработаны экспериментальные данные эксперимента по наблюдению изменения энергии нейтрона при прохождении через ускоренное вещество, проведенного на реакторе ИЛЛ (Гренобль). Существование эффекта следует из справедливости принципа эквивалентности и детальных нейтронно-оптических расчетов. Изменение энергии нейтрона,

зарегистрированное в опыте составляло величину порядка 2×10^{-10} эВчто является рекордным по уровню точности на сегодня. На пучке H8 импульсного нейтронного источника KENS (КЕК, Япония) проведен эксперимент, целью которого являлась проверка эффективности управления поляризацией тепловых и эпитепловых нейтронов с помощью радиочастотного поля. Поляризация нейтронов и анализ их поляризации осуществлялись устройствами на основе поляризованного ^{3}He с оптической накачкой, созданными коллаборацией КЕК-ЛНФ ОИЯИ в 2003-2005 гг. Результаты эксперимента хорошо согласуются с расчетами и показали высокую эффективность предложенного метода. Разработанная методика будет использована для управления нейтронной поляризацией в эксперименте по проверке Т-инвариантности во взаимодействии поляризованных нейтронов с поляризованными ядрами, постановка которого планируется на строящемся источнике JSNS. В рамках экспериментов по поиску нейтральных токов в нуклон-нуклонных взаимодействиях и определению слабой π-мезонной константы связи в коллаборации с ПИЯФ, ИЛЛ и ТУ Мюнхена проведен «нулевой» эксперимент по определению фоновой асимметрии на пучке холодных поляризованных нейтронов PF1B (ИЛЛ, Гренобль) для цикла измерений Р-нечетной асимметрии в реакции ^{6}Li(n,α)^{3}H.

В коллаборации Ювяскюля-Дармштадт-Дубна-Гатчина в JYFL (Финляндия) была проведена серия экспериментов по изучению деления с использованием двух мозаик полупроводниковых детекторов. В первом эксперименте исследовались угловые и массово-энергетические корреляции осколков деления в реакции ^{238}U + ^{4}He (40 МэВ). Угловое разрешение установки позволяло вести прямой поиск событий тройного коллинеарного распада. Был обнаружен ряд эффектов, которые могут давать косвенное указание на существование экзотических мод деления. Во втором эксперименте было проведено прецизионное измерение энергетических распределений α-частиц и ядер ^{6}He, испускаемых в процессе тройного спонтанного деления ^{252}Cf. Наблюдалось существенное отклонение спектров от Гауссовской формы в низкоэнергетической области.

В рамках сотрудничества с ИКИ РАН специалистами ЛНФ и ЛРБ были проведены расчеты угловой зависимости эффективности лабораторного прибора ЛЕНД, предназначенного для анализа нейтронного излучения на орбите Луны в составе орбитального аппарата НАСА Lunar Reconnaissance Orbiter 2008. Были также проведены экспериментальные калибровки лабораторного прототипа прибора.

В рамках международной программы «Атмосферные выпадения тяжелых металлов (ТМ) в Европе – оценки на основе анализа мхов-биомониторов» завершен большой цикл работ, связанных с одновременным сбором образцов в 2005–2006 гг в ряде районов Центральной России, Южного Урала, Белоруссии, Болгарии, Словакии, Польши, Румынии,

Сербии, Македонии, Хорватии и Греции для проведения многоэлементного активационного анализа на реакторе ИБР-2. Результаты анализа по 13 элементам: Al, As, Cd, Cr, Cu, Fe, Hg, Ni, Pb, Sb, Ti, V и Zn будут переданы в Европейский Атлас атмосферных выпадений ТМ. Аналогичные исследования проведены в Монголии и Вьетнаме. Особый интерес представляют результаты анализа мхов-биомониторов из биосферных заповедников (Приокско-Террасного и Воронежского), полученные в сотрудничестве с Институтом глобального климата и экологии (Москва).

В заключение можно отметить, что наблюдается рост интереса стран-участниц ОИЯИ к работам в области нейтронных исследований. Важно, что в последние годы в Лабораторию пришло довольно много молодежи. Все эти факты подтверждают, что Лаборатория продолжает успешно и динамично развиваться, проводя исследования в интересах стран-участниц ОИЯИ.

04.04.2007 ***А.В. Белушкин***

Директор

1. SCIENTIFIC RESEARCH

1.1. CONDENSED MATTER PHYSICS

In addition to the complex manganese oxides (manganites), whose main peculiarity is the effect of colossal magnetoresistance, growing interest is being shown in the complex cobalt oxides (cobaltites) of the $Ln_{1-x}M_xCoO_3$ type, where Ln – lanthanide, M – alkaline-earth element. From the scientific point of view, cobaltites are of interest due to strong correlations between lattice, charge, spin and orbital degrees of freedom. Cobalt oxides are important in practice since they are used as electrodes in current power supplies. The peculiarities of phase transitions in cobaltites are connected with the imbalance between the intra-atomic Hund energy and the energy of crystal field corresponding to the configuration of octahedrons of CoO_6. As a result, the Co^{3+} ion may be in three different spin states: low-spin (LS, $t_{2g}^6e_g^0$), intermediate (IS, $t_{2g}^5e_g^1$) and high-spin (HS, $t_{2g}^4e_g^2$) state.

At the IBR-2 reactor the investigations of atomic and magnetic structure of cobaltites were carried out (including experiments at high external pressures). At the HRFD diffractometer the composition of $Pr_{0.5}Sr_{0.5}CoO_3$ was studied, in which several magneto-structural phase transitions had been observed earlier. The diffraction spectra were measured in a wide range of temperatures (10 – 780 K) mainly in the mode of sample heating. In this range two phase transitions ($T_1 \approx 120$ K and $T_2 \approx 300$ K) have been detected, in the course of which magnetic and crystalline structures of the sample change. On heating the symmetry sequentially varies from triclinic to rhombic and then to rhombohedral one. The transitions are greatly spread over temperature, and between 120 K and 300 K the phases coexist (**Fig.1**). The magnetic measurements confirm that the structural transition at 300 K coincides with the Curie ferromagnetic point. The nature of the magnetic transition at 120 K remains unknown so far.

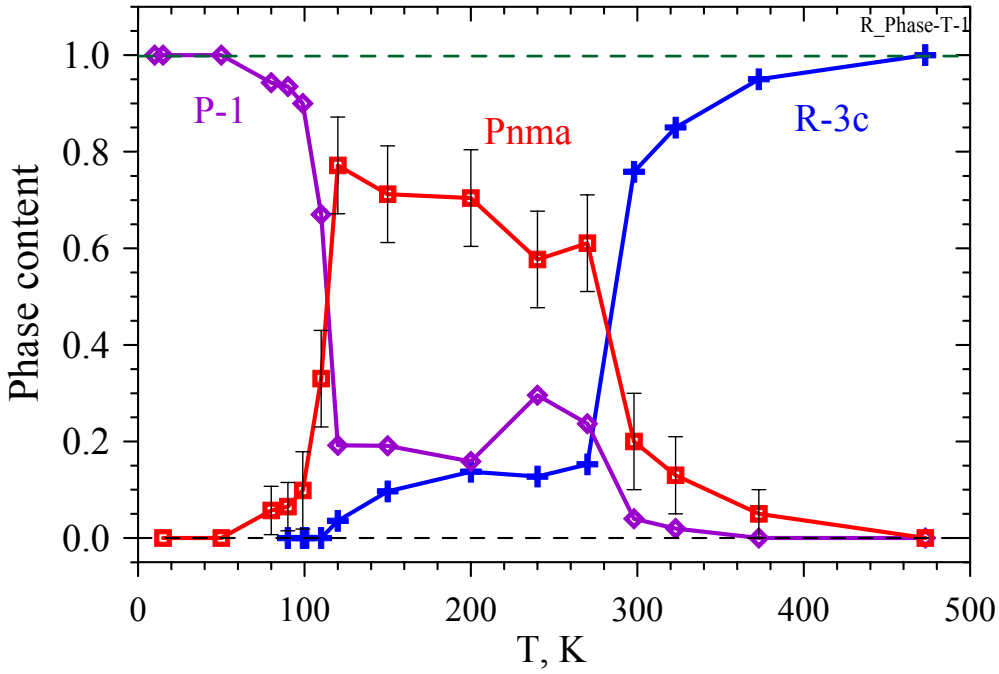

Fig. 1. *Structural phase content in a sample versus temperature.*

At the DN-12 diffractometer the investigation of the crystalline and magnetic structure of hexagonal frustrated manganites $RMnO_3$ (R=Y, Lu) was performed at high pressures of up to 6 GPa. The obtained experimental data along with the results of the previous investigations of other hexagonal manganites made it possible to relate the symmetry of triangular AFM state with the parameter of distortion of triangular lattice *s* formed by Mn and O atoms. The obtained generalized

magnetic phase diagram provides an explanation for the changes observed in the symmetry of the magnetic state caused by chemical substitution (change in the ion radius R of the element) and high pressure due to variation of *s* (**Fig. 2**).

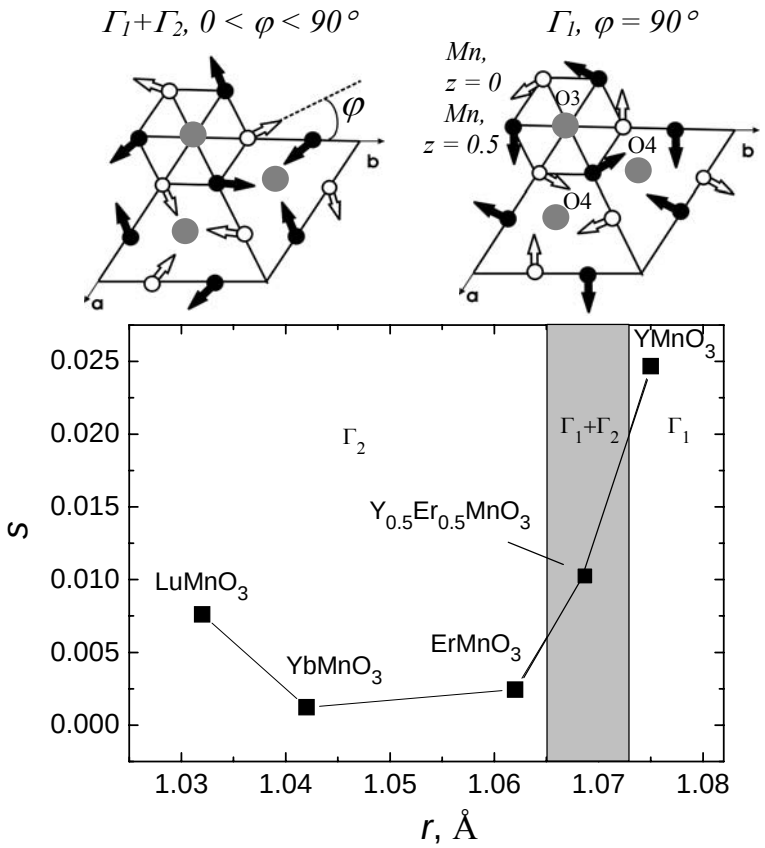

Fig. 2. *Phase diagram of hexagonal manganites $RMnO_3$ and schematic representation of AFM structures of the symmetry Γ_1 and $\Gamma_1+\Gamma_2$.*

In the framework of structural investigations of the factors influencing the stabilization of ferrofluids a planned study of the effect of surfactant excess in ferrofluids on their stability started. As the first system the classical ferrofluid based on magnetite dispersed into benzene and covered by a single layer of oleic acid was chosen. It is known that this system shows the most stability if the whole surfactant is adsorbed on a magnetite surface, i.e. in the absence of free surfactants in solution. In this connection, the solutions of oleic acid ($C_{17}H_{33}COOH$) in deuterated benzene (C_6D_6) were studied by small-angle neutron scattering. The aim of the study was to determine the character of interaction between molecules of the acid, and also to clarify the possibility of their clusterization. On the whole, scattering curves in the Guinier approximation (**Fig. 3**) point to the repulsion between the surfactant molecules. However, the value of the second virial coefficient B = –0.02 determined from these data is significantly larger than that for the system of hard spheres (B = –8). This suggests that the attraction component is essential in the pair potential of interaction between molecules. The volume of molecule of oleic acid, 657 $Å^3$, determined from the SANS data differs considerably from its Van der Waals volume, 523 $Å^3$, and, at the same time, practically coincides with the specific volume of pure oleic acid in its liquid state. In order to clarify the given observation, the simulation of the studied system by molecular dynamics methods started.

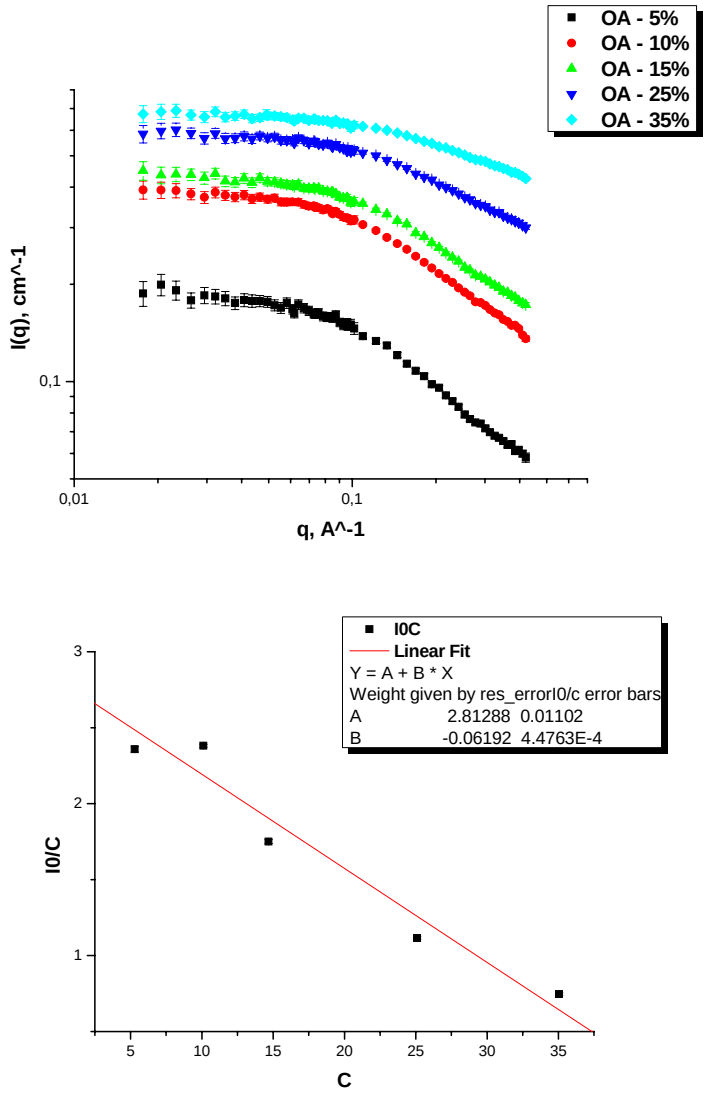

Fig. 3. *Scattering curves of oleic acid solution (OA) in deuterated benzene with various concentrations and dependence of scattering intensity at zero angle in the Guinier approximation on concentration. For the bottom graph a negative slope is observed, which is indicative of repulsion between oleic acid molecules in solution.*

At the REMUR spectrometer the investigation of the magnetic ordering and domain structure in the layers 20×[Fe(1.993nm)/Cr(1.2nm]/MgO was carried out. In this structure the magnetizations of neighboring iron layers are directed antiparallel. In the plane of layers there exist domains, which are also ordered antiferromagnetically. The type of interlayer ordering depends on the thickness of chromium layer. It was proposed to change the thickness of chromium layer by pressing and stretching it using a sound wave of megahertz range. In reflectometric experiments with polarized neutrons the effects of change in diffused neutron scattering from the domain structure and of occurrence of inelastic neutron scattering due to the onset of oscillations of the magnetic moments of layers were observed. The dependence of polarization ability on the Q_X component of momentum transfer (along the neutron beam) was determined at various values of the sound frequency $f_0 = 50$ MHz and $3f_0 = 150$ MHz (**Fig. 4**). It can be seen that with increasing frequency the Q_X distribution widens, which suggests that the size of the domain decreases. Thus, it has been shown that it is possible to control the magnetic structure of the antiferromagnetically-ordered structure 20×[Fe(1.993nm)/ Cr(1.2nm]/MgO by changing the level or frequency of the sound wave. This opens a new possibility to control the magnetic structure, which is characterized by a high speed of response.

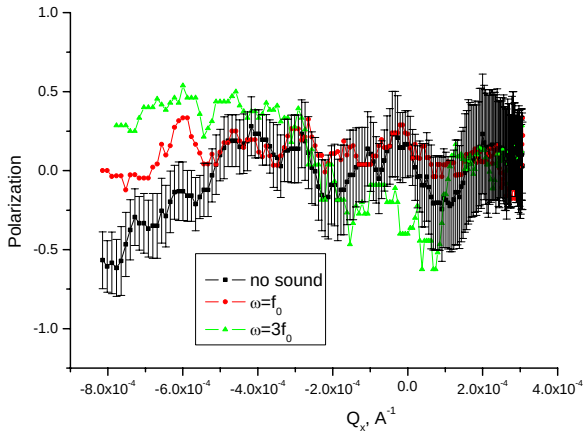

Fig. 4. *The dependence of polarization ability on the Q_X component of momentum transfer (along the neutron beam) at various values of sound frequency at neutron scattering from the films 20×[Fe(1.993nm)/Cr(1.2nm]/MgO.*

At the DN-2 diffractometer the decay of hydrated clathrate with deuterium (composition $32D_2$:$136D_2O$) was studied at heating up to 250 K with the fixation of stages of its decomposition. Short-term (15 min) heating of the sample with the subsequent hardening down to the temperature of liquid nitrogen (95 K) made it possible to perform stepwise removal of hydrogen from clathrate pores at the same conditions of long-term exposition to study interaction of the matrix with the molecules of interstitial deuterium. It turned out that the lattice parameter under these conditions did not depend on the deuterium concentration, i.e. no signs of increase of its interaction with the lattice were shown. In order to solve the question on the nature of deuterium extraction, the intensities of individual reflexes were analyzed. Thus, the compositions of hydrides at annealing were determined graphically by imposing the column of experimental intensities on the calculated raster (**Fig. 5**). The calculation of initial scattering by the Rietveld method gave the best agreement at the concentration of 32 molecules of D_2 per cell, where 16 molecules are in a large cage (8b, 2 mol. each) and 16 molecules – in a small one (16c, 1 mol. each). After short-term (15 min) heating up to the temperature of 145 K changes in the clathrate structure are minimal. Gradual removal of hydrogen is possible up to the temperature of 195 K, when the growth of impurity phase of ice starts and the composition reaches the minimal value $x=16_{8b}+16*0.7_{16c}=27.2\pm 0.5D_2$. On warming up to 220 K the decomposition of clathrate along with the appearance of intensive lines of ice crystalline phases (Ih, Ic) with a noticeable portion of amorphous ice of low density are observed.

Complex investigations of physical properties of synthetic single-crystal quartz and quartz powder in a temperature region of α-β transition were conducted by neutron diffraction and mechanical spectroscopy. The crystal structure of quartz powders with various average sizes of grains was determined in a temperature interval up to 620°C and at a temperature of α-β phase transition. Temperature dependences of values of internal friction and resonance frequency in quartz samples were obtained in the vicinity of the phase transition temperature at the excitation of vibrations in the planes parallel and perpendicular to the Z axis of quartz. Different values of temperatures of the points of maximum of internal friction lying in the interval of 560-620°C were registered. Possible reasons for the displacement of transition temperature were suggested. The maximum of internal friction, which is not associated with the structural transformations in quartz, was revealed in the vicinity of 350°C. The aim of further studies is to find reasons for the displacement of the point of phase α-β transition in quartz and the nature of the internal friction peak at 350°C.

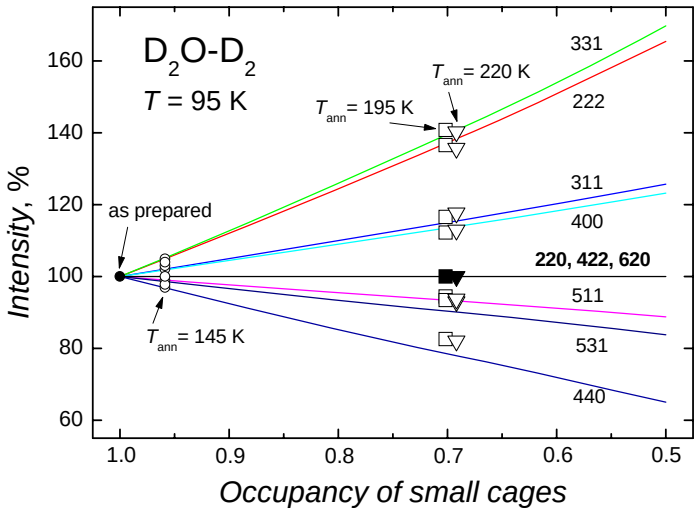

Fig. 5. *Calculated and experimental values of intensities for D_2O–D_2 clathrate as a function of occupancy of small cages.*

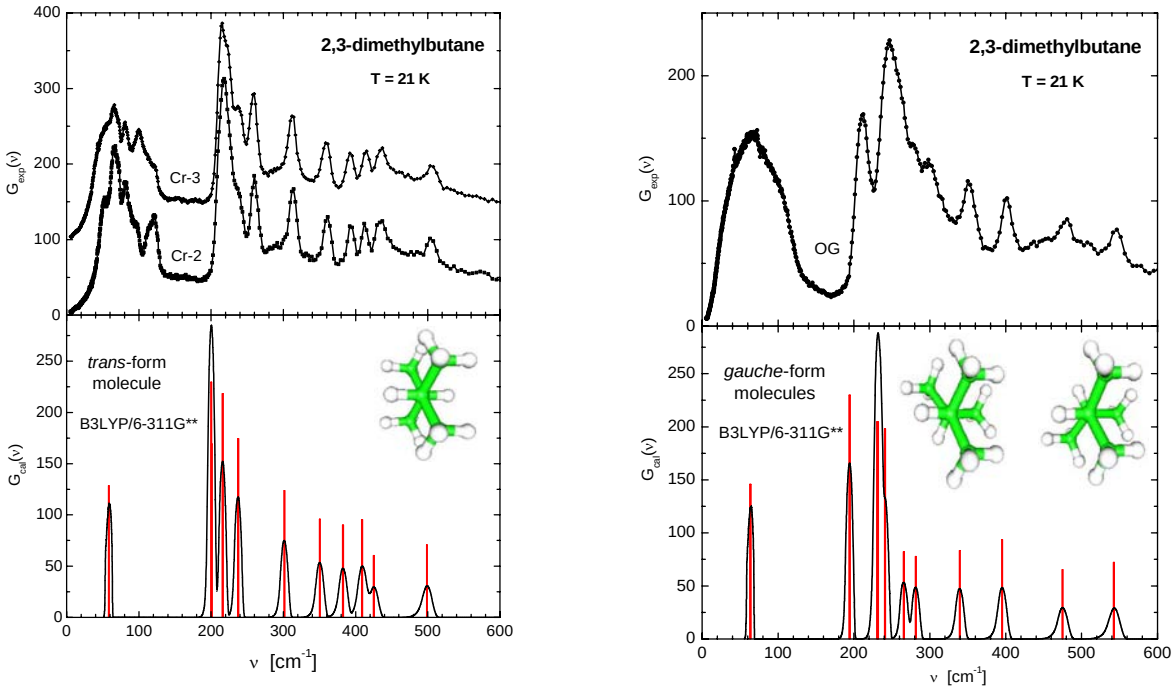

Fig. 6. *Comparisons of the $G_{exp}(\nu)$ spectra of crystalline (Cr-2 and Cr-3) and orientational glass (OG) solid phases of 2,3-dimethylbutane with the $G_{cal}(\nu)$ spectra of isolated molecules calculated within one phonon scattering approximation.*

At the inverted geometry spectrometer NERA the study of vibration spectra of hexane isomers was conducted accompanied by the calculations in the framework of the DFT method. Inelastic scattering spectra were measured for the isomers: 2- or 3-methyl-pentane and 2,2- or 2,3-dimethyl-butane with a general formula C_6H_{14}. Simultaneously, the diffraction spectra of these samples were measured, which allowed us to control the structure of solid phases. DFT calculations of the structure and dynamics of molecules of the studied isomers were performed to interpret a low-frequency part of the internal vibration spectrum, which is clearly seen in the experimental spectra measured at a low temperature. Special interest in these calculations was aroused by the fact that the inelastic scattering spectra of diisopropyl measured in the glassy and crystalline phases differ from each other. The comparison of the calculated and measured spectra (**Fig. 6**) shows that

internal vibrations in the orientation glass state correspond to the vibrations in a *gauche*-form of a molecule. This implies low potential barriers for internal rotations of molecular groups $CH(CH_3)_2$, which was also confirmed by the DFT calculations.

At the DIN-2PI spectrometer the investigation of atomic dynamics in superionic and non-superionic phases of AgCuSe was carried out for the first time using the slow neutron scattering technique. The analysis of the dynamic structural factor $S(Q,\omega)$ points to the presence of low-energy modes in the energy region of 3-4 MeV in the ordered state of AgCuSe, which presumably correspond to acoustic phonon modes. A correlation was established between the transition of AgCuSe into the superionic state and the changes in the dynamics of crystalline lattice involving an abrupt change in spectra of the dynamic structural factor, generalized density of phonon states, thermodynamic properties. An increase in thermal oscillation amplitude, a change in heat capacity at the transition into the superionic state are indicative of considerable softening of the phonon spectrum in α- AgCuSe. The phonon state density $G(\varepsilon)$ in α- and *β*- AgCuSe is characterized by the non-Debye behavior in the low energy region and by two pronounced maxima at ε ~ 10 and 20 MeV (**Fig. 7)**. The reason for $G(\varepsilon)$ deviation from the Debye dependence is the presence of low-energy excitation mode. At the transition from β to α phase the smearing of maxima is observed at ε ~ 10 and 20 meV, as a result of a change of many factors in the atomic dynamics of the studied system.

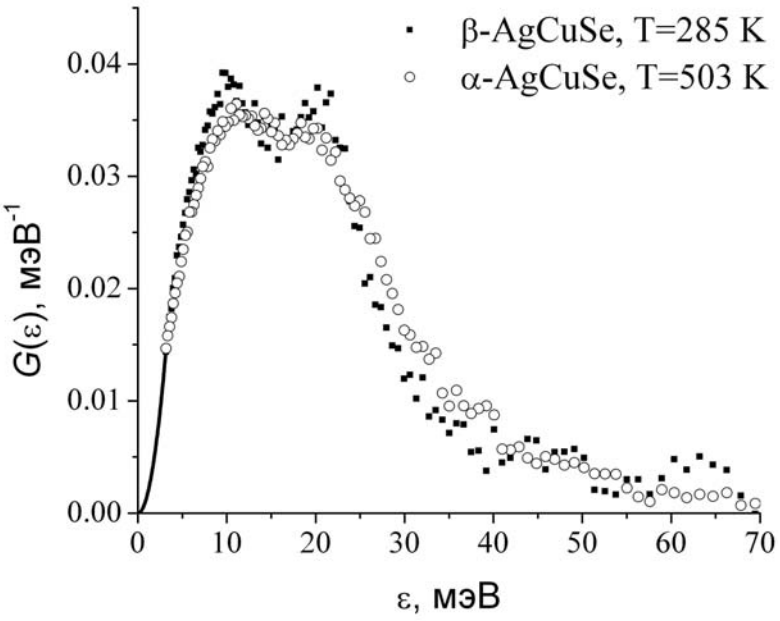

Fig. 7. *Neutron-weighted generalized density of phonon states G(ε) of AgCuSe in superionic and non-superionic phases.*

In 2006 a series of works on experimental determination of the universal constant of the interaction of fluctuating surfaces was completed. The interaction of this type (undulation forces) manifests itself in a wide class of objects – from biological membranes to strings in the modern field theory trying to describe all fundamental interactions from a single viewpoint. This accounts for close attention of modern theoretical physics to biomembranes and, in particular, to lipid membranes. The establishment of the law and an initial estimate of the universal constant of interactions of such objects made by W. Helfrich in 1978 became a significant result in the statistical physics of random surfaces. His estimate gave the value of the universal constant $3\pi^2/128$.

In 1986-89 C.R. Safinya et al. using the analysis of the shape of diffraction peaks from amphiphilic multilayers obtained at X-ray high-resolution diffractometers on synchrotron X-ray

sources, interpreted the results of their experiments as complete quantitative verification of the results of the undulation force theory including the distance dependence of the force and the constant value $3\pi^2/128$. That was a triumph of W. Helfrich's concept. But as the further advancement of research in this field showed, it was a short-time triumph. Several groups, including theoretical physicists concerned with the quantum field theory, independently of one another and using different theoretical methods succeeded in obtaining an exact value of the universal constant of these interactions. Their results coincided, but the obtained value (close to $3\pi^2/256$) was twice as large as the experimental value. Such contradiction of theoretical and experimental results has received the name "enigmatic" and actually meant severe crisis in this field.

In the work by V.I.Gordeliy, V.G.Cherezov and J.Teixeira a new approach to study intermembrane interactions and to determine the universal constant based on the investigation of temperature dependence of intermembrane interactions by means of complementary use of small-angle thermal neutron scattering and high-resolution diffraction on a synchrotron source has been developed. In particular, the value of the constant $3\pi^2/256$ has been obtained that coincides with the theoretical predictions. It also has been shown that the transition from multilamellar to unilamellar membranes proceeds in accordance with a two-state model. In addition, for the first time the true significance of undulation forces has been demonstrated – they really make a considerable contribution into the balance of intermembrane interactions, and what is more, become dominating at intermembrane distances larger than 20.5 Å.

Figure 8 illustrates the experimental dependence of the theoretical parameter η (derived from the analysis of diffraction data) on the structural parameters of membranes (membrane thickness d_b and repeat distance d) obtained using small-angle neutron scattering. This dependence made it possible to determine the value of the universal constant.

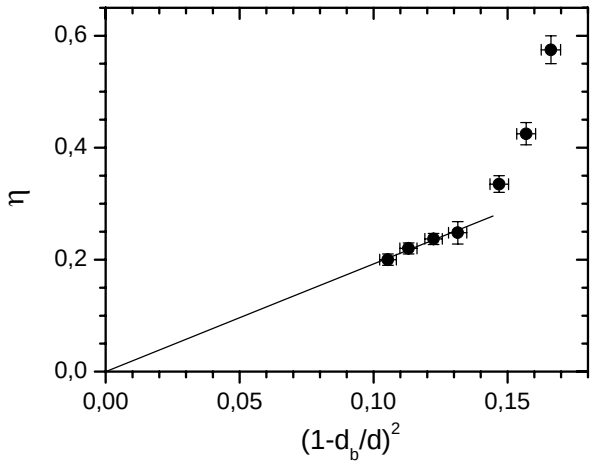

***Fig. 8**. Experimental dependence of the theoretical parameter η (derived from the analysis of diffraction data) on the structural parameters of membranes (membrane thickness d_b and repeat distance d) obtained using small-angle neutron scattering.*

1.2. NEUTRON NUCLEAR PHYSICS

Introduction

In the course of the year 2006 the main work in the field of neutron nuclear physics in the Frank Laboratory of Neutron Physics was carried out at the IBR-2 reactor, the EG-5 facility, on neutron beams of other nuclear centers of Russia, Bulgaria, Poland, Czech Republic, Germany, Republic of Korea, China, France, USA and Japan. The studies were in traditional directions, such as the investigation of time and spatial parity violation processes in the interaction of neutrons with nuclei, studying of the quantum-mechanical characteristics, energy and dynamics of the fission process, experimental and theoretical investigation of the electromagnetic properties and beta-decay of the neutron, gamma-spectroscopy of neutron-nuclear interactions, studies of atomic nucleus structure, obtaining of the new data for reactor applications and nuclear astrophysics, experiments with ultracold neutrons, and applied investigations.

1. Experimental investigations

1.1 Fundamental properties of the neutron

1.1.1 Experiment on the direct measurement of the cross section of neutron-neutron scattering

The work in the framework of preparation and carrying out of an experiment on the direct measurement of the cross section of neutron-neutron scattering at the YAGUAR reactor (RFNC-VNIITF, Snezhinsk).

In 2006 a complete set of collimators out of a mixture of the enriched boron and sulfur (for central collimators) and out of a mixture of the boron carbide and sulfur (for the rest of collimators) was manufactured. Vacuum tests of a lower part of the channel with the collimators installed in it were carried out. The tests showed that in the tested configuration (without an upper part of the channel) at the standard pumping the vacuum of $\sim 3 \cdot 10^{-6}$ mbar is reached, which is enough to perform measurements of the nn-scattering. (The assembled lower part of the facility during the tests is shown in **Fig. 1** and **Fig. 2**).

A test of an ion pump (of the «NORD-250» type) was carried out when it was installed instead of one of the turbo-molecular pumps. The test showed that the use of this pump does not lead to an improvement of the vacuum inside the vacuum system.

Fig. 1

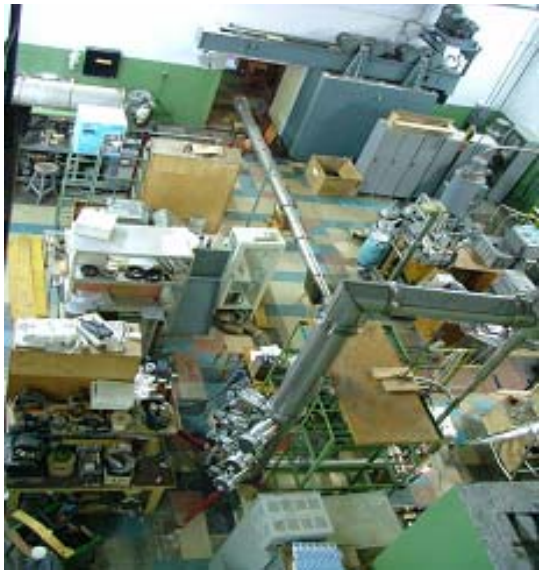

Fig. 2

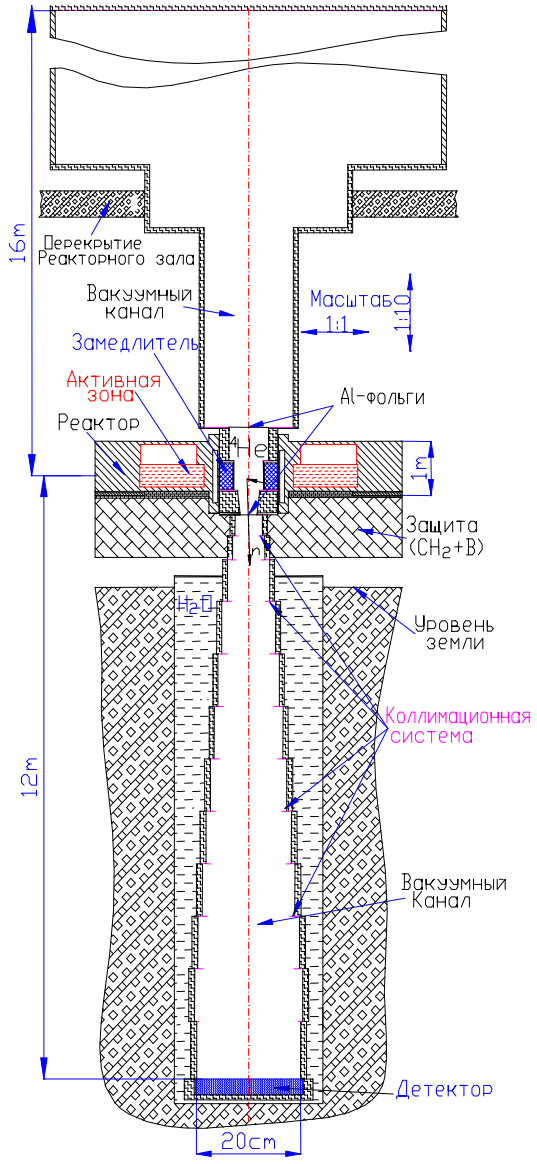

Fig. 3. *Diagram of the facility for calibration measurements on gases.*

Manufacturing of the additional equipment to assemble a neutron channel under the reactor and carrying out of the upper work (under the ceiling of the reactor hall) to assemble the elements of the neutron channel completed.

The main part of elements of the design of the modernized detector was manufactured. Tests of the vacuum density of the detector case were carried out. Various operating modes of the detector were studied in order to decrease maximally the pulse duration preserving the amplitude resolution.

Thus, the work to manufacture a full-scale facility to measure the cross section of neutron-neutron scattering at the YAGUAR reactor was completed.

The facility was successfully tested in Dubna, conveyed to Snezhinsk, mounted and adjusted at the YAGUAR reactor.

In order to check working capacity of all systems of the facility during the real measurements at the reactor and also to check the reliability of the obtained results first calibration measurements on gases have been carried out. The diagram of measurements is given in **Fig.3**. A cavity inside the reactor core, in which the neutron-neutron scattering is to take place, is filled by a rare gas with the well-known scattering cross section at the pressure of ~100 torr. The cavity is separated from the vacuum channel, by which the neutrons scattered on a gas hit the detector, by a thin aluminum foil. All other parts of the facility (except for the detector, the sensitivity of which has been lowered and has been equal to $6.6\ 10^{-5}$ in contrast to 100% efficiency for recording of the n-n scattering) are the same as for the measurement of n-n scattering 40 μm thick. Cross section of the neutron scattering on a gas filling the inner cavity of the reactor is calculated according to the number of recorded neutrons at the known energy-release of the reactor. Coincidence of the cross section measured in this way with a known tabulated cross section is the criterion of correctness of the system adjustment, correctness of the calculation of a neutron spectrum and solid angle, in which the neutron recording takes place. Furthermore, the whole recording channel is tested in this measurement.

Results of the measurements showed as follows:

1. All systems of the facility, except for the recording system, operate normally.

2. The role of γ-background has proved to be unexpectedly great – the overwhelming majority of events recorded by the detector during the pulse have been γ-quanta. A large flux of γ-quanta passing through the detector leads to the situation that the detector ceases to record any events (both neutrons and γ-quanta) and regenerates in more than 10 ms when the thermal neutron flow scattered on atoms of a gas has already bypassed the detector. Therefore, the neutron recording in the pulsed mode has proved to be impossible. It is necessary to perform an additional simulation to optimize the detector protection from the point of view of decreasing the γ-quanta flux passing through it,

and also a modernization of electronics of the recording system aimed at decreasing the regeneration time in case of overload.

3. The measurement carried out at constant power of the reactor showed that the channel adjusted correctly and in the absence of the detector overload the recording system also operates correctly. The measured cross section of thermal neutrons on ^{4}He was 0.87±0.13 b (tabulated value of this cross section – 0.760 b).

1.1.2 Investigation of the n-e scattering

A new method to obtain experimental value of the neutron scattering length on electron b_{ne} was applied to analyze the data on structural factors $S(q)$ (q – transmitted wave number) describing neutron diffraction in gases and liquids. The results of diffraction experiments were used obtained at the reactor in Grenoble by an international group of physicists, who kindly granted their numerical data for our calculations.

At first, $S(q)$ for gaseous isotope ^{40}Ar were processed, in which, due to an anomalously strong nuclear scattering, the relative contribution of n,e-scattering to the total scattering is by the order of 1 less than in natural Ar, Kr and Xe. Accordingly, the result proved to be quite modest but it demonstrated the effectiveness of the proposed method:

$b_{ne} = -(1{,}33 \pm 0{,}28 \pm 0{,}57) \cdot 10^{-3}$ Fm,

where the second error is systematic. The article was submitted to Eur. Phys. J.C. Naturally, the data processing on the diffraction on liquid Kr gave much better result. Three different variants of data processing led to very close values of b_{ne}, the most accurate of which is

$b_{ne} = -(1{,}38 \pm 0{,}04) \cdot 10^{-3}$ Fm.

This result is among the best 10-12 concerning the accuracy.

An experiment has been proposed aimed at the measurement of the n-e scattering length at the TS3000K facility on liquid metals. The first preliminary experiment is planned to be carried out on liquid lead, since the melting point of lead is somewhat higher than 300^{0}C. In case of successful experiment on lead, measurements on other liquid metals with higher melting temperature will also be carried out.

The TS3000K facility has been realized in the «Horia Hulubei» National Institute of Physics and Nuclear Engineering, Bucharest – Romania (IFIN-HH), and is intended for investigation of the structure and dynamics of the solid and liquid state using inelastic neutron scattering under conditions of super-high temperature and vacuum.

In 2006 theoretical estimations to measure the n-e scattering length on lead using several phenomenological models of liquid state and liquid lead have been carried out. These estimations show a possibility to obtain the length at the TS3000K facility on the DIN-2PI channel.

1.2 Neutron optics

1.2.1 Optics of strongly absorbing materials

The work on experimental check of validity of the 1/v law for the ultra-cold neutron capture cross section in natural gadolinium has been completed. The idea of the work is based on the circumstance that the interaction of neutron with matter may be described by the model of effective optical potential only in the case when the total cross section of interaction of neutrons with nuclei obey the 1/v law. At the same time, in general, the optical potential V is complex.

$$\mathbf{V = U + iW}. \qquad (1)$$

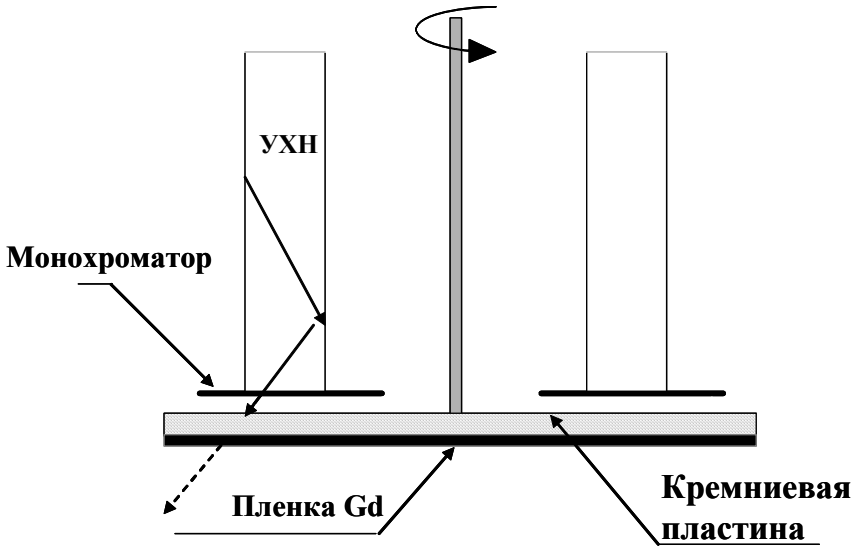

Fig. 4. *Diagram of the experiment to check the 1/V law for the UCN capture cross section in natural gadolinium.*

In case of natural gadolinium, which has a record value of the capture cross section owing to the presence of resonances in the thermal region of energies, in general, the model of potential is not valid. However, for cold and very cold neutrons it must hold true with a high accuracy. Values of the real and imaginary parts of the potential of natural gadolinium for the case of UCN have been determined in our previous papers [1.1, 1.2]: V = 45 neV, W = 82 neV.

The peculiarity of the model of potential is that, that in case of its validity both the reflection coefficient and the matter transparency depend only on the neutron velocity component, which is normal towards the surface of matter. It is this peculiarity that has been accepted as a basis for our experiment.

Ultracold neutrons passed through the peripheral part of a sample, which was a gadolinium film, 25 nm thick, applied on a silicon disk. Rotating the disk, one could change the relative velocity of neutrons and that of the sample retaining unchanged the normal velocity component (see **Fig.4**). Transmission does not vary with the speed of rotation and this testifies to the validity of the model of effective potential and, consequently, to the observance of the 1/v law. As a result, it has been determined that the 1/v law for the UCN capture cross section in natural gadolinium is valid with the accuracy on the order of 0.1% in the interval of change of the UCN velocities from 4 to 35 m/s.

1.2.2 Interaction of the neutron with accelerating matter

The experiment to observe a change of energy of the neutron at passing through the accelerating matter has been carried out. Existence of the effect follows both from the validity of the equivalence principle and from the detailed neutron-optical calculations [2.2]. For a flat sample moving with acceleration the value of effect is determined by the expression

$$\Delta E \approx wd\frac{1-n}{n}, \qquad (2),$$

where **d** – the sample thickness**, n** – the refraction index and **w** – acceleration of the sample. The aim of the work has been to measure such change of energy.

A silicon wafer, 0.6 mm thick, which could be set in harmonic motion, was used as a sample. Simultaneously, the neutron energy was to change according to the harmonic law in compliance with

$$\Delta E(t) = \frac{1-n}{n} A d \Omega^2 \mathrm{Sin}(\Omega t), \qquad (3),$$

where **A** and $\Omega=2\pi f$ – the amplitude and oscillation frequency of the sample, respectively. The maximal value of acceleration $w_{max} = A\Omega^2$ was a magnitude on the order of 7.5 g, which corresponded to the energy transfer $\Delta E \approx 2 \times 10^{-10}$ eV.

The experiment was conducted using the UCN gravitational spectrometer with interference filters. Here, a sample was placed between the filter-monochromator (and near it) and the filter-analyzer. Harmonic motion of a sample led to a periodic modulation of the count rate with the same frequency. This modulation was induced by two effects: a change of energy proportional to the sample acceleration, which was the subject of the search, and a change of the sample transparency caused by alternation of the relative velocity of the sample and that of the neutron. At various relations between these two effects, the desired one and the systematic one, oscillation phase of the neutron count rate was also different. It was this circumstance that was accepted as a basis for the experiment. In the experiment oscillation phase of the count rate was measured depending on the distance between the two filters.

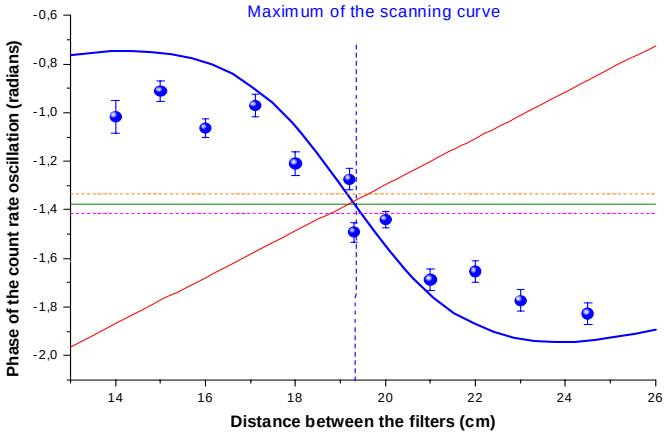

Fig. 5. *Oscillation phase of the count rate depending on the position between the filters.*

The obtained results are shown in **Fig. 5**. Blue closed points – the result of measurement of oscillation phase of the count rate depending on the distance between the filters. Solid blue curve – the theoretical calculation. Red inclined line – the calculation made on the assumption that a change of the oscillation phase is caused only by a periodic modulation of the sample transparency and the desired effect of energy change is absent. Horizontal solid and dotted lines – oscillation phase of the count rate (and a corridor of errors) when the filter-analyzer is absent. At correct measurements and calculations these lines must cross at one point.

The experiment undoubtedly testifies to the existence of the effect of neutron energy change observed for the first time at passing through an accelerating sample. Its value corresponds to the theoretical predictions with an accuracy on the order of 15%. Further experiments will show if this discrepancy relates to physical reasons or it is of purely methodological character. It is also should be mentioned, that although the effect of accelerated matter has been observed so far only in the neutron-optical experiment, it is of quite universal nature and should also exist for particles of different nature.

1.2.3 Verification of the weak equivalence principle and measurement of the neutron gravitational acceleration

At the UCN source in ILL (Grenoble) an experiment to measure the neutron gravitational acceleration has been carried out. The experiment has been carried out using the gravitational UCN spectrometer with the Fabry-Perot interferometer (FPI), and its idea earlier published in the paper is given in **Fig. 6**. After passing through the FPI-monochromator, the neutrons with a narrow interval of vertical velocities pass through a rotating phase diffraction grating. The neutrons corresponding to the 1-st order of diffraction decrease their energy by the value $\Delta E = \hbar\Omega$, where the frequency modulation Ω is proportional to the frequency of the grating rotation f and is equal to $\Omega = 2\pi\frac{f}{\varphi}$, where φ - angular period of the grating. On the way to the FPI-analyzer neutrons accelerate in the gravitational field increasing their energy by the value mgH, where H – the distance between FPI. The energy measurement is performed by way of scanning throughout the height by analyzing FPI. Simultaneously, maxima of the corresponding scanning curves are determined at various values of the grating rotation frequency and the modulation frequency proportional to it. Here, value of the gravitational acceleration is determined from the relation

$$g = \frac{\hbar}{m}\frac{\Delta\Omega}{\Delta H} \qquad (4).$$

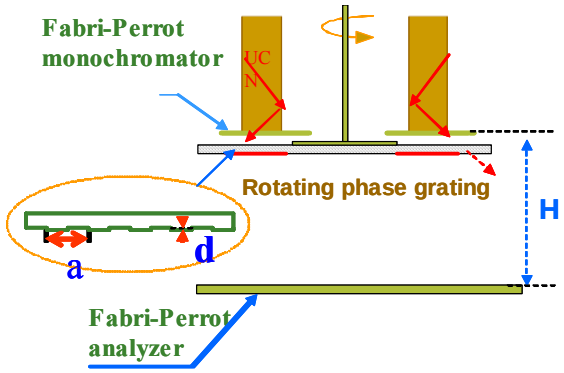

Рис.6. *Идея эксперимента по измерению ускорения свободного падения нейтрона.*

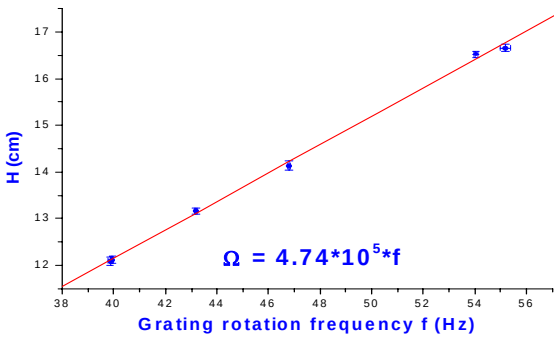

Fig.7. *Position of the maxima of scanning curves depending on the grating rotation frequency.*

Results of one of the experimental series is shown in **Fig. 7**.

At present, the experimental data processing continues. A preliminary result is that within the accuracy on the order of 0.2% the gravitational acceleration of the neutron is the same as that of the macroscopic body.

1.2.4 Designing of the neutron microscope

In 2006 the work on design of the neutron microscope oriented toward the advanced European UCN sources has started. The software to calculate mirror optical systems for UCN in the

presence of gravitation has been created. With the help of this program, calculations of the horizontal neutron microscope with compensation of the gravitational aberrations by refracting elements are conducted. The encouraging results have been obtained.

1.3 Investigation of the properties of ultracold neutrons

1.3.1 Works in the framework of investigation of the UCN interaction with the surface

In 2006 investigations of the surfaces of a number of materials have been carried out by the atomic-force microscope (AFM). The investigations have been aimed at testing of the hypothesis on surface nanoparticles as the reason for the so-called «low heating» of UCN at the interaction with surface. The surfaces of copper, iron, various grades of stainless steel and sapphire, and also the dependence of surface texture on the temperature of preliminary degassing, have been investigated. Typical data from the sample surfaces obtained on AFM are presented in **Fig. 8**.

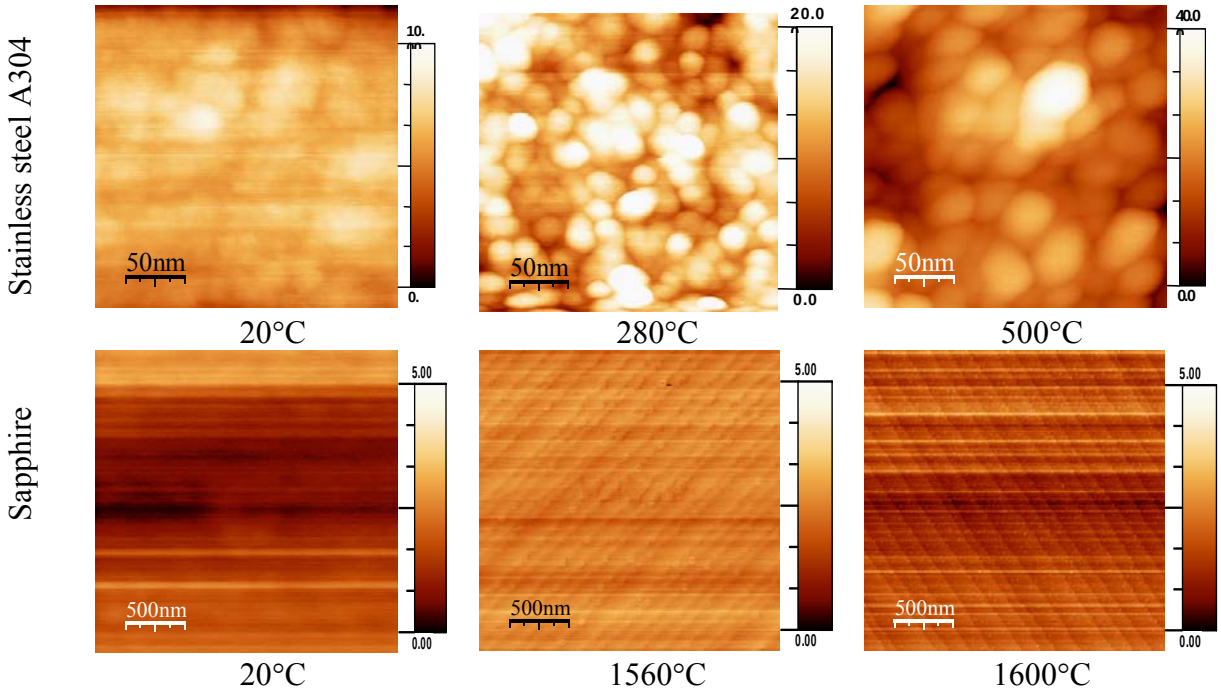

Fig. 8. *Data from the sample surfaces.*

The main conclusion drawn from the conducted measurements: nanoparticles of various size are present on all the studied surfaces (except for the polished monocrystalline sapphire). The sizes of nanoparticles increase with the growth of temperature of the preliminary warming-up of samples, the number of nanoparticles depends on this temperature and on the vacuum depth during the warming-up. Nanoparticles are formed on the monocrystalline sapphire at its warming-up up to the temperature ~1600°C, at the same time, after its warming-up to 800°C no nanoparticle formation is observed on its surface. Surface of the monocrystalline sapphire after its warming-up to 1600°C is a stepped structure with steps equaling to one atomic plane.

The observation of particles on the surface points to a possibility of inelastic neutron scattering with a low energy transfer on such particles if they prove to be free enough.

1.3.2 Investigation of the quasi-elastic UCN scattering

In ILL the work of the last year was continued by new measurements of the probability and spectra of the quasi-elastic UCN scattering on a series of samples: copper, diamond-like carbon, teflon, etc. In the previous experiments a considerable heating of neutrons was detected for the first time in the velocity region of 8-12 m/s.

The method has been to measure the neutron flux (after scattering on a sample) through calibrated samples with known neutron absorption cross section. In this case silicon single crystal wafers and rhodium foils have been used as absorbers. Absorption curves for neutrons of the total scattering spectrum: from ultracold ones to thermal ones, have been measured in this way. Absorption curves have been measured and spectra of scattered neutrons have been restored from them. Final processing of the results will be carried out at the beginning of 2007.

As before, the measurements have been carried out only at room temperature and on the samples, which have not been treated thermally in vacuum. The experiments are planned, in which the sample surface may be thermally degassed in vacuum, and the measurements may be carried out at low temperatures.

1.3.3 Works to create a UCN source at the TRIGA pulsed reactor

New detailed calculations have been performed and the generation of ultracold neutrons at the TRIGA-Mainz pulsed reactor (in common with the groups from Munich and Mainz) have been measured for the first time. This is the realization of the long-standing proposal by Yu. N. Pokotilovski „Production and storage of ultracold neutrons at pulsed neutron sources with low repetition rates“, Phys. Lett., A356 (1995) 412.

Results on the UCN generation and nonstationary transport on the mirror neutron guide are in good line with the calculations.

Neutrons were generated in the solid deuterium target at the temperature of 6-10 K and were transported along the mirror neutron guide 6 m of length. In a part of experiments the mesithylene moderator was used at the temperature of 20 K.

At the neutron recording three different neutron detectors were used in turn: the silicon detector with the enriched boron fluoride radiator, the proportional gas one with He-3, and, finally, due to the high count rate at the pulsed generation (up to 10^6 neutrons per second), the GEM-detector with the boron radiator. At the reactor pulse 10 MJ the number of recorded neutrons with the energy lower than 200 neV exceeded 10^5.

1.4 Spatial and time parity violation in the interaction of neutrons with nuclei

1.4.1 Measurement of P-odd asymmetry of the triton emission in the reaction $^6Li(n,\alpha)^3H$

At the PF1B beam of cold polarized neutrons of the ILL reactor (Grenoble) a “zero” experiment to determine background asymmetry for a series of experiments to measure P-odd asymmetry of the triton emission in the reaction $^6Li(n,\alpha)^3H$ has been carried out. The value $\alpha_0 = (0.0 \pm 0.5)\cdot10^{-8}$ has been obtained. Thus, one of two most important experiments conducted in the course of several last years to search for neutral currents in nucleon-nucleon interactions is successfully completed. Comparison of this result with the result of the main experiment: $\alpha_t = -(8.6 \pm 2.0)\cdot10^{-8}$ shows that the observed effect is caused by P-odd asymmetry of tritons from the reaction $^6Li(n,\alpha)^3H$. The aim of investigations is to determine weak π-meson constant of coupling f_π corresponding to the interaction of neutral currents in nucleon-nucleon processes. The restrictions: $f_\pi = (0.4 \pm 0.4)\cdot10^{-7}$ follow from the obtained asymmetry on the assumption that other constants are equal to the Desplanques «best values», etc., and $-1.2\cdot10^{-7} \le f_\pi \le 1.6\cdot10^{-7}$ taking into account theoretical and experimental uncertainties of other constants. This confirms the results of the experiment on ^{18}F and the conclusion that f_π is significantly smaller than the Desplanques «best

value», etc., ($4.6 \cdot 10^{-7}$). The works are carried out in common with PNPI (Gatchina), ILL (Grenoble, France), TU of Munich (Germany).

1.4.2 Control of neutron polarization by means of the Ramsey rotation

In 2006 an experiment aimed at verification of the effectiveness of control of the polarization of thermal and epithermal neutrons using the radio-frequency field has been carried out. The experiment has been conducted on beam H8 of the KENS pulsed neutron source (KEK, Japan). Layout of the facility is given in **Fig.9**.

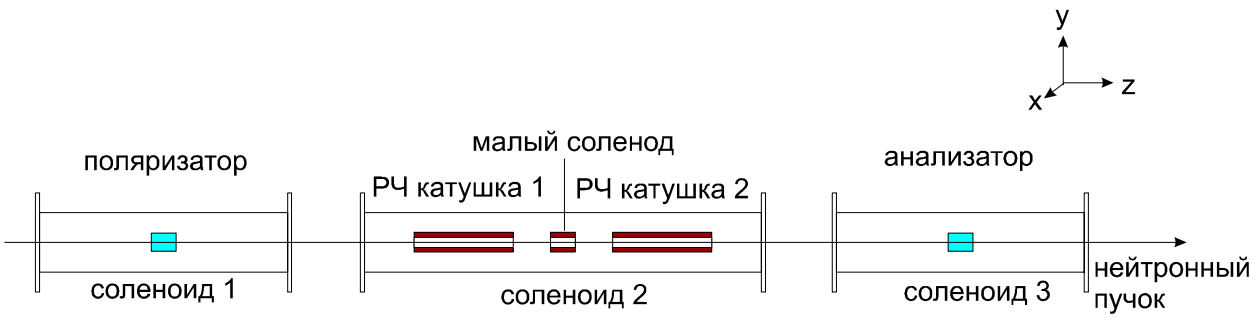

Fig. 9. *Diagram of the experiment.*

The polarization of neutrons and analysis of their polarization was carried out by devices on the basis of polarized ^{3}He with optical pumping created by the KEK-FLNP JINR collaboration in 2003-2005. In solenoid 2.80 cm of length and 12 in diameter, two rectangular radio-frequency coils RF1 and RF2 20 cm of length each were placed one after another. Each coil generated an oscillating field $2H_1\cos(\omega t)$ directed along the *y* axis. The measurement was conducted in the time-of-flight mode. The field was switched on at the moment when neutrons with $E_h = 80$ meV arrived at the input of the first coil and was switched off at the moment of arrival of neutrons with $E_l = 23.6$ meV. Simultaneously, the field amplitude H_1 was modulated in such a way so as to provide the turn of neutron polarization for the given angle φ round the y axis for all the neutrons in the interval $E_l \le E \le E_h$. To do this, execution of the condition $\gamma H_1 t = \varphi$ was necessary, where γ – the gyromagnetic ratio for the neutron, and t – the time of flight of a neutron of the given energy along the coil. In our experiment $\varphi = \pi/2$ was chosen. The second coil worked coherently with the first one and, thus, the total turn of neutron polarization at the analyzer input was π, i.e. the polarization reversal took place. A corresponding change of transmission of the neutron beam passed through the analyzer was recorded by the scintillation detector on the flight path 12.05 m long.

If one switches on the additional field between the first coil and the second one then due to the additional rotation of neutron polarization in this area, the character of neutron transmission changes.

In the experiment we measured neutron transmissions with the coils switched off T_{off} and with the coils switched on T_{on}. Then we constructed the relation:

$$R = \frac{T_{on}}{T_{off}} - 1 = \frac{1 + \alpha(E) P_1 P_2}{1 + P_1 P_2},$$

where P_1 and P_2 - neutron polarizations passed individually through the polarizer and analyzer, respectively. All the information on the fields, to which neutron polarization was subjected between

the polarizer and the analyzer is included in function $\alpha(E)$. **Figs. 10, 11** illustrate relations *R* for the cases with the small solenoid switched off/on. Red lines – the fitting. Energy dependence of relations R relates the dependence of values $\alpha(E)$, P_1 and P_2 on the neutron energy.

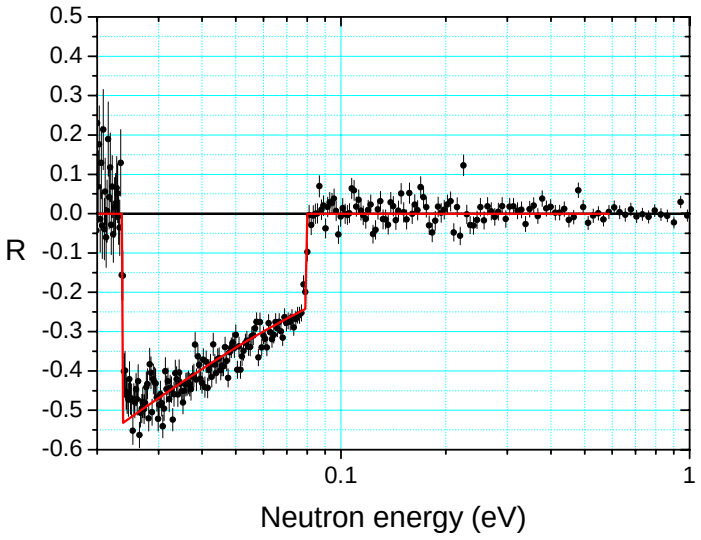

Fig. 10. *Relation R when the small solenoid is switched off.*

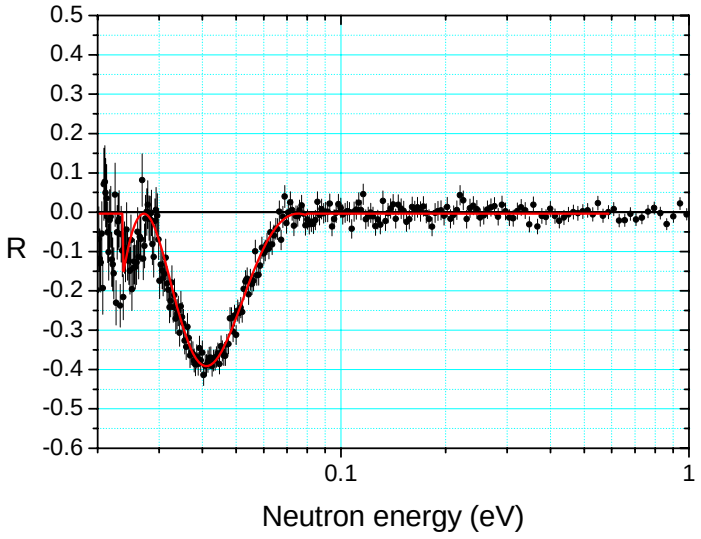

Fig. 11. *Relation R when the small solenoid is switched on.*

For 2007 carrying out of investigations on the technique of manufacturing and selection of $LaAlO_3$ single crystals is planned aimed at the creation of the polarized nuclear target to verify T-invariance in the interaction of polarized neutrons with polarized nuclei. In addition, the work to improve the existing cryostat of nuclear target will be carried out.

1.4.3 Search for and investigation of the structure of subthreshold neutron p-resonances in lead isotopes by the combined correlation gamma spectroscopy method

With the aim of testing the validity of the experimental data obtained previously on the existence of the negative neutron p-resonance in ^{207}Pb isotopes instead of ^{204}Pb as was expected on the basis of the work to observe spin rotation of thermal neutrons at the interaction with lead additional experiments have been carried out on the improved gamma-spectrometer COCOS at channel №1 of the IBR-2 reactor with the increased effectiveness and operating speed. In order to study the energy dependence of the radiative neutron capture cross section two samples with various weight and content of isotopes under investigation: a) 20 g with 90.4% enrichment in ^{207}Pb isotope and b) 9 g with 51% enrichment in ^{204}Pb isotope containing 0.94 g of ^{207}Pb isotope were used as targets.

As a result of conducting several series of measurements, ample experimental data are accumulated for a possible isotope identification of the sought negative p-resonance and estimation of its parameters.

1.5 Investigation of the nuclear fission

1.5.1 Search for exotic fission modes at the IBR-2 reactor using the «Mini-Fobos» facility

Events pointing to a possibility of existence of the ternary collinear cluster decay (TCCD) have been detected for the first time in a series of experiments to study spontaneous fission of ^{252}Cf nuclei carried out in the Flerov Laboratory of Nuclear Reactions. Experimental manifestations of such decay channel have been considered in the framework of assumption of the «missing» mass, i.e. of detection in coincidence of only two heavy collinear fragments having a smaller total mass than a mass of the initially fissionable nucleus. This «missing» or «lost» mass may correspond to one or several fragments, which escape at small angles to the fission axis and are not detected. It is presumed, that shell effects play the key role in such processes. The main results have been obtained on the FOBOS and Mini-FOBOS facilities. One of the main advantages of detector modules of the FOBOS spectrometer is a possibility of independent measurement of the velocity vector, mass and charge of each particle without attracting suppositions on kinematic peculiarities of the reaction mechanism.

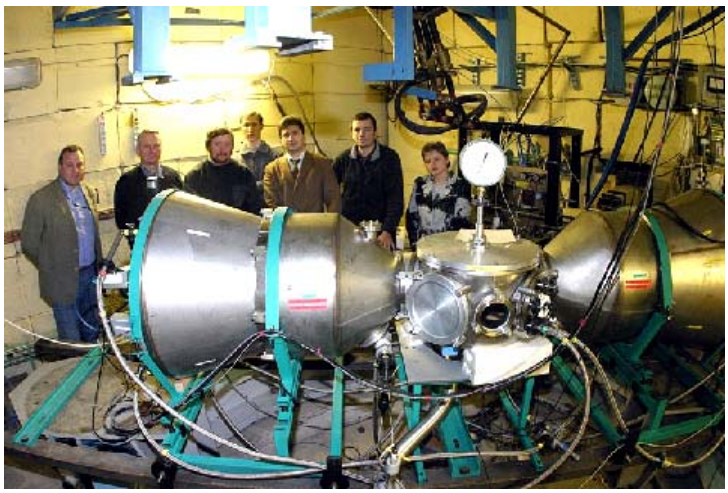

Fig.12. *The Mini-Fobos facility on channel 6b of the IBR-2 reactor.*

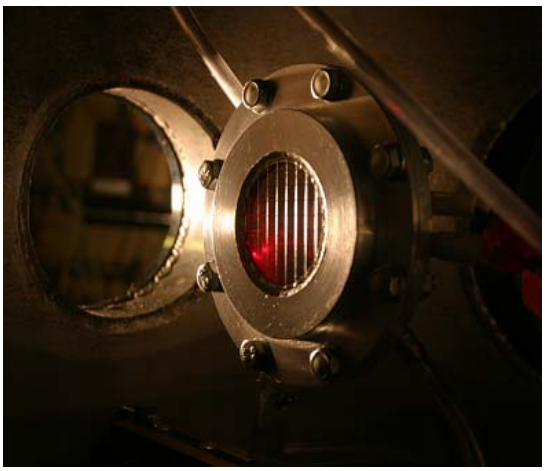

Fig.13. *Start avalanche counter with an internal target.*

The investigations continued in the Frank Laboratory of Neutron Physics in accordance with decisions of the working conference as of December, 21, 2004. In 2006 the Mini-FOBOS spectrometer was installed on neutron guide channel 6b of the IBR-2 reactor (see **Fig.12**), and a

series of measurements was carried out. For the operation under new conditions a support was manufactured, a start avalanche counter with an internal target was developed (**Fig. 13**). Stability of the data collection was provided by conditioning of both experimental canyon 6b and of the room with electronics. Within the framework of the technique described above the $^{236}U^{*}$ decay obtained in the reaction $^{235}U+ n_{th}$ was studied. Around $6x10^{6}$ events was collected in all and the spectrometer effectiveness was about 1.5%. The preliminary analysis points to the structures similar to those detected at the investigation of decay of ^{252}Cf nuclei.

1.5.2 Measurement of total energy spectra of light charged particles in spontaneous fission of ^{252}Cf

The experiment to measure total energy spectra of light charged particles in the spontaneous fission of ^{252}Cf was carried out in the JYFL laboratory (Jyväskylä, Finland). The experimental facility is shown in **Fig. 14**. Spontaneous source of the ^{252}Cf fission manufactured in the Radium Institute (Saint-Petersburg) had the activity on the order of 500 fission per second. The substrate, on which a thin layer of californium was applied, was a foil of aluminum oxide (Al_2O_3) 22.2 $\pm$ 3.4 μg/cm^2 of thickness with deposition of ~10 μg/cm^2 of gold layer. The energy loss of fragments at the perpendicular passing through the substrate was ≤ 1.5 MeV. Energy losses of the fragments escaping from the fore-part of the source were no more than 60 keV. The assessed thickness of the californium layer (Cf_2O_3) was 3.5 μg/cm^2.

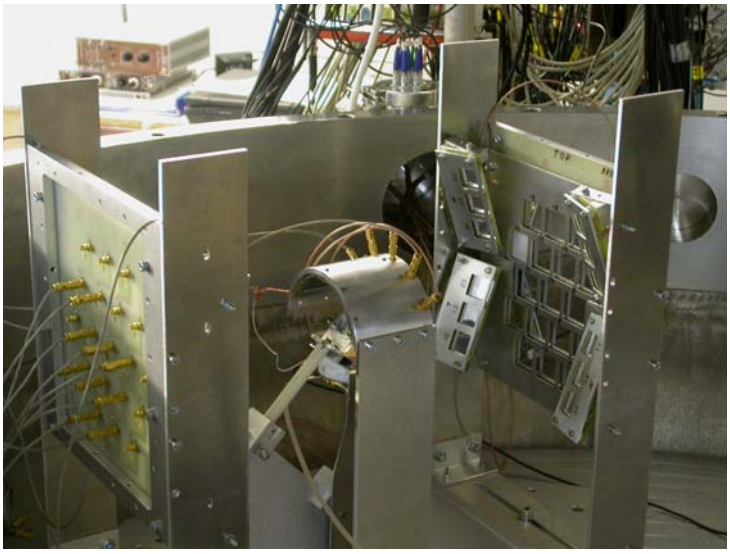

Fig. 14. *Experimental facility to measure energy spectra of light charged particles.*

In the experiment the energy and time of flight of the light charged particle were recorded, at the same time there were no absorbers on its way to the detector. This allowed one to measure energy spectra with a high accuracy down to the smallest energies of ~0.5 MeV, which is the lowest threshold ever reached in the experiments of such kind. Light charged particles were recorded by mosaics of silicon detectors located at the distance of ≈20 cm from the source. As a start signal, fission fragments were used recorded by the fast MCP detector located at right angles to the mosaic of silicon detectors at the distance of 2.5 mm from the source. In order to discriminate fission fragments from the 6-MeV alpha particles from the ^{252}Cf natural radioactivity, the coincidence circuit of the start signals with the signals from 10 silicon detectors located from the source side

opposite to MCP was applied. Geometry of the experiment covered the angular range from 70° to 110° of the light particle escape with regard to the fission fragments, i.e. for the most part, equatorial particles were recorded.

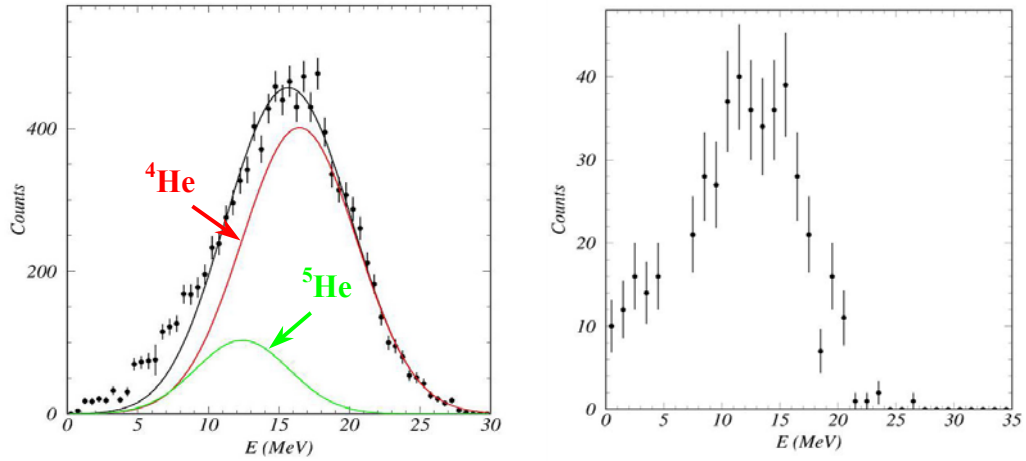

Fig. 15. *Experimental energy spectra for ^{4}He (to the left) and ^{6}He (to the right). Contributions from true α-particles are shown for ^{4}He and those from α-particles formed as a result of the ^{5}He decay.*

Results of the measurements for α-particles and ^{6}He are presented in **Fig. 15**. On the left figure two curves are depicted, which are the result of fitting of the experimental data for energies higher than 9 MeV with taking into account the 17% contribution from α-particles known from the previous measurements, which were formed as a result of decay of unstable ^{5}He isotopes in the ternary fission. It is seen that the deflection of shape of the experimental curve from the Gaussian one can not be explained by this component. Apparently, the presence of this deflection is related to a complex statistical distribution of initial configurations of the fission system at the moment of break of the nucleus. Such supposition is qualitatively confirmed by trajectory calculations. It is also should be pointed out that the measured energy spectrum of α-particles coincides with the data obtained by Tischenko in 2002, however, it significantly differs from the data obtained by Loveland in 1974. The total energy spectrum for ^{6}He was measured for the first time in this work.

1.5.3 Preparation of measurements of emission of prompt neutrons in the neutron-induced fission on the GELINA source (IRMM, Geel, Belgium)

At present, it is relevant to investigate the reaction ^{239}Pu(n_{res},f) ^{235}U(n_{res},f) aimed at the measurement of correlations of emission of prompt neutrons with mass distributions of fission fragments in several strongest resonances. Taking into account the high alpha-radioactivity of plutonium, the acceptable quality of spectrometry of fission fragments could be reached using the up-to-date technique of digital signal processing (DSP). To diminish the effect of pulse pile-up due to the natural radioactivity of targets, it was also important to develop the technique of spectrometry of fission fragments using current preamplifiers, which allowed one to improve the quality of spectroscopy of fission fragments in the reaction ^{239}Pu(n_{res},f). In order to solve the stated problems, in collaboration with the IRMM specialists, the unique DSP technique with current preamplifiers for the spectrometry of fission fragments was developed for the first time. A mathematical apparatus of digital analysis of pulsed signals of nuclear particle detector was created, also, software for sampling and data acquisition from ionization chambers and neutron detectors were developed. The above-mentioned technique and software were approved using ^{252}Cf(sf) with the activity of 30 kilobecquerel. The results were obtained, which are in good line with the literary data.

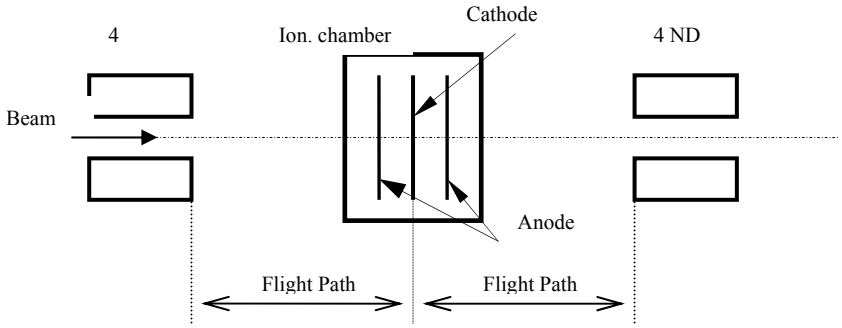

Fig. 16. *Diagram of the experimental facility.*

Also, in collaboration with the IRMM specialists, the technique to measure the fission neutron multiplicity was developed with the use of neutron detectors based on the liquid scintillator NE213 granted by the DEMON collaboration. The DSP program library was created implementing functions of the standard modules of nuclear electronics, such as spectrometric amplifiers, discriminators with tracking threshold, analog-to-digital and analog-to-time conversion, etc. The software for digital oscillographs by the Tektronix firm was developed, which allow one to use them as the equipment to digitalize pulses of the nuclear particle detectors.

The facility was located on the flight path 8 m long of the GELINA pulsed neutron source (**Fig. 16**). Altogether 8 neutron detectors (ND) with the capacity of 4 litre each were used. The distance between the target under investigation and ND was 0.75 м. For calibration measurements the ^{252}Cf(sf) target with the activity of 30 kilobecquerel was used.

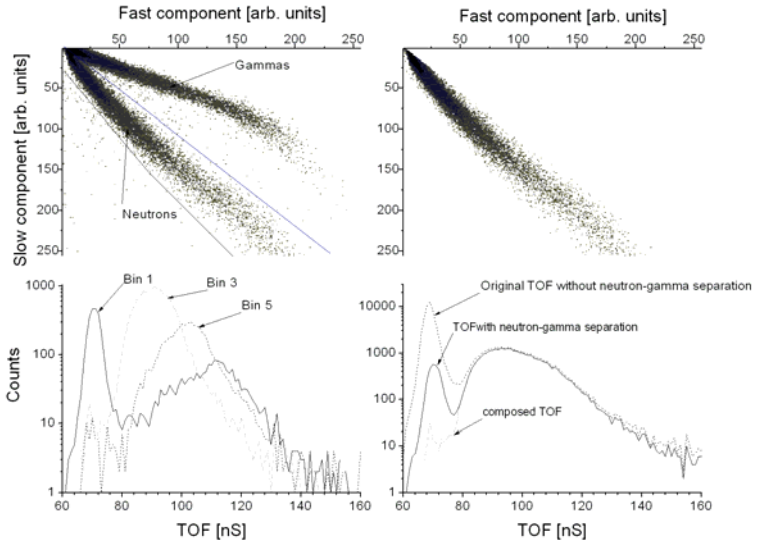

Fig. 17. *Suppression of the background of gamma quanta at the recording of prompt neutrons of fission with the analysis of pulse shape and time of flight for ^{252}Cf(sf).*

To suppress the background of gamma quanta, the analysis of pulse shape and the measurement of time of flight of prompt neutrons of fission were used (**Fig. 17).** Calibration measurements were conducted with the neutron beam from GELINA both switched on and off.

1.6 Gamma-spectroscopy of neutron-nuclear interactions

Analysis and interpretation of experimental data for level density and radiative strength functions of dipole gamma transitions in the region of neutron binding energy in nuclei from the mass range 39<A<201 were continued. Purpose of the analysis: a) estimation of the value and shape of the energy dependence of correlation functions of Cooper pairs of nucleons in the heated nucleus; б) extraction of potentially accessible information on the dynamics of interaction of the ordinary component and the superfluid one of the nuclear matter at the change of energy of the nucleus up to neutron resonances.

In particular, the approximation of level densities by partial level densities was carried out with various number of quasi-particles with the parameters taking into account the shell inhomogeneity of the single-particle spectrum.

The factors, which should be taken into account at the precision approximation of sums of radiative strength functions in various nuclei, were estimated.

Comparison of the calculated and experimental total gamma spectra in cobalt and iron-57 was carried out. It demonstrated that the level density and radiative strength functions determined in accordance with the technique developed in Dubna provide for the best data reproduction of such type and also for light nuclei.

Preparation to the experimental measurement of the two-step cascade of the thermal neutron capture is carried out with Dubna assistance in Hanoi.

1.7 Investigation of (n,p) and (n,α) reactions

At the EG-5 facility in FLNP the experiments to measure angular correlations in the reaction $^{14}N(n,p)^{14}C$ in the region of neutron energies up to 1 MeV are carried out. The reaction $^{7}Li(p,n)^{7}Be$ is used as a neutron source. The aim of the studies is to determine partial neutron and proton resonance widths for spins of the channels j = 1/2 and 3/2 and using these data to estimate the weak matrix element from the results of polarization experiments obtained earlier. By now, (preliminary) experimental values of the forward-backward correlation are obtained at E_n = 450, 476, 521, 557, 627, 640, 693 keV and are equal to 0.046 ± 0.033, -0.029 ± 0.027, -0.147 ± 0.056, -0.042 ± 0.016, 0.454 ± 0.072, 0.065 ± 0.028, 0.013 ± 0.024, respectively (see **Fig. 18**). Rather high values of α_{fb} at E_n = 521 and 627 keV may be caused by instability/drift of the neutron energy in the course of long exposures at the measurement in the forward-backward direction. Along with these measurements, works to improve the technique aimed at the refinement of accuracy of the obtained results are carried out. They involve both equipping of experiment by new detectors and development of the data processing procedure. Theoretical calculations and computer simulation continue.

Within the framework of the program to study mechanisms of nuclear reactions and to obtain data for nuclear power engineering on the EG-4.5 accelerator of the Institute of Heavy Ion Physics, Peking University, China, investigations of the reaction $^{64}Zn(n,\alpha)^{61}Ni$ for neutrons with the energies 2.6 and 4.0 MeV have been carried out. The reactions $T(p,n)^{3}He$ on the solid Ti-T target and $D(d,n)^{3}He$ on the gas deuterium target were used as a neutron source. Energy spectra and angular distributions of α-particles have been obtained, the data are being processed. Data processing of the previous measurements at E_n = 5 and 6 MeV has been completed, values of the total and differential cross section of the reaction $^{64}Zn(n,\alpha)^{61}Ni$ for these energies have been obtained.

Data processing to measure cross sections of the reaction $^{6}Li(n,\alpha)T$ at the neutron energy of 1.05, 1.54 and 2.25 MeV has been completed. The works are performed in common with Peking University (China) and the University of Lodz (Poland).

The equipment has been prepared to carry out experiments using the time-of-flight method at the pulsed neutron source of the Moscow Meson Factory, INR RAS, Troitsk, and then at IREN in Dubna.

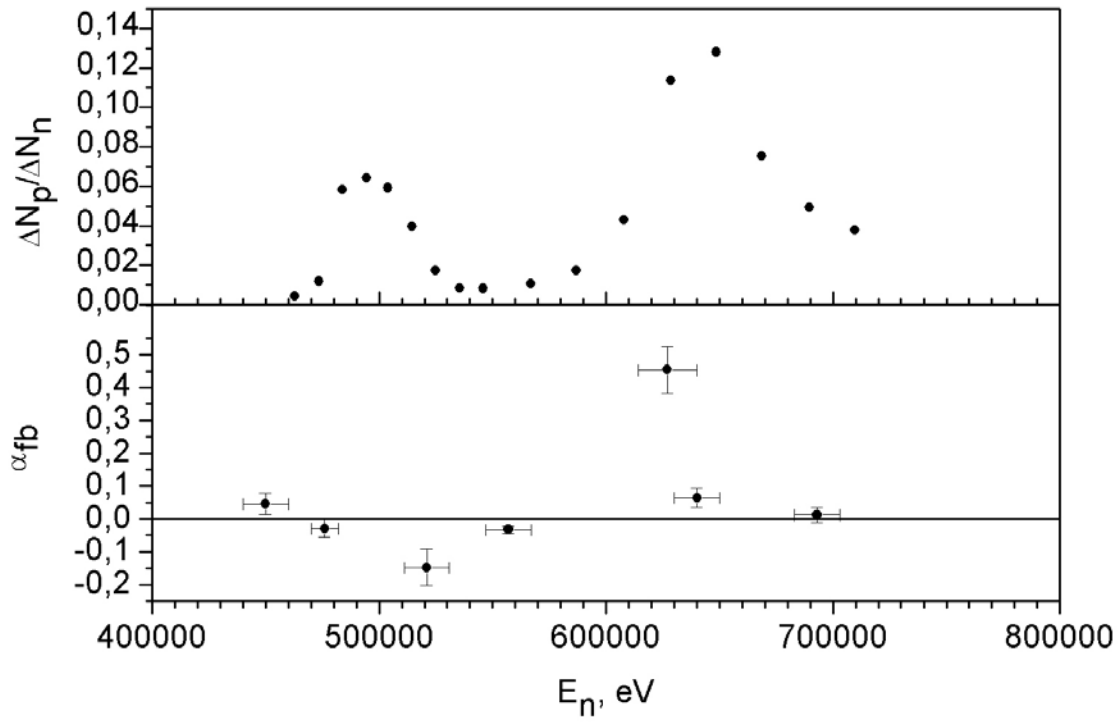

Fig. 18. *Upper diagram – relative proton escape from the reaction $^{14}N(n,p)^{14}C$; lower diagram – preliminary values of the forward-backward correlation.*

2. Theoretical investigations

The effect of neutron striction has been detected in neutron stars, and its influence on the parameters of neutron stars has been calculated. In particular, neutron-nuclear elastic scattering is characterized by a coherent scattering length, which leads to the optical interaction potential between the neutron and the medium: the positive length – to the repulsive potential, the negative length – to the attractive one. Neutron-neutron scattering is also characterized by a coherent scattering length, and this length is negative. Therefore, the optical potential inside the neutron star is attractive for each neutron, and it compresses (striction) the star further to the gravitation. This contraction does not lead to the star collapse because the scattering length decreases with an increase of the density, however, the calculation shows that the influence of neutron striction on the star parameters may be more than the relativity. Furthermore, dependence of the scattering length on the density leads to such phenomena as pulsation and explosions. The latter is possible at the resonance dependence of the scattering length on the neutron energy. The work opens new prospects in studying stars and elementary particles.

Complete solution of the task on neutron reflection from the medium with helical magnetization has been found. It has been shown that the resonance reflection with spin flip takes place. In **Fig. 19** the dependence of the reflection coefficient without spin flip (solid curve) and with spin flip (broken curve) on the wave vector k is shown at the initial neutron polarization in the direction opposite to the z axis, which is parallel to the inner normal to the mirror. Simultaneously, the matter magnetization is supposed to be rotating anticlockwise at moving away from the surface.

Theoretical investigation of the process of nucleon charge exchange $n + p \rightarrow p + n$ was continued. In particular, using the interchange operator of spin projections of the neutron and the proton, spin structure of the interchange amplitude $n + p \rightarrow p + n$ at zero angle and spin structure of the

«backward» elastic scattering amplitude of the neutron on the proton were considered in detail. Relations between the corresponding coefficients in these amplitudes were obtained. It was determined that for the charge exchange processes $n + p \rightarrow p + n$ at zero angle and for the «backward» elastic *np*- scattering the separation of a cross section into the spin-dependent and independent parts *is different in principle*. It is in the case of charge exchange at zero angle that the spin-dependent part of a cross section is proportional to a cross section of the charge-exchange breakup of deuteron $n + d \rightarrow p + (nn)$ in the «forward» direction. The spin-dependent part makes the main contribution to the charge exchange cross section at the neutron kinetic energies of > 200 MeV .

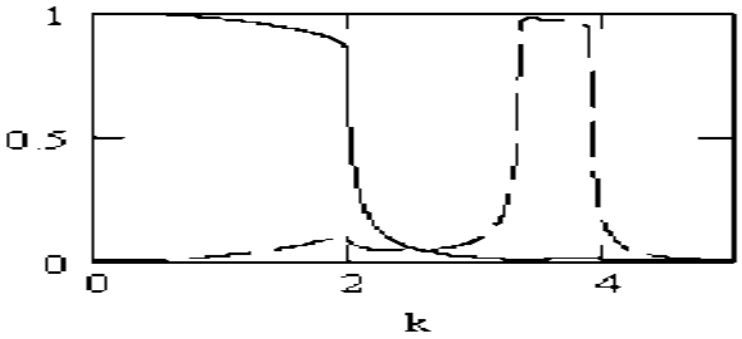

Fig.19. *Dependence of the reflection coefficient on the wave vector.*

Calculation of the spectrum of relative pulses of two finite neutrons at the charge-exchange breakup of deuteron $n + d \rightarrow p + (nn)$ was performed taking into account the strong *nn*-interaction in the finite state using analytical solutions of the Schroedinger equation for the *S*-wave function of deuteron and the function of relative motion of two neutrons in the potentials of the square well type. In particular, it was shown that at small relative pulses the contribution of *nn*-interaction in the finite state prevails greatly. With an increase of relative pulses, an abrupt decline of the distribution function was observed.

In 2006 investigation of the neutron $\beta-$decay continued. In order to extract the characteristics of electroweak interactions from half-lepton decays of hadrons, the accurate calculation of radiative correction to these processes with the successive taking into account of strong interactions and hadron structure is necessary. To do this, in 2006 the Ward-Takahashi identities have been obtained and investigated connecting the top parts of weak hadron decays and the corresponding properly energy parts and amplitudes of hadron interactions with the electroweak (calibration) fields. Results of the work allow one to conclude definitely to which extent the accounting of strong interactions in electroweak processes may be carried out precisely without referring to approximate evaluations.

3. Applied and methodical research

3.1 Investigation of element composition and structure of near-surface layers of solids at the EG-5 accelerator

In 2006 in cooperation with the Institute of Physics of the Maria Curie-Sklodovska University the experiments to investigate the properties of GaAs implanted by In ions with the energy 250 keV and the dose $3x10^{16}$ cm^{-2} were conducted. In order to determine diffusion constants of indium in gallium arsenide a part of the samples after implantation was subjected to the isobaric annealing in the argon atmosphere at the temperatures of 600^0 and 800^0C for 0.5 and 2 hours. After that, the surface of samples was coated by a protective layer of Si3N4. Studies of depth profiles of elements were carried out at the EG-5 accelerator using the method RBS. As a result, earlier unknown diffusion constants of In in GaAs were determined in the temperature region 600-800^0C. Also,

optical parameters (n, k) of the GaAs implanted surfaces were investigated using the ellipsometric technique.

Depth profiles of hydrogen implanted in silicon at the energy of 12 keV were investigated using the ERD technique on the basis of the electrostatic generator EG-5. At the implantation dose of hydrogen $2x10^{16}$ cm^{-2} it proved to be possible to determine the limiting atomic concentration, which can be measured using the ERD technique at the helium ion energy of 2.332 MeV. It was 0.5 at.%. At the implantation dose of hydrogen 10^{17} cm^{-2} the atomic concentration of hydrogen in silicon was 3% and was determined rather accurately. At the processing of the corresponding spectrum of proton recoil, the evaluation of limiting depth was carried out, which was obtained using the ERD technique. At the helium ion energy of 2.332 MeV it was 2 μm.

In 2006 instrument developments also continued. With the purpose of developing the implantation technology, the mechanism of generation of ions in plasma sources, their extraction and ion beam shaping was investigated. In particular, for the plasma ion source the simplified analysis of processes occurring in plasma was performed, on the basis of which analytic formulae were obtained for ion current and effectiveness of the ion source, and also the factors determining the two parameters were indicated.

In cooperation with the Electrotechnical Institute SAS (Slovak Republic) the experiments to investigate temperature stability of lamellar structures of the $Ru/HfO_2/Si$, $Ru/HfSiO_x/Si$ и Ru/HfSiON/Si types manufactured using the CMOS (complementary metal-oxide-semiconductor) technology continued. The RBS technique on the basis of the electrostatic generator EG-5 made it possible to detect a significant difference between these structures. Whereas insulating layers of the HfO_2 composition showed weak diffusion on both boundaries already after the annealing at 800^0, the structures with $HfSiO_x$ layers demonstrated complete stability at the this temperature. And the initial diffusion of these layers was observed at the annealing temperature of 900^0C. However, at the annealing up to 1000^0C significant diffusion both towards the substrate and towards the external layer occurred in the layers of both types. This investigation showed that the presence of Si atoms in dielectric layers on the basis of Hf increased thermal stability of these layers, which was significant for the CMOS technology.

Development of the technique of “labeled” neutrons on the second channel of EG-5 and the first results of its use to detect hidden substances were presented in the report at the XVI International conference on electrostatic accelerators and beam technologies in Obninsk.

Investigation of the content of heavy elements in teeth of people of various age and professions living in different conditions was conducted. Element analysis was carried out using the nuclear physical analytic methods PIXE and RBS.

3.2 Analytical studies using the neutron activation analysis (NAA) at the IBR-2 reactor

Biomonitoring

Within the framework of international program «Atmospheric depositions of heavy metals (HM) in Europe – assessments based on the analysis of moss-biomonitors» a large series of studies has completed, which is related to the simultaneous collection of samples in 2005–2006 in a number of regions in Central Russia, Southern Urals, Belarus, Bulgaria, Slovakia, Poland, Romania, Serbia, Macedonia, Croatia and Greece to perform multielement activation analysis at the IBR-2 reactor. Results of the analysis on 13 elements: Al, As, Cd, Cr, Cu, Fe, Hg, Ni, Pb, Sb, Ti, V and Zn will be submitted to the European Atlas of atmospheric depositions of HM. Similar studies have been carried out in Mongolia and Vietnam. The results of the analysis of moss-biomonitors from biosphere reserves (Prioksko-Terrasny and Voronezh biosphere reserves) obtained in collaboration with the Institute of Global Climate and Ecology (Moscow) are of particular interest. Along with the moss samples from the biosphere reserves, aerosol filters were analyzed, which will allow one to determine correlation between the elemental content in the air and atmospheric depositions in moss-biomonitors.

Air pollution studies were carried out using the active biomonitoring – exposure of moss-bags – under the conditions of urban environment in Poznan (Poland); Baia Mare (Romania), Sofia (Bulgaria), Athens (Greece) and in Dubna, in the area of domestic waste disposal site.

Ecological assessment

The NAA of bottom sediment columns collected at the Black Sea shelf of the Romanian coast was completed. In common with IFIN (Bucharest) and the University of Bucharest the assessment of retrospective pollution of this region will be made.

The multielement NAA of aerosol filter collection of different years obtained from Bratislava will allow one to characterize the dynamics of atmospheric pollution of the Slovak capital by heavy metals for the last 15 years.

The work to study weekly cycles of the atmospheric condition (elemental content of aerosol filters) of the Great Cairo valley (Egypt) continued. New results confirmed the data obtained earlier on the existence of the so-called "effect of days off", which in Arabian countries fall at Thursday-Friday.

In common with the University in Opole (Poland) the complex investigation to assess the environmental condition at the "anomalous territory" in the west of Poland characterized by an increased radioactive background owing to the Chernobyl accident and man-caused influence of industry was carried out. The natural migration of a series of elements in soil profiles was traced, and also NAA of plants-biomonitors and mushrooms as accumulators of toxic elements was performed.

In collaboration with the «Dubna» University the distribution of a series of heavy metals near road interchanges in Dubna and Moscow (Schiolkovskoe and Minskoe highways) was studied.

The work to analyze 200 soil samples from the region of lead-zinc industrial complex in Macedonia was completed and maps of distribution of the main elements-toxicants were plotted.

Foodstuffs and human health

In 2006 a large cycle of works to analyze foodstuffs with the purpose of assessing the intake of microelements by a human organism with foodstuffs (Central Russia) and the influence of detrimental industries on the quality of foodstuffs (Romania) was completed.

Within the framework of the IAEA Coordination Program «Exposure to toxic and potentially toxic elements in women of childbearing age in developing countries» in collaboration with the Russian State Medical University (Moscow) and the Analytical Centre of the Geological Institute of RAS the multielement analysis of blood samples of 60 specially selected patients was conducted. The analysis was carried out using NAA on the IBR-2 reactor in Dubna and MEPhI; lead, cadmium and mercury were determined by the atomic adsorption spectrometry in GIN RAS.

Biotechnologies

In collaboration with the Institute of Physics of Georgian AS new results in determining chromium in bacterial samples of *Arthrobacter oxidans* were obtained. These bacteria extracted from natural basalts may be used to change the chromium valency (conversion of the toxic Cr-VI into the nontoxic form Cr-III), which is of great scientific and practical interest. These results published in the prestigious journal Analytical Chemistry (USA) were highly evaluated by the IAEA specialists.

Archeology

Within the framework of cooperation with the University in Skopje and the Museum of History and Archeology of Macedonia the analysis of ceramics of ritual vessels (amphorae) and scrapes from their inner surfaces was carried out. Results of the analysis will make it possible to accept or reject the hypothesis on the contents of these amphorae.

New materials

NAA of rubidium-containing compounds used in experiments of the Condensed Matter Department on the X-ray and neutron diffraction was carried out.

Educational process

In 2006 on the basis of the REGATA facility in the radioanalytical laboratory at IBR-2 Practical training for students of senior courses of the «Dubna» University and International Schools organized by the JINR University Centre was held. For the reporting period on the basis of the NAA sector 2 Bachelor's theses and 5 Master's theses were written. In 2006 2 Ph.D. theses based on the materials obtained in the NAA sector were defended.

Organization of meetings

In 2006 preparation to the International meeting of the Commission of the United Nations Organization "The 20th Task Force Meeting of the UNECE ICP Vegetation and Long-Range Atmospheric Transport of Pollutants" was underway, which will take place in Dubna in March, 2007.

1. НАУЧНЫЕ ИССЛЕДОВАНИЯ

1.1. ФИЗИКА КОНДЕНСИРОВАННЫХ СРЕД

Вслед за сложными оксидами марганца (манганитами), основной особенностью которых является эффект колоссального магнитного сопротивления, растущий интерес проявляется к сложным оксидам кобальта (кобальтитам) типа $Ln_{1-x}M_xCoO_3$, где Ln – лантанид, M – щелочноземельный элемент. С научной точки зрения кобальтиты интересны сильными корреляциями между решеточными, зарядовыми, спиновыми и орбитальными степенями свободы. Оксиды кобальта важны для практики в связи с их использованием в качестве электродов в источниках тока. Особенности фазовых переходов в кобальтитах связаны с нарушением баланса между внутриатомной энергией Хунда и энергией кристаллического поля, связанной с конфигурацией октаэдров CoO_6. В результате, ион Co^{3+} может находиться в трех разных спиновых состояниях: низкоспиновом (LS, $t_{2g}^6e_g^0$), промежуточном (IS, $t_{2g}^5e_g^1$) высокоспиновом (HS, $t_{2g}^4e_g^2$).

На реакторе ИБР-2 ведутся исследования атомной и магнитной структуры кобальтитов, в том числе при высоких внешних давлениях. На дифрактометре ФДВР изучался состав $Pr_{0.5}Sr_{0.5}CoO_3$, в котором ранее наблюдались несколько магнито-структурных фазовых переходов. Дифракционные спектры были измерены в широком диапазоне температур (10 – 780 K), в основном в режиме нагрева образца. В этом диапазоне обнаружены два фазовых перехода ($T_1 \approx 120$ K и $T_2 \approx 300$ K), в ходе которых изменяются магнитная и кристаллическая структуры образца. При нагревании симметрия последовательно повышается от триклинной до ромбической и затем до ромбоэдрической. Переходы сильно размыты по температуре а между 120 K и 300 K фазы сосуществуют (**Рис. 1**). Магнитные измерения подтверждают, что структурный переход при 300 K совпадает с ферромагнитной точкой Кюри. Природа магнитного перехода при 120 K пока остается неизвестной.

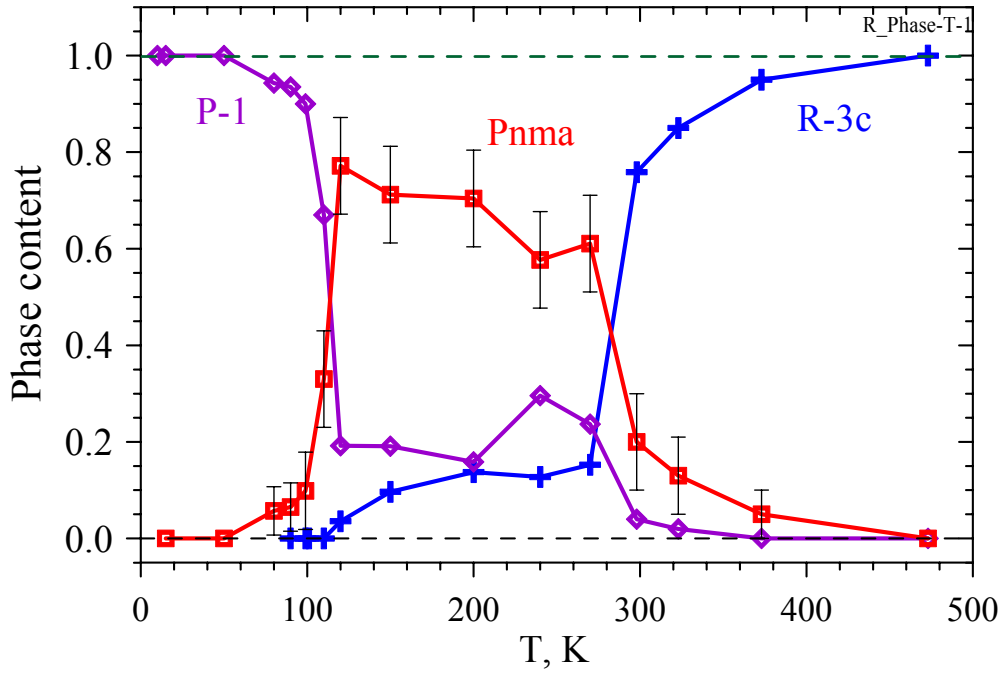

Рис. 1. *Содержание структурных фаз в образце в зависимости от температуры.*

На дифрактометре ДН-12 проведено исследование кристаллической и магнитной структуры гексагональных фрустрированных манганитов $RMnO_3$ (R=Y, Lu) при высоких давлениях до 6 ГПа. Полученные экспериментальные данные, вместе с результатами

предыдущих исследований других гексагональных манганитов, позволили установить взаимосвязь между симметрией треугольного АФМ состояния с параметром искажения треугольной решетки *s*, образованной атомами Mn и O. Полученная обобщенная магнитная фазовая диаграмма позволяет объяснить наблюдаемые изменения симметрии магнитного состояния при химическом замещении (изменении ионного радиуса R элемента) и приложении высокого давления за счет вариации *s* (**Рис. 2**).

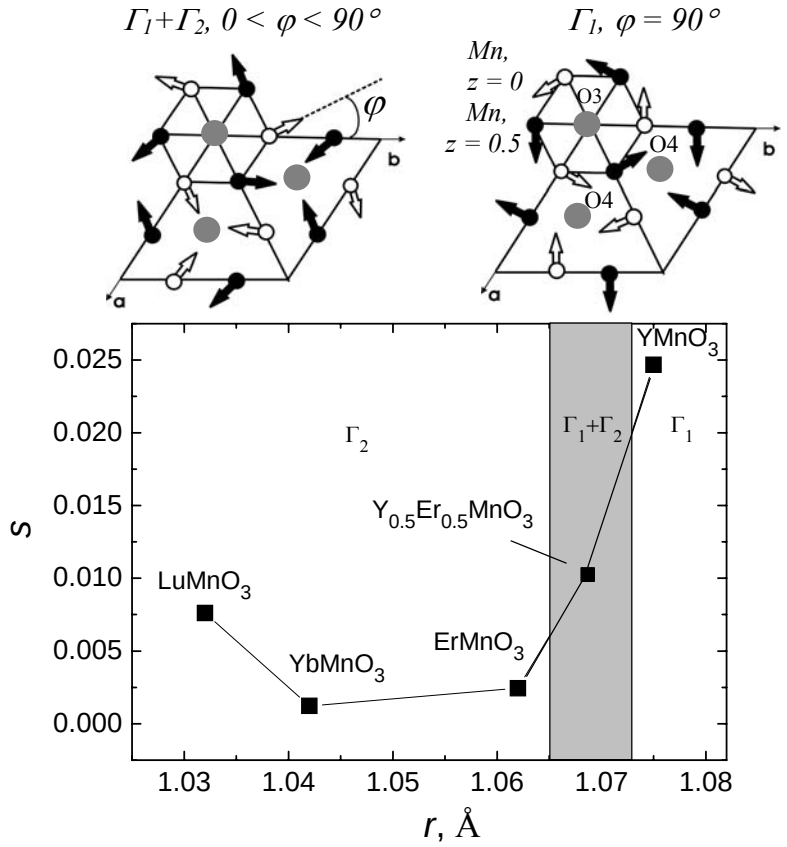

Рис. 2. *Фазовая диаграмма гексагональных манганитов $RMnO_3$ и схематическое изображение АФМ структур симметрии Γ_1 и $\Gamma_1+\Gamma_2$.*

В рамках структурных исследований факторов, влияющих на стабилизацию магнитных жидкостей, начато планомерное изучение эффекта избытка поверхностно-активного вещества (ПАВ) в магнитных жидкостях на их стабильность. В качестве первой системы выбрана классическая магнитная жидкость на основе магнетита, диспергировнного в бензол и покрытого одинарным слоем олеиновой кислоты. Известно, что эта система наиболее стабильна, когда весь ПАВ адсорбирован на поверхности магнетита, т.е. в отсутствие свободного ПАВ в растворе. В этой связи с помощью малоуглового рассеяния нейтронов были исследованы растворы олеиновой кислоты ($C_{17}H_{33}COOH$) в дейтерированном бензоле (C_6D_6). Целью работы было определение характера взаимодействия между молекулами кислоты, а также прояснение возможности их кластеризации. Кривые рассеяния (**Рис. 3**) в приближении Гинье указывают в целом на отталкивание между молекулами ПАВ. Однако, определенное из этих данных значение второго вириального коэффициента B = -0.02 значительно больше, чем для системы твердых шаров (B = -8). Это говорит о том, что компонента притяжения существенна в парном потенциале взаимодействия между молекулами. Определенный из данных МУРН объем молекулы олеиновой кислоты, 657 $Å^3$, значительно отличается от ее Ван-дер-Ваальсовского объема, 523 $Å^3$, и, в то же время, практически совпадает с удельным объемом чистой олеиновой кислоты в ее жидком состоянии. Для прояснения данного

наблюдения начаты работы по моделированию изучаемой системы методами молекулярной динамики.

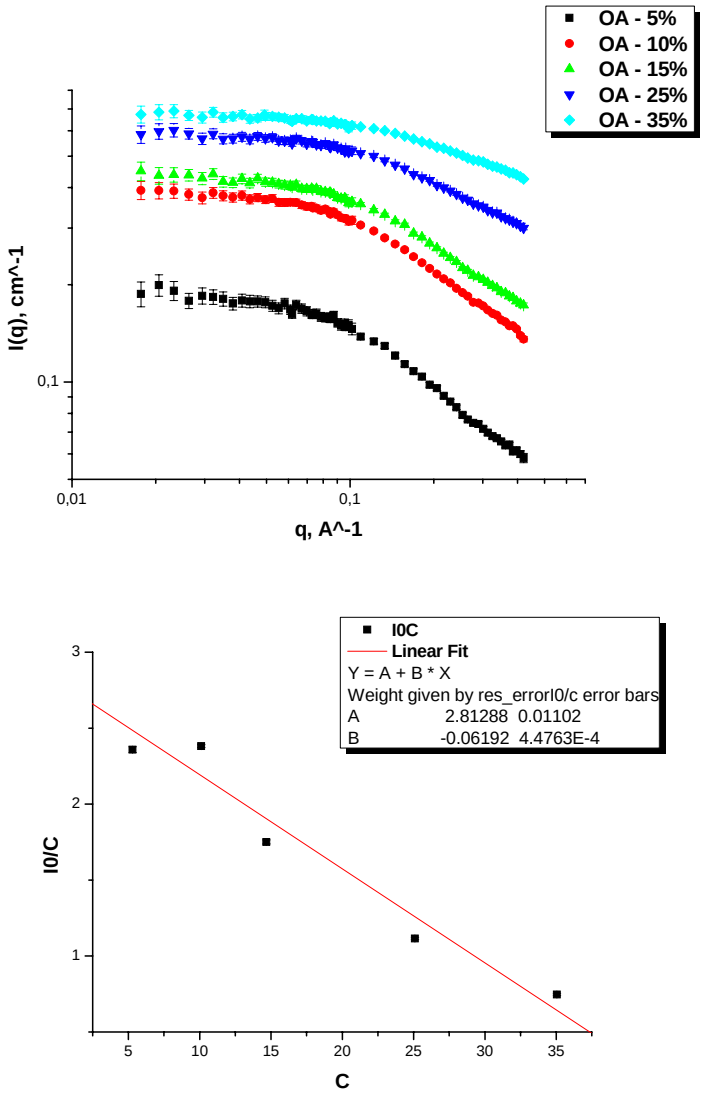

Рис. 3. *Кривые рассеяния на растворе олеиновой кислоты (ОА) в дейтерированном бензоле с различной концентрацией и зависимость интенсивности рассеяния в нулевой угол из приближения Гинье в зависимости от концентрации. Для последнего графика наблюдается отрицательный наклон, что свидетельствует об отталкивании молекул олеиновой кислоты в растворе.*

На спектрометре РЕМУР проведено исследование магнитного упорядочения и доменной структуры в слоях 20×[Fe(1.993nm)/Cr(1.2nm]/MgO. В этой структуре намагниченности соседних слоёв железа направлены антипараллельно. В плоскости слоёв существуют домены, которые также упорядочены антиферромагнитно. Тип магнитного межслоевого упорядочения зависит от толщины слоя хрома. Было предложено изменять толщину слоя хрома его сжатием и растяжением с помощью звуковой волны мегагерцового диапазона. В рефлектометрических экспериментах с поляризованными нейтронами наблюдены эффекты изменения диффузного рассеяния нейтронов от доменной структуры и появления неупругого рассеяния нейтронов благодаря возникновению колебаний магнитных моментов слоёв. На **рис. 4** показана зависимость поляризационной способности от переданной компоненты волнового вектора Q_X (вдоль пучка нейтронов) при различных значениях частоты звука f_0= 50 МГц и $3f_0$= 150 МГц.

Видно, что с увеличением частоты Q_X распределение уширяется, что говорит об уменьшении размера домена. Таким образом, показано, что можно управлять магнитной структурой антиферромагнитно-упорядоченной структуры 20×[Fe(1.993nm)/ Cr(1.2nm]/MgO изменяя уровень или частоту звуковой волны. Это открывает новую возможность управления магнитной структурой, которая характеризуется большим быстродействием.

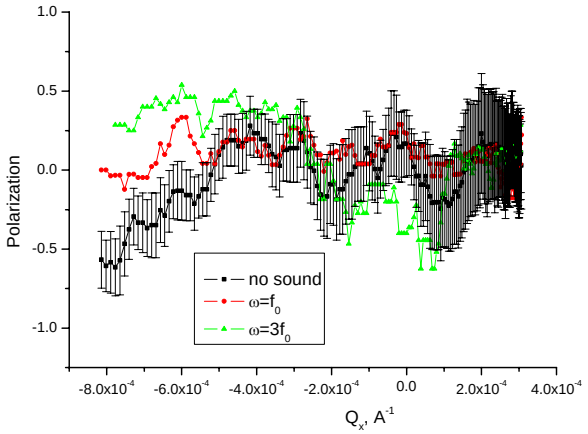

Рис. 4. *Зависимость поляризационной способности от переданной компоненты волнового вектора Q_X (вдоль пучка нейтронов) при различных значениях частоты звука при отражении нейтронов от пленок 20×[Fe(1.993nm)/Cr(1.2nm]/MgO.*

На дифрактометре ДН-2 изучался распад гидратного клатрата с дейтерием состава $32D_2$:$136D_2O$ при нагреве до 250 К с фиксированием отдельных этапов его разложения. Кратковременный (15 мин.) нагрев образца с последующей закалкой до температуры жидкого азота (95 К) позволил осуществить ступенчатое удаление водорода из пор клатрата при одинаковых условиях длительной съемки для изучения взаимодействия матрицы с молекулами внедренного дейтерия. Оказалось, что параметр решетки в этих условиях не зависит от концентрации дейтерия, т.е. никаких признаков усиления его взаимодействия с решеткой не обнаружено. Для решения вопроса о характере экстракции дейтерия анализировались интенсивности отдельных рефлексов. Так, графически (**Рис. 5**), наложением на расчетный растр (hkl) столбца экспериментальных интенсивностей были установлены составы гидридов при отжиге. Расчет исходной картины методом Ритвельда дал наилучшее согласие при концентрации 32 молекулы D_2 на ячейку, где 16 молекул находятся в большой поре (8b, по 2 мол.) и 16 молекул – в малой поре(16c, по 1 мол.). После кратковременного (15 мин.) нагрева до температуры 145 К изменения в структуре клатрата минимальны. Постепенное удаление водорода возможно до температуры 195 К, когда начинается рост примесной фазы льда, а состав достигает минимального значения $x=16_{8b}+16*0.7_{16c}=27.2 \pm 0.5D_2$. После отогрева до 220 К наблюдается разложение клатрата и появление интенсивных линий кристаллических фаз льда (Ih, Ic) с заметной долей фазы аморфного льда низкой плотности.

Проведены комплексные исследования физических свойств синтетического монокристаллического кварца и кварцевого порошка в температурной области α-β перехода методами нейтронной дифракции и механической спектроскопии. Определена кристаллическая структура кварцевых порошков с разной средней величиной зерен в температурном интервале до 620°С и температуры α-β фазового перехода. Получены температурные зависимости величины внутреннего трения и резонансной частоты у образцов кварца в окрестности температуры фазового перехода при возбуждении колебаний в параллельной и перпендикулярной оси Z кварца плоскостях. Зарегистрированы различные значения температур точек максимума внутреннего трения, лежащие в интервале от 560 – 620°С. Высказаны предположения о возможных причинах

смещения температуры перехода. Обнаружен максимум внутреннего трения вблизи значения 350°C, не связанный со структурными превращениями в кварце. Цель дальнейших работ – определение причин смещения точки фазового α-β перехода в кварце и природы пика внутреннего трения при 350°C.

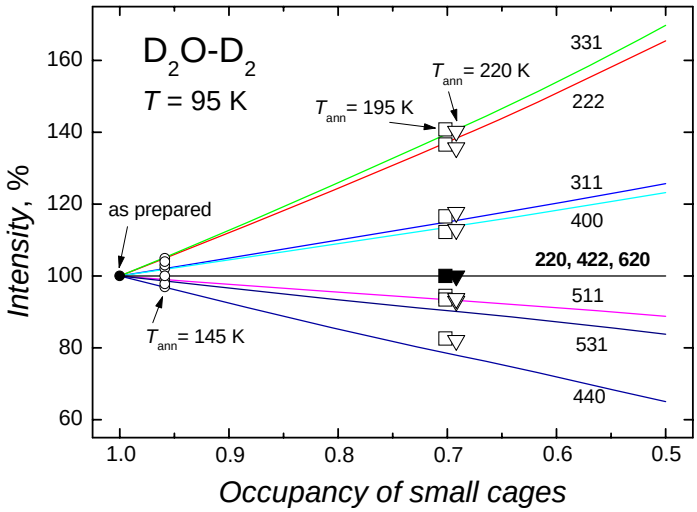

Рис. 5. *Вычисленные и экспериментальные значения интенсивностей D_2O–D_2 клатрата как функции заселенности малы пор.*

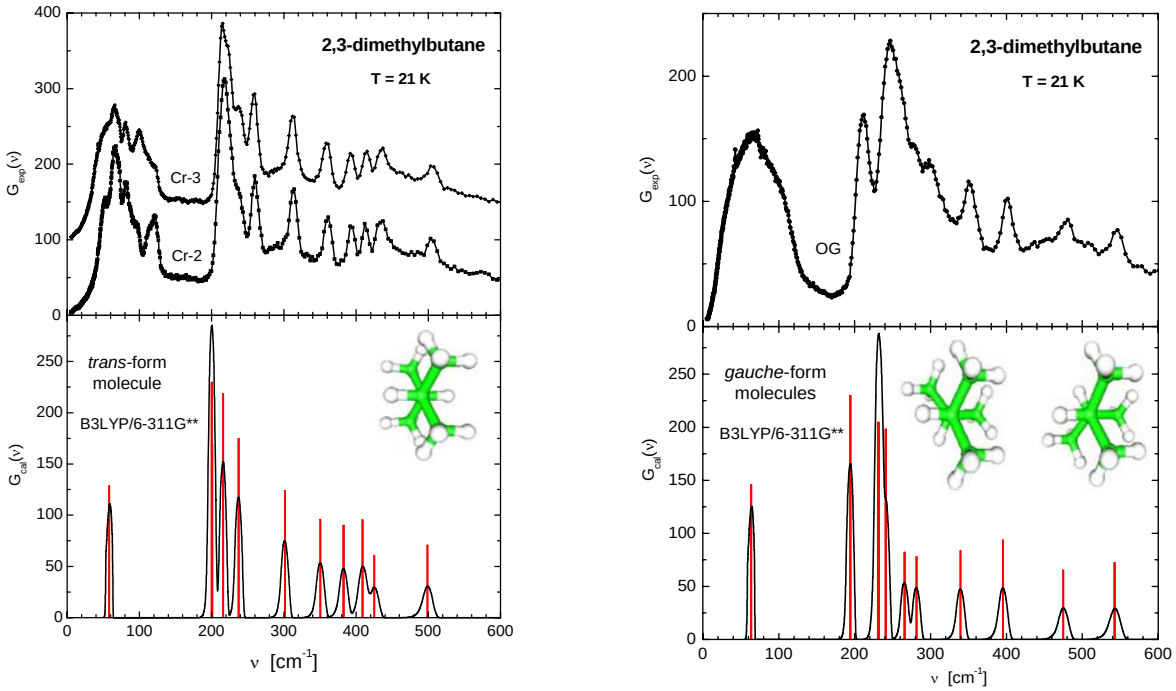

Fig. 6. *Comparisons of the $G_{exp}(\nu)$ spectra of crystalline (Cr-2 and Cr-3) and orientational glass (OG) solid phases of 2,3-dimethylbutane with the $G_{cal}(\nu)$ spectra of isolated molecules calculated within one phonon scattering approximation.*

На спектрометре обратной геометрии HEPA изучены вибрационные спектры изомеров гексана, для которых также проведены расчеты в рамках метода DFT. Спектры неупругого рассеяния измерены для изомеров: 2- или 3-метил-пентан и 2,2- или 2,3-диметил-бутан с общей формулой C_6H_{14}. Одновременно измерялись дифракционные спектры этих образцов, что позволяло контролировать структуру твердых фаз. DFT

вычисления структуры и динамики молекул изученных изомеров были сделаны для интерпретации низкочастотной части спектра внутренних колебаний, которая хорошо видна на экспериментальных спектрах, измеренных при низкой температуре. Особый интерес в этих вычислениях был связан с тем, что спектры неупругого рассеяния диизопропила, измеренные в стеклоподобной и кристаллической фазах, отличались друг от друга. Сравнение вычисленных и измеренных спектров (**Рис. 6**) показывает, что внутренние колебания в состоянии ориентационного стекла (OG) соответствуют колебаниям в *gauche*-форме молекулы. Это предполагает низкие потенциальные барьеры для внутренних вращений молекулярных групп $CH(CH_3)_2$, что также было подтверждено DFT вычислениями.

На спектрометре ДИН-2ПИ на образцах AgCuSe впервые с использованием метода рассеяния медленных нейтронов проведено исследование атомной динамики в суперионной и несуперионной фазах этого соединения. Анализ динамического структурного фактора $S(Q,\omega)$ указывает на наличие низкоэнергетических мод в области энергий 3 – 4 мэВ в упорядоченном состоянии AgCuSe, предположительно отвечающим акустическим фононным модам. Установлена корреляция между переходом в суперионное состояние AgCuSe и изменениями в динамике кристаллической решетки, заключающаяся в резком изменении спектров динамического структурного фактора, обобщенной плотности фононных состояний, термодинамических свойств. Увеличение амплитуды тепловых колебаний, изменение теплоемкости при переходе в суперионное состояние свидетельствует о значительном смягчении фононного спектра в α- AgCuSe. Плотность фононных состояний $G(\varepsilon)$ в α- и *β*- AgCuSe характеризуется недебаевским поведением в области малых энергий и двумя выраженными максимумами при ε ~ 10 и 20 мэВ (**Рис. 7**). Причиной отклонения $G(\varepsilon)$ от дебаевской зависимости является присутствие моды низкоэнергетических возбуждений. При переходе от β к α фазе наблюдается размытие максимумов при ε ~ 10 и 20 мэВ, как следствие изменения многих факторов атомной динамики исследуемой системы.

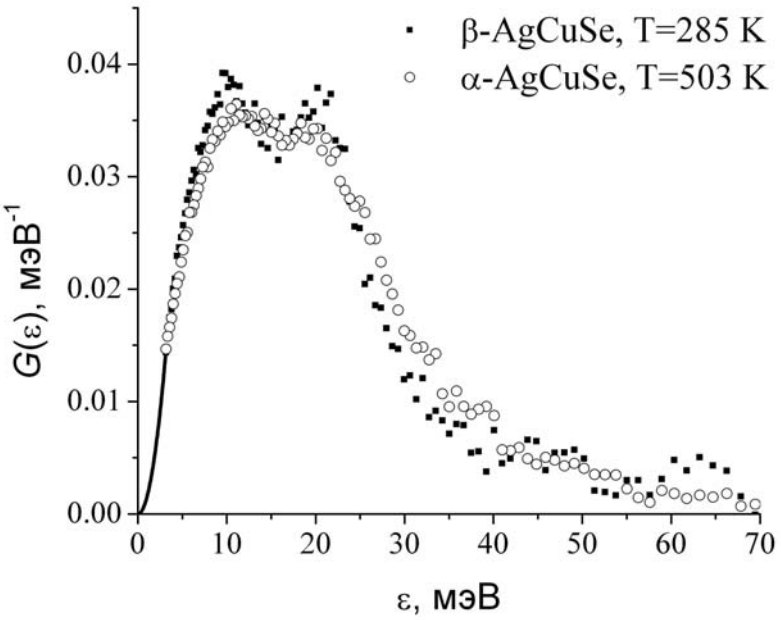

Рис. 7. *Нейтронно-взвешенная обобщенная плотность фононных состояний G(ε) AgCuSe в суперионной и несуперионной фазах.*

1.2. НЕЙТРОННАЯ ЯДЕРНАЯ ФИЗИКА

Введение

В течение 2005 основные работы в области нейтронной ядерной физики в ЛНФ им. И. М. Франка проводились на реакторе ИБР-2, установке ЭГ-5, на нейтронных пучках других ядерных центров России, Болгарии, Польши, Чехии, Германии, Республики Корея, Китая, Франции, США, и Японии. Исследования проводились в традиционных направлениях: изучение процессов нарушения пространственной и временной четности при взаимодействии нейтронов с ядрами; изучение квантово-механических характеристик, энергетики и динамики процесса деления; экспериментальное и теоретическое исследование электромагнитных свойств нейтрона и его бета-распада; гамма-спектроскопия нейтронно-ядерных взаимодействий; структура атомного ядра; получение новых данных для реакторных приложений и для ядерной астрофизики; эксперименты с ультрахолодными нейтронами; прикладные исследования.

1. Экспериментальные исследования

1.1 Фундаментальные свойства нейтрона

1.1.1 Эксперимент по прямому измерению сечения рассеяния нейтрона на нейтроне

Работы в рамках подготовки и проведения эксперимента по прямому измерению сечения рассеяния нейтрона на нейтроне на реакторе ЯГУАР (РФЯЦ-ВНИИТФ, г.Снежинск)

В 2006 г. был изготовлен полный комплект коллиматоров из смеси обогащённого бора с серой (для центральных коллиматоров) и из смеси карбида бора с серой в очехловке из кадмия (для остальных коллиматоров). Проведены вакуумные испытания нижней части канала с установленными в неё коллиматорами. Испытания показали, что в испытываемой конфигурации (без верхней части канала) при штатной откачке достигается вакуум $\sim 3 \cdot 10^{-6}$ мбар, что достаточно для проведения измерения nn-рассеяния. (Собранная нижняя часть установки во время испытаний представлена на **Рис. 1** и **Рис. 2**)

Проведено испытание магниторазрядного насоса (тип «НОРД-250»), установив его вместо одного из турбомолекулярных насосов. Испытание показало, что использование этого насоса не приводит к улучшению вакуума внутри вакуумной системы.

Рис. 1

Рис. 2

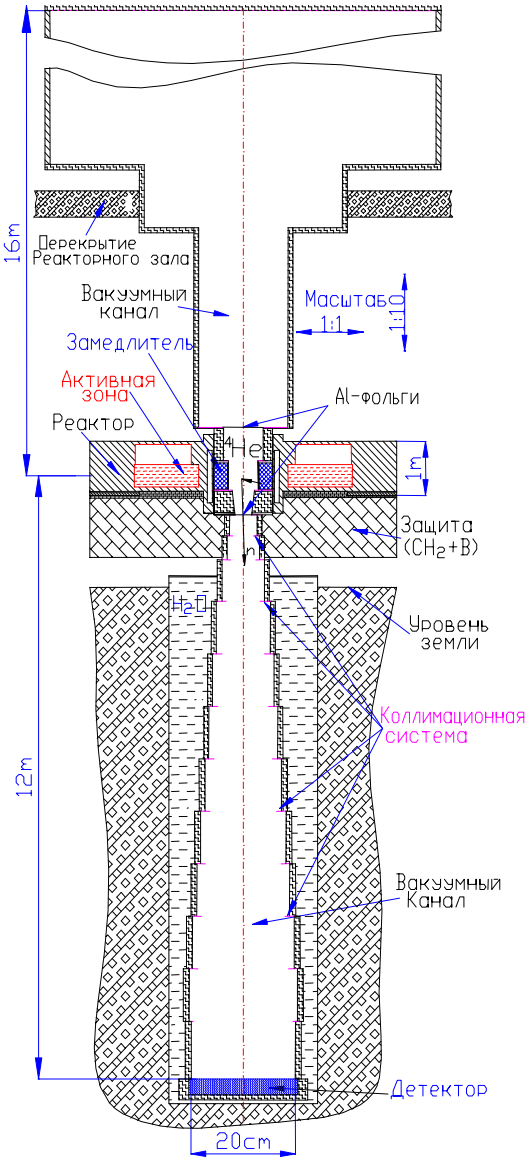

Рис. 3. *Схема установки для калибровочных измерений на газах.*

Завершено изготовление дополнительной оснастки для монтажа нейтронного канала под реактором и проведения верховых работ (под потолком реакторного зала) по монтажу элементов нейтронного канала.

Изготовлена основная часть элементов конструкции модернизированного детектора. Проведены испытания вакуумной плотности корпуса детектора. Исследовались различные режимы работы детектора с целью максимально уменьшить длительность импульса при сохранении амплитудного разрешения.

Таким образом, были завершены работы по изготовлению полномасштабной установки для измерения сечения рассеяния нейтрона на нейтроне на реакторе ЯГУАР.

Установка успешно прошла тестовые проверки в Дубне, была переправлена в Снежинск, смонтирована и отъюстирована на реакторе ЯГУАР.

Для проверки работоспособности всех систем установки в условиях реальных измерений на реакторе, а также для проверки достоверности получаемых результатов были выполнены первые калибровочные измерения на газах. Схема измерений представлена на **Рис.3**. В полость внутри активной зоны реактора, в которой должно происходить рассеяние нейтронов друг на друге, заполняется инертный газ с хорошо известным сечением рассеяния при давлении ~100 торр. Полость отделена от вакуумного канала, по которому нейтроны, рассеянные на газе попадают в детектор, тонкой алюминиевой фольгой. Вся остальная установка (за исключением детектора, чувствительность которого была понижена, и составляла 6,6 10^{-5}, в отличие от 100% эффективности для регистрации n-n рассеяния) такая же, как и при измерении n-n рассеяния толщиной 40 мкм. По числу зарегистрированных нейтронов, при известном энерговыделении реактора, вычисляется сечение рассеяния нейтронов на газе, заполняющем внутреннюю полость реактора. Совпадение измеренного таким образом сечения с заранее известным табличным сечением, является критерием правильности юстировки системы, правильности вычисления нейтронного спектра и телесного угла, в котором происходит регистрация нейтронов. Кроме того, в этом измерении тестируется весь регистрационный канал.

Результаты измерений показали следующее:

1. Все системы установки, за исключением системы регистрации работают нормально.

2. Неожиданно велика оказалась роль γ-фона – подавляющее большинство регистрируемых детектором событий во время импульса реактора это γ-кванты. Большой

поток γ-квантов, проходящий через детектор, приводит к тому, что детектор перестаёт регистрировать какие-либо события (как нейтроны так и γ-кванты) и восстанавливается спустя более чем 10 мс, когда поток тепловых нейтронов, рассеявшихся на атомах газа, уже миновал детектор. Поэтому регистрация нейтронов в импульсном режиме оказалась невозможна. Необходимо провести дополнительное моделирование, для оптимизации защиты детектора с точки зрения уменьшения потока γ-квантов, проходящего через него, и модернизацию электроники системы регистрации с целью уменьшения времени восстановления в случае перегрузки.

3. Проведенное измерение на постоянной мощности реактора показало, что канал отъюстирован правильно и, что при отсутствии перегрузки детектора система регистрации также правильно работает. Измеренное сечение рассеяния тепловых нейтронов на ^{4}He составило 0,87±0,13 б (табличное значение этого сечения – 0,760 б).

1.1.2 Исследование n-e рассеяния

Новый метод получения экспериментальной величины длины рассеяния нейтрона на электроне b_{ne} был применен для анализа данных по структурным факторам $S(q)$ (q - переданное волновое число), описывающих дифракцию нейтронов в газах и жидкостях. Использовались полученные на реакторе в Гренобле результаты дифракционных экспериментов интернациональной группы физиков, любезно предоставивших для наших расчетов свои числовые данные.

Сначала обрабатывались $S(q)$ для газообразного изотопа ^{40}Ar, у которого из-за аномально сильного ядерного рассеяния относительный вклад n,e-рассеяния в полное рассеяние примерно на порядок меньше, чем у естественных Ar, Kr и Xe. Соответственно, результат оказался весьма скромным, но продемонстрировал действенность предложенного метода:

$b_{ne} = -(1{,}33 \pm 0{,}28 \pm 0{,}57) \cdot 10^{-3}$ Фм,

где вторая ошибка – систематическая. Статья направлена в Eur. Phys. J.C. Естественно, гораздо лучший результат дала обработка данных по дифракции на жидком Kr. Три разных варианта обработки данных привели к очень близким величинам b_{ne}, наиболее точная из которых

$b_{ne} = -(1{,}38 \pm 0{,}04) \cdot 10^{-3}$ Фм.

Этот результат входит в число 10 – 12 лучших по точности.

Предложен эксперимент с целью измерения длины n-e рассеяния на установке TS3000K на жидких металлах. Первый предварительный эксперимент планируется проводить на жидком свинце поскольку точка плавления свинца находится чуть выше 300^0C. В случае удачного эксперимента на свинце будут сделаны измерения и на других жидких металлах с более высокой температурой плавления.

Установка TS3000K реализована в Национальном Институте Ядерной Физики им. “Хоря Хулубей”, Бухарест – Румыния (IFIN-HH) и предназначена для исследования структуры и динамики твердого и жидкого состояния с помощью неупругого рассеяния нейтронов в условиях сверхвысоких температур и вакуума.

В 2006 г. были проведены теоретические оценки для измерения длины n-e рассеяния на свинце с использованием нескольких феноменологических моделей жидкого состояния и жидкого свинца. Эти оценки показывают возможность получения длины на установке TS3000K на канале DIN-2PI.

1.2 Нейтронная оптика

1.2.1 Оптика сильно поглощающих веществ

Закончена работа по экспериментальной проверке справедливости закона 1/v для сечения захвата ультрахолодных нейтронов в естественном гадолинии. Идея работы основана на том обстоятельстве, что взаимодействие нейтронов с веществом может быть описана моделью эффективного оптического потенциала в том и только в том случае, когда полное сечение взаимодействия нейтронов с ядрами вещества подчиняется закону 1/v. При этом оптический потенциал V вообще говоря комплексен.

$$\mathbf{V = U + iW}. \qquad (1)$$

В случае естественного гадолиния, обладающего рекордным значением сечения захвата благодаря наличию резонансов в тепловой области энергий, модель потенциала вообще говоря не справедлива. Однако для холодных и очень холодных нейтронов она должна выполняться с большой точностью. Значения действительной и мнимой частей потенциала естественного гадолиния для случая УХН были определены в наших предшествующих работах [1.1, 1.2]: V = 45нэВ, W = 82нэВ.

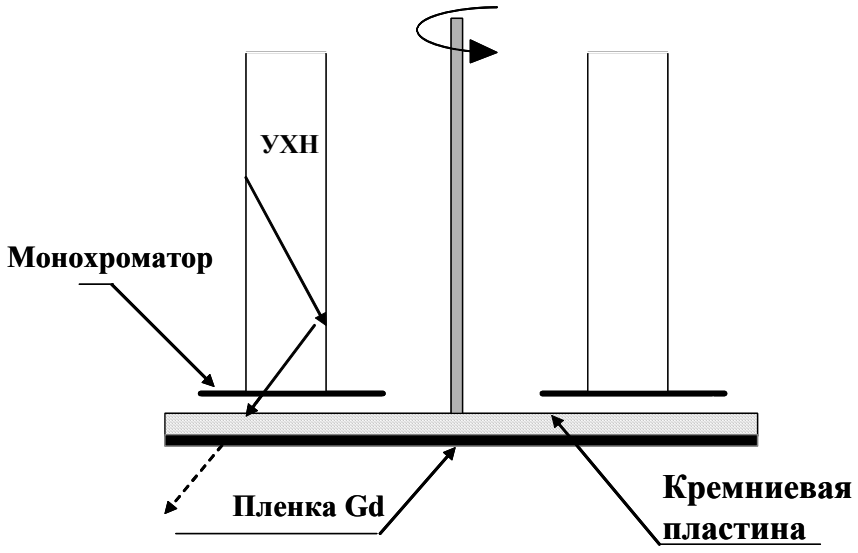

Рис. 4. *Схема эксперимента по проверке закона 1/V для сечения захвата УХН в естественном гадолинии.*

Особенность модели потенциала состоит в том, что в случае ее сраведливости как коэффициент отражения, так и прозрачность вещества зависят только от компоненты скорости нейтрона, нормальной к поверхности вещества. Именно эта особенность и была положена в основу нашего эксперимента.

Ультрахолодные нейтроны проходили через периферическую часть образца, представляющего собой пленку гадолиния, толщиной около 25нм, нанесенную на кремниевый диск. Вращая диск, можно было менять относительную скорость нейтронов и образца, сохраняя неизменной нормальную компоненту скорости (см. **Рис.4**). Неизменность пропускания от скорости вращения свидетельствовала о справедливости модели эффективного потенциала и, следовательно, о выполнении закона 1/v. В результате установлено, что закон 1/v для сечения захвата УХН в естественном гадолинии справедлив с точностью порядка 0.1% в интервале изменения скоростей УХН от 4 до 35м/сек.

1.2.2 Взаимодействие нейтрона с ускоряющимся веществом

Был поставлен эксперимент по наблюдению изменения энергии нейтрона при прохождении через ускоренное вещество. Существование эффекта следует как из справедливости принципа эквивалентности, так и из детальных нейтронно-оптических расчетов [2.2]. Для плоского образца, двигающегося с ускорением, величина эффекта определяется выражением

$$\Delta E \approx wd\frac{1-n}{n}, \qquad (2),$$

где **d** – толщина образца**, n** – показатель преломления и **w** – ускорение образца. Целью работы было измерение такого изменения энергии.

В качестве образца использовалась кремниевая пластина, толщиной 0.6мм, которую можно было приводить в гармоническое движение. При этом энергия нейтрона также должна была меняться по гармоническому закону в соответствии с

$$\Delta E(t) = \frac{1-n}{n} Ad\Omega^2 Sin(\Omega t), \qquad (3),$$

где **A** и $\Omega=2\pi f$ – амплитуда и частота осцилляции образца соответственно. Максимальное значение ускорения $w_{max} = A\Omega^2$ составляло величину порядка 7.5g, чему соответствует передача энергии $\Delta E \approx 2\times10^{-10}$ эВ.

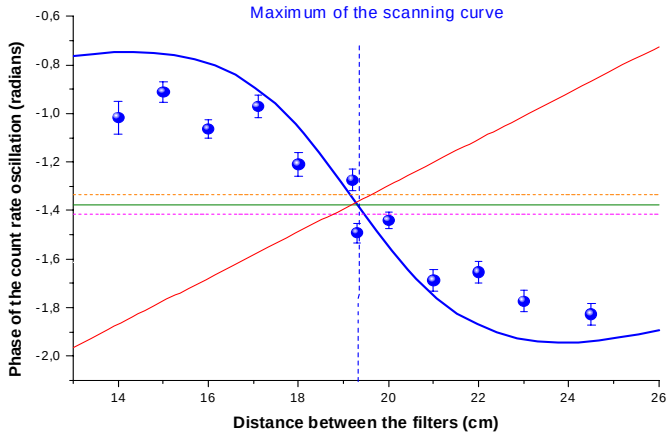

Рис. 5. *Фаза осцилляции скорости счета в зависимости от положения между фильтрами.*

Эксперимент был поставлен с гравитационным спектрометром УХН с интерференционными фильтрами. При этом образец размещался между фильтром-монохроматором (и вблизи него) и фильтром-анализатором. Гармоническое движение образца приводило к периодической модуляции скорости счета с той же частотой. Эта модуляция порождалась двумя эффектами: изменением энергии, пропорциональным ускорению образца, что и являлось предметом поиска, и изменением прозрачности образца, обусловленным периодическим изменение относительной скорости образца и нейтрона. При различных соотношениях между этими двумя эффектами, искомым и систематическим, фаза осцилляции скорости счета нейтронов также различно. Это обстоятельство и было положено в основу эксперимента. В нем измерялась фаза осцилляции скорости счета в зависимости от расстояния между двумя фильтрами.

Полученные результаты иллюстрируются **рисунком 5**. Синие закрытые точки – результат измерения фазы осцилляции скорости счета в зависимости от расстояния между фильтрами. Сплошная синяя кривая – теоретический расчет. Красная наклонная прямая – расчет, сделанный в предположении, что изменение фазы осцилляции обусловлено только периодической модуляцией прозрачности образца, а искомый эффект изменения энергии отсутствует. Горизонтальная сплошная и пунктирная линии – фаза осцилляции скорости счета (и коридор погрешностей) в отсутствии фильтра-анализатора. При корректных измерениях и расчетах эти линии должны пересекаться в одной точке.

Эксперимент с несомненностью свидетельствуют о существовании впервые наблюдаемого эффекта изменения энергии нейтронов при прохождении через ускоряющийся образец. Его величина соответствует теоретическим предсказаниям с точностью порядка 15%. Дальнейшие эксперименты покажут, связано ли это расхождение с физическими причинами или оно носит чисто методический характер. Отметим еще, что хотя эффект ускоренного вещества наблюдался пока только в нейтронно-оптическом эксперименте, он имеет весьма универсальную природу и должен существовать и для частиц иной природы.

1.2.3 Проверка слабого принципа эквивалентности и измерение ускорения свободного падения нейтрона

На источнике УХН в ИЛЛ (Гренобль) поставлен эксперимент по измерению ускорения свободного падения нейтрона. Эксперимент поставлен с помощью гравитационного спектрометра УХН с интерферометрами Фабри-Перо (ИФП), а его идея, опубликованная ранее в работе, иллюстрируется **рисунком 6**. После прохождения ИФП-монохроматора нейтроны с узким интервалом вертикальных скоростей проходят через вращающуюся фазовую дифракционную решетку. Нейтроны, соответствующие - 1-му порядку дифракции уменьшают свою энергию на величину $\Delta E = \hbar\Omega$, где частота модуляции Ω пропорциональна частоте вращения решетки f и равна $\Omega = 2\pi\frac{f}{\varphi}$, где φ-угловой период решетки. На пути к ИФП-анализатору нейтроны ускоряются в гравитационном поле, увеличивая свою энергию на величину mgH, где H – расстояние между ИФП. Измерение энергии производится путем сканирования по высоте анализирующим ИФП. При этом определяется максимумы соответствующих кривых сканирования при различных значениях частоты вращения решетки и пропорциональной ей частоты модуляции. Величина ускорения свободного падения определяется при этом из соотношения

$$g = \frac{\hbar}{m}\frac{\Delta\Omega}{\Delta H} \qquad (4)$$

Результаты одной из экспериментальных серий приведены на **рисунке 7**.

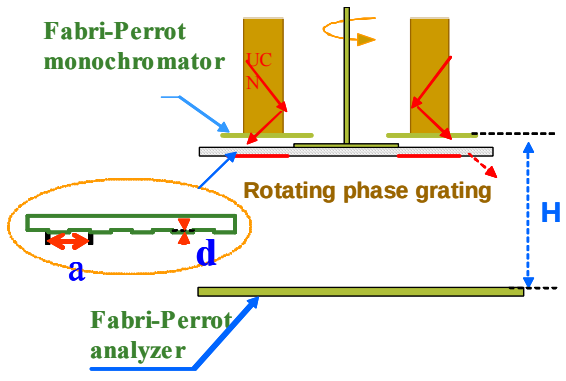

Рис. 6. *Идея эксперимента по измерению ускорения свободного падения нейтрона.*

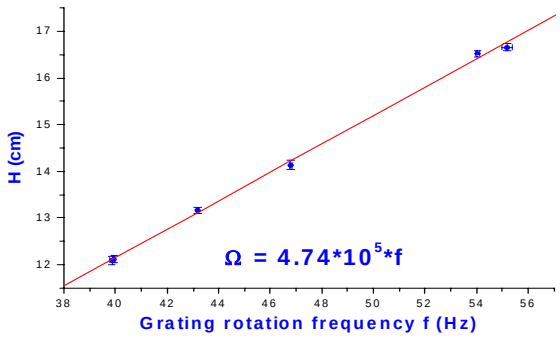

Рис. 7. *Положение максимумов кривых сканирования в зависимости от частоты вращения решетки.*

В настоящее время продолжается обработка экспериментальных данных. Предварительный результат состоит в том, что в пределах точности порядка 0.2%. ускорение свободного падения нейтрона такое же, что и для макроскопических тел.

1.2.4 Проектирование нейтронного микроскопа

В 2006 году начаты работы над проектом нейтронного микроскопа, ориентированного на европейские источники УХН нового поколения. Создано математическое обеспечение для расчета зеркальных оптических систем для УХН в присутствии гравитации. С помощью этой программы ведутся расчеты горизонтального нейтронного микроскопа с компенсацией гравитационных аберраций преломляющими элементами. Получены обнадеживающие результаты.

1.3 Исследование свойств ультрахолодных нейтронов

1.3.1 Работы в рамках исследования взаимодействия УХН с поверхностью

В 2006 году были проведены исследования поверхностей ряда материалов микроскопом атомных сил (AFM). Исследования проводились с целью проверки гипотезы о поверхностных наночастицах как причине так называемого «малого нагрева» УХН при взаимодействии с поверхностью. Исследовалась поверхность меди, железа, различных марок нержавеющей стали и сапфира, а так же зависимость структуры поверхности от температуры предварительного обезгаживания. Типичные данные, полученные на AFM, с поверхности образцов представлены на **Рис. 8**.

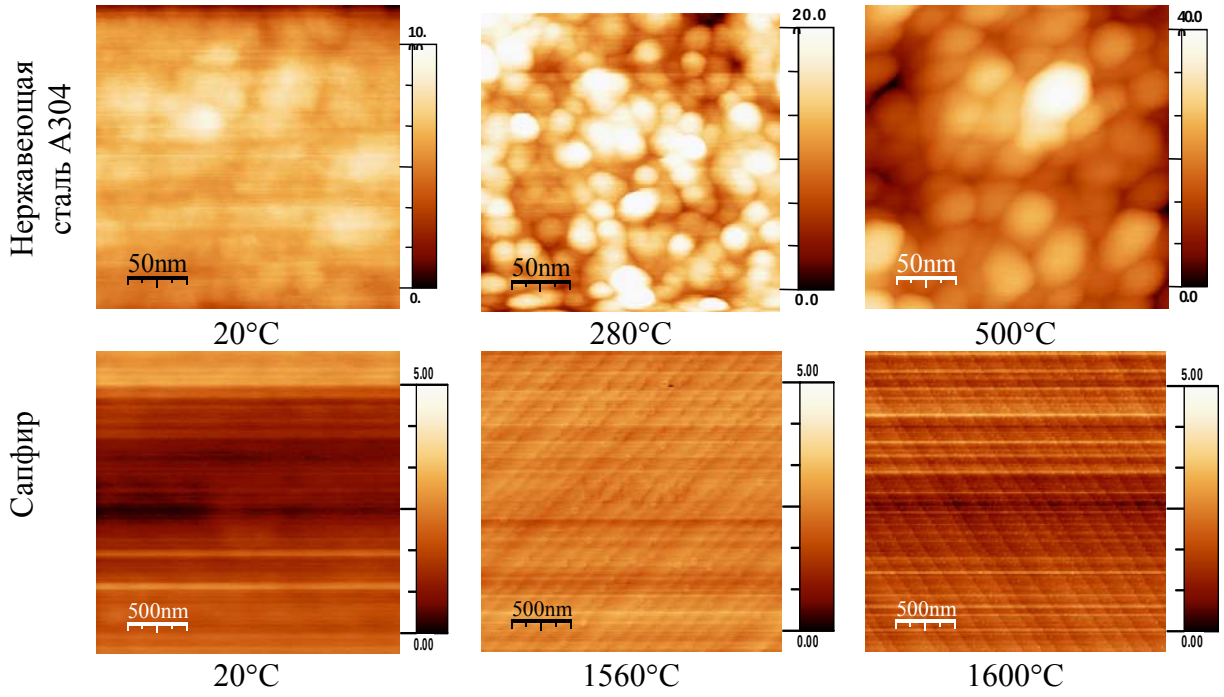

Рис. 8. *Данные с поверхности образцов.*

Основной вывод из проведённых измерений: на всех исследованных поверхностях (за исключением полированного монокристаллического сапфира) присутствуют наночастицы различных размеров. Размеры наночастиц увеличиваются с ростом температуры предварительного прогрева образцов, количество наночастиц зависит от этой температуры и от глубины вакуума во время прогрева. На монокристаллическом сапфире при прогреве до температур ~1600°C образуются наночастицы в то же время после прогрева до 800°C образование наночастиц на его поверхности не замечено. Поверхность монокристаллического сапфира после прогрева до 1600°C представляет собой ступенчатую структуру со ступеньками в одну атомарную плоскость.

Обнаружение частиц на поверхности указывает на возможность неупругого рассеяния нейтронов с малой передачей энергии на таких частицах если они окажутся достаточно свободными.

1.3.2 Исследование квазиупругого рассеяния УХН

В продолжение работы прошлого года проведены в ILL новые измерения вероятности и спектров квазиупругого рассеяния УХН на ряде образцов: медь, алмазоподобный углерод, тефлон и др. В предыдущих экспериментах был впервые обнаружен значительный нагрев нейтронов в область скоростей 8-12 м/с.

Метод заключался в измерении потока нейтронов (после рассеяния на образце) сквозь калиброванные образцы с известным сечением поглощения нейтронов. В данном случае в качестве поглотителей использовались пластины монокристаллов кремния и родиевые фольги. Таким образом измерялись кривые поглощения для нейтронов полного спектра рассеяния: от ультрахолодных до тепловых. Измерены кривые поглощения и восстановлены из них спектры рассеянных нейтронов. Окончательная обработка результатов будет проведена в начале 2007 г.

Как и в прежнем случае, измерения проводились только при комнатной температуре и на образцах термически в вакууме не обработанных. Планируются эксперименты, в которых поверхность образцов может в вакууме термически обезгаживаться, а измерения могут проводиться при низких температурах.

1.3.3 Работы по созданию источника УХН на импульсном реакторе TRIGA

Проведены новые детальные расчеты и впервые измерена генерация ультрахолодных нейтронов на импульсном реакторе TRIGA-Майнц (совместно с группами из Мюнхена и Майнца). Это есть реализация давнего предложения Yu. N. Pokotilovski, „Production and storage of ultracold neutrons at pulsed neutron sources with low repetition rates“, Phys. Lett., A356 (1995) 412.

Результаты по генерации УХН и нестационарному транспорту по зеркальному нейтроноводу хорошо согласуются с расчетами.

Нейтроны генерировались в твердой дейтериевой мишени при температуре 6-10 К, и транспортировались по зеркальному нейтроноводу длиной 6 м. В части экспериментов использовался мезитиленовый предзамедлитель при температуре 20 К.

При регистрации нейтронов использовались попеременно три разных детектора нейтронов: кремниевый с радиатором из обогащенного фторида лития, пропорциональный газовый с He-3, и окончательно из-за высокой скорости счета при импульсной генерации (до 10^6 нейтронов в секунду) GEM-детектор с борным радиатором. При импульсе реактора 10 МДж количество зарегистрированных нейтронов с энергией ниже 200 нэВ превышало 10^5.

1.4 Нарушение пространственной и временной четности при взаимодействии нейтронов с ядрами

1.4.1 Измерение P-нечетной асимметрии эмиссии тритонов в реакции ^{6}Li(n,α)^{3}H

На пучке холодных поляризованных нейтронов PF1B реактора ИЛЛ (Гренобль) проведен «нулевой»-эксперимент по определению фоновой асимметрии для серии экспериментов по измерению P-нечетной асимметрии эмиссии тритонов в реакции ^{6}Li(n,α)^{3}H. Получено значение $\alpha_0 = (0.0 \pm 0.5)\cdot 10^{-8}$. Таким образом, успешно завершен один из двух важнейших, ведущихся в течение нескольких последних лет, экспериментов по поиску нейтральных токов в нуклон-нуклонных взаимодействиях. Сопоставление этого результата с результатом основного эксперимента: $\alpha_t = -(8.6 \pm 2.0)\cdot 10^{-8}$ показывает, что наблюдаемый эффект обусловлен P-нечетной асимметрией тритонов из реакции ^{6}Li(n,α)^{3}H. Целью исследований является определение слабой π-мезонной константы связи f_π, соответствующей взаимодействию нейтральных токов в нуклон-нуклонных процессах. Из полученной асимметрии следуют ограничения: $f_\pi = (0.4 \pm 0.4)\cdot 10^{-7}$, в предположении, что другие константы равны «лучшим значениям» Дипланка и др., и $-1.2\cdot 10^{-7} \le f_\pi \le 1.6\cdot 10^{-7}$ с учетом теоретических и экспериментальных неопределенностей других констант. Это подтверждает результаты эксперимента на ^{18}F и вывод, что f_π существенно меньше «лучшего значения» Дипланка и др. ($4.6\cdot 10^{-7}$). Работы выполняются совместно с ПИЯФ (Гатчина), ИЛЛ (Гренобль, Франция), ТУ Мюнхена (Германия).

1.4.2 Управление нейтронной поляризацией посредством рамсеевского вращения

В 2006 г. был проведен эксперимент, целью которого являлось проверка эффективности управления поляризацией тепловых и эпитепловых нейтронов с помощью радиочастотного поля. Эксперимент проводился на пучке H8 импульсного нейтронного источника KENS (КЕК, Япония). Схема установки приведена на **рис.9**.

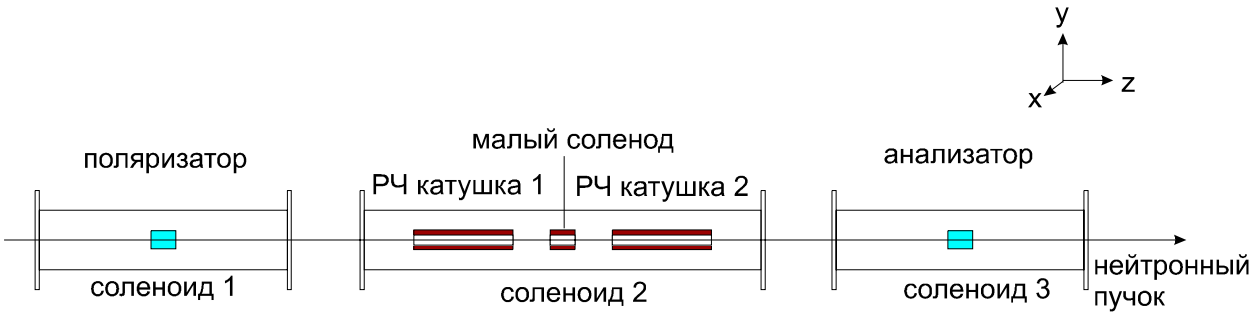

Рис. 9. *Схема эксперимента.*

Поляризация нейтронов и анализ их поляризации осуществлялись устройствами на основе поляризованного ^{3}He с оптической накачкой, созданными коллаборацией КЕК-ЛНФ ОИЯИ в 2003-2005 гг. В соленоиде 2 длиной 80 см и диаметром 12 см последовательно располагались две прямоугольные радиочастотные катушки РЧ 1 и РЧ 2 длиной 20 см каждая. Каждая катушка создавала осциллирующее поле $2H_1\cos(\omega t)$, направленное вдоль оси *y*. Измерение осуществлялось по времени пролета. Поле включалось в момент, когда на вход первой катушки приходили нейтроны с $E_h = 80$ мэВ и выключались в момент прихода нейтронов с $E_l = 23.6$ мэВ. При этом, амплитуда поля H_1 модулировалась так, чтобы обеспечить поворот нейтронной поляризации на заданный

угол φ вокруг оси y для всех нейтронов в интервале $E_l \le E \le E_h$. Для этого необходимо выполнение условия $\gamma H_1 t = \varphi$, где γ - гиромагнитное отношение для нейтрона, а t – время пролета нейтрона данной энергии вдоль катушки. В нашем эксперименте было выбрано $\varphi = \pi/2$. Вторая катушка работала когерентно с первой и, таким образом, полный поворот нейтронной поляризации на входе анализатора составлял π, т.е., происходил реверс поляризации. Соответствующее изменение трансмиссии, прошедшего через анализатор нейтронного пучка регистрировалось сцинтилляционным детектором на пролетной базе 12.05 м.

Если между первой и второй катушками включить дополнительное поле, то из-за дополнительного вращения нейтронной поляризации на этом участке, характер нейтронной трансмиссии изменяется.

В эксперименте мы измеряли нейтронные трансмиссии с выключенными катушками T_{off} и включенными T_{on}. Затем строили отношение:

$$R = \frac{T_{on}}{T_{off}} - 1 = \frac{1 + \alpha(E) P_1 P_2}{1 + P_1 P_2},$$

где P_1 и P_2 - поляризации нейтронов прошедших по отдельности сквозь поляризатор и анализатор соответственно. Вся информация о полях, действию которых нейтронная поляризация подвергалась на участке от поляризатора к анализатору содержится в функции $\alpha(E)$. На **рис. 10,11** показаны отношения R для случаев с выключенным и включенным малым соленоидом. Красные линии – подгонка. Энергетическая зависимость отношений R связана с зависимостью от энергии нейтронов величин $\alpha(E)$, P_1 и P_2.

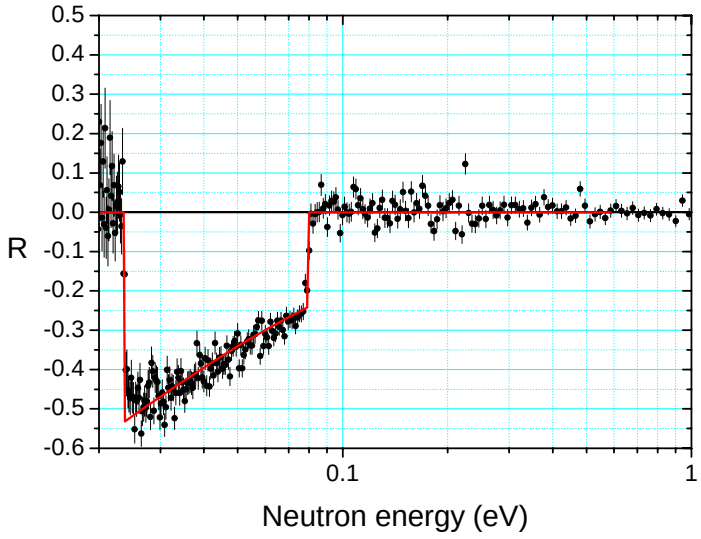

Рис. 10. *Отношение R, когда малый соленоид выключен.*

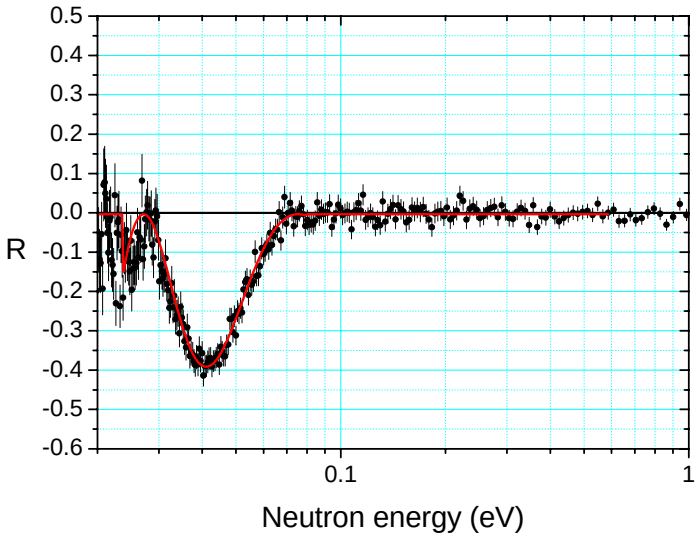

Рис. 11. *Отношение R, когда малый соленоид выключен.*

На 2007 запланированы проведения исследований по методике изготовления и отбора монокристаллов $LaAlO_3$ с целью создания поляризованной ядерной мишени для проверки Т-инвариантности во взаимодействии поляризованных нейтронов с поляризованными ядрами. Кроме того, будут проводится работы по совершенствованию существующего криостата ядерной мишени.

1.4.3 Поиск и исследование структуры подпороговых нейтронных p-резонансов на изотопах свинца методом комбинированной корреляционной гамма-спектроскопии

С целью проверки полученных ранее экспериментальных данных о существовании отрицательного нейтронного p-резонанса у изотопа ^{207}Pb, вместо ^{204}Pb, как ожидалось на основании работ по наблюдению поворота спина тепловых нейтронов при взаимодействии со свинцом, были проведены дополнительные эксперименты на усовершенствованном гамма-спектрометре COCOS канала №1 реактора ИБР-2 с повышенной эффективностью и быстродействием. Для изучения энергетической зависимости хода сечения радиационного захвата нейтронов в качестве мишеней использовались два образца с различным весом и содержанием изучаемых изотопов: а) 20 г с обогащением 90,4% по изотопу ^{207}Pb и б) 9 г с обогащением 51% по изотопу ^{204}Pb, содержащим 0,94 г изотопа ^{207}Pb.

В результате проведения нескольких серий измерений накоплен достаточный экспериментальный материал, для возможной изотопной идентификации искомого отрицательного p-резонанса и оценки его параметров.

1.5 Исследования деления ядер

1.5.1 Поиск экзотических мод деления на реакторе ИБР-2 с использованием установки «Мини-Фобос»

События, указывающие на возможность существования тройного коллинеарного кластерного распада (ТККР), были впервые обнаружены в серии экспериментов по

изучению спонтанного деления ядер ^{252}Cf, проведенных в Лаборатории ядерных реакций. Экспериментальные проявления такого канала распада рассматривались в рамках предположения “недостающей” массы, т.е. детектирования в совпадении только двух тяжёлых коллинеарных фрагментов, имеющих меньшую суммарную массу, чем масса исходно делящегося ядра. Данная “недостающая” или “потерянная” масса может соответствовать одному или нескольким фрагментам, которые вылетают под малыми углами к оси деления и не детектируются. Как предполагается, для подобных процессов ключевую роль играют оболочечные эффекты. Основные результаты были получены на установках ФОБОС и мини-ФОБОС. Одним из главных преимуществ детекторных модулей спектрометра ФОБОС является возможность независимого измерения вектора скорости, массы и заряда каждой частицы без привлечения предположений о кинематических особенностях механизма реакции.

Рис.12. *Установка Мини-Фобос на канале 6б реактора ИБР-2.*

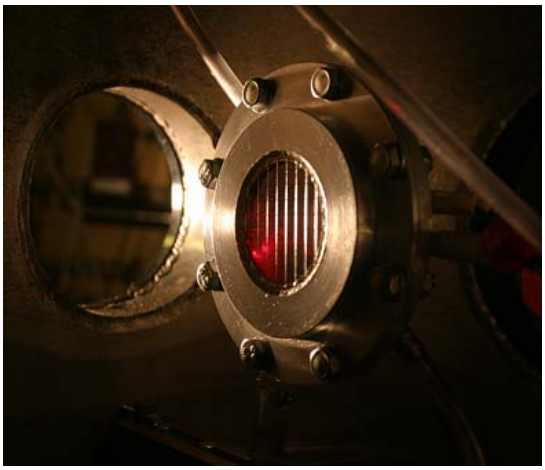

Рис.13. *Стартовый лавинный счетчик с внутренней мишенью.*

Исследования продолжились в Лаборатории нейтронной физики в соответствии с решениями рабочего совещания от 21 декабря 2004 г. В 2006 году спектрометр мини-ФОБОС был установлен на канале нейтроновода 6Б реактора ИБР-2 (см. **Рис.12**), и выполнена серия измерений. Для работы в новых условиях была изготовлена поддерживающая стойка, разработан стартовый лавинный счётчик с внутренней мишенью (**Рис. 13**). Стабильность набора данных обеспечивалась кондиционированием как экспериментального каньона 6Б, так и помещения с электроникой. В рамках вышеописанного метода изучался распад $^{236}U^{*}$, полученного в реакции $^{235}U+ n_{th}$. Всего было набрано около $6x10^{6}$ событий, при этом эффективность спектрометра составила примерно 1.5%. Предварительный анализ указывает на структуры, подобные обнаруженным при исследовании распада ядер ^{252}Cf.

1.5.2 Измерение полных энергетических спектров легких заряженных частиц в спонтанном делении ^{252}Cf

Эксперимент по измерению полных энергетических спектров легких заряженных частиц в спонтанном делении ^{252}Cf был проведен в лаборатории JYFL (г. Ювяскюля, Финляндия). Экспериментальная установка показана на **Рис. 14**. Спонтанный источник деления ^{252}Cf, изготовленный в Радиевом институте (С.Петербург), имел активность

порядка 500 делений в секунду. Подложка, на которую был нанесен тонкий слой калифорния, представляла собой фольгу из окиси алюминия (Al_2O_3) толщиной 22.2 $\pm$ 3.4 мкг/см^2 с напылением ~10 мкг/см^2 слоя золота. Потеря энергии осколков при перпендикулярном прохождении через подложку составляла ≤ 1.5 МэВ. Потери энергии осколков, вылетающих с передней части источника были не ьбольше 60 кэВ. Оценочная толщина слоя калифорния (Cf_2O_3) равняется 3.5 мкг/см^2.

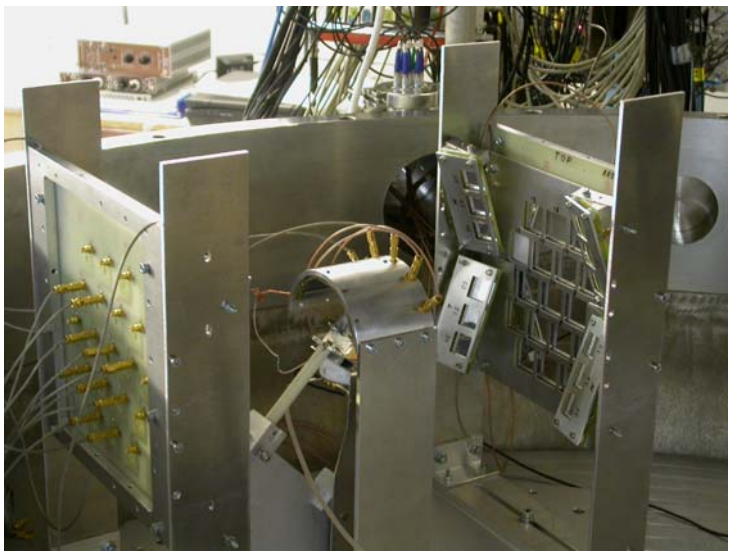

Рис. 14. *Экспериментальная установка для измерения энергетических спектров легких заряженных частиц.*

В эксперименте регистрировалась энергия и время пролета легкой заряженной частицы, при этом отсутствовали какие-либо поглотители на ее пути к детектору. Это позволило измерить энергетические спектры с высокой точностью вплоть до самых маленьких энергий ~0.5 МэВ, что является самым низким порогом, когда-либо достигнутым в экспериментах такого рода. Легкие заряженные частицы регистрировались мозаиками из кремниевых детекторов, расположенными на расстоянии ≈20 см от источника. В качестве стартового сигнала использовались осколки деления, зарегистрированные быстрым МКП детектором, расположенным под прямым углом к мозаике кремниевых детекторов на расстоянии 2.5 мм от источника. Для дискриминации осколков деления от 6-мэвных альфа-частиц от естественной радиоактивности ^{252}Cf была применена схема совпадения стартовых сигналов с сигналами от 10 кремниевых детекторов, расположенных с противоположной от МКП стороны источника. Геометрия эксперимента покрывала угловой диапазон от 70° до 110° вылета легких заряженных частиц относительно осколков деления. Т.е в основном регистрировались экваториальные частицы.

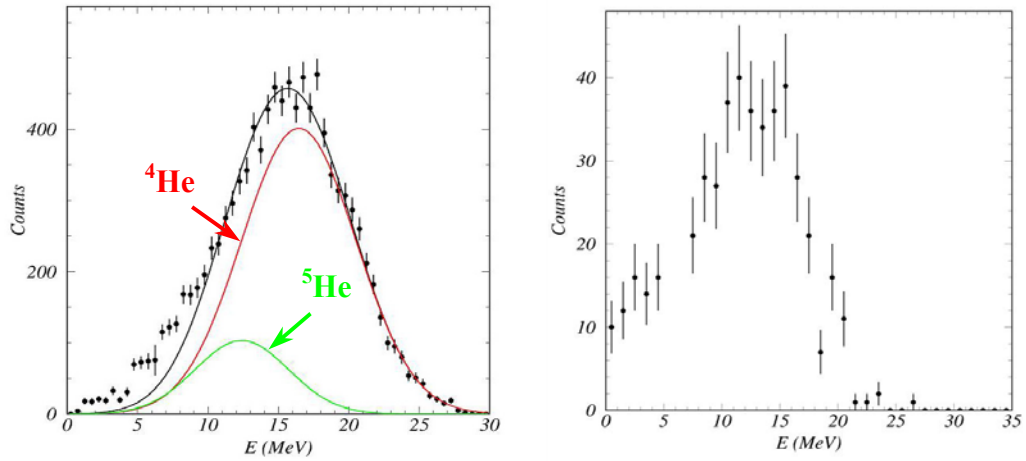

Рис. 15. *Экспериментальные энергетические спектры для ^{4}He (слева) и ^{6}He (справа). Для ^{4}He показаны вклады от истинных α-частиц, и от α-частиц образующихся в результате распада ^{5}He.*

Результаты измерений для α-частиц и ^{6}He представлены на **Рис. 15**. На левом рисунке нанесены две кривые, которые представляют собой результат подгонки экспериментальных данных для энергий выше 9 МэВ с учетом известного из предыдущих измерений 17% вклада от α-частиц, образующихся в результате распада нестабильных изотопов ^{5}He в тройном делении. Видно, что отклонение формы экспериментальной кривой от Гауссовской не может быть объяснено этой компонентой. По-видимому, наличие этого отклонения связано со сложным статистическим распределением начальных конфигураций делящейся системы в момент разрыва ядра. Такое предположение качественно подтверждается траекторными расчетами. Следует также заметить, что измеренный энергетический спектр α-частиц совпадает с данными, полученными Тищенко в 2002 г, однако существенно расходится с данными Лавланда 1974 года. Полный энергетический спектр для ^{6}He был измерен впервые в этой работе.

1.5.3 Подготовка измерений эмиссии мгновенных нейтронов в нейтронно-индуцированном делении на источнике GELINA (IRMM, Geel, Бельгия)

В настоящее время актуальным является исследование реакций ^{239}Pu(n_{res},f) ^{235}U(n_{res},f) с целью измерения корреляций эмиссии мгновенных нейтронов с массовыми распределениями осколков деления в нескольких наиболее сильных резонансах. Учитывая высокую удельную альфа-радиоактивность плутония, приемлемое качество спектрометрии осколков деления могло быть достигнуто с применением современной техники цифровой обработки сигналов (ЦОС). Для уменьшения эффекта наложения импульсов из-за естественной радиоактивности мишеней было также необходимо разработать методику спектрометрии осколков деления с помощью токовых предусилителей, которые позволяли улучшить качество спектроскопии осколков деления в реакции ^{239}Pu(n_{res},f). Для решения указанных задач в колаборации с сотрудниками IRMM впервые была разработана уникальная методика ЦОС с токовыми предусилителями для спектрометрии осколков деления. Был создан математический аппарат цифрового анализа импульсных сигналов детекторов ядерных частиц, а также разработано программное обеспечения (ПО) для дискретизации и сбора информации с ионизационных камер и нейтронных детекторов. Вышеуказанная методика и ПО были апробированы с использованием ^{252}Cf(sf) активностью 30 килобекерель. Были получены результаты, хорошо согласующиеся с литературными данными.

Также в колаборации с сотрудниками IRMM была разработана методика измерения множественности нейтронов деления с использованием нейтронных детекторов на базе жидкого сцинтиллятора NE213, предоставленных колаборацией DEMON. Была создана библиотека программ ЦОС, реализующих функции стандартных модулей ядерной электроники таких, как спектрометрические усилители, дискриминаторы со следящим порогом, аналого-цифровое и аналогово-временное преобразование и т.д. Было разработано ПО для цифровых осциллографов фирмы Tektronix, позволяющих использование их в качестве аппаратуры для оцифровывания импульсов детекторов ядерных частиц.

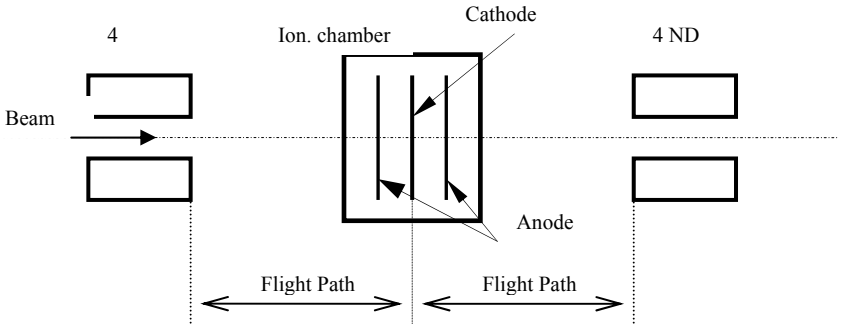

Рис. 16*. Схема экспериментальной установки.*

Установка располагалась на 8 метровой пролетной базе импульсного нейтронного источника GELINA (**Рис. 16**). Всего было использовано 8 нейтронных детектора (НД) емкостью по 4 литра каждый. Расстояние между исследуемой мишенью и НД составило - 0.75 м. Для калибровочных измерений использовалась мишень ^{252}Cf(sf) активностью 30 килобекерель.

Для подавления фона гамма квантов использовался анализ формы импульсов и измерение времени пролета мгновенных нейтронов деления (**Рис. 17).** Калибровочные измерения проводились как с включением, так и с выключением пучка нейтронов от GELINA.

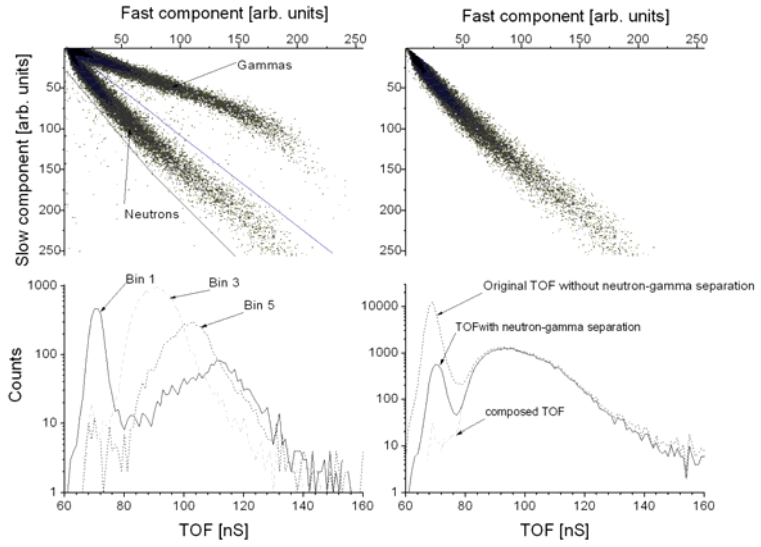

Рис. 17. *Иллюстрация подавления фона гамма квантов при регистрации мгновенных нейтронов деления с анализом формы импульса и времени пролета для ^{252}Cf(sf).*

1.6 Гамма-спектроскопия нейтронно-ядерных взаимодействий

Продолжается анализ и интерпретация экспериментальных данных для плотности уровней и радиационных силовых функций дипольных гамма-переходов в диапазоне энергии связи нейтрона в ядрах из области масс $39<A<201$. Цель анализа: а) оценка величины и формы энергетической зависимости корреляционных функций куперовских пар нуклонов в нагретом ядре; б) экстракция потенциально доступной информации о динамике взаимодействия обычной и сверхтекучей компонент ядерной материи при изменении энергии возбуждения ядра вплоть до нейтронных резонансов.

В частности, выполнена аппроксимация плотности уровней парциальными плотностями уровней с различным числом квазичастиц с параметрами, учитывающими оболочечные неоднородности одночастичного спектра.

Оценены факторы, которые следует учитывать при прецизионной аппроксимации сумм радиационных силовых функций в различных ядрах.

Выполнено сопоставление расчетных и экспериментальных полных гамма-спектров в кобальте и железе-57. Оно продемонстрировало, что плотность уровней и радиационные силовые функции, определенные по разработанной в Дубне методике обеспечивают наилучшее воспроизведение экспериментальных данных такого типа и для легких ядер.

При содействии Дубны в Ханое выполняется подготовка к экспериментальному измерению двухквантовых каскадов захвата тепловых нейтронов.

1.7 Исследование реакций (n,p) и (n,α)

На ускорителе ЭГ-5 ЛНФ проводятся эксперименты по измерению угловых корреляций в реакции $^{14}N(n,p)^{14}C$ в области энергий нейтронов до 1 МэВ. В качестве источника нейтронов используется реакция $^{7}Li(p,n)^{7}Be$. Цель исследований – определение парциальных нейтронных и протонных ширин резонансов для спинов каналов j = 1/2 и 3/2 и, с использованием этих данных, оценка слабого матричного элемента из результатов поляризационных экспериментов, полученных ранее. Текущие (предварительные) экспериментальные значения корреляции вперед-назад получены при E_n = 450, 476, 521, 557, 627, 640, 693 кэВ и равны 0.046 ± 0.033, -0.029 ± 0.027, -0.147 ± 0.056, -0.042 ± 0.016, 0.454 ± 0.072, 0.065 ± 0.028, 0.013 ± 0.024, соответственно (см. **Рис. 18**). Достаточно высокие значения α_{fb} при E_n = 521 и 627 кэВ могут быть обусловлены нестабильностью/дрейфом энергии нейтронов в течении длительных экспозиций при измерении в направлении вперед и назад. Вместе с этими измерениями производятся работы по усовершенствованию методики с целью улучшения точности получаемых результатов. Они включают в себя как оснащение эксперимента новыми детекторами, так и отработку процедуры обработки данных. Продолжаются теоретические расчеты и компьютерное моделирование процессов.

В рамках программы по изучению механизмов ядерных реакций и получению данных для ядерной энергетики на ускорителе ЭГ-4.5 Института физики тяжелых ионов при Пекинском университете, Китай, проведены исследования реакции $^{64}Zn(n,\alpha)^{61}Ni$ для нейтронов с энергиями 2.6 и 4.0 МэВ. Источником нейтронов служили реакции $T(p,n)^{3}He$ на твердой Ti-T мишени и $D(d,n)^{3}He$ на газовой дейтериевой мишени. Получены энергетические спектры и угловые распределения α-частиц, данные обрабатываются. Завершена обработка данных предыдущих измерений при E_n = 5 и 6 МэВ, получены значения полного и дифференциального сечения реакции $^{64}Zn(n,\alpha)^{61}Ni$ для этих энергий.

Завершена обработка данных по измерению сечений реакции $^{6}Li(n,\alpha)T$ при энергии нейтронов 1,05, 1,54 и 2,25 МэВ. Работы проводятся совместно с Пекинским университетом (Китай) и Лодзинским университетом (Польша).

Подготовлено оборудование для проведения экспериментов с использованием метода времени пролета на импульсном источнике нейтронов Московской мезонной фабрики ИЯИ РАН в Троицке и затем на ИРЕН в Дубне.

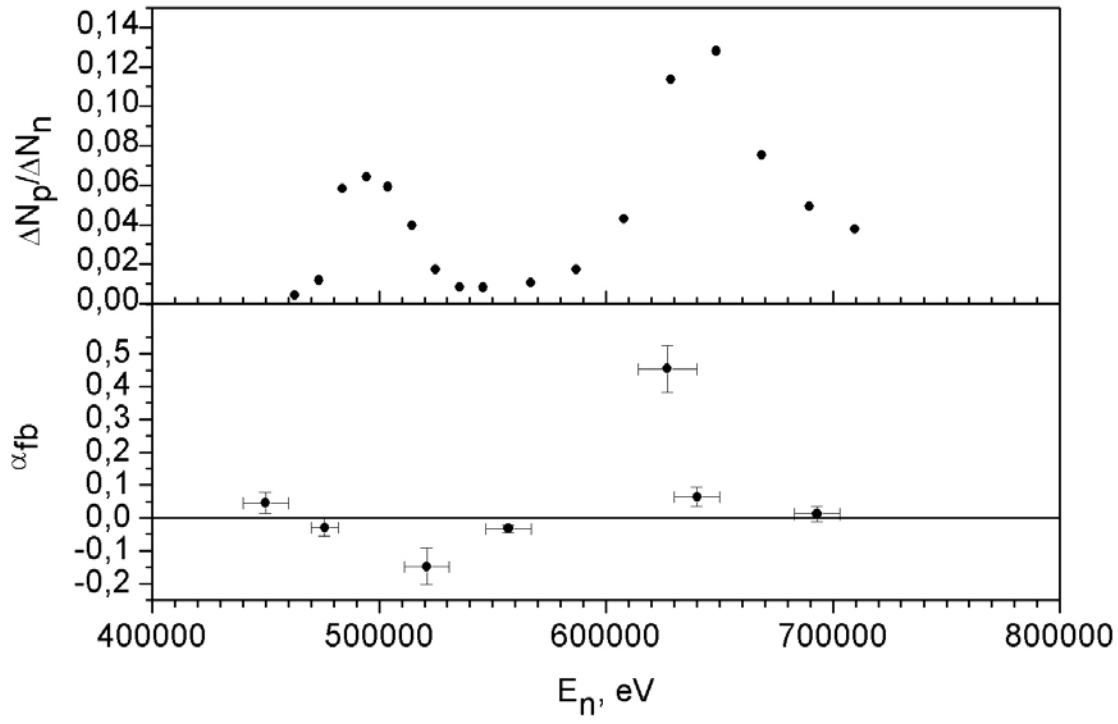

Рис. 18. *Верхний график – относительный выход протонов из реакции $^{14}N(n,p)^{14}C$; нижний график – предварительные значения корреляции вперед-назад.*

2. Теоретические исследования

Обнаружен эффект нейтростриктции в нейтронных звездах и рассчитано его влияние на параметры нейтронных звезд. Нейтрон-ядерное упругое рассеяние характеризуется, в частности, когерентной длиной рассеяния, которая приводит к оптическому потенциалу взаимодействия нейтрона со средой. Положительная длина – к отталкивающему, отрицательная – к притягивающему. Нейтрон-нейтронное рассеяние также характеризуется когерентной длиной рассеяния, и эта длина отрицательна. Следовательно, оптический потенциал внутри нейтронной звезды является притягивающим для каждого нейтрона, и он сжимает (стрикция) звезду в дополнение к гравитации. Это сжатие не приводит к коллапсу звезды, потому что длина рассеяния уменьшается с увеличением плотности, однако расчет показывает, что влияние нейтростриктции на параметры звезды может быть больше релятивизма. Кроме того, зависимость длины рассеяния от плотности приводит к таким явлениям как пульсация и взрывы. Последнее возможно при резонансной зависимости длины рассеяния от энергии нейтрона. Работа открывает новые перспективы в изучении звезд и элементарных частиц.

Найдено полное решение задачи об отражении нейтронов от среды с геликоидальной намагниченностью. Показано, что имеет место резонансное отражение с переворотом спина. На **рисунке 19** показана зависимость от волнового вектора k коэффициента отражения без переворота спина (сплошная кривая) и с переворотом (пунктирная кривая) при начальной поляризации нейтронов в направлении,

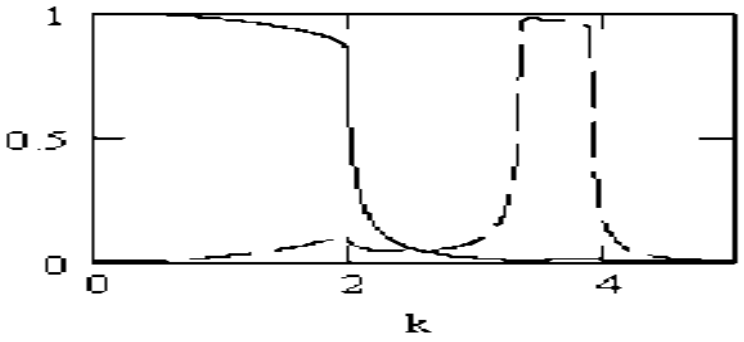

Рис. 19. *Зависимость коэффициента отражения от волнового вектора.*

противоположном оси z, которая параллельна внутренней нормали к зеркалу. При этом предполагается, что намагниченность вещества при удалении от поверхности вращается против часовой стрелки.

Продолжено теоретическое исследование процесса нуклонной перезарядки $n + p \rightarrow p + n$. В частности, с помощью оператора перестановки спиновых проекций нейтрона и протона, детально рассмотрены спиновая структура амплитуды перезарядки $n + p \rightarrow p + n$ при нулевом угле и спиновая структура амплитуды упругого рассеяния "назад" нейтрона на протоне. Получены соотношения между соответствующими коэффициентами в этих амплитудах. Установлено, что для процессов перезарядки $n + p \rightarrow p + n$ при нулевом угле и упругого *np*- рассеяния "назад" разделение дифференциального сечения на спин-зависящую и не зависящую от спина части *принципиально различно* . Именно в случае перезарядки при нулевом угле спин-зависящая часть сечения пропорциональна сечению зарядово-обменного развала дейтрона $n + d \rightarrow$

$p + (nn)$ в направлении "вперед". Спин-зависящая часть дает основной вклад в сечение перезарядки при кинетических энергиях нейтронов > 200 MeV .

Выполнен расчет спектра относительных импульсов двух конечных нейтронов при зарядово-обменном развале дейтрона $n + d \rightarrow p + (nn)$ с учетом сильного *nn*-взаимодействия в конечном состоянии, используя аналитические решения уравнения Шредингера для *S*-волновой функции дейтрона и функции относительного движения двух нейтронов в потенциалах типа прямоугольной ямы. Показано, в частности, что при малых относительных импульсах вклад *nn*-взаимодействия в конечном состоянии сильно превалирует. С ростом относительных импульсов наблюдается резкий спад функции распределения.

В 2006 году продолжалось исследование $\beta-$распада нейтрона. Для извлечения характеристик электрослабых взаимодействий из полулептонных распадов адронов необходимо точное вычисление радиационных поправок к этим процессам с последовательным учетом сильных взаимодействий и строения адронов. С этой целью в 2006 году были получены и исследованы тождества Уорда-Такахаши, связывающие вершинные части слабых распадов адронов и соответствующие собственно-энергетические части и амплитуды взаимодействия адронов с электрослабыми (калибровочными) полями. Результаты работы дают возможность определенно заключить, в какой мере учет сильных взаимодействий в электрослабых процессах может быть выполнен точно, без обращения к приближенным оценкам.

3. Прикладные и методические исследования

3.1 Исследования элементного состава и структуры приповерхностных слоёв твердых тел на ускорителе ЭГ-5

В 2006 году в сотрудничестве с Институтом Физики УМКС были выполнены эксперименты по исследованию свойств GaAs имплантированного ионами In с энергией 250 кэВ и дозой $3x10^{16}$ см$^{-2}$. Для того, чтобы определить коэффициенты диффузии индия в арсениде галлия часть образцов после имплантации подвергалась изобарическому отжигу

в атмосфере аргона при температурах 600^0 и 800^0C в течение 0,5 и 2-х часов. Затем, поверхность образцов покрывалась защитным слоем Si3N4. Исследования глубинных профилей элементов выполнялись на ускорителе ЭГ-5 с использованием методики RBS. В результате были определены неизвестные ранее коэффициенты диффузии In в GaAs в температурном диапазоне 600-800^0C. Также исследовались оптические параметры (n, k) имплантированных поверхностей GaAs с помощью элипсометрической методики.

Глубинные профили водорода, имплантированного в кремний при энергии 12 кэВ, были исследованы с помощью методики ERD на базе электростатического генератора ЭГ-5. При дозе имплантации водорода $2x10^{16}$ $см^{-2}$ оказалось возможным определить предельную атомную концентрацию, которая может быть измерена с помощью методики ERD при энергии ионов гелия 2,332 МэВ. Она составила 0,5 ат.%. При дозе имплантации водорода 10^{17} $см^{-2}$ атомная концентрация водорода в кремнии составляла 3% и определялась достаточно точно. При обработке соответствующего спектра протонов отдачи проведена оценка предельной глубины, достижимой с помощью методики ERD при энергии ионов гелия 2,332 МэВ, она составляет 2мкм.

В 2006 году продолжались также методические разработки. С целью развития техники имплантации был исследован механизм генерации ионов в плазменных источниках, их экстракции и формирования ионных пучков. В частности, для плазменного источника ионов выполнен упрощённый анализ процессов, происходящих в плазме, на основе которого получены аналитические выражения для ионного тока и эффективности ионного источника, а также указаны факторы, определяющие оба параметра.

В сотрудничестве с Электротехническим институтом Словацкой АН продолжались эксперименты по исследованию температурной стабильности слоистых структур типа $Ru/HfO_2/Si$, $Ru/HfSiO_x/Si$ и Ru/HfSiON/Si, изготовленных с помощью CMOS (complementary metal-oxide-semiconductor) технологии. Методика RBS на базе электростатического генератора ЭГ-5 позволила обнаружить существенную разницу между этими структурами. В то время как изолирующие слои состава HfO_2 показывают слабую диффузию на обеих границах уже после отжига при 800^0, структуры с $HfSiO_x$ слоями демонстрируют полную стабильность при этой температуре. А начальная диффузия этих слоёв наблюдается при температуре отжига 900^0C. Однако при отжиге до 1000^0C существенная диффузия, как в сторону подложки, так и в сторону внешнего слоя происходит у слоёв обоих типов. Это исследование показало, что присутствие атомов Si в диэлектрических слоях на основе Hf повышает термостабильность этих слоёв, что является существенным для CMOS технологии.

Разработка методики «меченых» нейтронов на втором канале ЭГ-5 и первые результаты её использования для обнаружения скрытых веществ были представлены в докладе на XVI Международной конференции по электростатическим ускорителям и пучковым технологиям в Обнинске.

Проведено исследование содержания тяжёлых элементов в зубах людей различного возраста и профессий, проживающих в различных условиях. Элементный анализ был выполнен с помощью ядерно-физических аналитических методик PIXE и RBS.

3.2 Аналитические исследования с применением метода нейтронно-активационного анализа (НАА) на реакторе ИБР-2

Биомониторинг

В рамках международной программы «Атмосферные выпадения тяжелых металлов (ТМ) в Европе – оценки на основе анализа мхов-биомониторов» завершен большой цикл работ, связанных с одновременным сбором образцов в 2005–2006 гг в ряде районов Центральной России, Южного Урала, Белоруссии, Болгарии, Словакии, Польши, Румынии, Сербии, Македонии, Хорватии и Греции для проведения многоэлементного активационного анализа на реакторе ИБР-2. Результаты анализа по 13 элементам: Al, As,

Cd, Cr, Cu, Fe, Hg, Ni, Pb, Sb, Ti, V и Zn будут переданы в Европейский Атлас атмосферных выпадений ТМ. Аналогичные исследования проведены в Монголии и Вьетнаме. Особый интерес представляют результаты анализа мхов-биомониторов из биосферных заповедников (Приокско-Террасного и Воронежского), полученные в сотрудничестве с Институтом глобального климата и экологии (Москва). Параллельно с образцами мха из заповедников проанализированы аэрозольные фильтры, что позволит установить корреляцию между элементным содержанием в воздухе и атмосферных выпадениях во мхах-биомониторах.

Проведены исследования воздушных загрязнений с помощью активного биомониторинга - экспозиции сухого мха (moss-bags) - в условиях городской среды в Познани (Польша); Байа Марэ (Румыния), Софии (Болгария), Афины (Греция) и в Дубне, в районе полигона бытовых отходов.

Оценка состояния экосистем

Завершен НАА колонок донных отложений, отобранных на шельфе Черноморского побережья Румынии. Совместно с ИФИН (Бухарест) и Бухарестским Университетом будет сделана оценка ретроспективного загрязнения этого региона.

Многоэлементный НАА коллекции аэрозольных фильтров разных лет, полученных из Братиславы, позволит охарактеризовать динамику загрязнения атмосферы столицы Словакии тяжелыми металлами за последние 15 лет.

Продолжена работа по изучению недельных циклов состояния атмосферы (элементного содержания аэрозольных фильтров) Великой Каирской долины (Египет). Новые результаты подтвердили ранее полученные данные о существовании так называемого «эффекта выходных дней», которые в арабском мире приходятся на четверг-пятницу.

Совместно с Университетом в Ополе (Польша) выполнено комплексное исследование по оценке состояния окружающей среды на «аномальной территории» на западе Польши, характеризующейся повышенным радиоактивным фоном вследствие Чернобыльской аварии и техногенным воздействием промышленности. Прослежена естественная миграция ряда элементов в почвенных разрезах, а также проведен НАА растений-биомониторов и грибов как аккумуляторов токсичных элементов.

При участии университета «Дубна» изучено распределение ряда тяжелых металлов вблизи транспортных развязок в Дубне и Москве (Щелковское и Минское шоссе).

Завершена работа по анализу 200 образцов почв из района свинцово-цинкового комбината в Македонии и построены карты распределений основных элементо-токсикантов.

Продукты питания и здоровье человека

В 2006 году завершен большой цикл работ по анализу продуктов питания из с целью оценки поступления микроэлементов в организм человека с продуктами питания (Центральная Россия) и воздействия вредных производств на качество продуктов питания (Румыния).

В рамках координационной программы МАГАТЭ «Воздействие токсичных и потенциально токсичных элементов на женщин репродуктивного возраста в развивающихся странах» (Exposure to toxic and potentially toxic elements in women of childbearing age in developing countries) совместно с Российским государственными медицинским университетом (Москва) и Аналитическим центром Геологического института РАН был проведен многоэлементный анализ образов крови 60-и специально подобранных пациентов. Анализ проводился с применением НАА на реакторах ИБР-2 в Дубне и МИФИ; свинец, кадмий и ртуть определялись методом атомной абсорбционной спектрометрии в ГИН РАН.

Биотехнологии

Совместно с Институтом физики АН Грузии получены новые результаты по определению хрома в бактериальных образцах Arthrobacter oxidans. Эти бактерии, выделяемые из природных базальтов, могут использоваться для изменения валентности хрома (перевод токсичного Cr-VI в нетоксичную форму Cr-III), что представляет большой научно-практический интерес. Эти результаты, опубликованные в журнале Analytical Chemistry (США) получили высокую оценку специалистов МАГАТЭ.

Археология

В рамках сотрудничесива с Университетом в Скопье и Музея Истории и археологии Македонии выполнен анализ керамик ритуальных сосудов (амфор) и соскобов с их внутренней поверхности. Результаты анализа позволят принять или отвергнуть гипотезу о содержимом этих амфор.

Новые материалы

Проведен НАА рубидий-содержащих соединений, используемых в экспериментах НЭОФКС по рентгеновской и нейтронной дифракции.

Учебный процесс

На базе установки РЕГАТА в радиоаналитической лаборатории на ИБР-2 в 2006 году проводился Практикум для студентов старших курсов Университета «Дубна» и Международных Школ, организуемых УНЦ ОИЯИ. За отчетный период на базе сектора НАА были выполнены 2 бакалаврских и 5 магистерских работ. В 2006 году защищены 2 кандидатские диссертации по материалам, полученным в секторе НАА.

Организация совещаний

В 2006 году велась подготовка в Международному совещанию Комиссии организации объединенных наций “The 20^{th} Task Force Meeting of the UNECE ICP Vegetation and Long-Range Atmospheric Transport of Pollutants”, которое будет проходить в Дубне в марте 2007 года.

2. NEUTRON SOURCES

2.1. PULSED REACTOR IBR-2

In the year 2006 the IBR-2 reactor operated for ~2334 hours for physical experiments (see **Table 1**).

The main results on the IBR-2 modernization in 2006:

1) The main task of the year – manufacturing of fuel assemblies (FA) for the IBR-2M reactor – has been successfully fulfilled. In July the license for manufacturing FA in JINR was obtained, and on 12.07.2006 the first FA was made in the presence of a special commission. On 16.11.2006 the work was completed: 89 FA were manufactured, which provided an initial charge of the new reactor (63 FA) and burn up margin (~ 40 %). The FLNP specialists have performed the work with a high quality.

2) In JINR EW:
   - The manufacturing of rolling shielding was completed, its check assembly and tests were carried out;

   - The control systems of the reactor were manufactured (emergency system units, compensating regulators, manual regulator).

The operation parameters of the IBR-2 reactor in 2006. ***Table 1***

№	Cycle №	1	2	3	4	5	6*	7	8	9	Всего:
	Time of cycle	**16.01–27.01.**	**13.02.–24.02.**	**13.03.–24.03.**	**10.04 – 21.04**	**16.05 – 26.05.**	**04.09. – 29.09.**	**16.10.–27.10.**	**13.11. – 27.11.**	**04.12. – 18.12**	
1	Operation for physical experiment, hr	258	261	265	259	260	142	261	316	312	2334
2	Operation of MR-3, hr	272	296	276	273	276	205	276	336	339	2549
3	Generated power, MW·hr	390	394	400	393	395	215	395	479	473	3534
4	Number of emergency shutdowns (AES)	1	0	0	1	2	1	1	1	2	9
5	Due to:										
	• Voltage drops				1	2	1	1	1	2	8
	• Instrumental malfunction or failure										
	• Electronic equipment failure	1									1
	• Personnel errors										

3) Safety Control System (SCS) of IBR-2M:
   - The prototype model of ASCS (SNIIP-SYSTEMATOM) was manufactured and tested at the IBR-2 reactor.
   - In SNIIP-SYSTEMATOM the work on standard ASCS (including a new control panel) was started.
   - In INEUM the work to develop CM system was continued.
   - In JINR EW a prototype model of KO drive was manufactured, work on a prototype model of emergency shutdown system drive is in progress.
4) Moderator complex for IBR-2M.
   The following work is in the completion stage:
   - manufacturing of CHF-700/15 in "Heliymash";
   - detail design of moderators for 3 directions: beams 2-3, beams 4-6, beams 7-11 (NIKIET);
   - design of technological part (SSDI);
   - detail design of cryogenic pipeline and intermediate heat exchanger (Heliymash).

   In FLNP the calculations and experimental work on transportation of C_9H_{12} pellets were performed; design documentation on pellet generator was worked out.
5) "The program of works at the IBR-2 reactor during temporary shutdown (2007-2010)" as well as the schedule of works on modernization of IBR-2 in this period were developed, agreed upon and approved.

The financing of works on the IBR-2 modernization in 2006 can be seen from **Table 2**.

Table 2

Financing of the IBR-2 modernization in 2006 (k$)

		1995-2005	**2006**
JINR	Plan	2840	700
	Actual	2280	675
	%	80	96
Rusatom	Plan	2370	420
	Actual	2144	420
	%	90,5	100
Total:	Plan	5210	1120
	Actual	4424	1095
	%	85	98

Plans for 2007.

1. Defueling of the IBR-2 reactor.
2. Design and manufacturing of the IBR-2M safety control system (SCS).
3. Delivery of the IBR-2M reactor vessel from NIKIET.
4. Beginning of dismantling of the primary equipment.
5. Completion of works on stationary reflectors in JINR EW.
6. Design of working documentation of cryogenic moderators in NIKIET.
7. Manufacturing and delivery of cryogenic equipment from "Heliymash".

Development of the complex of broad spectrum neutron moderators («combi-moderators») for the modernized research reactor IBR-2M in 2006:

1. The technical project of the complex of neutron moderators for IBR-2M was worked out.
2. The contract (with SSDI and "Heliymash") on the project of engineering design of the cooling system for cold moderators and the contract with the Barber-Nichols firm on the supply of helium coolant circulator were signed.
3. The project of tracing of helium tubes was fulfilled.
4. The calculations of spectral characteristics of neutron beams were completed, taking into account the real geometry of the moderators determined by the technical project.
5. The experiments to obtain spectra of cold neutrons from the moderator composed of a mixture of mesitylene and m-xylene in the temperature range from 10 K to 50 K were conducted. The results of preliminary processing were obtained.
6. The experiments to transport pellets in a gas flow both in a straight tube and in smooth bends of the tube in the range of gas rate of 5 – 12 m/s, as well as the experiments to fill the pellets into a prototype of the moderator chamber were completed.
7. The work on mathematical computer simulation of gas-dynamic forces and pulses influencing a pellet moving in the tube was performed; resistance coefficients as functions of the pellet and gas rate were obtained.
8. The concept was experimentally substantiated and the engineering documentation was worked out in order to manufacture a "pilot" copy of a device for the dosed feed of pellets.
9. The manufacturing of a "pilot" copy of the device for mass production of solid pellets of the mixture of mesitylene and m-xylene was started.

In 2006 the research and design works, which are necessary to issue the working documentation of the whole moderator complex and its technological part were completed.

Plans for 2007:

1. To publish reports and papers on research works carried out in the frameworks of the project of the complex of neutron moderators.
2. To work out (partially, according to the amount of financing) working documentation of the whole complex of moderators and its technological part.

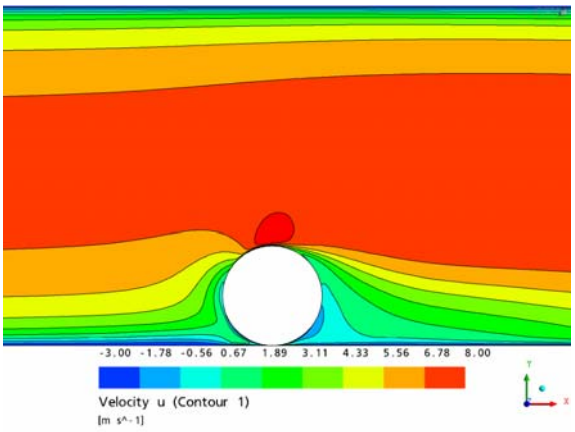

Fig.1. *Profile of gas rates (longitudinal, along the tube), when a pellet 5mm in diameter moves in the tube 17mm in diameter; gas rate – 8 m/s, pellet rate – 3 m/s.*

2.2. The IREN Project

The main tasks of the Frank Laboratory of Neutron Physics and the Laboratory of Particle Physics in 2006 were the completion of disassembling of the IBR-30 reactor and assembling of the available equipment of the first stage of the LUE-200 linac.

1. Decommissioning of IBR-30:

In accordance with the approved working schedule of the decommissioning the following works were carried out:

- «The report on the estimation of condition of the nuclear and radiation safety of the Research Pulsed Reactor IBR-30 in 2005» was prepared and submitted to the Rostehnadzor of RF.
- All the equipment from the reactor hall except for beam shutters, which will be used for the first stage of IREN, was dismantled and moved to building 117/b.
- All rooms of building 43 adjacent to the reactor hall were cleared.
- The inspection and repair of the entrance into the reactor hall were performed.
- The decontamination and preparation to the repair of the reactor hall were carried out.

Fig. 1. *The IBR-30 reactor hall in the process of fuel assembly unloading and after the preparation to the repair.*

2. Works on the LUE-200 linac:

- Theoretical substantiation of a possibility to obtain the necessary parameters of the electron beam at the first stage of the linac completed.
- The MK1 klystron modulator was mounted at the regular place and adjusted.

Fig. 2. *Mounting of the focusing solenoid (left) and electron gun (right).*

- The modulator was mounted at the regular place and also the pulsed transformer for the electron gun.
- Test assembly of the SHF path of the first section was carried out.
- Power frame of the vacuum pump system of the LUE-200 first section was completed. The test assembly was carried out.
- Test assembling and certification of the buncher coil were carried out.
- In building 43 mounting of the focusing solenoid of the first accelerating section was performed with geodetic tie.
- The electron gun was mounted at the regular place.
- By the end of the year pipeline laying-out of the water supply for the system of water-cooling and thermostabilization of LUE-200 will be completed.

3. Plans for 2007:

All the works planned for 2007 are in the framework of the approved budget of theme 0993:

- Completion of working drafts of power supply, water supply and automated radiation control (ARC) for LUE-200.
- Development of the project documentation for the non-multiplying target.
- Manufacturing and mounting of the non-multiplying target.
- To complete equipment and to mount the power and water supply systems, as well as ARC.
- Completion of repair of the room for the main control panel (MCP) and rooms 204-209, 306 in building 43.
- Repair of the hall for the non-multiplying target.
- Mounting of equipment for the automated monitoring and control system (AMCS) including MCP.
- Completion of mounting of the LUE-200 equipment: 1-st accelerating section, klystron 5045 (SLAC), SHF-feeder, intermediate areas with beam diagnostics devices, simulator of the 2-nd section, quadrupoles, transport channel, vacuum system, power supply system for electromagnets of the focusing system, magnetic spectrometer.
- Start-up and commissioning work, testing of the linac equipment.
- Complex start-up of the linac.

2. НЕЙТРОННЫЕ ИСТОЧНИКИ
2.1. ИМПУЛЬСНЫЙ РЕАКТОР ИБР-2

В 2006 г. ИБР-2 отработал на физический эксперимент ~ 2334 часа (см. таблицу 1).

Основные результаты по модернизации ИБР-2 в 2006 г.:

1) Была успешно решена главная задача года – изготовление тепловыделяющих сборок (ТВС) для реактора ИБР-2М. В июле 2006 г. была получена лицензия на изготовление ТВС в ОИЯИ, а 12.07.2006 г. собрана первая ТВС в присутствии специальной комиссии. 16.11.2006 г. работа была завершена: изготовлено 89 ТВС, что обеспечивает стартовую загрузку нового реактора (63 ТВС) и запас на выгорание (~ 40 %). Работа выполнена специалистами ЛНФ с высоким качеством.

2) В ОП ОИЯИ:
   - Завершено изготовление откатных защит, проведена их контрольная сборка и испытания;

   - Изготовлены органы регулирования реактора (блоки аварийной защиты, компенсирующие регуляторы, ручной регулятор).

Показатели работы реактора ИБР-2 в 2006 г. ***Таблица 1***

№	№ цикла	1	2	3	4	5	6*	7	8	9	Всего:
	Время цикла	**16.01–27.01.**	**13.02.–24.02.**	**13.03.–24.03.**	**10.04 – 21.04**	**16.05 – 26.05.**	**04.09. – 29.09.**	**16.10.–27.10.**	**13.11. – 27.11.**	**04.12. – 18.12**	
1	Работа на физический эксперимент, час	258	261	265	259	260	142	261	316	312	2334
2	Наработка ПО-3, час	272	296	276	273	276	205	276	336	339	2549
3	Энергонаработка, МВт·час	390	394	400	393	395	215	395	479	473	3534
4	Количество срабатываний аварийной защиты (АЗ)	1	0	0	1	2	1	1	1	2	9
5	Причины срабатываний АЗ										
	• посадки напряжения				1	2	1	1	1	2	8
	• неисправности и отказы оборудования										
	• сбои в электронной аппаратуре	1									1
	• ошибки персонала										

3) СУЗ ИБР-2М:
   - Завершен опытный образец АСУЗ (СНИИП-СИСТЕМАТОМ), проводятся его испытания на реакторе ИБР-2.
   - В СНИИП-СИСТЕМАТОМ начаты работы по штатной АСУЗ, включая новый пульт управления;
   - В ИНЭУМ продолжались работы по созданию системы контроля технологических параметров;
   - В ОП ОИЯИ изготовлен опытный образец привода КО, ведется работа над опытным образцом привода аварийной защиты.
4) Комплекс замедлителей ИБР-2М.
   В стадии завершения следующие работы:
   - Изготовление КГУ-700/15 в «Гелиймаше»;
   - Технический проект собственно замедлителей для 3-х направлений: 2-3 пучки, 4-6 пучки, 7-11 пучки (НИКИЭТ);
   - Проект технологической части (ГСПИ);
   - Рабочий проект криогенных трубопроводов и промежуточных теплообменников (Гелиймаш);

   В ЛНФ выполнены расчетные и экспериментальные работы по транспортировке шариков C_9H_{12}, разработана КД на генератор шариков.
5) Разработана, согласована и утверждена «Программа работ на реакторе ИБР-2 в режиме временного останова (2007-2010 г.г.»), а также график работ по модернизации ИБР-2 в период временного останова.

Финансовое обеспечение работ по модернизации ИБР-2 в 2006 г. видно из таблицы 2:

Таблица 2

Финансирование проекта модернизации ИБР-2 в 2006 г. (k$)

		1995-2005	**2006**
ОИЯИ	План	2840	700
	Факт	2280	675
	%	80	96
Росатом	План	2370	420
	Факт	2144	420
	%	90,5	100
Всего:	План	5210	1120
	Факт	4424	1095
	%	85	98

Планы на 2007 г.

1. Разгрузка активной зоны ИБР-2.
2. Разработка и изготовление СУЗ.
3. Поставка корпуса реактора ИБР-2М из НИКИЭТ.
4. Начало демонтажных работ по основному оборудованию.
5. Завершение работ по стационарным отражателям в ОП ОИЯИ.
6. Разработка РД криогенных замедлителей в НИКИЭТ
7. Изготовление и поставка из «Гелиймаша» криогенного оборудования.

Разработка комплекса замедлителей нейтронов широкого спектра («комби-замедлителей») для модернизируемого исследовательского реактора ИБР-2М:

1. Выполнен технический проект комплекса замедлителей нейтронов для ИБР-2М.
2. Заключен договор (с ГСПИ и «Гелиймаш») на проект технологической части охлаждения холодных замедлителей; заключен договор на поставку гелиевой газодувки фирмой Barber-Nichols.
3. Выполнен проект трассировки гелиевых труб.
4. Завершены расчеты спектральных характеристик нейтронных пучков с учетом реальной геометрии замедлителей, определенной техническим проектом.
5. Проведены эксперименты по измерению спектра холодных нейтронов из замедлителя в виде смеси мезитилена и m-ксилола при температуре от 10 К до 50 К. Получены результаты предварительной обработки.
6. Завершены опыты по транспортировке шариков в потоке газа в прямой трубе и в плавных изгибах трубы в диапазоне скоростей газа 5 – 12 м/с, а также опыты по засыпке шариков в макет камеры замедлителя.
7. Выполнена работа по математическому компьютерному моделированию газодинамических сил и моментов, действующих на шарик, движущийся в трубе; получены коэффициенты сопротивления как функции скорости шарика и газа.
8. Экспериментально обоснована концепция и подготовлена рабочая документация на изготовление «пилотного» экземпляра устройства дозированной подачи шариков.
9. Начато изготовление «пилотного» экземпляра устройства для массового приготовления твердых шариков смеси мезитилена и m-ксилола .

В 2006 году завершены исследовательские и конструкторские работы, необходимые для выпуска рабочей документация всего комплекса замедлителей и его технологической части.

В 2007 году планируется:

1. Выпустить отчеты и публикации по исследовательским работам, проведенным в ходе проекта комплекса замедлителей.
2. Выполнить (частично, в соответствии с объемом финансирования) разработку рабочей документация всего комплекса замедлителей и его технологической части.

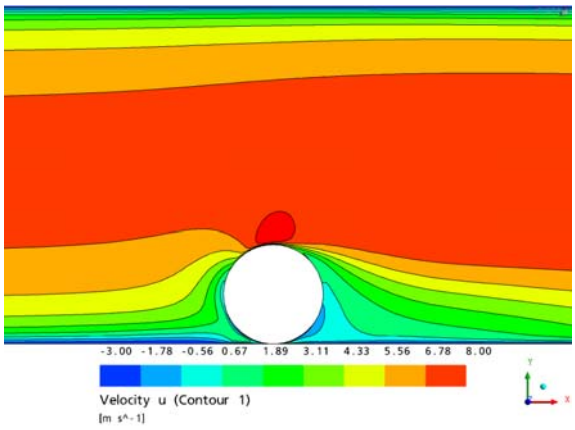

Рис.1. *Профиль скоростей газа (продольный, вдоль трубы) при качении шарика диаметром 5 мм в трубе 17 мм; скорость газа 8 м/с, шарика – 3 м/с.*

2.2. ПРОЕКТ ИРЕН

Главными задачами Лаборатории нейтронной физики и Лаборатории физики частиц в 2006 году являлось завершение демонтажа реактора ИБР-30 и монтаж имеющегося оборудования первой очереди ускорителя ЛУЭ-200.

1. Вывод из эксплуатации ИБР-30:

В соответствии с утвержденным планом-графиком вывода из эксплуатации, были выполнены следующие работы:

- Подготовлен и представлен в Ростехнадзор РФ «Отчет по оценке состояния ядерной и радиационной безопасности ИИР ИБР-30 в 2005 году».
- Демонтировано и транспортировано в здание 117/6 все оборудование из зала реактора за исключением шиберов пучков, которые будут использованы для первой очереди ИРЕН.
- Освобождены все смежные с залом реактора помещения здания 43.
- Проведена ревизия и ремонт входной двери в зал реактора.
- Проведена дезактивация и подготовка зала реактора к ремонту.

Рис. 1. *Зал реактора ИБР-30 на момент проведения выгрузки кассет и после подготовки к ремонту.*

2. Работы по ускорителю ЛУЭ-200:

- Завершено теоретическое обоснование возможности получения нужных параметров пучка электронов в 1-ой очереди ускорителя.
- Смонтирован на штатном месте и налажен модулятор клистрона МК1.

Рис. 2. *Монтаж фокусирующего соленоида (слева) и электронной пушки (справа).*

- Смонтирован на штатном месте модулятор и импульсный трансформатор для электронной пушки.
- Проведена контрольная сборка СВЧ-тракта первой секции.
- Укомплектована стойка питания системы вакуумных насосов первой секции ЛУЭ-200. Проведена контрольная сборка.
- Произведена контрольная сборка и паспортизация катушки группирователя.
- В здании 43 произведен монтаж с геодезической привязкой фокусирующего соленоида первой ускоряющей секции.
- Смонтирована на штатном месте электронная пушка.
- До конца года будет завершена прокладка трассы водоснабжения для системы водоохлаждения и термостабилизации ЛУЭ-200.

3. Планы на 2007 год:

Все запланированные на 2007 год работы находятся в рамках утвержденного бюджета по теме 0993:

- Завершение рабочих проектов электроснабжения, водоснабжения и автоматизированного радиационного контроля (АСРК) ЛУЭ-200.
- Разработка проектной документации на неразмножающую мишень.
- Изготовление и монтаж неразмножающей мишени.
- Комплектование и монтаж систем электроснабжения, водоснабжения и АСРК.
- Завершение ремонта помещения главного пульта управления (ГПУ) и комнат 204-209, 306 здания 43.
- Ремонт зала неразмножающей мишени.
- Монтаж оборудования системы автоматизированного контроля и управления (АСКУ), включая ГПУ.
- Завершение монтажа оборудования ЛУЭ-200: 1-я ускорительная секция, клистрон 5045 (SLAC), СВЧ – фидер, промежуточные участки с устройствами диагностики пучка, имитатор 2-й секции, квадрупольные линзы, канал транспортировки, вакуумная система, система источников питания э/магнитов системы фокусировки, магнитный спектрометр,.
- Пусконаладочные работы, тренировка оборудования ускорителя.
- Комплексный запуск ускорителя.

3. DEVELOPMENT AND CREATION OF ELEMENTS OF NEUTRON SPECTROMETERS FOR CONDENSED MATTER INVESTIGATIONS

In 2006 work in the framework of the theme was focused on the following main activities:

- Creation of gas and scintillation neutron detectors;
- development of sample environment systems;
- development of data acquisition systems and computing infrastructure.

1. Creation of neutron detectors

a) Gas detectors

In 2006 1-D position-sensitive detector based on multiwire proportional chamber was put into operation at the HRFD diffractometer. The software for acquisition and accumulation of data from this detector is integrated into the control software package Sonix.

A similar detector system (including a detector, electronics, PC and software) was constructed for the REFLEX spectrometer. The detector was tested on a test bench with a ^{252}Cf source and on beam 6b. At present, it is used in current measurements. In one of the experiments a study of multilayer structure [MgO / (4.7nm) Fe / (4.7nm) V] 10 / [(1ML) Fe / (1ML) V] 17 / (36.5nm) V / (2nm) Pd was carried out by the polarized neutron reflectometry technique. The coordinate spectrum is presented in **Fig. 1**. A horizontal line in the spectrum corresponds to specular neutron reflection and provides information on nuclear structure deep inside the sample (nuclear profile). A slanting line tells about the presence of non-specular (diffuse) reflection. Characteristic inhomogeneities in the sample plane (at layer interface) can be judged from it.

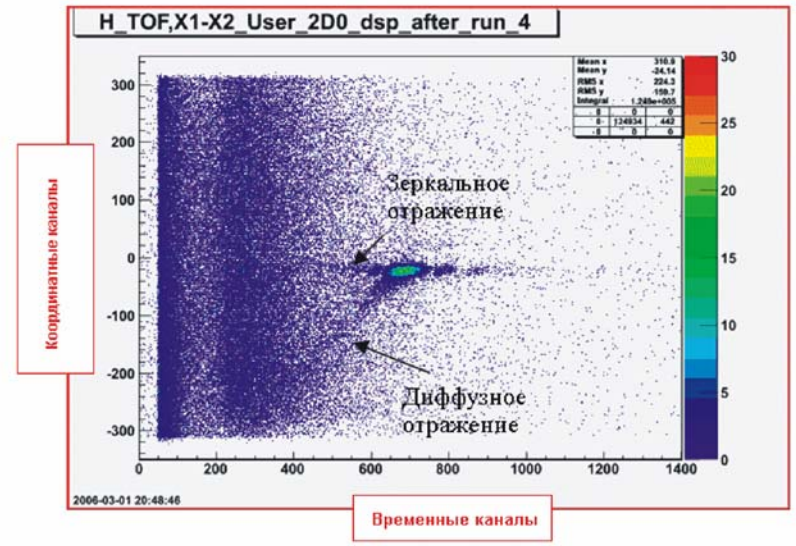

***Fig. 1**. Spectrum from [MgO/(4.7nm)Fe/(4.7nm)V]10/[(1ML)Fe/(1ML)V]17/(36.5nm)V/(2nm)Pd in the study using polarized neutron reflectometry at the REFLEX setup. A slanting line due to diffuse reflection can be seen. The scale division value of coordinate channel is 0.32 mm. The scale division value of time channel is 64 μs.*

Using the same technology, 2D PSD with a sensitive area of 225×225 mm^2 was developed. On the basis of experience gained in the process of development and tests of 1D PSD and 2D monitor, the following characteristics of 2D detector (**Table 1**) were specified:

Table 1

Gas mixture	2000 mbar He^3+2000mbar CF_4
Efficiency	60%
Sensitive area	225×225 mm^2
Coordinate resolution X,Y	2-3 mm
Count rate	Up to 10^6 events/s.
Differential nonlinearity	<10%
Readout	Delay lines, start from anode

The design and engineering documentation of the detector case, anode and cathode electrodes was worked out. All mechanical units were manufactured in JINR EW. **Figure 2** shows an assembly drawing of the detector.

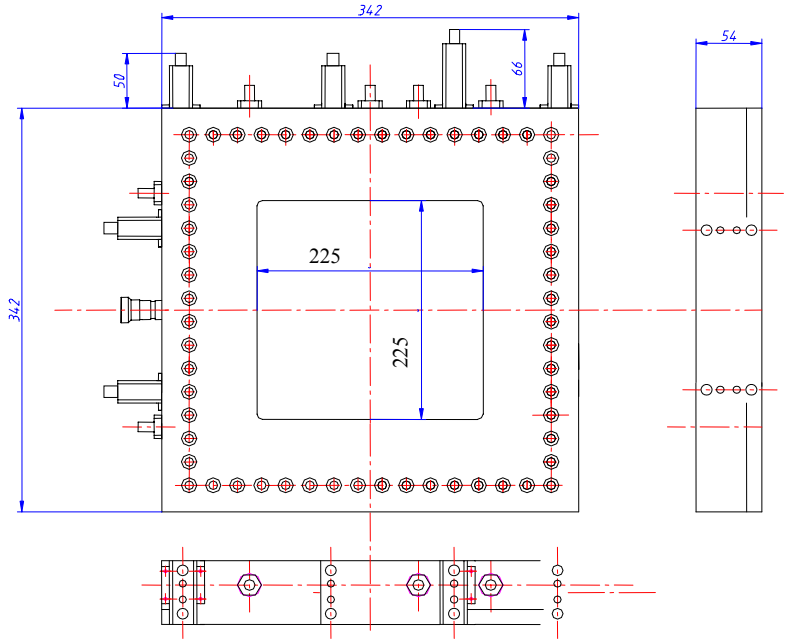

Fig. 2. *Assembly drawing of 2D detector.*

The detector is a multiwire proportional chamber with delay line data readout. Overall dimensions of the chamber are 342×342×54 mm. The entrance window is 7 mm thick, which only minimally weakens an incident neutron flux and makes it possible to endure mechanical loads that arise when filling the detector with a gas mixture. High voltage of positive polarity is fed via an MHV connector. Five BNC connectors serve for signal output. The detector has 2 gas connectors of the "Swagelock" type and this permits the use of the detector in a flow-operating mode.

In the chamber volume two cathode, two drift and one anode electrodes are positioned. Each of the electrodes is a textolite frame with a cut window with wound fine wires of gold plated tungsten for anode and cathode planes and a mylar film with aluminum spray coating for drift planes. The thickness of anode wires is 10 μm and of the cathode wires – 50 μm. The anode wire spacing is 1 mm. A common bus connects the anode wires. The cathode wire spacing is 1 mm. The cathode wires are connected together in pairs and brought out to the delay line, each unit of which delays signals by 2.9 ns. The distance between the electrodes is 3 mm; the anode is positioned in the middle. The drift electrodes are placed close against the detector walls, which rules out the presence of a shielding gap of working mixture. To detect neutrons, the chamber volume is filled with a

mixture of neutron converter gas He^3 and quenching gas CF_4. The total pressure of the gas mixture is 4000 mbar.

The detector was tested at a pressure of up to 6 atm. The technological degassing procedure was carried out. Limit voltages at anode are +4500V and -2000V at drift electrodes, working voltages are 3400V and 1000V, respectively.

Signals from both delay lines and an anode signal through preamplifiers come to a constant fraction timing five-channel discriminator and are registered in data acquisition and accumulation block (DAAB). This block contains signal level converter NIM-TTL, 8-channel integrated time-to-code converter (TDC-GPX) with time resolution of 80 ps and count rate of 10M events/s; field programmable gate array (FPGA) containing about 6K of logic elements; 1 Gbyte histogram memory, which makes it possible to accumulate three-dimensional spectra X-Y-TOF of up to 512×512×1024 32-bit words; and high-speed interface with optical communication link to a personal computer (**Fig. 3**). The data acquisition and accumulation system can operate in two modes: in the mode of histogram accumulation in internal memory and in the list mode, when "raw" data are accumulated directly on a PC hard disk.

All functions of the block are programmable. Different versions of firmware programs are recorded by the PC control program into FPGA, which makes it possible to realize various functions and to use this block for data accumulation both from 1D and 2D detectors without any changes in hardwareAmong the firmware programs are the programs for digital signal processing, data filtering, for counting the number of accepted and rejected events, for recording data in required format, etc. The multilevel modular structure of PC-programs allows modules of lower levels having access to hardware to be integrated into other program complexes. The software of the upper level provides a full set of functions that make it possible to set parameters, to choose several variants of measurement modes, to visualize data on-line, to store information and to protocol the operation of the system. The main distinction of the DAAB software as compared to that of the PCI DAQ block now in use is that DAAB has no digital signal processor (DSP), which essentially reduces data accumulation rate (down to 100K events/s). In the new version of the block the functions of DSP (filtering, histogramming, data formatting, etc.) are performed by FPGA.

The use of very large-scale integration circuits has made it possible to mount DAAB on one six-layer printed board of the NIM standard (182.9×150 mm^2). Optical receiver-transmitters and parallel-serial and serial-parallel converters are placed on a daughter board (mezzanine), which allows the use of interfaces of various types without changing the block circuit design. The counterpart of an optical interface is installed directly in a computer.

Logic and time simulation of operation of the block was performed using Quartus II package from ALTERA. It was shown that the rate of reception, filtering and accumulation of events in the block may amount to 2 million events/s. Real registration rate (taking into account data transfer and recording to a computer) is no less than 1 million events/s. The detector was tested on a test bench. Tests on an IBR-2 beam with the available DAQ board were carried out in December. Tests of DAAB are scheduled for the first half of 2007.

Electronics and software of the microstrip detector were debugged. A series of tests of the detector on a test bench and on an IBR-2 beam were conducted.

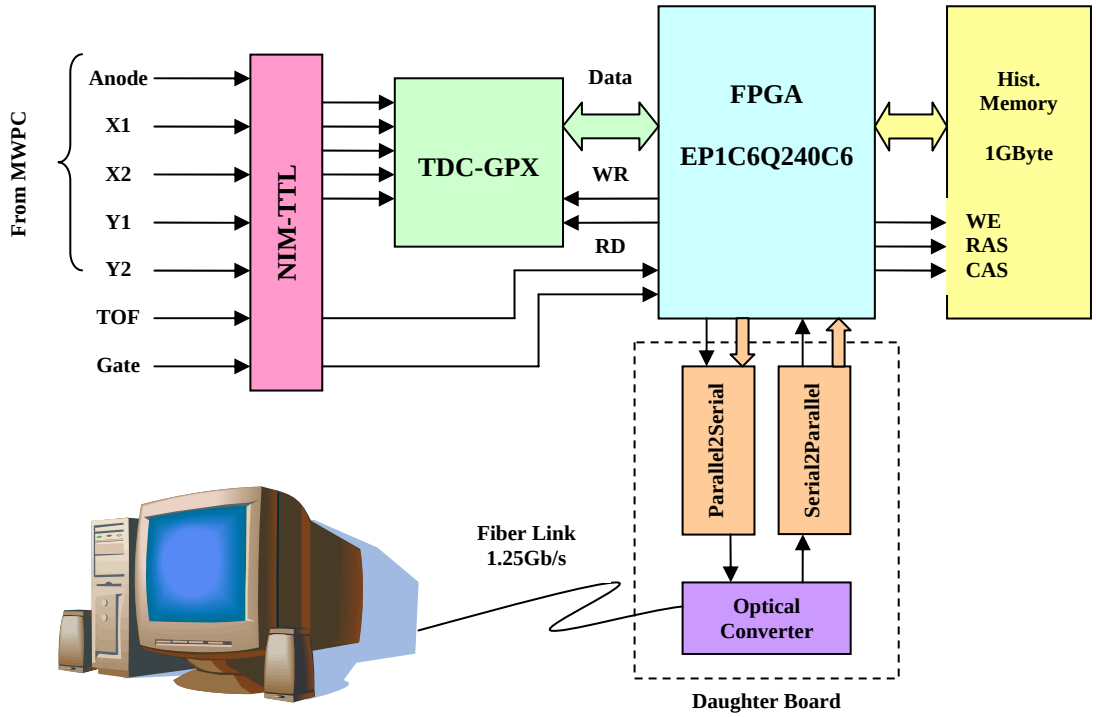

Fig. 3. *Architecture of data acquisition and accumulation system from PSD.*

b) Scintillation detectors

The 4-th and 3-rd sections of the FSD diffractometer were designed. The detector modules were not manufactured for lack of financing.

The design of the detector system for the DN-6 diffractometer was developed. It has provision for using 2 groups of detectors located in the region of scattering angle of 90° and scattering angle of 45° (laboratory system). The 3D model of the detector system is given in **Fig. 4**.

In cooperation with the Institute of Metal Physics RAS (Yekaterinburg) 100-channel scintillation thermal neutron detector for the D7A spectrometer located at the IVV-2M reactor of Sverdlovsk branch of NIKIET was developed, manufactured and put into operation.

The detector is constructed on the modular principle, which makes it possible to arrange channel sensitive areas on a cylindrical surface of arbitrary radius. The channel sensitive volume is a multilayer composition of plates of scintillation screen ND and spectrum-shifting fibers. Dimensions of entrance aperture of channel sensitive area are S = 3 × 120 mm. Average detection efficiency in channels for neutrons with a wavelength of $\lambda = 1.53$ Å is $\eta = 70$ %. Gamma sensitivity of the detector channels does not exceed $\xi \leq 1 \cdot 10^{-7}$. Maximum count rate of a single channel is no less than $\nu \geq 1 \cdot 10^{5}$ n/s. Each module of the detector is an independent device and contains 10 neutron detection channels, signal processing electronics, high-voltage power supply system and computer communication electronics. Data acquisition from modules, setting of detection parameters and control over modules are carried out via interface CAN.

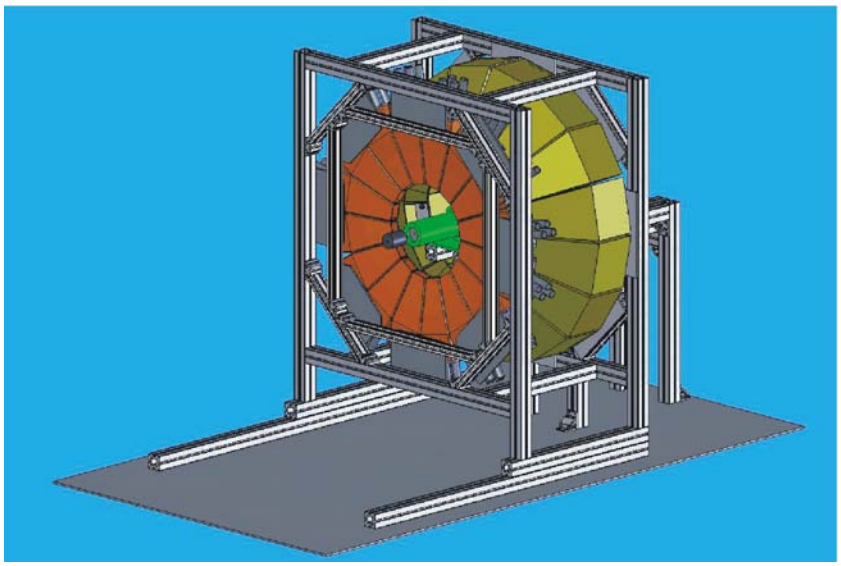

***Fig. 4**. Three-dimensional model of the detector system for the DN-6 diffractometer.*

2. Development of sample environment systems

In 2006 the following devices were included into the structure of control systems of spectrometer actuators:

- a device for placing a scatterer into a neutron beam in front of PSD at the YuMO spectrometer (**Fig. 5**);
- a device for rotating about vertical and horizontal axes and for vertical sample movement on the basis of the HUBER goniometer at the SKAT spectrometer.

Controller SMC-32-CAN for control systems of spectrometer actuators was developed and tested.

On beam 9 the modernization of the chopper control system was carried out on the basis of direct-current electric drive. More stable amplifiers of the electric drive were included into the structure of the system. The control system software was replaced.

***Fig. 5.** Device for placing a scatterer into a neutron beam.*

In 2006 a closed-cycle cryostat with cryocooler PT-405 with pulse tubes was manufactured for operation in a temperature range of 8-300K. Its construction allows it to be installed in the shaft of the DN-2 spectrometer. **Figure 6** shows this cryostat before sinking it into the shaft. The cryostat was used to obtain spectra of scattered neutrons from mesitylene, which is considered to be the most promising material for cold moderators of the modernized reactor IBR-2M.

Fig.6. *Cryostat.*

3. Development of data acquisition systems and computing infrastructure

A new central server *Sun Fire X4200* (AMD-64 platform) with the operating system *OS Solaris 2.10* and bulk storage device *Storage Array* (6.4 T byte) were put into service. The replacement of the basic server of the FLNP computer cluster (*Enterprize 3000*) by the modern system on the basis of AMD Opteron 64 and the use of bulk storage device made it possible to significantly enhance computing power of the cluster and to increase the shared disk space. At present, the former central server is used for work with applications written for the old operating system.

The first stage of work to create a new architecture of the FLNP computer cluster and to optimize network communication lines was fulfilled (**Fig. 7**). A change-over of the available switches of the central network core to routing switches Cisco 3750, the installation of 1Gbit/s interface to switch Cisco 8510 CSR and the application of high-speed communication in the main FLNP LAN links made it possible to enhance the reliability of network operation and to provide connection with the JINR network and other networks at Gigabit rates. The reorganization of the FLNP Web server was carried out as well.

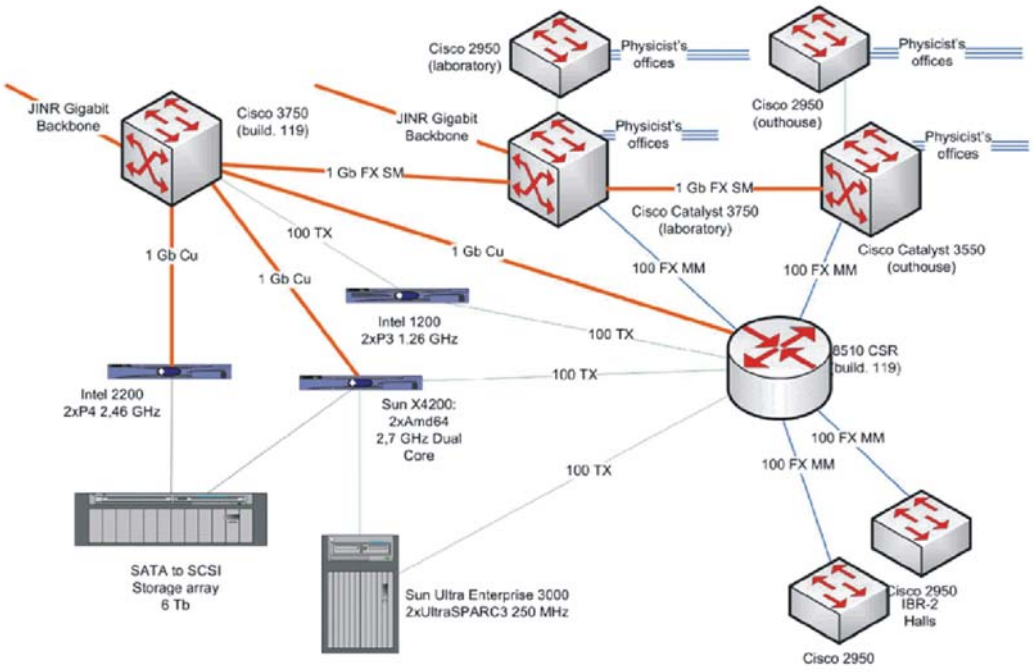

Fig. 7. *New architecture of FLNP LAN.*

A large amount of work to manufacture and adjust blocks of analog electronics for gas detectors and monitor counters was carried out.

A new electronic block for data acquisition from multi-counter systems was designed. Digital simulation of the block for accumulating data from 64 counters was performed.

The following work was conducted on the data acquisition system software.

- Position-sensitive detectors under the Sonix+ software (PC, Windows) were put into operation at the YuMO and HRFD spectrometers.
- A version of Sonix+ for the DSD spectrometer (IMP RAS Yekaterinburg) was prepared and tested in Dubna.
- Work to install the Sonix+ complex at the MOND diffractometer (SSC RRC KI, Moscow) started.
- The software complex Sonix+ was elaborated in its service part and upgraded to improve its performance characteristics.
- Work to design the software for remote control over experiments at the IBR-2 spectrometers via network started.

Electronic and software support was constantly provided during the IBR-2 reactor cycles.

The following main problems are to be solved in the year 2007 in the framework of the theme:

1. Design of neutron position-sensitive detector based on multi-wire proportional chamber with individual data readout from each wire (design and manufacturing of the detector case and electrodes, design of read-out electronics and data acquisition electronics, purchase of materials and components).

2. Creation of module scintillation detector on the basis of matrix photomultipliers (development of the detector design, design of data accumulation electronics, measurement of characteristics of the assembly – matrix photomultiplier + scintillation screen).
3. Manufacturing of 8 modules of the ASTRA detector for the FSD diffractometer.
4. Creation (in cooperation with PNPI) of bent reflector neutron guide on beam 7a of the IBR-2 reactor (calculations and selection of a variant of optical channel, design, purchase of materials, manufacturing of optical elements (PNPI) and mechanical constructions of the head part of the neutron guide).
5. Modeling, manufacturing and testing of electronic blocks for multicounter systems and PSD with delay lines.
6. Creation of cable infrastructure of the network segment of the IBR-2 experimental halls (Gigabit Ethernet).
7. Development of a control block of actuating mechanisms of the IBR-2 spectrometers on the basis of industrial standard CAN.
8. Modernization and support of infrastructure of engineer and programmer work places.
9. Creation of vacuum test bench to improve “cryogen free” technology for the IBR-2M spectrometers.
10. Development of the Sonix+ software package for remote control over experiments.

3. РАЗРАБОТКА И СОЗДАНИЕ ЭЛЕМЕНТОВ НЕЙТРОННЫХ СПЕКТРОМЕТРОВ ДЛЯ ИССЛЕДОВАНИЯ КОНДЕНСИРОВАННЫХ СРЕД

Работы по теме велись в следующих основных направлениях:

— Создание газовых и сцинтилляционных нейтронных детекторов;
— развитие систем окружения образца;
— развитие систем сбора данных и вычислительной инфраструктуры.

1.Создание нейтронных детекторов

а) Газовые детекторы

В 2006 г. на дифрактометре ФДВР введен в эксплуатацию разработанный ранее однокоординатный позиционно-чувствительный детектор на основе многопроволочной пропорциональной камеры.Программное обеспечение для сбора и накопления данных с этого детектора интегрировано в управляющий комплекс Sonix.

Аналогичная детекторная система, включающая в себя собственно детектор, электронику, PC и программное обеспечение, была создана для спектрометра РЕФЛЕКС. Детектор был протестирован на стенде с источником ^{252}Cf и на пучке №6б ИБР-2, в настоящее время на нем ведутся рабочие измерения. В одном из экспериментов проводилось исследование многослойной структуры [MgO / (4.7nm) Fe / (4.7nm) V] 10 / [(1 ML) Fe / (1 ML) V] 17/(36.5nm) V / (2nm) Pd методом рефлектометрии поляризованных нейтронов. Координатный спектр, полученный при данном измерении, приведен на **рис.1**. Горизонтальная линия на спектре соответствует зеркальному отражению нейтронов, и дает информацию о ядерной структуре вглубь образца (ядерном профиле). Наклонная линия говорит о наличии незеркального (диффузного) отражения. По ней можно судить о характерных неоднородностях в плоскости образца (на границе раздела слоев).

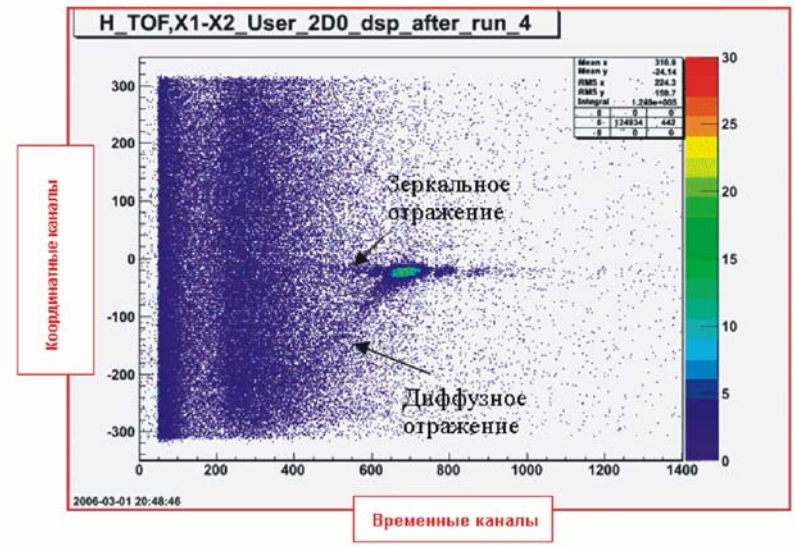

***Рис.1**. Спектр от [MgO/(4.7nm)Fe/(4.7nm)V]10/[(1ML)Fe/(1ML)V]17/(36.5nm)V/(2nm)Pd при исследовании с помощью метода рефлектометрии поляризованных нейтронов на установке «РЕФЛЕКС» Видна линия, обусловленная диффузным отражением. Цена деления координатного канала 0,32 мм. Цена деления временного канала 64 микросекунды.*

По такой же технологии была выполнена разработка двухкоординатного ПЧД с размерами чувствительной области 225x225 мм^2. На основе опыта, полученного при разработке и испытаниях

1D ПЧД и 2D монитора, были заданы следующие технические характеристики двухкоординатного детектора (**Табл.1**):

Таблица 1

Газовая смесь	2000 мбар He^3+2000мбар CF_4
Эффективность	60%
Чувствительная область	225×225 $мм^2$
Координатное разрешение X,Y	2-3 мм
Скорость счета	до 10^6 соб./с
Диффер. неоднородность	<10%
Съем сигнала	Линии задержки, старт от анода

Разработана конструкторская и технологическая документация на корпус детектора, анодный и катодные электроды. Все механические узлы изготовлены в ОП ОИЯИ. На **рис.2** показан сборочный чертеж детектора.

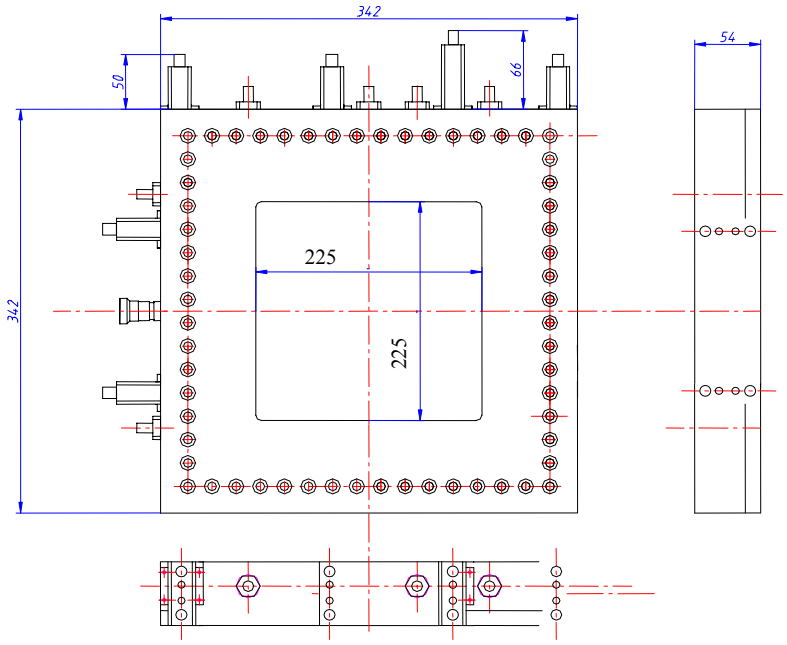

Рис.2. *Сборочный чертеж 2D детектора.*

Детектор представляет собой многопроволочную пропорциональную камеру со съемом информации с линий задержки. Внешние габариты камеры составляют 342×342×54 мм, толщина входного окна 7 мм, что в минимальной степени ослабляет падающий нейтронный поток, и позволяет выдерживать механические нагрузки, возникающие при заполнении детектора газовой смесью. Высокое напряжение положительной полярности подается через разъем MHV, для вывода сигналов служат 5 разъемов BNC. Детектор имеет 2 газовых разъема типа «Swagelock», что позволяет использовать его в проточном режиме работы.

В объеме камеры расположены два катодных, два дрейфовых и один анодный электроды. Каждый из электродов представляет собой текстолитовую рамку с выфрезерованным окном, в котором натянуты тонкие проволоки из позолоченного вольфрама, для анодной и катодных плоскостей, и майларовая пленка с алюминиевым напылением, для дрейфовых плоскостей. Толщина анодных проволочек 10 микрон, катодных – 50 микрон. Анодные проволочки намотаны с шагом 1 мм и соединены общей шиной, катодные проволочки намотаны с шагом в 1 мм,

объединены по две и выведены на линию задержки, одно звено которой задерживает на 2,9 наносекунд. Расстояние между электродами составляет 3 мм, анод расположен посередине. Дрейфовые электроды прижаты к стенкам детектора, что, практически, исключает наличие экранирующего промежутка рабочей смеси. Для регистрации нейтронов внутренний объем камеры заполнен смесью, состоящей из газа-конвертера нейтронов He^3 и гасящего газа CF_4. Полное давление газовой смеси 4000 миллибар.

Детектор испытан на давление до 6 атм. Проведена технологическая процедура обезгаживания. Предельные напряжения на аноде составляет +4500В, на дрейфовых электродах -2000В, рабочие напряжения 3400В и 1000В соответственно.

Сигналы с обоих концов линий задержки и анодный сигнал усиливаются и формируются предусилителями, установленными на корпусе детектора. Затем эти сигналы поступают в пятиканальный дискриминатор с точной временной привязкой и далее регистрируются в блоке сбора и накопления данных (БСНД). Этот блок содержит преобразователь уровня сигналов NIM-TTL, 8-канальный интегральный преобразователь время-код (TDC-GPX) с временным разрешением 80пс и быстродействием 10М событий/с; программируемую логическую матрицу (FPGA), содержащую порядка 6К логических элементов; гистограммную память емкостью 1Гбайт, которая позволяет накапливать трехмерные спектры X-Y-TOF размером до 512×512×1024 32-разрядных слов; и высокоскоростной интерфейс с оптической линией связи к персональному компьютеру (**рис**.**3**). Система сбора и накопления данных предусматривает два режима работы: режим гистограммирования во внутренней памяти блока и списочный режим, при котором “сырые” данные накапливаются непосредственно на диске персонального компьютера (PC).

Все функции блока являются программируемыми. Различные версии firmware программ записываются управляющей программой PC в FPGA, что позволяет реализовать различные функции и использовать этот блок для накопления данных как с 1D, так и с 2D детекторов без каких-либо изменений в hardware. К числу firmware программ относятся программы цифровой обработки сигналов, фильтрации данных , счета числа принятых и отбракованных событий, записи данных в требуемом формате и др.. Многоуровневая модульная структура PC-программ позволяет встраивание модулей нижних уровней, производящих обращения к аппаратуре, в другие программные комплексы. На верхнем программном уровне реализованы функции задания параметров, выбора нескольких вариантов режимов измерений, on-line визуализации, сохранения данных и протоколирования работы системы. Главное отличие в программном обеспечении БСНД по сравнению используемым в настоящее время блоком PCI DAQ состоит в том, что в БСНД нет цифрового сигнального процессора (ЦСП), который существенно ограничивал скорость накопления данных (до 100К соб./с). В новой версии блока функции ЦСП (фильтрация, гистограммирование, форматирование данных и др.) выполняет FPGA.

Благодаря использованию схем сверхбольшой интеграции, БСНД смонтирован на одной шестислойной печатной плате стандарта NIM (182,9 x 150 мм²). Оптические приемо-передатчики и преобразователи кодов (параллельного кода в последовательный и наоборот) размещены на дочерней плате (мезонине), что позволяет использовать различные типы интерфейсов, не меняя схемотехнику самого блока. Ответная часть оптического интерфейса монтируется непосредственно в компьютере.

Логическая и временная симуляция работы блока выполнена с использованием пакета Quartus II фирмы ALTERA. В результате показано, что скорость приема, фильтрации и сборки событий в блоке достигает 2 млн. соб./с. Реальная скорость регистрации (с учетом передачи и записи данных в компьютер) составляет не менее 1 млн.соб./с. В настоящее время детектор собран и проверен на стенде, испытания на пучке планируется провести в декабрьском цикле ИБР-2 с существующей платой DAQ. Тестирование БСНД будет выполнено в первом полугодии 2007 г.

Завершена отладка электроники и программного обеспечения микростripового детектора, а также проведена серия стендовых испытаний детектора. В декабре будут проведены испытания на пучке ИБР-2.

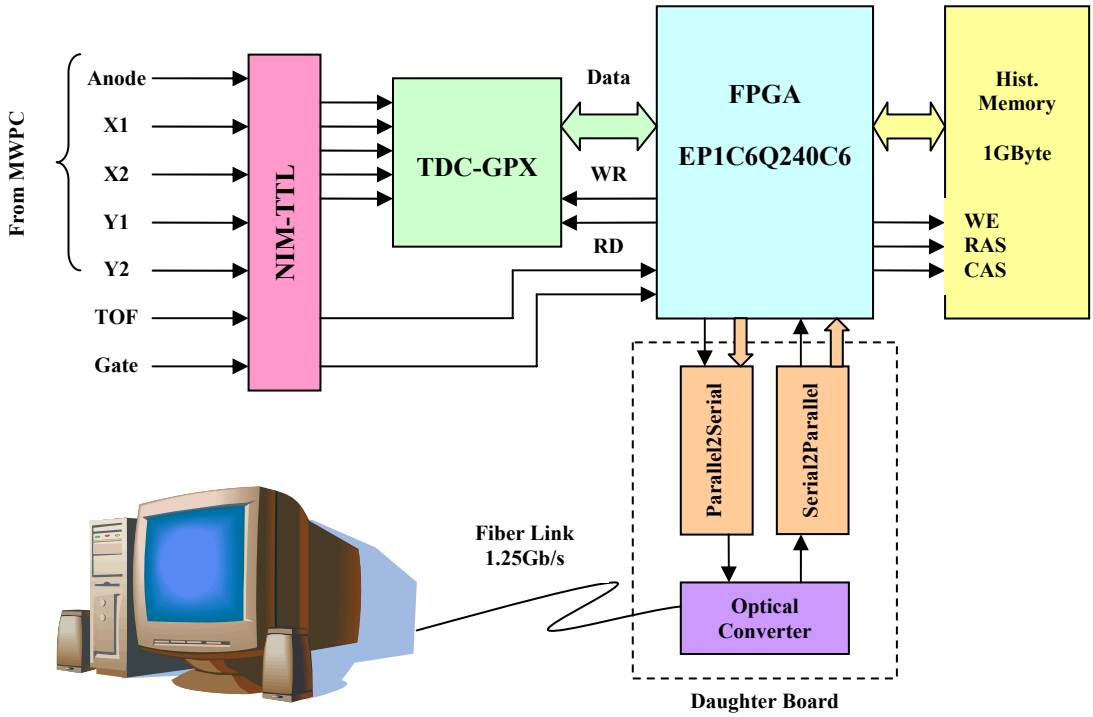

Рис.3. *Архитектура системы сбора и накопления данных с ПЧД.*

б) Сцинтилляционные детекторы

Разработана конструкция 4-й и 3-й секций дифрактометра ФСД, изготовление модулей детектора не проводилось из-за отсутствия финансирования.

Разработана конструкция детекторной системы дифрактометра ДН-6. В конструкции предусмотрено использование 2 групп детекторов – расположенных в области угла рассеяния 90 градусов и угла рассеяния 45 градусов (лабораторная система). Трехмерная модель детекторной системы представлена на **рис. 4**.

Совместно с Институтом физики металлов РАН (Екатеринбург) разработан, изготовлен и сдан в эксплуатацию 100-канальный сцинтилляционный детектор тепловых нейтронов для спектрометра Д7А , установленного на реакторе ИВВ-2М Свердловского филиала НИКИЭТ. Детектор построен по модульному принципу, что позволяет разместить чувствительные поверхности каналов на цилиндрической поверхности с произвольным радиусом. Чувствительный объем канала представляет собой многослойную композицию из пластин сцинтилляционного экрана ND и спектросмещающих волокон. Размеры входной апертуры чувствительной области канала S = 3 × 120 мм. Средняя эффективность регистрации в каналах для нейтронов с длиной волны λ = 1.53 Å составляет η = 70%. Гамма чувствительность каналов детектора не превышает $\xi \leq 1 \cdot 10^{-7}$. Максимальная скорость счета отдельного канала не менее $\nu \geq 1 \cdot 10^{5}$ н./сек. Каждый модуль детектора представляет собой независимое устройство и содержит 10 каналов регистрации нейтронов, электронику обработки сигнала, систему высоковольтного питания и электронику связи с компьютером. Сбор информации с модулей, установка параметров регистрации и управление модулями осуществляются по интерфейсу CAN.

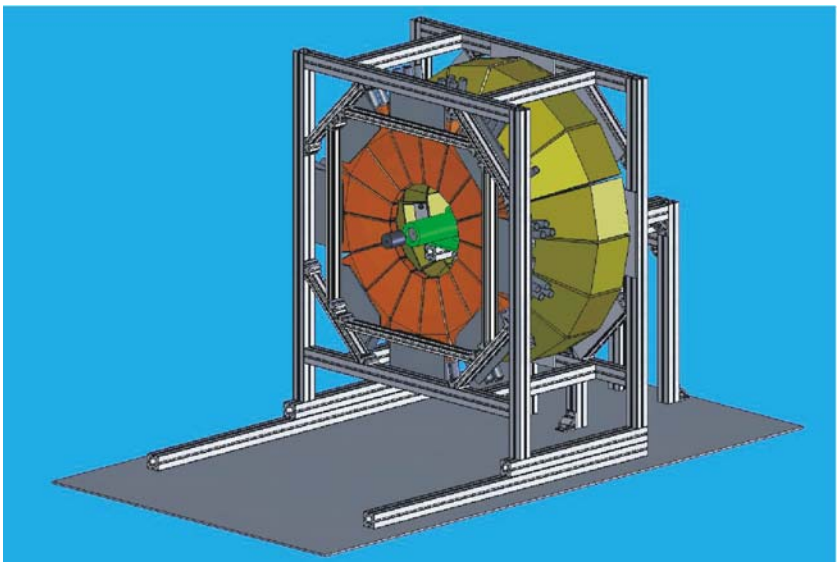

Рис. 4*. Трехмерная модель детекторной системы дифрактометра ДН-6.*

2.Развитие систем окружения образца

В 2006 г. в состав систем управления исполнительными механизмами спектрометров введены:

- устройство ввода рассеивателя в нейтронный пучок перед ПЧД детектором спектрометра ЮМО (р**ис.5**).
- устройство вращения вокруг вертикальной и горизонтальной осей и вертикального перемещения образца на базе гониометра HUBER спектрометра СКАТ.

Рис.5. *Устройство ввода рассеивателя в нейтронный пучок.*

Выполнена разработка и проведены испытания контроллера SMC-32-CAN прототипа контроллера систем управления исполнительными механизмами спектрометров при их модернизации во время остановки реактора ИБР-2.

На 9 пучке проведена модернизация системы управления прерывателем на базе электропривода постоянного тока. В состав системы включены более стабильные усилители электропривода. Проведена замена программного обеспечения системы управления.

В 2006 г. был изготовлен криостат на основе замкнутого цикла с криокулером РТ-405 на импульсных трубках для работы в диапазоне 8-300К. Криостат выполнен в виде, пригодном для установки его в шахту спектрометра ДН-2. На **рис. 6** показан этот криостат перед погружением в шахту ДН-2. Криостат был использован для проведения измерений спектров рассеянных нейтронов на мезитилене, который рассматривается как наиболее перспективный материал для холодных замедлителей модернизированного реактора ИБР-2.

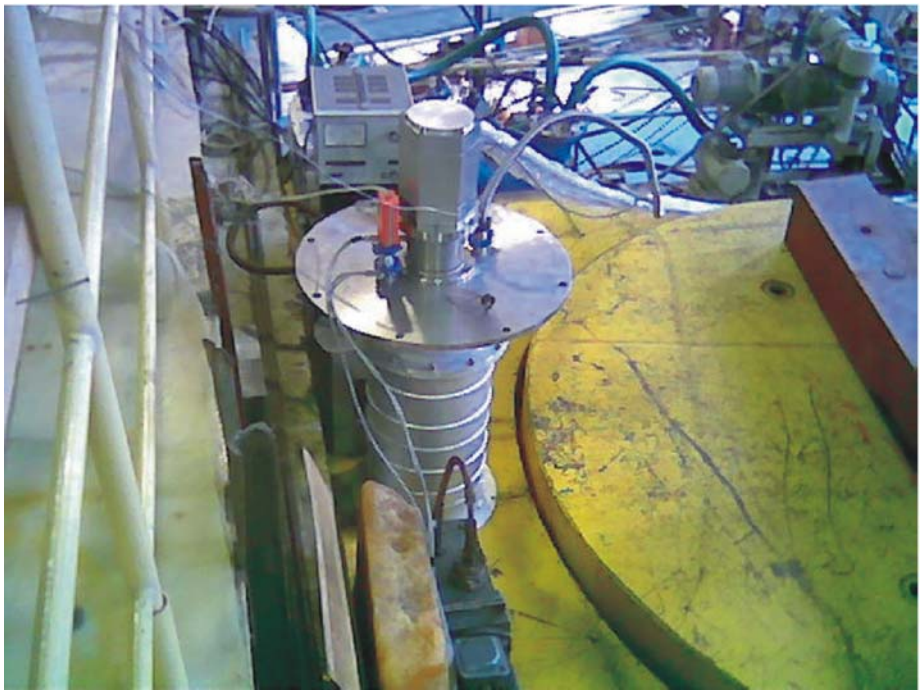

Рис.6. *Криостат.*

3. Развитие систем сбора данных и вычислительной инфраструктуры

Новый центральный сервер *Sun Fire X4200* (AMD-64 platform) с операционной системой *OS Solaris 2.10* и устройством массовой памяти *Storage Array* (6.4 T byte) введен в эксплуатацию. Замена базового сервера компьютерного кластера ЛНФ (*Enterprise 3000*) на современную систему на основе AMD Opteron 64 и использование массовой памяти позволило значительно увеличить вычислительную мощность кластера и расширить предоставляемое пользователям дисковое пространство. Бывший центральный сервер используется в настоящее время для работы с приложениями, написанными под старую операционную систему.

Выполнен первый этап работ по созданию новой архитектуры компьютерного кластера ЛНФ и оптимизации коммуникационных линий сети (**рис.7**). Замена существующих коммутаторов центрального ядра сети на маршрутизирующие коммутаторы Cisco 3750, установка 1Гбит/с интерфейса в коммутатор Cisco *8510 CSR* и применение высокоскоростных соединений на основных линиях сети позволили повысить надежность сетевых операций и обеспечить связь с сетью ОИЯИ и другими сетями на гигабитных скоростях. Была также выполнена реорганизация Web сервера ЛНФ.

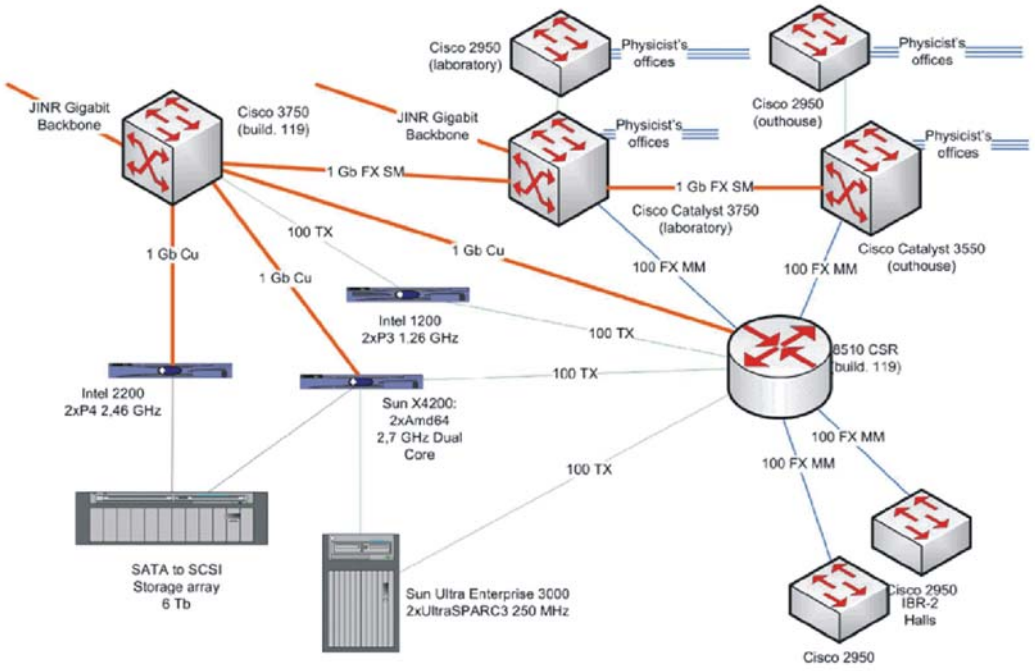

Рис.7. *Новая архитектура LAN ЛНФ.*

Выполнен большой объем работ по изготовлению и наладке блоков аналоговой электроники для газовых детекторов и мониторных счетчиков.

Разработан новый электронный блок для сбора данных с многосчетчиковых систем. Проведено цифровое моделирование блока для накопления данных с 64-х счетчиков.

По программному обеспечению систем сбора данных выполнены следующие основные работы:

- на спектрометрах ЮМО и ФДВР введены в эксплуатацию ПЧД под управлением Sonix+ (PC, Windows);
- подготовлена и протестирована в Дубне версия Sonix+ для спектрометра ДСД (ИФМ РАН, Екатеринбург).
- начаты работы по постановке комплекса Sonix+ на нейтронный диффрактометр МОНД (РНЦ им Курчатова, Москва).
- программный комплекс Sonix+ был дополнен в сервисной части, а также усовершенствован для улучшения эксплуатационных характеристик.
- начата разработка программного обеспечения для удаленного наблюдения за экспериментами на спектрометрах ИБР-2 по сети.

Во время циклов ИБР-2 постоянно осуществлялась электронная и программная поддержка экспериментов.

Основные задачи по теме в 2007 г.:

1. Разработка позиционно-чувствительного детектора нейтронов на основе многопроволочной пропорциональной камеры с индивидуальным считыванием информации с каждой нити (проектирование и изготовление корпуса и электродов детектора, проектирование readout электроники и электроники сбора данных, приобретение материалов и комплектующих изделий).

2. Разработка и изготовление (совместно с ИЯИЯЭ БАН, София) элементов изогнутого позиционно-чувствительного детектора рентгеновского излучения.
3. Создание модульного сцинтилляционного детектора на основе матричных фотоумножителей (разработка конструкции детектора, проектирование регистрирующей электроники, измерение характеристик сборки – матричный ФЭУ + сцинтилляционный экран).
4. Изготовление 8 модулей детектора АСТРА для дифрактометра ФСД.
5. Создание изогнутого зеркального нейтроновода на канале 7а реактора ИБР-2 (расчеты и выбор варианта оптического канала, проектирование, приобретение материалов и оптических элементов, изготовление механических конструкций головной части нейтроновода, демонтаж старого нейтроновода).
6. Моделирование, изготовление и тестирование электронных блоков для многосчетчиковых систем и ПЧД с линиями задержки.
7. Создание кабельной инфраструктуры сетевого сегмента экспериментальных залов ИБР-2 (Гигабит Ethernet).
8. Разработка системы управления исполнительными механизмами спектрометров ИБР-2 на базе индустриального стандарта CAN.
9. Модернизация и поддержка инфраструктуры рабочих мест инженеров и программистов.
10. Создание вакуумного стенда для отработки технологии “cryogen free” криостатов для спектрометров ИБР-2М.
11. Развитие программного комплекса Sonix+ для удаленного контроля за экспериментами.

4. EXPERIMENTAL REPORTS

4.1. CONDENSED MATTER PHYSICS

Diffraction

Crystal Structure of Chromium Hydrides
V.E.Antonov, A.I.Beskrovnyy, P.E.Butorin, V.K.Fedotov, M.K.Sakharov, M.Tkacz, S.G.Vasilovskiy

Analysis of Lipid Multilamellar Neutron Diffraction Patterns Measured in Real Time
N.Yu.Ryabova, A.I.Beskrovnyy, M.A.Kiselev, A.M.Balagurov

Anomalies of Structure and Properties for Titanium Diselenide Interclated by Iron
E.A.Galieva, N.A.Danilova, S.V.Pryanichnikov, S.G.Titova, A.N.Titov, I.A.Bobrikov, A.M.Balagurov, V.G.Simkin

Structural Phase Transition in Pyridinium Perrhenate at High Pressure
S.E.Kichanov, D.P.Kozlenko, J.Wasicki, W.Nawrocik, P.Czarnecki, B.N. Savenko, V.P.Glazkov and C.Lathe

Generalized Phase Diagram of Hexagonal Frustrated Manganites
D.P.Kozlenko, S.E.Kichanov, B.N.Savenko, S.Lee, J.-G.Park, V.P.Glazkov

A Neutron Diffraction Study of the Structure and Thermal Behaviour of Framework Phosphates of Zirconium and Tantalum
A.I.Orlova, V.A.Orlova, S.V.Nagornova, Ye.V.Bortsova, A.K.Koryttseva, A.I.Beskrovnyy , P.E.Butorin, S.G.Vasilovskiy

The Study of $La_{1-x}Sr_xCoO_3$ (x = 0.0 ÷ 0.5) by X-Ray Absorption Spectroscopy and High-Resolution Neutron Diffraction Methods
V.V.Efimov, E.A.Efimova, D.I.Kochubey, V.V.Kriventsov, A.Kuzmin, V.V.Sikolenko, V.G.Simkin, S.I.Tiutiunnikov, I.O.Troynchuk

Acoustic Emission of Quasi-Isotropic Rock Samples Initiated by Temperature Gradients
R.N.Vasin, A.N.Nikitin, T.Lokajicek, V.Rudaev

Inelastic Neutron Scattering

The Molecular Structure and Dynamics of 2-Aminopyridine-3-Carboxylic Acid by X-Ray Diffraction at 100K, Inelastic Neutron Scattering, Infrared, Raman Spectroscopy and from First Principles Calculations
A.Pawlukojć, W.Starosta, J.Leciejewicz, I.Natkaniec and D.Nowak

Microdynamics of Liquid Lithium–Hydrogen Alloy: Investigation by Inelastic Neutron Scattering
N.M.Blagoveshchenskii, V.A.Morozov, A.G.Novikov, M.A.Pashnev, V.V.Savostin, A.L.Shimkevich

QENS Studies of Durene and TCNB–Durene Charge Transfer Complex
J.Krawczyk, M.Nowina Konopka, I.Natkaniec, I.V.Kalinin, O.Steinsvoll

Internal Dynamics of 17-α-Methyltestosterone Studied by ^{1}H NMR and IINS
Krystyna Holderna-Natkaniec, Ireneusz Natkaniec, Dorota Nowak

Vibrational Density of States of Photosynthetic Pigment-Protein Complexes
J.Pieper, I.Natkaniec, A.Skomorokhov, G.Renger

Lattice Vibrations in an α- and β- AgCuS Superionic Conductor
A.N.Skomorokhov, D.M.Trots, S.G.Ovchinnikov, H.Fuess

Influence of Intercalation on Phonon Spectra of Titanium Dichalcogenides
A.N.Titov, A.N.Skomorokhov, A.A.Titov, S.G.Titova, V.A.Semenov

Small-Angle Neutron Scattering

Structure and Magnetic Changes of Co-Based Nanocomposite after Percolation Threshold
E.B.Dokukin, A.Kh.Islamov, A.I.Kuklin, M.E.Dokukin, E.A.Gan'shina, N.S.Perov, Yu.E.Kalinin and A.V.Sitnikov

Structure of Ferrofluids with Excess of Surfactant by Small-Angle Neutron Scattering
Viktor I.Petrenko, Mikhail V.Avdeev, Leonid A.Bulavin, Viktor L.Aksenov

Neutron Reflectometry

Investigations of the Non-Locality Effects in Type I Superconductor by Means of the Polarized Neutron Reflectometry
V.L.Aksenov, D.S.Drannikov, Yu.N.Khaidukov, V.F.Kozhevnikov, Yu.V.Nikitenko, A.V.Petrenko, V.V.Proglyado

4.2. NEUTRON NUCLEAR PHYSICS

Fundamental Research

"Zero" Experiment in the Measurement of the P-Odd Asymmetry in the Reaction ^{6}Li(n,α)^{3}H
V.A.Vesna, Yu.M.Gledenov, V.V.Nesvizhevsky, A.K.Petukhov, P.V.Sedyshev, T.Soldner, E.V.Shulgina, O.Zimmer

Ramsey Resonance for a Pulsed Beam
Yasuhiro Masuda[1], Vadim Skoy, Takashi Ino, Sun-Chang Jeong , Yutaka Watanabe

Applied Research

Temperature Dependence of Neutron Scattering on He-4 Gas
V.Ignatovich

JINR Contribution to the European Programme «Atmospheric Heavy Metal Deposition»: from 1995 to 2005/2006 Moss Surveys
M.V.Frontasyeva

CRYSTAL STRUCTURE OF CHROMIUM HYDRIDES

V.E. Antonov[a], A.I. Beskrovnyy[b], P.E. Butorin[b], V.K. Fedotov[a],
M.K. Sakharov[a], M. Tkacz[c], S.G. Vasilovskiy[b]

[a] *Institute of Solid State Physics RAS, 142432 Chernogolovka, Moscow District, Russia*
[b] *Frank Laboratory of Neutron Physics, Joint Institute for Nuclear Research, 141980 Dubna, Moscow District, Russia*
[c] *Institute of Physical Chemistry PAS, Kasprzaka 44/52, 01-224 Warsaw, Poland*

1. Introduction

Chromium hydrides with compositions close to CrH can be produced electrolytically [1,2] and under high hydrogen pressure [3,4]. Depending on the synthesis conditions, the hydrides can have a *hcp* (ε) or *fcc* (γ) metal lattice [2,4]. A room-temperature neutron diffraction investigation of the ε-CrH produced electrolytically showed that hydrogen atoms occupy octahedral interstitial positions in the *hcp* chromium lattice and that the hydride is not magnetically ordered [5]. The γ-CrH hydride has never been studied by neutron scattering.

In the present work, the γ-CrH and ε-CrH hydrides were prepared electrolytically and studied by neutron diffraction at liquid helium temperatures.

2. Sample preparation and experimental details

The samples of γ-CrH and ε-CrH, each weighing about 1.5 g, were prepared from 99.99% CrO_3 by cathodic electrodeposition as described in [2,6,7]. Chromium hydrides produced in this way are rather stable at room temperature and do not noticeably loose hydrogen during a few hours [7]. The γ-CrH and ε-CrH samples were ground in an agate mortar and, when not in use, stored in liquid nitrogen to prevent thermal decomposition. A small portion of a few milligrams of each sample was analysed by X-ray diffraction and hot extraction.

The room-temperature X-ray diffraction examination (SIEMENS D-500 diffractometer, monochromated Cu$K_{\alpha 1}$ radiation) showed that the ε-CrH sample was a single-phase ε-CrH compound, while the γ-CrH sample contained a few percent admixture of ε-CrH and Cr metal. The hot extraction into a calibrated volume at temperatures up to 500ºC gave the atomic H-to-metal ratio $x = 0.98(4)$ for the ε-CrH sample and $x = 0.93(4)$ for the γ-CrH sample.

Both samples were studied by neutron diffraction at 8 K with the DN-2 diffractometer. A powdered sample was enclosed in a cylindrical, thin-walled vanadium can and placed in a helium refrigerator. The diffraction data were analysed with a computer program [8] based on the Rietveld profile refinement technique.

3. Results and discussion

The neutron diffraction patterns of the ε-CrH and γ-CrH samples and the results of their profile analysis are presented in Figs. 1 and 2, respectively. The smooth background has been subtracted from the shown spectra to allow a better visual comparison with the calculated profi les. Thankfully, the samples proved to be rather well-crystallised and homogeneous. Most diffraction lines are well resolved and the profile fit of the pattern requires the Debye-Waller factors $B_{Cr} = 0.4$ Å^{-1} and $B_H = 2.0$ Å^{-1}. Similar values of *B*-factors are typical of powder *d*-metal hydrides prepared by gas-phase absorption and this suggests a comparable degree of lattice disorder in our electrolytical samples.

As seen from Fig. 1, the neutron diffraction pattern of the single-phase ε-CrH sample contains no new lines in addition to the lines of the *hcp* structure. The crystal structure of this phase therefore belongs to the same space group, $P6_3/mmc$, as the *hcp* structure of its metal lattice. In the *hcp* structure, there are two types of highly symmetrical interstitial positions conforming to the $P6_3/mmc$ space group. These are the octahedral positions (which are as many as the metal sites) and

tetrahedral positions (which are twice as many). As can be seen from the difference curve b in Fig. 1, a model assuming that hydrogen occupies every octahedral site gives a satisfactory profile fit of the experimental spectrum. At the same time, this spectrum is qualitatively different from profile c calculated for hydrogen randomly distributed over the tetrahedral sites. Correspondingly, any admixture of tetrahedral hydrogen makes the agreement between the calculation and experiment worse, and the model allowing partial occupancy of sites of both types converges to 100% occupancy of the octahedral ones.

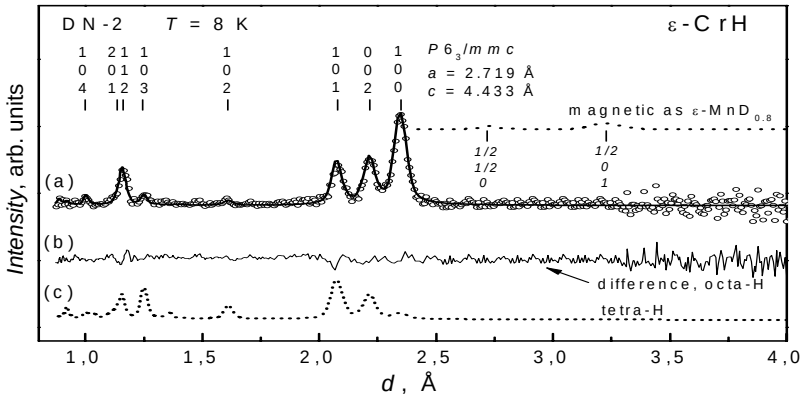

Fig. 1. Neutron powder diffraction pattern of the ε-CrH sample measured for 10 h at 8 K with the time-of-flight DN-2 diffractometer at JINR in Dubna (open circles) and results of its Rietveld analysis (lines). Curve (a) is the profile fit calculated for the NiAs-type $P6_3/mmc$ structure with hydrogen atoms occupying every octahedral site in the *hcp* Cr lattice with a = 2.719(3) Å and c = 4.433(4) Å. Curve (b) is the difference between the experimental (circles) and calculated (curve a) spectra. Curve (c) is the spectrum calculated for x = 1 hydrogen atoms randomly occupying one half of the tetrahedral interstices in *hcp* Cr, the other fitting parameters being the same as for curve (a). The dashed curve labelled "magnetic as ε-$MnD_{0.8}$" shows the calculated profile of the magnetic contribution, which would be observed in addition to the structure lines of ε-CrH if it were an antiferromagnet with the same magnetic structure and magnetic moments of 0.73 μ_B/metal atom as ε-$MnD_{0.83}$ [14].

In agreement with the preliminary X-ray examination, the neutron diffraction pattern of the γ-CrH sample (Fig. 2) presents a superposition of diffraction lines of γ-CrH and ε-CrH and chromium metal. The γ-CrH phase shows no new lines in addition to those of the *fcc* structure therefore the structure of this hydride belongs to the same space group, $Fm\bar{3}m$, as its *fcc* metal lattice. In full analogy with the said about the ε-CrH phase, there are octahedral and tetrahedral interstitial sites in the metal lattice of the γ-CrH phase. A model with hydrogen atoms occupying the tetrahedral sites is qualitatively inapplicable (see the calculated profile d in Fig. 2), while a model with octahedral hydrogen allows a satisfactory profile fit. Assuming the octahedral hydrogen coordination in the γ-CrH phase, the profile analysis of the experimental spectrum gives a mixture of 86% γ-CrH and 11% ε-CrH and 3% *bcc* Cr metal for the phase composition of the γ-CrH sample.

The lattice parameters of ε-CrH and γ-CrH determined in the present work well agree with X-ray results of Ref. [9]. The NiAs-type crystal structure of ε-CrH agrees with earlier neutron diffraction data [5]. The octahedral hydrogen coordination established for both ε-CrH and γ-CrH is characteristic of all hydrides with close-packed metal lattices that are formed by transition metals of groups VI-VIII (see review [10] and recent paper on γ-CoH [11]).

Of special interest are the magnetic properties of chromium hydrides because chromium is the leftmost 3*d*-metal in the periodic table that shows magnetic ordering. This problem, however, needs introductory remarks.

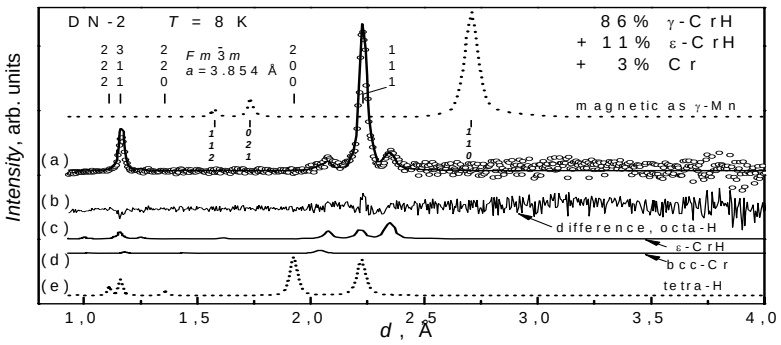

Fig. 2. Neutron powder diffraction pattern of the γ-CrH sample measured for 10 h at 8 K with the DN-2 diffractometer (open circles) and results of its Rietveld analysis (lines). Curve (a) presents the sum of calculated profiles for γ-CrH (86%) and ε-CrH (11%, curve (c)) and *bcc* Cr metal (3%, curve (d)). The profile for γ-CrH is calculated assuming a NaCl-type $Fm\bar{3}m$ structure with hydrogen atoms occupying every octahedral site in the *fcc* Cr lattice with a = 3.854(3) Å. Curve (b) is the difference between the experimental (circles) and calculated (curve a) spectra. Curve (e) is the profile calculated for x = 1 hydrogen atoms randomly occupying one half of the tetrahedral interstices in *fcc* Cr, the other fitting parameters being the same as in the model with hydrogen on octahedral sites. The dashed curve labelled "magnetic as γ-MnH" shows the calculated profile of the magnetic contribution, which would be observed in addition to the structure lines of γ-CrH if it were an antiferromagnet with the same magnetic structure and magnetic moments of 2.4 μ_B/metal atom as γ-Mn [15].

Concentration dependences of the spontaneous magnetization σ_0 at T = 0 K (for ferromagnets) and of the Néel temperature T_N (for antiferromagnets) of *fcc* (γ) alloys of 3*d*-metals which are close neighbours in the periodic table, are well described by the rigid band model and can be represented as unique functions of the average number N^e of external (3*d* + 4*s*) electrons per atom of the alloy (the so-called Slater-Pauling curves). These dependences are plotted by thin solid lines in Fig. 3. Our studies of γ hydrides of *fcc* Ni-based and Fe-based alloys showed [12] that the magnetic properties varied with increasing hydrogen content as if the hydrogen were merely a donor of a fractional number of $\eta \approx 0.5$ electrons per H atom in the otherwise unchanged metal *d*-band. This approximation, which we call the rigid *d*-band model for brevity, is a rather straightforward consequence of the available *ab initio* band structure calculations, and its applicability to alloys with different types of band structure has been thoroughly discussed in [12]. In particular, if the properties of the alloy obey the rigid band model, the properties of its γ hydrides considered as functions of the effective electron concentration $N^e(x) = N^e(0) + \eta \cdot x$ are described by the thin lines of Fig. 3.

Due to the relatively narrow intervals of mutual solubility of 3*d*-metals in hexagonal phases, the concentration dependences of their magnetic properties (two segments of thick solid line in Fig. 3) are known to a much lesser extent than those of the *fcc* alloys. However, if the available experimental points for hexagonal hydrides are added to the graph as a function of $N^e(x)$ with η = 0.5 electrons per H atom, the properties of both hexagonal metals and hydrides can be described by the same curves (dashed lines in Fig. 3). These curves are similar to those for the γ alloys and are likely to represent the Slater-Pauling plot for the (hypothetical) hexagonal alloys [13].

As seen from Fig. 3, the Néel points of the hexagonal alloys monotonically increase from 0 K at $N^e \approx 8.1$ el./metal atom to 350 K at $N^e \approx 7.4$ el./metal atom (the point for ε-$MnD_{0.83}$), and the Néel points of the *fcc* alloys increase from 0 K at $N^e \approx 8.3$ el./metal atom to 660 K at $N^e = 7$ el./metal atom (the point for γ-Mn). Both ε-CrH and γ-CrH have $N^e \approx 6.5$ el./metal atom. The dashed curves labelled "magnetic as..." in the upper parts of Figs. 1 and 2 show the calculated profiles of the magnetic contribution, which would be observed in addition to the structure lines if ε-CrH and γ-CrH were antiferromagnets with the same magnetic structures and magnetic moments as the earlier studied phases with the nearest N^e-values, namely, ε-$MnD_{0.83}$ [14] and γ-Mn [15].

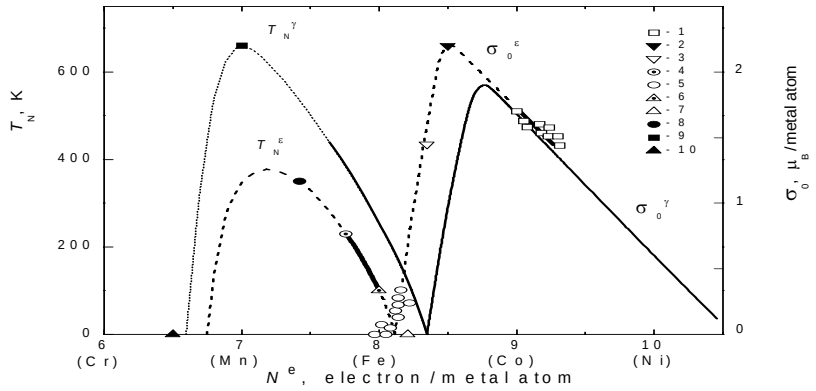

Fig. 3. Slater-Pauling curves for *fcc* (γ) alloys (experiment – thin solid lines) and *hcp* (ε) alloys (experiment – two sections of thick solid lines; an estimation – dashed lines) of 3*d*-metals that are nearest neighbours in the periodic table. The symbols for hydrides show experimental data presented as a function of the effective electron concentration, $N^e(x) = N^e(0) + \eta \cdot x$, with $\eta = 0.5$ electrons per H atom: 1 – σ_0 of ε-CoH_x solid solutions; 2 – σ_0 of ε′-FeH with a *double hcp* metal lattice; 3 – σ_0 of $Fe_{0.947}Cr_{0.053}H_{0.92}$ with a 9*R*-type metal lattice; 4 – T_N of ε-$Fe_{0.776}Mn_{0.224}$; 5 – σ_0 of ε-$Fe_{0.776}Mn_{0.224}H_x$ solid solutions; 6 – T_N of ε-Fe; 7 – σ_0 of ε-$FeH_{0.42}$ (references to the original experimental papers are given in Ref. [13]); 8 – T_N of ε-$MnD_{0.83}$ [14]; 9 – T_N of γ-Mn [15]; 10 – T_N of ε-CrH and γ-CrH [2]. *x* is the H-to-metal atomic ratio.

The calculated magnetic contribution to the neutron diffraction pattern of ε-CrH (Fig. 1) is too small to be seen against the background. The magnetic contribution to the pattern of γ-CrH (Fig. 2) is significant, and the absence of corresponding diffraction lines in the experimental pattern of γ-CrH measured at 8 K therefore corroborates the conclusion [2] that this hydride is paramagnetic down to helium temperatures. Assuming, in accordance with the NMR data [2], that ε-CrH and γ-CrH are not magnetically ordered at temperatures down to 3 K, the Néel points of antiferromagnetic *hcp* and *fcc* 3*d*-alloys as a function of decreasing electron concentration should reach a maximum and then go down to helium temperatures at the N^e values not less than 6.5 el./metal atom. This is schematically shown by the dashed curves in Fig. 3.

Fig. 3 therefore presents the Slater-Pauling curves for *hcp* and *fcc* 3*d*-alloys delineated over the entire range of electronic concentrations, where the alloys undergo magnetic ordering. Interestingly, the steep decrease in the Néel temperature (and, correspondingly, in the magnetic moments) of antiferromagnetic *fcc* alloys with N^e decreasing in the range 7.0–6.5 el./atom is similar to the steep decrease in σ_0 of ferromagnetic *fcc* alloys occurring in the invar range 8.8–8.4 el./atom. One can speculate that the strong dependence of magnetic properties on the electron concentration suggests their strong dependence on the interatomic distances, and the antiferromagnetic *fcc* phases (for example, hydrides of Cr-Mn alloys) in the range 7.0–6.5 el./atom would show invar anomalies as well.

4. Conclusions

Phases of *fcc* (γ) CrH and *hcp* (ε) CrH prepared electrolytically using the technique of Ref. [7] show a good homogeneity and crystallinity comparable to those of ε-CrH samples prepared by gas-phase absorption at high pressure. The present neutron diffraction investigation and earlier NMR investigation [2] of electrolytically prepared samples showed γ-CrH and ε-CrH to be magnetically disordered down to helium temperatures. This allowed completing the construction of the Slater-Pauling curves for *fcc* and *hcp* 3*d*-alloys over the entire range of electronic concentrations, where the alloys undergo magnetic ordering (see Fig. 3).

This work was supported by grants Nos. 02-02-16859 and 05-02-17733 from the Russian Foundation for Basic Research and by the Program "Physics and Mechanics of Strongly Compressed Matter" of the Russian Academy of Sciences.

References

[1] C.A. Snavely, Trans. Electrochem. Soc. 92 (1947) 537.
[2] J. Poźniak-Fabrowska, B. Nowak, M. Tkacz, J. Alloys Comp. 322 (2001) 82.
[3] B. Baranowski, K. Bojarski, Roczn. Chem. 46 (1972) 525.
[4] Y. Fukai, M. Mizutani, Mater. Trans. 43 (2002) 1079.
[5] G. Albrecht, F.-D. Doenitz, K. Kleinstück, M. Betzl, Phys. Stat. Sol. 3 (1963) K249.
[6] B. Dorner, I.T. Belash, E.L. Bokhenkov, E.G. Ponyatovsky, V.E. Antonov, L.N. Pronina, Solid State Commun. 69 (1989) 121.
[7] M. Tkacz, Polish J. Chem. 71 (1997) 1735.
[8] V.B. Zlokazov, V.V. Chernyshev, J. Appl. Crystallogr. 25 (1992) 447.
[9] A.D. Stock, K.J. Hardcastle, J. Inorg. Nucl. Chem. 32 (1970) 1183.
[10] V.E. Antonov, J. Alloys Comp. 330-332 (2002) 110.
[11] V.E. Antonov, T.E. Antonova, V.K. Fedotov, T. Hansen, A.I. Kolesnikov, A.S. Ivanov, J. Alloys Comp. 404-406 (2005) 73.
[12] E.G. Ponyatovskii, V.E. Antonov and I.T. Belash, Usp. Fiz. Nauk 137 (1982) 663 [Engl. Trans. Sov. Phys. Usp. 25 (1982) 596]
[13] V.E. Antonov, M. Baier, B. Dorner, V.K. Fedotov, G. Grosse, A.I. Kolesnikov, E.G. Ponyatovsky, G. Schneider, F.E.Wagner, J. Phys.: Condens. Matter 14 (2002) 6427.
[14] A.V. Irodova, V.P. Glazkov, V.A. Somenkov, S.Sh. Shil'shtein, V.E. Antonov, E.G. Ponyatovskii, Fiz. Tverd. Tela 29 (1987) 2714 [Engl. Trans. Sov. Phys. Solid State 29 (1987) 1562].
[15] G.E. Bacon, I.W. Dunmur, J.H. Smith, R. Street, Proc. Roy. Soc. A241 (1957) 223.

ANALYSIS OF LIPID MULTULAMELLAR NEUTRON DIFFRACTION PATTERNS MEASURED IN REAL TIME

Ryabova N.Yu., Beskrovnyy A.I., Kiselev M.A., Balagurov A.M.

Frank Laboratory of Neutron Physics, Joint Institute for Nuclear Research, Dubna, Russia

To understand the lipid bilayers organization and their behaviour it is very important first of all to know their structure features. Neutron diffraction method is a powerful tool for the study of biological and model membrane systems. Using standard Fourier transformation of lamellar neutron pattern one can obtain the Fourier profile of scattering length density along axis normal to membrane plane. Fourier profile analysis let us to determine such important parameters as the membrane thickness, hydrophobic and hydrophilic regions, and the value of the intermembrane space. Using high luminosity neutron diffractometer on pulsed reactor it is possible to carry out the real-time experiments on the investigation of the kinetic processes in model membranes. If the collection of the neutron diffraction pattern consisted of four Bragg peaks at least is a fast enough as against the characteristic time of such process, it allows us to calculate the Fourier profiles, and to define the internal membrane structure in addition to the standard repeat membrane distance measurement [1].

Present Fourier profile analysis is especially relevant for the investigation of slower in comparison with one in phospholipids bilayers kinetic processes in co-called Stratum Corneum membranes. These multicomponent membranes are a lipid matrix model of the human skin outermost layer, which is the main water penetration pathway.

We demonstrate here an example of the Fourier profile analysis application for the investigation of the dipalmitoylphosphatidylcholine (DPPC) membrane hydration. Neutron diffraction patterns from the oriented sample were collected at the diffractometer DN-2 of the IBR-2. Diffraction pattern were recorded at fixed angles ($2\theta = 11^{o}$) of the two-dimensional position sensitive ^{3}He detector. Figure 1 presents the set of spectra measured from the DPPC membrane during hydration and dehydration at temperature of $20^{o}C$ and at relative humidity of 98% and 58% respectively. A concentration of D_2O in H_2O is 8% and corresponds to the zero scattering length density of water.

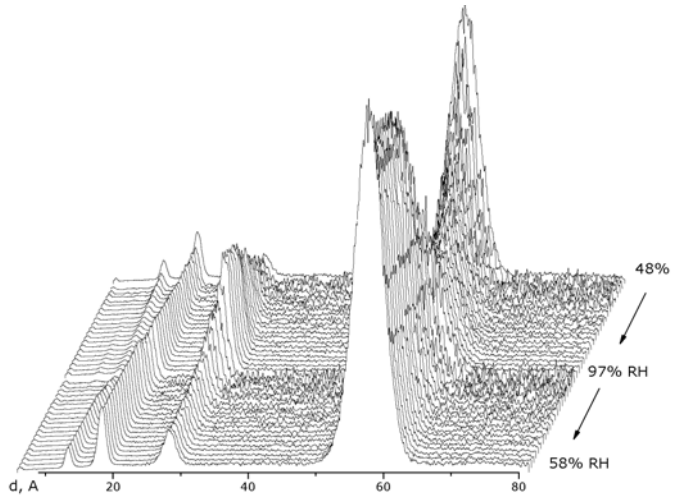

Fig. 1. Set of neutron diffraction patterns from DPPC membrane collected during hydration and dehydration.

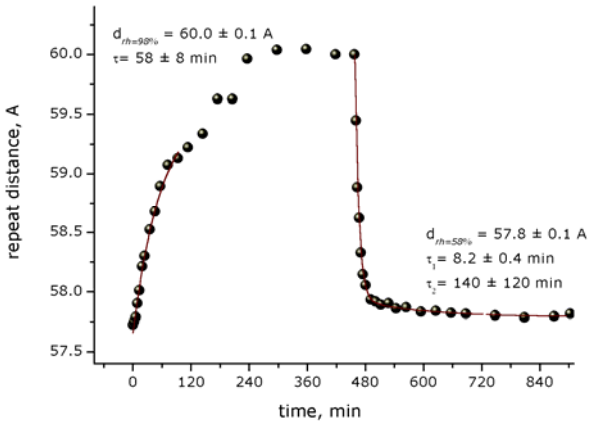

Fig. 2. Change of the DPPC membrane repeat distance under hydration and dehydration.

The neutron scattering length density across the bilayer $\rho_s(x)$ is restored as Fourier synthesis:

$$\rho_s(x) = \frac{2}{d}\sum_{h=1}^{h_{max}} F_h \cdot \cos\left(\frac{2\cdot\pi\cdot h\cdot x}{d}\right), \quad (1)$$

where h is the diffraction order, and F_h is the structure factor calculated from the integrated peak intensity. For Fourier profile analysis we used Gauss function (2) corresponding to methyl group, and two functions (3) which describe symmetrical scattering length density distribution relative to $x = 0$ and corresponding to the "polar head" molecular groups, and to the methylen groups.

$$\rho_{CH3}(x) = \frac{A}{\sqrt{2\pi}\cdot\sigma}\cdot\exp\left[-\frac{1}{2}\cdot\left(\frac{x-x_0}{\sigma}\right)^2\right] \quad (2)$$

$$\rho^{sym}(x) = \frac{A}{\sqrt{2\pi}\cdot\sigma}\cdot\left(\exp\left[-\frac{1}{2}\cdot\left(\frac{x-x_0}{\sigma}\right)^2\right] + \exp\left[-\frac{1}{2}\cdot\left(\frac{x+x_0}{\sigma}\right)^2\right]\right) \quad (3)$$

Thus, the Fourier profile $\rho_s(x)$ was fitted by the function

$$\rho_{fit}(x) = \rho_{CH3}(x) + \rho^{sym}_{CH2}(x) + \rho^{sym}_{PH}(x) \quad (4)$$

The membrane thickness and the "water" layer are estimated as $d_B = 2(x_0 + FWHH/2)$, where $FWHH = 2\cdot\sigma\cdot\sqrt{2\cdot\ln 2}$ is the width of the polar head group, and $d_w = d - d_w$, respectively.

Figures 3 and 4 show the time dependences of these membrane parameters.

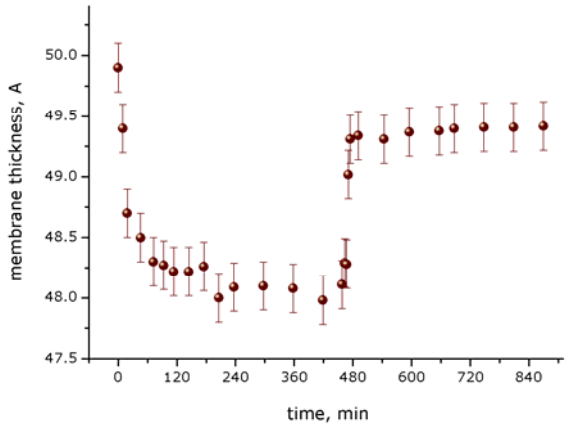

Fig. 3. Change of the DPPC membrane thickness under hydration and dehydration.

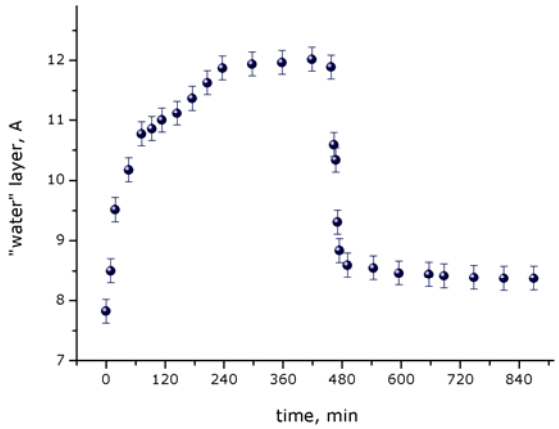

Fig. 4. Change of the "water" layer under hydration and dehydration.

The obtained data show that under membrane dehydration the membrane repeat distance (see Fig. 2) is decreasing by 2.2 Å, and it comes out of the following two processes with the similar time behaviour: increasing of the membrane thickness and decreasing the "water" layer by 1.4 Å and 3.6 Å, respectively.

References

[1] Balagurov A.M. et.al., JINR P19-84-862, Dubna, 1984.

ANOMALIES OF STRUCTURE AND PROPERTIES FOR TITANIUM DISELENIDE INTERCLATED BY IRON

E.A. Galieva[1], N.A. Danilova[1], S.V. Pryanichnikov[2], S.G. Titova[2], A.N. Titov[1], I.A. Bobrikov[3], A.M. Balagurov[3], V.G. Simkin[3]

[1]*Ural State University, Ekaterinburg*
[2]*Institute of Metallurgy UrD RAS, Elaterinburg*
[3]*Neutron Physics Laboratory, JINR, Dubna*

For Fe_xTiSe_2 intercalation compound the transition between regimes of heavy and localized polarons, accompanying with structure anomaly, was studied using thermal analysis, high-resolution neutron diffraction and DC-conductivity measurements.

Intercalation materials on a basis of titanium dichalcogenides demonstrate a polaron type of localization of charge carriers [1]. The basic phenomenon found in such systems is a presence of phase transition of the first order accompanying the change of a degree of charge carrier localization at transition from a heavy polaron regime (HP, non-activated type of conductivity) to regime of localized polarons (LP, activated conductivity). Moreover, delocalized state can be fixed by quench; the transition between localized and delocalized states is accompanied by endo-thermal effect [2]. Thus, there is a base to consider the transition between HP and LP regimes as first order phase transition.

In the present work, the features of structure and conductivity for Fe_xTiSe_2 are investigated using high-temperature high-resolution neutron diffraction and differential thermal analysis (DTA) at change of a degree of localization of charge carriers at change of temperature.

Fe_xTiSe_2, x=0.1 и 0.25 samples were synthesed by ampoule method using elements [1,2]. The choice of composition is explained by absence of iron ordering effect for x≤0.25. Electric conductivity measured by standard four-probe method for ceramic samples quenched from 800, 600, 400 and 200^{0}C and slowly cooled from 800^{0}C (the last one is marked as MO-sample) is shown in Fig. 1. It is visible, that the temperature of localization of charge carriers is T_{loc}≈500^{0}C.

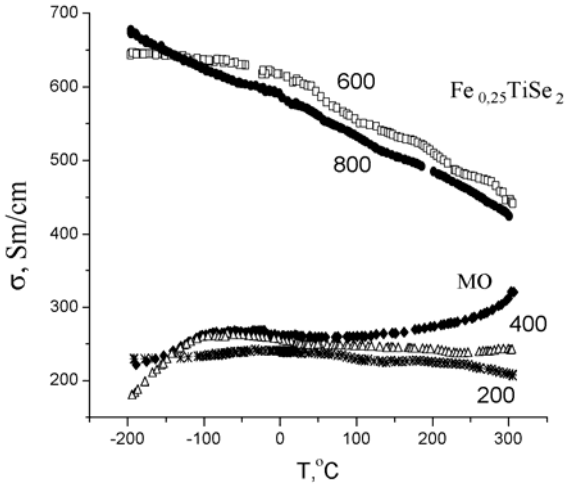

Fig. 1. Electric conductivity for quenched $Fe_{0.25}TiSe_2$ samples as function of temperature. The temperature of quench is specified near to each curve. MO means slowly cooled sample.

DTA experiment was carried out using Q-1500 automatic installation. Samples were placed in pumped (out up to 10^{-5} torr.) quartz ampoule with a special groove for the thermocouple. It has allowed to carry out preliminary heat treatments and DTA measurements, not taking a sample on air to avoid degradation because of oxidation, uncontrollable chalcogen evaporation and so forth. The sample weight was ~1 g, heating rate 5 °C/min, accuracy of DTA signal ~1 mkV. For MO-samples small endo-effect is observed close 500^{0}C, corresponding to HP→LP transition. At the range 350–800^{0}C for quenched samples there are no thermal effects. For both groups of samples the break

close 250-300^{0}C is observed. The effect observed at 500^{0}C is close to a point of transition between modes of conductivity whereas the break at 300^{0}C is not connected to a change of conductivity.

Neutron diffraction data were obtained using Furie diffractometer of the high resolution (HRFD). Diffraction spectra were measured in a mode of sample heating from 25°C up to 650°C, time of an exposition at each temperature 4 hours. The example of the spectrum measured at T=25°C for MO-$Fe_{0.25}TiSe_2$, calculated and difference spectra obtained by Rietveld method using MRIA program are shown in Fig. 2. Calculation was made using the following structure model: space group $P\bar{3}m$ (№164), Z=1, Ti atoms are located in *(1a)* (0 0 0) position, Fe atoms are in (1*b*) (0 0 ½)-position, Se in (2*c*) (⅓ ⅔ z)-position. At 25^{0}C structure parameters were the following: *a*=3.5927(1) Å, *b*=5.9904(1) Å, z(Se)=0.2553(2).

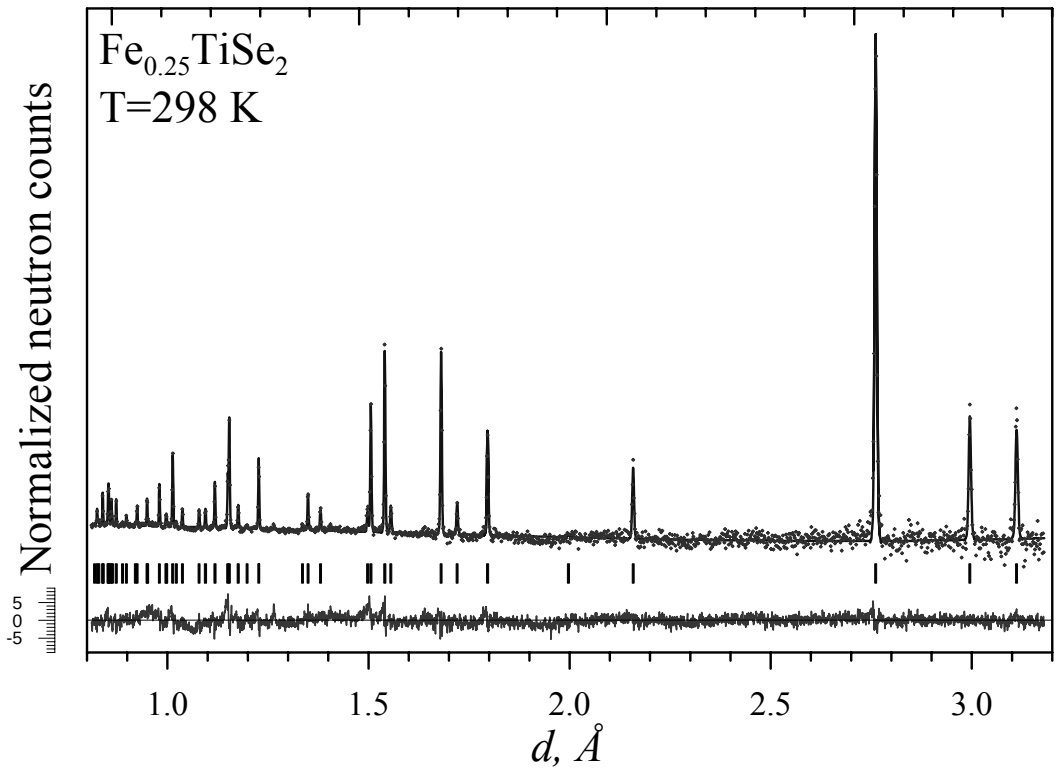

Fig. 2. Neutron diffraction experimental, calculated and difference spectrum for MO- $Fe_{0.25}TiSe_2$ sample measured at room temperature and processed using Rietveld method. Vertical strokes specify calculated positions of diffraction peaks.

On temperature dependences of unit cell parameters for both investigated compounds with *x*=0.1 and 0.25 the abnormal behavior is observed; for MO- $Fe_{0.25}TiSe_2$ sample in a range 200-400^{0}C the deviation of temperature dependence of unit cell constants from linear is visible (Fig. 3). For compound with small iron content x=0.10 the linear dependence of unit cell parameters is kept in all a range, however in the same interval 200-400^{0}C the thermal expansion coefficient has an abnormal behavior, i.e. actually, the first derivative of functions ***a***(T) and ***c***(T). It shows that structural anomaly still exists, but becomes much weaker when iron content is small that specifies connection of structure anomaly with intercalated iron. Similar anomalies of unit cell parameters as function of temperature with local minima of ***a***(T) and ***c***(T) were observed earlier close T_{loc}~130°C for Ag_xTiTe_2 [3]. For compounds with silver the structural anomaly at T_{loc} was accompanied by endo-effect at the same temperature ~130°C [3]. For researched structures with iron the thermal effect is present at higher temperature 500°C, in the same temperature where the jump of electrical conductivity is observed (Fig. 1), while at 500°C no any structure anomaly was found.

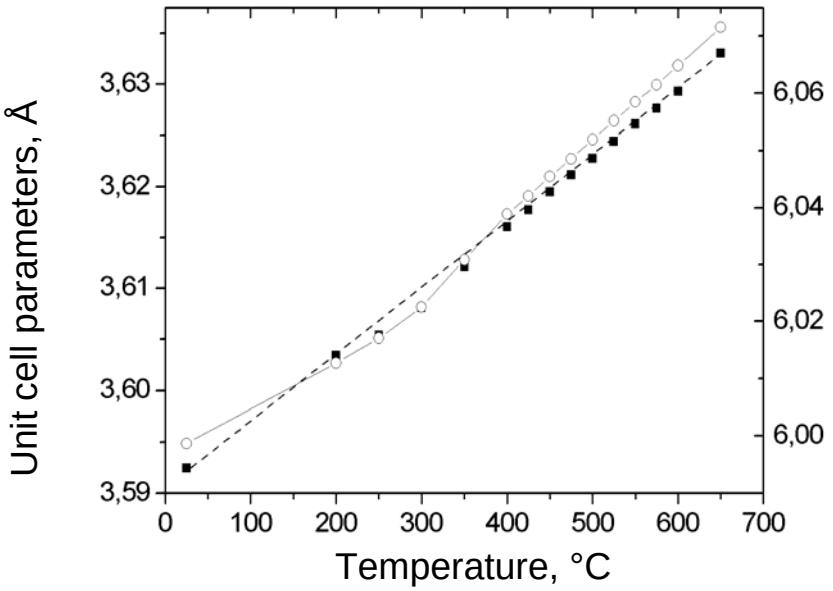

Fig. 3. Uni cell parameters ***a***(T) (the left axis, dark symbols) and ***c***(T) (the right axis, light symbols) as function of temperature for MO- $Fe_{0.25}TiSe_2$ sample. It is visible, that near 300°C the deviation from a linear line occurs for both ***a***(T) and ***c***(T)

It is possible to assume, that difference between temperatures of anomalies of structure close 300°C and physical properties at 500°C is a consequence of the fact, that the band of the localized impurity state for Fe_xTiSe_2 is located below 0.3 eV relatively Fermi level in comparison with Ag_xTiTe_2 system where it gets directly on Fermi level [3]. Then in case of Fe_xTiSe_2 the increase in a degree of localization for charge carriers should not affect kinetic properties, keeping electronic states at Fermi level without change. The change should arise only in a case when the top of the impurity band of localized states reaches Fermi level owing to thermal broadening of a band. Thus, localization of impurity polarons, accompanying with lattice deformation, occurs at 300°C, and transition to the metal conductivity, connected with an output of polaron band top on Fermi level, is observed only at 500°C. Probably, this condition is fixed by quench.

Thus, in this work the direct data concerning influence of degree of localization of charge carriers on crystal structure features are reported for iron intercalation compound based on titanium diselenide.

The work is supported by RFBR, grant № 06-03-32900 and Programs of Ministry of Education and Science of RF «Development of scientific potential of the high school» (RNP.2.1.1.6945).

1. *Titov A., Titova S., Neumann M. et al.* // Mol. Cryst. Liq. Cryst. 1988. V. 311. P. 161.
2. *Titov A.N., Schennikov V.V., Krasavin L.S., Titova S.G.* // Izvestia RAN. Ser. Phys. 2002. V. 66. № 6. P. 869.
3. *Titov A.N., Titova S.G.*// J. Alloys and Comp. 1997. V. 256, P.13.

STRUCTURAL PHASE TRANSITION IN PYRIDINIUM PERRHENATE AT HIGH PRESSURE

S.E.Kichanov[a], D.P.Kozlenko[a], J.Wasicki[b], W.Nawrocik[b], P.Czarnecki[b], B.N. Savenko[a], V.P.Glazkov[c] and C.Lathe[d]

[a]*Frank Laboratory of Neutron Physics, JINR, 141980 Dubna, Moscow Region, Russia*
[b]*Faculty of Physics, A.Mickiewicz University, Umultowska 85, 61-614 Poznań, Poland*
[c]*RRC 'Kurchatov Institute', 123182, Moscow, Russia.*
[d]*HASYLAB am DESY, Notkestrasse 85, D-22603 Hamburg, Germany*

Pyridinium salts belong to the group of molecular-ionic crystals with hydrogen bonds, which exhibit a reach variety of interesting phenomena such as structural phase transitions, ferroelectricity and dynamical orientational disorder of the pyridine cations [1-4]. Two latter compounds are of special interest because their Curie temperatures are above room temperature. The para-ferroelectric transition is accompanied by the structural phase transformation, resulting in the change of the disorder degree of pyridinium and perrhenate ions [5].

The precise determination of crystal and molecular structure is essential for explaining the nature of the ferroelectric properties of pyridinium salts. The more complete structural information for $PyHReO_4$, including hydrogen atoms coordinates, can be obtained from neutron diffraction investigations, if deuterated sample is used, while the pressure behavior of lattice parameters may be investigated by X-ray diffraction. In order to study the structural *P-T* phase diagram in the extended pressure range than previously and obtain more detailed information about structural parameters of different phases, we have performed combined energy dispersive X-ray diffraction and neutron diffraction measurements with a deuterated pyridinium perrhenate $(d_5PyH)ReO_4$.

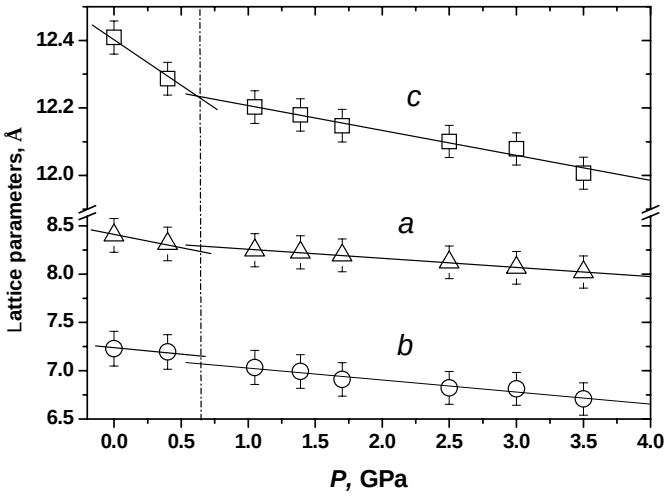

Figure 1. The pressure dependence of the lattice parameters of the pyridinium perrhenate. The solid lines represent the linear fit of the experimental data.

The X-ray diffraction experiments at high pressures up to 3.5 GPa and room temperature were performed with the F3.1 beamline using white synchrotron X-rays from the storage ring DORIS III, Hamburg, Germany. At ambient conditions the orthorhombic phase II with space group $Cmc2_1$ was evidenced. At pressures $P > 0.7$ GPa changes in the diffraction patterns were observed. They correspond to the appearance of the orthorhombic phase I with space group Cmcm under high

pressure. The dependence of the lattice parameters of both phases are shown in figure 2. The linear compressibility of lattice parameters and bulk modules of both phases are calculated.

Neutron diffraction measurements at high pressures up to 2 GPa and temperatures 10-300 K were performed with the DN-12 spectrometer at the IBR-2 high flux pulsed reactor, Dubna, Russia. No changes in diffraction patterns at P=2 GPa on cooling down to 10 K were observed, indicating the stability of the phase I in the whole studied temperature range of 10-293 K. The atomic coordination for phase I, II and III were obtained. The behaviour of hydrogen bond at high pressure is discussed.

The *P-T* phase diagram of deuterated pyridinium perrhenate constructed on the basis of the obtained experimental data and data from ref. [5] for protonated compound are shown in figure 6. The stabilization of the paraelectric phase I under high pressure implies the suppression of the ferroelectricity in $(d_5PyH)ReO_4$.

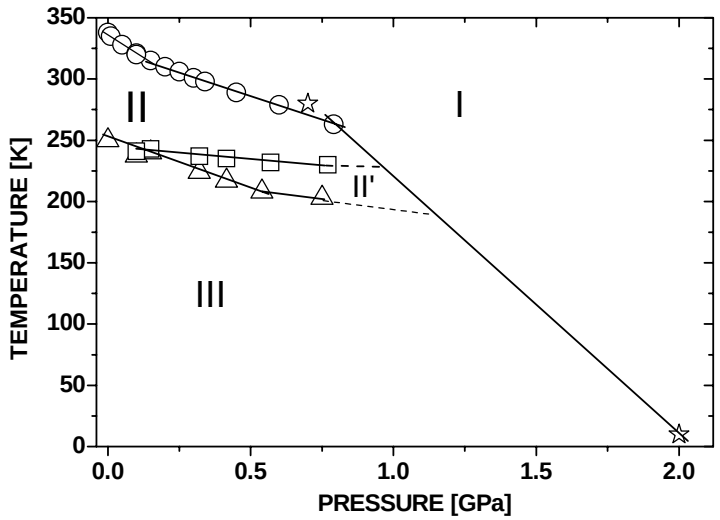

Figure 2. Phase diagram of $(d_5PyH)ReO_4$ constructed on the basis of the present data and data from ref. [5].

References

[1] Czarnecki P, Nawrocik W, Pajak Z and Wasicki J 1994 *Phys. Rev.* B **49** 1511

[2] Czarnecki P, Nawrocik W, Pajak Z and Wasicki J 1994 *J. Phys.: Condensed Matter* **6** 4955

[3] Wasicki J, Czarnecki P, Pajak Z, Nawrocik W and Szczepanski W 1997 *J. Chem. Phys.* **107** 576

[4] Pajak Z, Czarnecki P, Wasicki J and Nawrocik W 1996 *J. Chem. Phys.* **109** 6420

[5] Czarnecki P, Beskrovny A I, Bobrovicz-Sarga L, Lewicki S and Wasicki J, 2005 *J. Phys.: Condensed Matter* **17** S3131

GENERALIZED PHASE DIAGRAM OF HEXAGONAL FRUSTRATED MANGANITES

D.P. Kozlenko[1], S.E. Kichanov[1], B.N. Savenko[1], S. Lee[2], J.-G. Park[2,3], V.P. Glazkov[4]

[1] *Frank Laboratory of Neutron Physics, JINR, 141980 Dubna, Russia*
[2] *Department of Physics and Institute of Basic Science, Sung Kyun Kwan University, Suwon 440-746, Korea*
[3] *Center for Strongly Correlated Materials Research, Seoul National University, Seoul 151-742, Korea*
[4] *Russian Research Center "Kurchatov Institute", 123182, Moscow, Russia*

The hexagonal manganites $RMnO_3$ belong to unusual type of multiferroic materials showing coexistence of ferroelectric behavior and magnetic ordering and the ferroelectric transition temperature $T_C \sim 600$ - 900 K is found to be much higher in comparison with antiferromagnetic (AFM) ordering temperature $T_N \sim 70 - 130$ K [1]. Magnetic properties of $RMnO_3$ manganites depend substantially on the ionic radius of R cation *r*. A rich variety of magnetic properties of hexagonal manganites reflects the modification of the balance between different in-plane and inter-plane magnetic interactions due to changes of the geometry of Mn-O-Mn network upon variation of the *r* value [2]. Apart from the variation of ionic radius of R cation, interatomic distances and angles in the structure can be modified directly by application of high external pressure. In order to study the interplay between a modification of structural parameters and relevant changes of the magnetic structure of the hexagonal manganites, neutron diffraction experiments at high external pressures up to 6 GPa with $YMnO_3$ and $LuMnO_3$ compounds having initial triangular AFM states of Γ_1 and Γ_2 symmetry were performed.

The obtained results provided evidence that a direct relationship between the distortion of the triangular network formed by Mn and O ions and magnetic state exists [3]. Such a distortion can be characterized by the parameter $s = (l_{Mn\text{-}O4} - l_{Mn\text{-}O3})/(l_{Mn\text{-}O4} + l_{Mn\text{-}O3})$, where $l_{Mn\text{-}O3}$ and $l_{Mn\text{-}O4}$ are Mn-O3 and Mn-O4 bond lengths in the triangular (*ab*) planes. The generalized magnetic phase diagram in terms of parameter *s* is shown in fig. 1. At ambient pressure the hexagonal $RMnO_3$ compounds with a relatively large $s \sim 0.025$, like $YMnO_3$, exhibit the triangular AFM state of Γ_1 symmetry. The compounds with a small $s < 0.010$, like $LuMnO_3$, exhibit the triangular AFM state of Γ_2 symmetry.

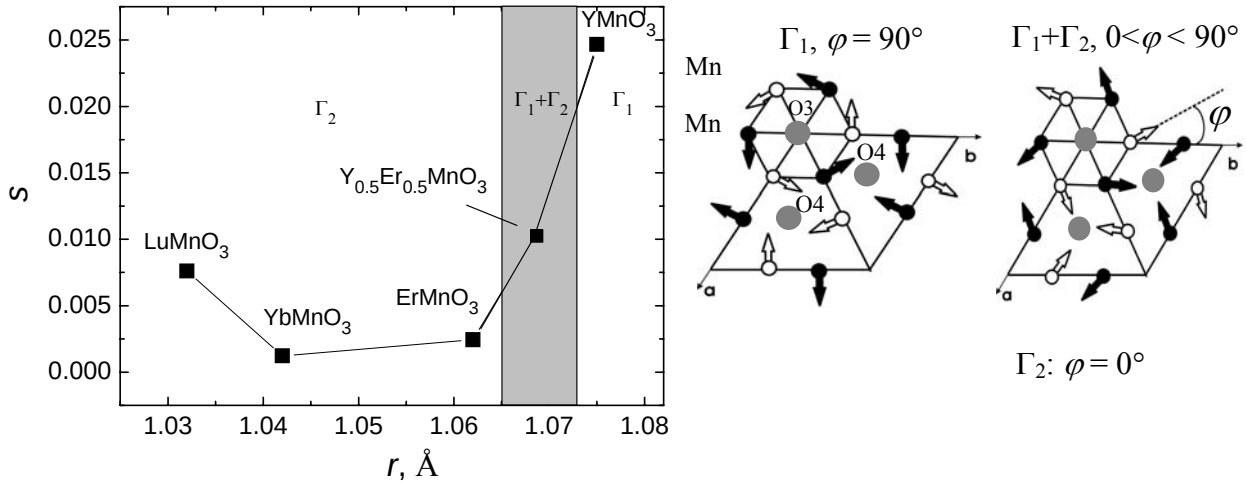

Fig. 1. Generalzied magnetic phase diagram of hexagonal manganites $RMnO_3$ (left) and the relevant magnetic structures (right). Open and filled circles correspond to Mn positions at planes with z = 0 and 0.5

In $YMnO_3$ the *s* value decreases from 0.025 to 0.016 with increasing pressure to 5 GPa while it remains nearly constant in $LuMnO_3$ (Fig. 2). Such a rapid decrease of *s* in $YMnO_3$ correlates with a change of the triangular AFM state symmetry from Γ_1 to Γ_2 through the mixed $\Gamma_1 + \Gamma_2$ representation consistent with the proposed generalized magnetic phase diagram (Fig. 1), as well as with a rapid decrease of the ordered Mn magnetic moment (see the inset of Fig. 2). The observed weak pressure dependence of *s* in $LuMnO_3$ under high pressure (Fig. 2) is also in good agreement with a stability of the triangular AFM state symmetry of Γ_2 representation in terms of the magnetic phase diagram of Fig. 1. It may as well explain why we observe a considerably small decrease of the ordered Mn magnetic moment under high pressure (Fig. 2) in comparison with that of $YMnO_3$. The decrease of *s* is expected to enhance geometrical frustration effects due to symmetrization of triangular lattice, leading to the decrease of ordered magnetic moment.

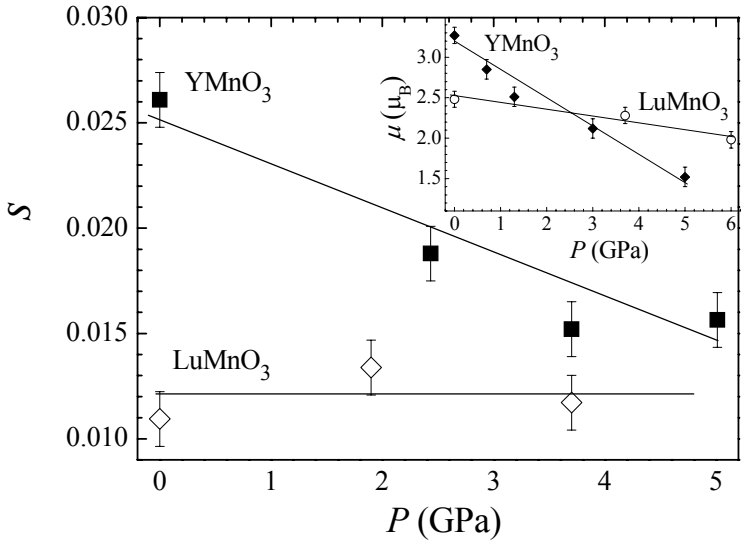

Fig. 2. Pressure dependence of the distortion parameter of triangular network formed by Mn and O ions (at 295 K) and the ordered Mn magnetic moment (at 10 K) in $YMnO_3$ and $LuMnO_3$.

[1] T.Katsufuji, M.Masaki, A.Machida et.al., Phys. Rev. B **66**, 134434 (2002).
[2] J.E.Greedan, M.Bieringer, J.F.Britten et.al., J. Solid State Chem. **116**, 118 (1995).
[3] D.P. Kozlenko, S.E. Kichanov, S.Lee et.al. JETP Lett., **83**, 346 (2006).

A NEUTRON DIFFRACTION STUDY OF THE STRUCTURE AND THERMAL BEHAVIOUR OF FRAMEWORK PHOSPHATES OF ZIRCONIUM AND TANTALUM

A.I. Orlova[a], V.A. Orlova[a], S.V. Nagornova[a], Ye.V. Bortsova[a], A.K. Koryttseva[a], A.I. Beskrovnyy [b], P.E. Butorin[b], S.G. Vasilovskiy[b]

[a]*Chemical Department of Nizhny Novgorod State University, Nizhny Novgorod, Russia*
[b]*Frank Laboratory of Neutron Physics, JINR, Dubna, Russia*

Investigations of new materials being stable under large thermal gradients are of importance. There exists a demand in them in different fields of modern technologies. These are ceramics having different applications (e.g. immobilization of radwastes) and also construction materials (containers for transportations and containment of nuclear materials; spaceships coatings; carriers for space mirrors and catalysts, size-preserving equipment **[1]**.

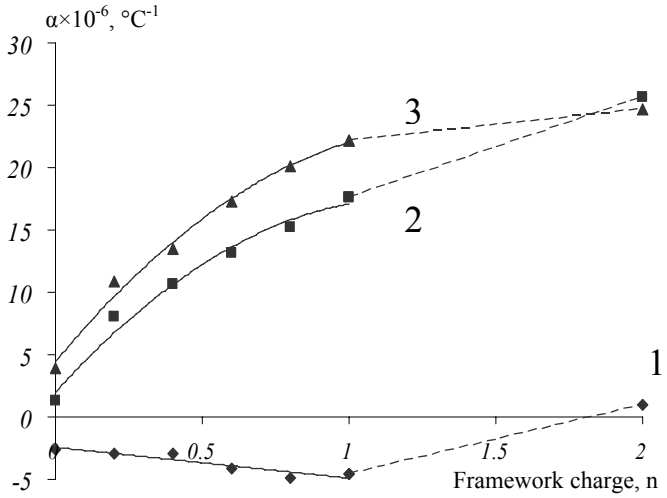

Fig. 1. Dependence of the axial coefficients of thermal expansion α_a (1), α_c (2) and anisotropy of thermal expansion $|\alpha_a - \alpha_c|$ (3) on the framework $[Fe_{1/2+x}Nb_{3/2-x}(PO_4)_3]^{n-}$ charge n in the phosphate series $Na_{2x}[Fe_{1/2+x}Nb_{3/2-x}(PO_4)_3]$ ($0 \le n \le 2$, $n = 2x$).

In this connection we carry out investigations of framework type orthophosphates, the structural analogues of sodium zirconium phosphate $NaZr_2(PO_4)_3$ (NZP). Their high stability under the influence of different types of energy is accounted for the considerable contribution of the covalent component into framework-forming bonds. Crystallochemical modeling of new compositions of pentavalent elements (Nb, Ta) phosphates with expected thermal behavior, in particular, ultralow and tailorable thermal expansion is carried out by our scientific group **[2]**. The dependence of thermal expansion parameters (axis coefficients α_a , α_c and thermal expansion anisotropy $|\alpha_a - \alpha_c|$) on the framework charge and occupation extent of the interstitial sites is established (fig.1).

In order to reveal the character of thermal deformation mechanism and to determine the evolution of structure parameters upon heating we have experimentally studied the structure of $Na_2Fe_{3/2}Nb_{1/2}(PO_4)_3$ phosphate in the temperature range 20-600°C.

The samples were synthesized by solid-state reaction method with the heat treatment at 450, 600, 800, 900°C and characterized by X-ray powder diffraction and IR-spectroscopy. Structure refinement of $Na_2Fe_{3/2}Nb_{1/2}(PO_4)_3$ phosphate was carried out assuming $R\bar{3}c$ space group by Rietveld technique using VMria computer programme. Neutron diffraction spectrum of powder sample was detected at the room temperature and at 600°C using the time-of-fligth diffractometer DN-2, installed on the impulse reactor IQR-2. The structure of $Na_{1,9}Ti_{1,1}Al_{0,9}(PO_4)_3$ was used as a structural analogue **[3].**

Lattice parameters and results of crystal structure refinement of $Na_2Fe_{3/2}Nb_{1/2}(PO_4)_3$ are presented in table 1; the corresponding selected interatomic distances are showed in fig.2.

The framework is built up from the units ("dimmers") consisting of two octahedra ($(Fe/Nb)O_6$ in this case) linked by three bridging PO_4-tetrahedra. The presence of these units is typical for all compounds of NZP-type **[4,5]**. Iron and niobium cations statistically occupy a 12-fold site (00z).

$[Fe_{3/2}Nb_{1/2}(PO_4)_3]^{2-}$ units are located on the three-fold axis and joined together by common oxygen atoms thus forming a three-dimensional lattice. There are two types of interstitial sites: M1 and M2 (they differ in location and size) in the ratio M1:M2=1:3.

Table1. Lattice parameters and results of the structure refinement of $Na_2Fe_{3/2}Nb_{1/2}(PO_4)_3$

	sp. gr.	a, Å	c, Å	Z	d-range.	number of reflections	R_{exp}	R_{wp}	R_p	χ^2
T = 17˚C	$R\bar{3}c$	8,6812	21,9732	6	0,95-4,68	204				3,43
T = 592˚C	$R\bar{3}c$	8,7726	22,4936	6	0,92-4,79	238				4,18

Na atoms in $Na_2Fe_{3/2}Nb_{1/2}(PO_4)_3$ structure fully occupy six-fold site of M1-type, whereas the eight-fold site of M2-type is occupied by one third with Na atoms.

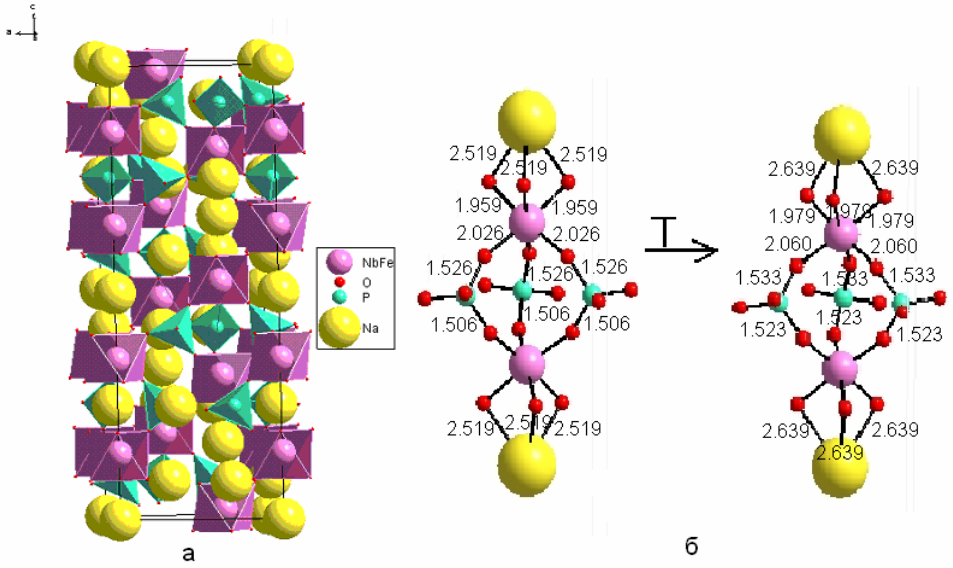

Fig. 2. Structure fragement of $Na_2Fe_{3/2}Nb_{1/2}(PO_4)_3$ (a) and thermal deformation of the "dimmer" (б)

High temperature powder neutron diffraction allowed to evaluate the contribution of different bonds, polyhedra and interpolyhedra angles to the total thermal structure deformation.

It was established that Na-O bonds are the most subjected to the influence of temperature. The increase of Na-O bond lengths leads to the expansion of the structure along the *c*-axis to greater extent than in other structural dimensions. The increase of all bond lengths is accompanied by the correlated turning of all polyhedra. This fact prevents the expansion of the "dimmer" columns along the *a*-axis and so the *a*-parameter does not significantly increase.

In this work we have also discussed the influence of occupation of the M2-sites by Na-cations and interpolyhedra angle distortion on the thermal strain of the whole structure.

In order to examine heating induced changes in cubic structure of langbeinite-mineral type we have also carried out the investigation of $Cs_2Mg_{0.5}Zr_{1.5}(PO_4)_3$ phosphate by high temperature neutron diffraction. Whole pattern (Rietveld) method has been used. Temperatures of the experiments were: 15, 150, 300, 450 and 600 ^{0}C.

Framework forming polyhedra strains can be estimated by means of the value of maximum difference Δ in the bond length. These values were found to be different at different temperatures **[6]**. At 15 °C the phosphorous tetrahedra are slightly strained: Δ=0.05 Å, and the values of the O-P-O valent angles are close to the ideal tetrahedra angle and equal to 109.5°. With temperature increase, bond length changes and Δ-value reaches 0.21 Å at 600 °C. Strains of metal-oxygen MgO_6- and ZrO_6- octahedra change to the less extent: Δ=0.23 Å at 15 °C and Δ=0.35 Å at 600 °C. Turning of polyhedra also takes place upon heating (fig.3).

Thermal expansion coefficients of $Cs_2Mg_{0.5}Zr_{1.5}(PO_4)_3$ phosphate are α_a = (3.93 - 5.05) $\times 10^{-6}$ °C^{-1} .

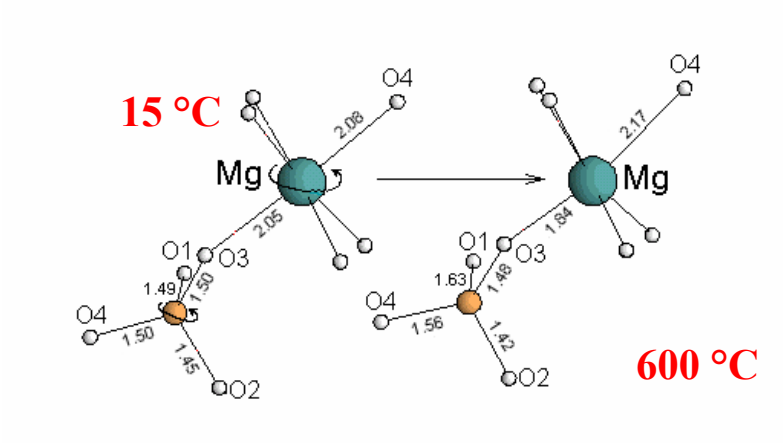

Fig.3. Deformations of the framework forming polyhedra upon heating

Thus, we can consider that the thermal expansion of langbeinite and NZP-type phosphates differs in the value and character of deformations. NZP-like phosphates expand anisotropically. Thermal expansion parameters depend on the nature of cations, occupying the interstitial sites and also on the extent of occupation. The decrease in occupation of interstitial M-sites leads to the decrease of structure deformation upon heating. Some NZP phosphates have near zero thermal expansion anisotropy.

Framework phosphates with cubic structure expand isotropically. The nature of cations, occupying interstitial sites does not significantly affect the thermal structure deformation α_a ($K_2Mg_{0.5}Zr_{1.5}(PO_4)_3$) = $5.3 \cdot 10^{-6}$ $°C^{-1}$ at 600 °C, and α_a($Cs_2Mg_{0.5}Zr_{1.5}(PO_4)_3$)= $5.05 \cdot 10^{-6}$ $°C^{-1}$ at 600 °C.

References

1. Orlova A.I. et al, J. Matt. Sci. Lett. 40 (2005) 2741,
2. Orlova A.I. et al., Kristallographiya (Rus. J. Cryst.) 49 (2004) 724,
3. Mouahid F. E.et al., J. Mat. Chem. 10 (2000) 2748,
4. Voronkov A.A. et al, Kristallographiya (Rus. J. Cryst.) 20 (1979) 556,
5. Sizova R.G. et al, Kristallographiya (Rus. J. Cryst.) 26 (1981) 293,
6. Orlova A.I. et al, Radiochimia (Rus. J. Radiochem.) 47 (2005) 213.

THE STUDY OF $La_{1-x}Sr_xCoO_3$ (x = 0.0 ÷ 0.5) BY X-RAY ABSORPTION SPECTROSCOPY AND HIGH-RESOLUTION NEUTRON DIFFRACTION METHODS

V.V. Efimov[1], E.A. Efimova[1], D.I. Kochubey[2], V.V. Kriventsov[2], A. Kuzmin[3], V.V.Sikolenko[1,4], **V.G.Simkin[1]**, S.I.Tiutiunnikov[1], I.O.Troynchuk[5]

[1]*Joint Institute for Nuclear Research, Dubna 141980, Moscow region, Russia*
[2]*Boreskov Institute of Catalysis, Lavrentiev prosp. 5, Novosibirsk 630090, Russia*
[3] *Institute of Solid State Physics, Kengaraga str. 8, LV-1063 Riga, Latvia*
[4]*Hahn-Meitner-Institut Glienicker str. 100, Berlin D-14109, Germany*
[5]*Institute of Solid State and Semiconductor Physics, 220072 Minsk, Belarus*

Correlations of the local atomic and electronic structure with crystal lattice structural parameters changes have been studied by X-ray absorption spectroscopy (EXAFS/XANES) and high-resolution neutron diffraction in $La_{1-x}Sr_xCoO_3$ (x = 0.0, 0.2, 0.3 и 0.5). The valence state of the cobalt ions has been probed by XANES. It has been shown that the substitution of La^{3+} for Sr^{2+} leads to the small increase of the Co–Co interatomic distances and to an appearance of the mixed Co^{3+}/Co^{4+} intermediate spin state configuration. The crystal structure of cobaltites has been refined using the Rietveld method. The variations of the Co-O distance and the Co-O-Co angle in $La_{1-x}Sr_xCoO_3$ (x = 0.0, 0.2, 0.3 и 0.5) have been precisely established and analysed.

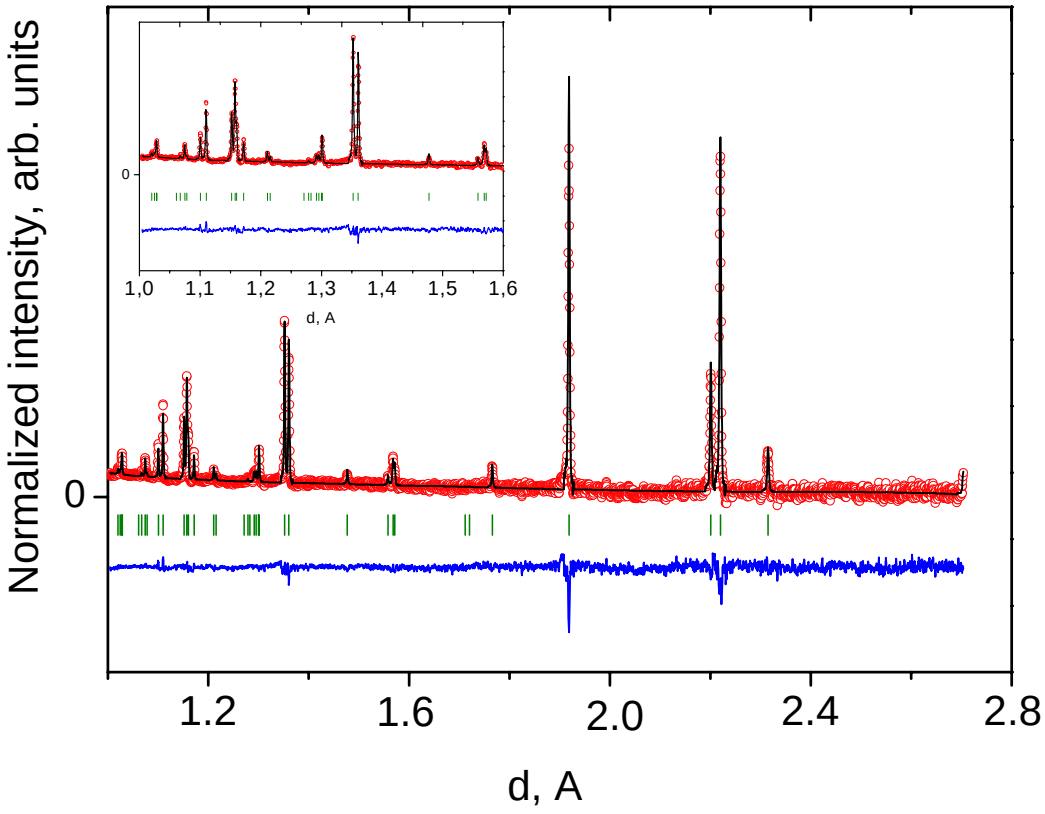

Fig. 1 Neutron diffraction pattern of $LaCoO_3$: experimental curve (continuous line), refinement points (open circles) and their difference (continuous line below). Ticks show the predicted 2θ positions for the Bragg peaks.

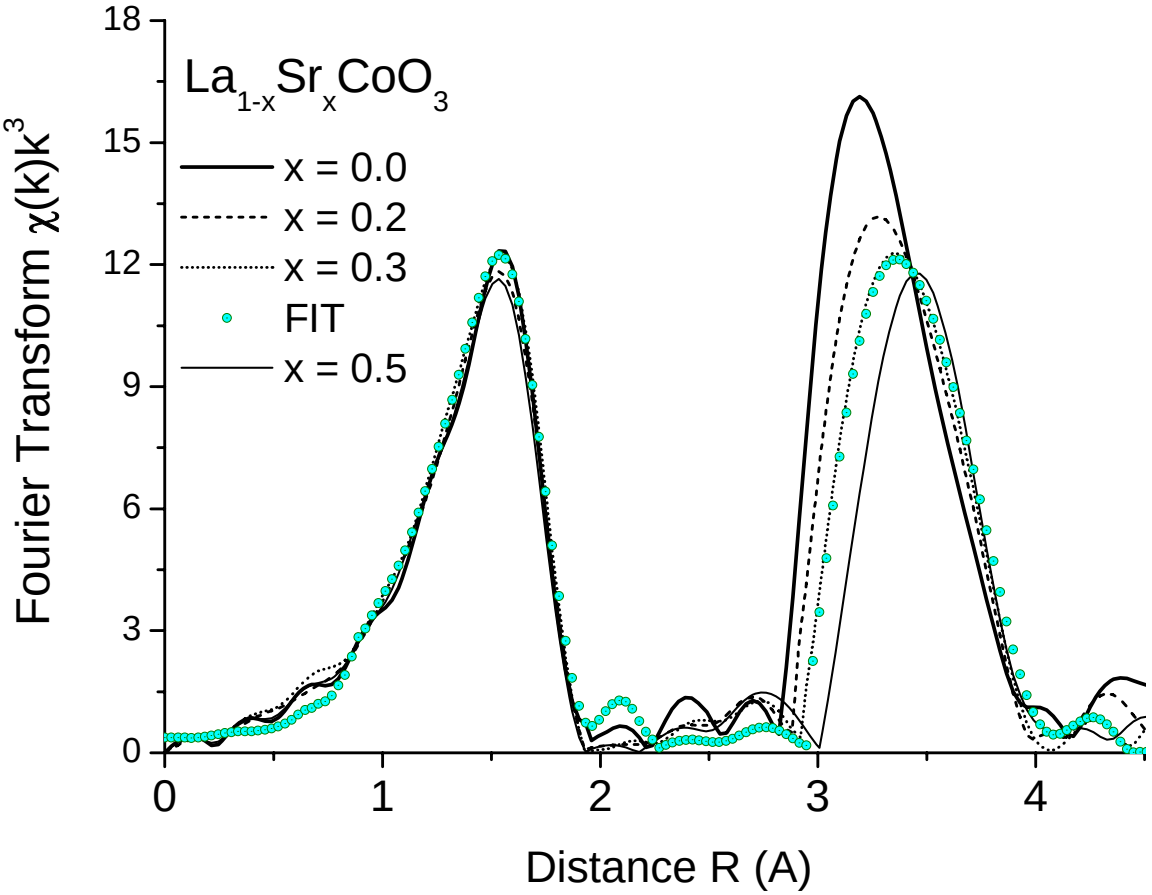

Fig. 2. Fourier transforms of the Co *K*-edge EXAFS $\chi(k)k^3$ signals for the $La_{1-x}Sr_xCoO_3$ powder at the 290 K.

Literature

1. V.V. Efimov, E.A. Efimova, D.I. Kochubey, V.V. Kriventsov, A. Kuzmin, V.V.Sikolenko, **V.G.Simkin**, S.I.Tiutiunnikov, I.O.Troynchuk// The investigation of $La_{1-x}Sr_xCoO_3$ (x = 0.0 ÷ 0.5) X-ray absorption spectroscopy and neutron difraction // ***Surface investigation X-ray, Synchrotron and Neutron Techniques*** **6**, 23-29 (2006) (in Russian).
2. V. V. Efimov, E.A. Efimova, S. Khasanov, D.I. Kochubey, V.V. Kriventsov, A. Kuzmin, V. Sikolenko, A.N. Shmakov, S.I. Tiutiunnikov, I.O.Troynchuk. Effect of high-current pulsed electron beam irradiation on the structure of $La_{0.7}Sr_{0.3}CoO_3$ powder // ***Journal of Physics and Chemistry of Solids*** **67**, 2001-2006 (2006).

ACOUSTIC EMISSION OF QUASI-ISOTROPIC ROCK SAMPLES INITIATED BY TEMPERATURE GRADIENTS

R.N. Vasin[a], A.N. Nikitin[a], T. Lokajicek[b], V. Rudaev[b]

[a] Joint Institute for Nuclear Research, Frank Laboratory of Neutron Physics, 141980, Dubna, Russia
[b] Institute of Rock Structure and Mechanics, Academy of Sciences of the Czech Republic, 18209, Prague, Czech Republic

Introduction

The comprehensive knowledge and description of the geodynamic effects (rockbursts, earthquakes, and others) in Earth's lithosphere requires the improvement and further elaboration of existing physical models of the geological medium. Studies of physical processes and phenomena causing mechanical instability of rocks under the effect of high temperatures, pressures, tectonic stresses, and other factors are important. Anomalous properties of rock minerals have to be taken into account. It should be noticed that physical fields in lithosphere have gradient nature due to the anisotropy and heterogeneity of the geological medium and spatially inhomogeneous distribution of thermodynamic parameters. Temperature gradients have a significant effect on processes in the Earth's interior (in particular, the prefracture processes).

This essay discusses registered acoustic activity of marble and sandstone caused by temperature gradients, and the influence of non-uniform heating on propagation of elastic waves in samples and on their crystallographic texture.

Samples selection

This work continues the systematic studies of rock properties at high temperatures and mechanical loads [1-3]. Thus, next samples which was selected. Coarse-grained marble from Koneprusy cave, 30 km southwest of Prague, contained more than 98% calcite. Laminated sandstone of the Cretaceous from SE Germany consisted of more than 95% quartz. Six samples of cylindrical form (30 mm in diameter and 60 mm in length) were prepared: vap00, vap04, vap05 (marble) and sandstone0, sandstone1, sandstone2 (sandstone). Samples vap00 and sandstone0 were used only for texture measurements.

Study of the crystallographic texture of the samples

The crystallographic texture controls the anisotropy of material. At this stage of experiment it was preferable to avoid the influence of anisotropy on the crack formation e.g. to select samples with nearly chaotic crystallographic textures. According to [4] slow heating may not cause the acoustic activity due to plastic flows. Measurements of texture before and after heating can reveal plastic deformations in samples.

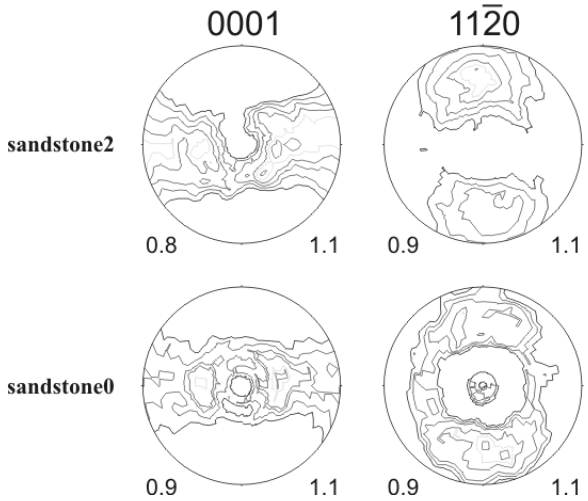

Fig.1. Pole figures (0001) and (11-20) of quartz in sandstone samples sandstone0 and sandstone2. Maximum and minimum intensities are shown.

Texture measurements have been carried out at the neutron texture diffractometer SKAT at the beam 7a of reactor IBR-2. Pole figures of quartz in sandstone samples sandstone0 and sandstone2 are shown on Fig.1.

All of the samples show a weak texture, which is almost completely unaffected by heating. Therefore, samples can be considered as quasi-isotropic in physical properties on a macroscopic scale. In addition, we may assume that plastic flow is absent in the samples.

Method and results of acoustic experiment

In the experiment, a temperature gradient was created along the radius of sample. For this purpose, axial holes 3 mm in diameter were drilled in samples and a heating element was placed inside this holes. The temperature was controlled by two thermal resistors on the sample surface and one inside the sample. To record acoustic emission and determine the velocities and attenuation of elastic waves in sample, six resonance piezoelectric transducers were used. The Vallen AMSY-5 multichannel system was used for data recording.

Samples sandstone1 and vap05 were heated gradually, with a step of up to 20˚C (the mean rate of heating of the sample surface was ~0.5˚C). Thus, the temperature gradient increased also slowly from 0 to ~400˚C/cm. The maximum temperature (~800˚C) inside samples sandstone2 and vap04 was created almost instantaneously, which resulted in temperature gradients of up to 520˚C/cm. With time this gradient reduced to ~400˚C/cm. Sample sandstone2 also was subsequently held under stable thermal conditions for four hours (at surface temperature ~236˚C and inside ~800˚C).

Some results of acoustic experiments are shown on Fig.2 and Fig.3.

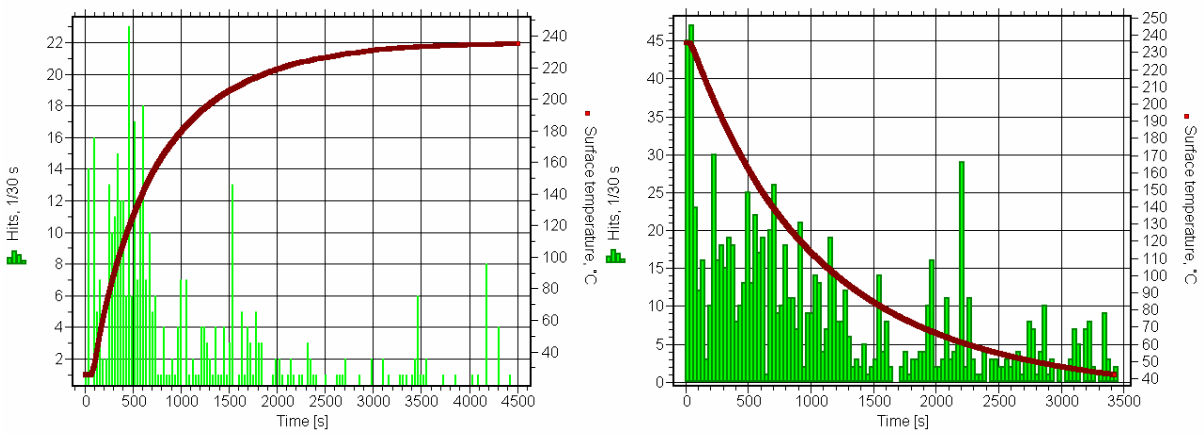

Fig.2. Surface temperature (solid line) and acoustic activity (histogram) of sample sandsone2 (left – rapid heating, right – rapid cooling).

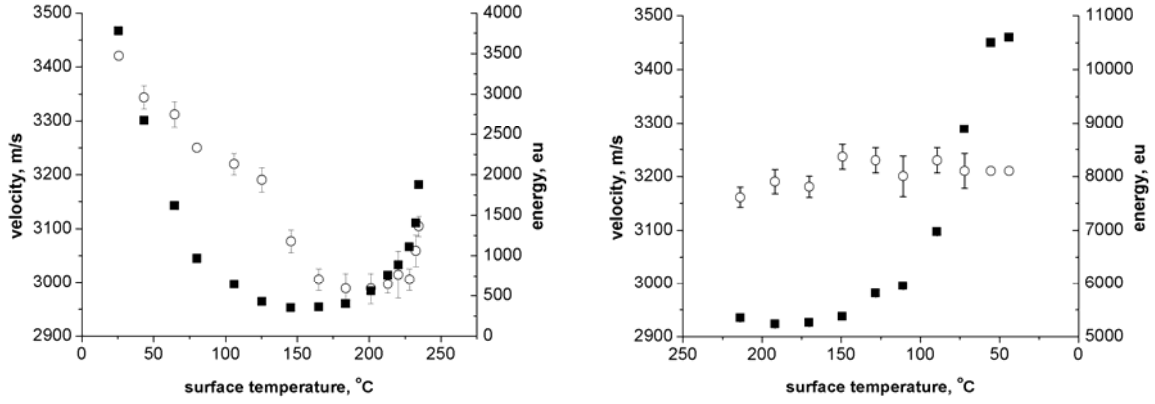

Fig.3. Velocity (○) and energy (■) of propagating P-waves in sample sandstone2 (left – rapid heating, right – rapid cooling).

The following features of acoustic activity of marble and sandstone should be noted:

- at a slow stepwise heating local maxima of acoustic activity are attained at the initial stage of heating with the rise of the temperature gradient;
- in the sandstone samples, a maximal acoustic activity is attained at maximal temperature gradient in the sample;
- the intensity of acoustic activity of sandstone subjected to slow heating is two orders of magnitude higher than in case of rapid heating;
- temperature dependencies of acoustic activity in the marble samples are similar at different heating rates, acoustic activity attains maxima at surface temperatures of 30-60˚C and higher than 200˚C;
- during cooling, all samples demonstrate maximal acoustic activity at the moment of switching-off the heater, and the emission intensities of different samples are comparable.

The following features of elastic wave velocities and attenuation behavior should be noted:

- regardless of heating regime, the elastic wave velocities decrease throughout the temperature range; during cooling, velocities increase linearly;
- attenuation of the elastic waves virtually independent of the heating regime;
- at sandstone samples, the temperature dependence of the attenuation shows essentially non-linear behavior;
- in sandstone held at a constant high temperature and high temperature gradient, the energy of passing waves dropped in a jumplike manner by ~20% 3.5 hours after beginning of the experiment; drop was preceded by an increase in the temperature by 2˚C.

Acknowledgements
We are grateful to Dr. A. Frishbutter (GFZ, Potsdam, Germany), who kindly provided us with sandstone samples, and staff members of the Institute of Rock Structure and Mechanics, Academy of Sciences of the Czech Republic, Prague, for their assistance in conducting the acoustic experiments.

References

[1] Ivankina T.I., Nikitin A.N., Telepnev A.S. et al. The effect of temperature and long-term mechanical stresses on the deformational, thermal, and textural characteristics of marble. *Izvestiya, Phys. Solid Earth*. **37**, No.1, 46-58 (2001).
[2] Sobolev G.A., Ponomarev A.V., Nikitin A.N. et al. Dynamics of the polymorphic α-β-transition in quartzite from data of neutron diffractometry and acoustic emission. *Izvestiya, Phys. Solid Earth*. **40**, No.10, 788-797 (2004).
[3] Nikitin A. N., Vasin R. N., Balagurov A. M. et al. Investigation of thermal and deformation properties of quartzite in a temperature range of polymorphous α-β transition by neutron diffraction and acoustic emission methods. *Physics of Particles and Nuclei, Letters.* **3**, No.1, 46-53 (2006).
[4] Dahm T., Manthei G., Eisenblatter J. Relative moment tensor of thermally induced microcracks in salt rocks. *Tectonophysics*. **289**, No.1-3, 61-74 (1998).

THE MOLECULAR STRUCTURE AND DYNAMICS OF 2-AMINOPYRIDINE-3-CARBOXYLIC ACID BY X-RAY DIFFRACTION AT 100K, INELASTIC NEUTRON SCATTERING, INFRARED, RAMAN SPECTROSCOPY AND FROM FIRST PRINCIPLES CALCULATIONS

A,Pawlukojć[a,d], W. Starosta[a], J. Leciejewicz[a], I. Natkaniec[b,d] and D. Nowak[c,d]

[a]*Institute of Nuclear Chemistry and Technology, ul.Dorodna 16, 03-195 Warszawa, Poland*
[b]*H. Niewodniczański Institute of Nuclear Physics, ul. Radzikowskiego 152, 31-342 Kraków, Poland*
[c]*Faculty of Physics, Mickiewicz University, ul. Umultowska 85, 61-614 Poznań, Poland*
[d]*Joint Institute of Nuclear Research, Frank Laboratory of Neutron Physics, 141980 Dubna, Russia*

In contrast to the aliphatic aminoacids which in majority exhibit zwitterionic structures, N-heterocyclic aminoacids show a variety of hydrogen configurations. For example, no transfer of a proton has been reported in the molecule of 3-aminopyrazine-2-carboxylic acid. Its molecules interact via rather weak hydrogen bonds [1-3]. Dimeric molecular units formed by two acid molecules bridged by O-H…O bonds are observed in the structure of 3-aminobenzenecarboxylic acid [4, 5]. On the other hand, an X-ray crystallographic study of 2-aminopyridine-3-carboxylic acid revealed a transfer of the proton from the carboxylic group to the hetero-ring nitrogen atom. A zwitterionic molecule is formed in this way [6]. For this reason, as a successive step in our research on aminoacids by Inelastic Neutron Spectroscopy (INS) a combined study of the molecular structure of the latter compound by X-ray diffraction, INS, IR and Raman spectroscopy supplemented by DFT calculations was undertaken.

Neutron scattering data collection was carried out at the pulsed reactor IBR-2 in Dubna using the inverted time-of –flight spectrometer NERA-PR [9]. The temperature of the sample was maintained at 20(2) K. The spectra were converted from neutron per channel to $S(Q,\omega)$ function per energy transfer. In the energy transfer range from 5 to 100 meV the relative INS resolution was about 3%. The $S(Q,\omega)$ against energy transfer range is shown in Fig.1. The structure of the sample could be controlled in the temperature range from 20 K to 300 K because the NERA-PR spectrometer can record simultaneously powder diffraction patterns of the sample in this temperature range.

The total energy optimization and the harmonic force field calculations have been performed using the DMol3 program [10, 11] as a part of Materials Studio package [12]. The results have been obtained for solid 2-aminopyridine-3-carboxylic acid within the local density approximation (LDA) at PWC [13] and VWN [14] functionals and within generalized gradient approximation (GGA) at PW91 (Perdew-Wang generalized gradient approximation [13]), PBE (Perdew-Burke-Ernzerhof correlation [15]) and BLYP (Becke exchange [16] plus Lee-Yang-Parr correlation [17]) functionals. Calculations have been performed using DNP basis set as implemented in DMol3. For the system of 64 atoms in crystallographic unit cell has been obtained 189 frequency modes, in which, 168 describe normal vibrations of four molecules and 21 describe a translation and rotation modes.

Inelastic neutron scattering spectra (including overtones, combinations and interaction with lattice modes) were calculated from mass weighted normal vibrational coordinates using auntieCLIMAX program [19] adapted to the parameters of the NERA-PR spectrometer. The calculated INS spectra are presented on Fig. 1.

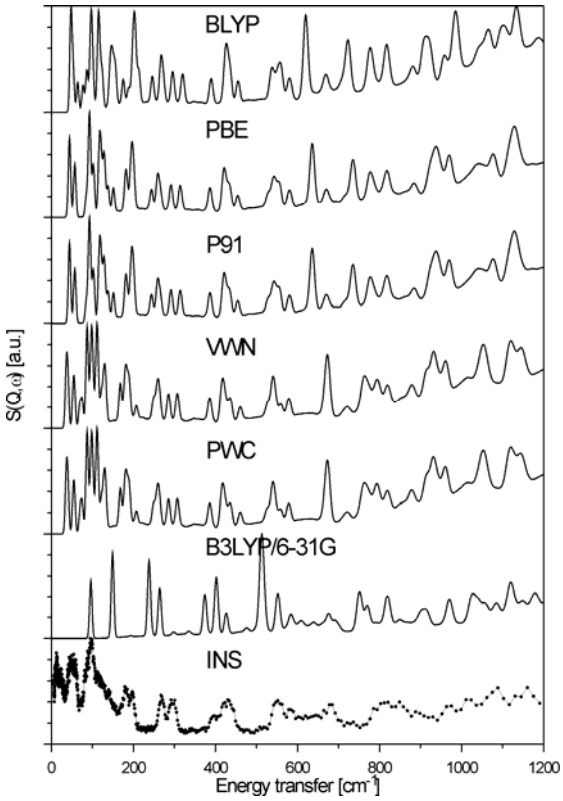

Fig.1. Experimental and calculated INS spectra of 2-aminopyridine-3-carboxylic acid.

References

[1] A. J. Dobson, R. E. Gerkin, Acta. Cryst**., C52** (1996) 1512.
[2] H. Ptasiewicz-Bąk, J .Leciejewicz, Polish J.Chem., **71** (1997) 1350.
[3] A. Pawlukojć, I. Natkaniec , Z. Malarski, J. Leciejewicz, J. Mol. Struct., **516** (2000) 7.
[4] J. Voogd, B. H. M.Verzul, A. J. M. Duisenberg, Acta Cryst., **B36** (1998) 2805.
[5] A. Pawlukojć, J. Leciejewicz, Chem.Phys**., 299** (2004) 39.
[6] A. J. Dobson, R. E. Gerkin, Acta Cryst., **C53** (19997) 1427.
[7] A. Pawlukojć, L. Sobczyk, Trends Appl. Spectr., **5** (2004) 117.
[8] G. M. Sheldrick, SHELXL97. Program for crystal structure solution and refinement, (1997) University of Goetingen, Germany.
[9] I. Natkaniec, S. I. Bragin, J. Brańkowski, J. Mayer, Proc. ICANS XIII, Abingdon 1993, RAL Report 94-025 vol.1, p.89.
[10] B. Delley, J. Chem. Phys., **92** (1990) 508.
[11] B. Delley, J. Chem. Phys., **113** (2000) 7756.
[12] http://www.accelrys.com/
[13] J. P. Perdew, Y. Wang, Phys. Rev. B, **45** (1992) 13244.
[14] S. J. Vosko, L. Wilk, M. Nusair, Can. J. Phys., **58** (1980) 1200.
[15] J. P. Perdew, K. Burke and M. Ernzerhof, Phys. Rev. Lett., **77** (1996) 3865.
[16] A. D. Becke, J. Chem. Phys., **88** (1988) 2547.
[17] C. Lee, W. Yang, R. G. Parr, Phys. Rev. B, **37** (1988) 786.
[18] Gaussian 98, Revision A.6, M. J. Frisch, et al., Gaussian Inc., Pittsburgh PA, 1998.
[19] A.J. Ramirez-Cuesta, Comput. Phys. Commun., 157 (2004) 226.

MICRODYNAMICS OF LIQUID LITHIUM–HYDROGEN ALLOY: INVESTIGATION BY INELASTIC NEUTRON SCATTERING

N.M. Blagoveshchenskii, V.A. Morozov, A.G. Novikov, M.A. Pashnev, V.V. Savostin, A.L. Shimkevich*

State Scientific Center of Russian Federation – Institute of Physics and Power Engineering, Obninsk

**Russian Research Center "Kurchatov Institute", Moscow*

The usage of liquid lithium as a coolant in nuclear power devices stipulate the necessary investigation of this metal alloys peculiarities during development of coolant technology and its rectifying with respect of admixtures [1]. It is widely appreciated that the further progress in this area of utilization, and in the liquid state theory as well, is impossible without detail study of liquids microstructure, their atomic movement, and admixtures behavior in them. The method of inelastic slow neutron scattering is the powerful one to get a very useful information [2].

Experiments by inelastic neutron scattering on liquid Li–H alloy were carried out with double time-of-flight DIN-2PI spectrometer [3] incorporated with pulsed reactor IBR-2 (FLNP, JINR, Dubna). Initial energy of neutrons was 30.8 meV. Energy resolution of elastic peak was about 3.5 meV. Container of sample – liquid lithium and Li–H alloy – was the coaxial cylinder of outer and inner diameters, 80 mm and 65 mm respectively and 110 mm in height. The walls of the container were made from ARMCO-iron foil, 0.15mm-thick. The hydrogen-admixture concentration was held at 2 % at. The samples temperature was 557°C.

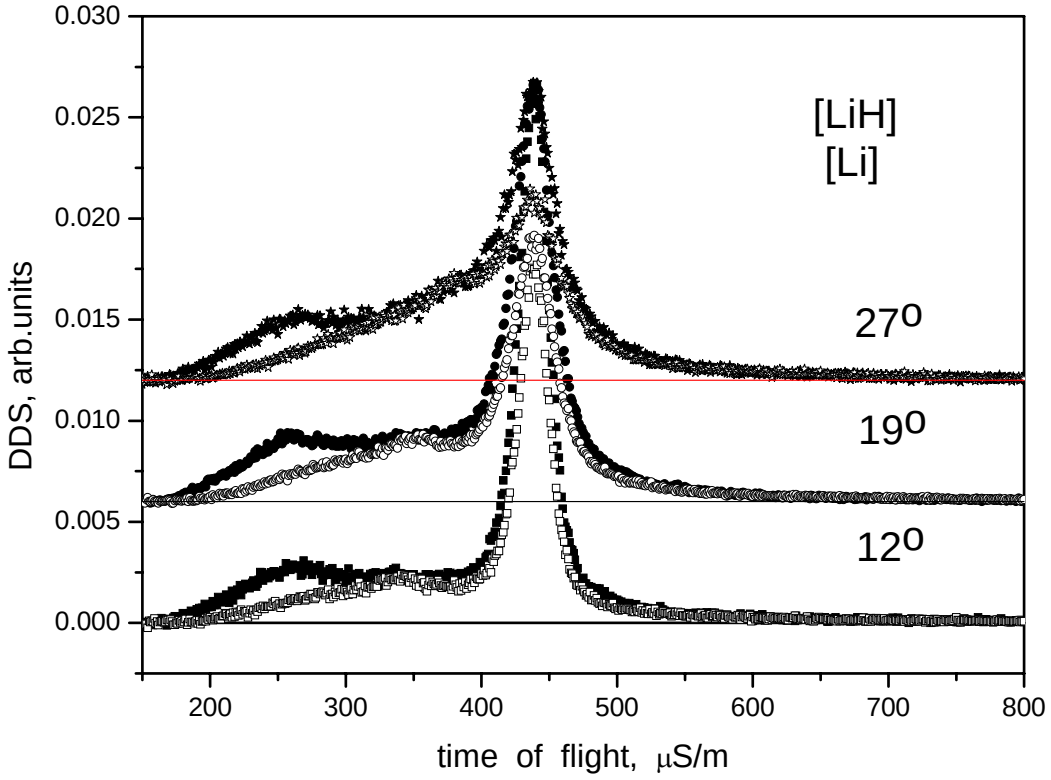

Fig.1. Typical DDS of scattered neutrons by Li (open symbols, [2]) and Li–H (full symbols).

During inferring the double-differential scattering cross sections (DDS) from the measured spectra the corrections on neutron flux attenuation by the transmission through the sample (with the presence of container matter), as well as the self-screening effect of empty container were introduced. The energy dependence of detector efficiency was taken into account. The corrections on multiple scattering and multiphonon processes were calculated by the method described in [2]. Some typical DDS of scattering are shown in fig. 1 and can be understood as demonstration of the additive nature of them at small scattering angles: it is clear that the metal (Li) matrix forms the acoustic part of the excitation spectra while the proton (hydrogen) forms the optic one.

Basing on the assumption of the experimental spectra additivity (fig. 1) the frequency spectra of lithium atoms and protons oscillations were obtained with the help of program complex SLOWN [4]. Each partial frequency spectrum was established as belonging to the "monoatomic liquid", lithium, and hydrogen respectively.

During the estimation of the frequency spectrum for alloy Li–H one can bear in mind that for the multicomponent mixture the following formula of one-phonon incoherent scattering takes place [5]:

$$\left(\frac{d^2\sigma}{d\Omega d\varepsilon}\right)^1_{INC} = \frac{k}{2k_O N}\frac{\hbar Q^2}{\varepsilon}\frac{\theta(\varepsilon)}{e^{\varepsilon/k_B T}-1} \qquad (1)$$

Here k_0 and k are wave vectors of incident and scattered neutron, $Q = k\text{-}k_O$, $\varepsilon = E - E_0$, N is nuclear density of scatterer. According to the formula (1), from the experimental data one can infer not the frequency spectrum of atoms oscillation, g(ε/h), but the so-called spectral neutron-weighted function, θ(ε):

$$\theta(\varepsilon) = g(\varepsilon/\hbar)\sum_{j=1}^{r} f_j \frac{a^2_{INC\,j}}{M_j} e^{-2W_j}\left[C_j(\varepsilon/\hbar)\right]^2 \qquad (2)$$

Here a_{INC} is the length of incoherent scattering, $P_j = [C_j(\varepsilon/h)]^2$ is average squares of polarization vectors for the partial components of phonons in alloy, being $f_1P_1+f_2P_2+\ldots= 1$, and f_j is relative concentration of atoms (sort j) by mass M_j. The function θ(ε) can be written in the another form:

$$\theta(\varepsilon) = \sum_{j=1}^{r} f_j \frac{a^2{}_{INC\,j}}{M_j} e^{-2W_j} g_j(\varepsilon/\hbar) \qquad (3)$$

Here $g_j(\varepsilon/h)$ is the frequency spectra of the partial monoatomic liquids. Taking into account the partial frequency spectra for lithium and hydrogen found earlier [2], we can estimate the function θ(ε) for Li–H alloy (see Fig.2, curve 3). Now, with known function θ(ε), and using the relation (2), the sought-after frequency spectrum of this alloy can be obtained, if the corresponding polarization vectors are known. Having no the other possibility, we use the polarization vectors counted [6] for the solid lithium hydride. The frequency spectrum for Li–H (2 % at.) alloy estimated so is demonstrated by Fig. 2 (curve 4). The frequency spectrum for Li–H alloy reveals, in general features, the resemblance with the one for the solid lithium hydride [6].

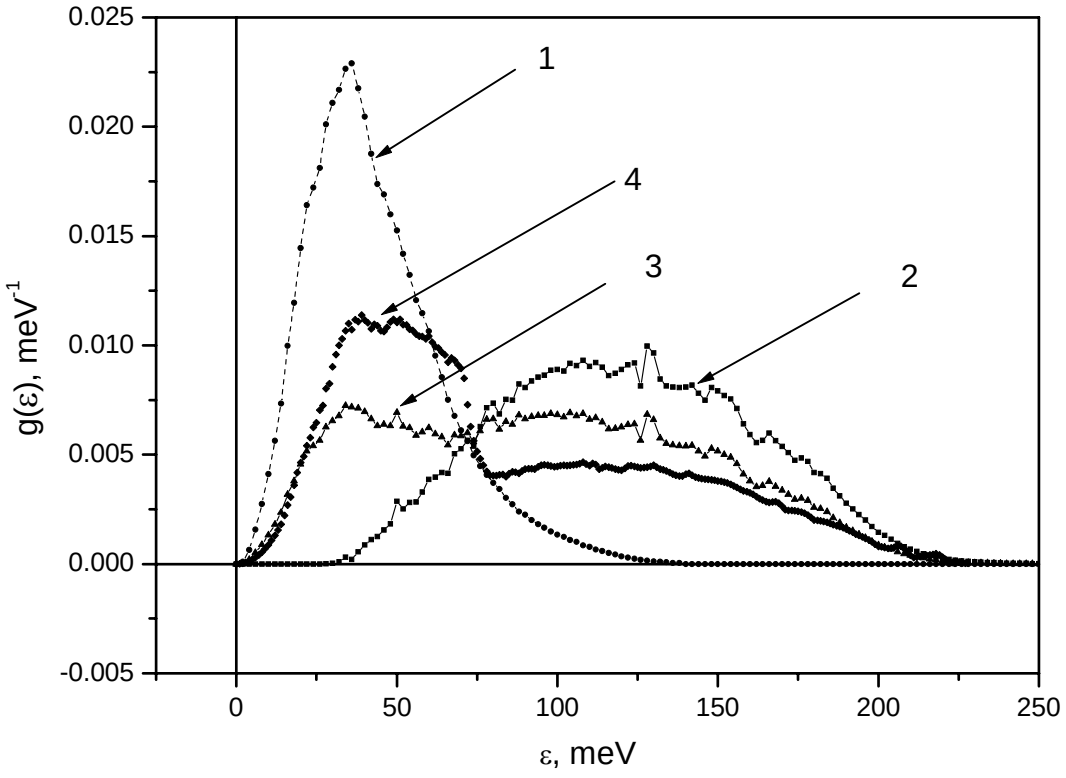

Fig.2 The frequency spectra:
1 – for pure liquid lithium; 2 – for proton liquid; 3 – spectral function θ(ε);
4 – the sought-after frequency spectrum for Li-H(2 % at.) alloy.

REFERENCES

1. *В.Н. Михайлов, В.А. Евтихин, И.Е. Люблинский, А.В. Вертков, А.Н. Чуманов.* Литий в термоядерной и космической энергетике XXI века**.** М.: Энергоатомиздат, 1999.
2. *Благовещенский Н.М., Морозов В.А., Новиков А.Г. и др.* Изучение микродинамики жидкого лития методом неупругого рассеяния нейтронов: Кристаллография. – в печати.
3. User Guide. Neutron Experimental Facilities for Condensed Matter Investigation at JINR. Ed. by Sikolenko V. Dubna: JINR Press. - 1997. - P.25.
4. *Лисичкин Ю.В., Довбенко А.Г., Ефименко Б.А. и др.* Учет конечных размеров образца при обработке измерений дважды-дифференциальных сечений рассеяния медленных нейтронов: ВАНТ.- Сер. Ядерные константы.-1979.-Вып.2.-С.12-24.
5. *Гуревич И.И., Тарасов Л.В*. Физика нейтронов низких энергий-М..:Наука, 1965. 608 с.
6. *Землянов М.Г., Бровман Е.Г., Черноплеков Н.А., Шитиков Ю.Л.*. Исследование динамики гидрида и дейтерида лития по неупругому рассеянию холодных нейтронов: IAEA proceedings of a Symposium on Inelastic Scattering of Neutrons. IAEA, Vienna -1965.-P.431-451.

QENS STUDIES OF DURENE AND TCNB–DURENE CHARGE TRANSFER COMPLEX

J. Krawczyk[a], M. Nowina Konopka[a], I. Natkaniec[a,b], I.V. Kalinin[c], O. Steinsvoll[d]

[a] *H.Niewodniczański Institute of Nuclear Physics PAN, 31-342 Kraków, Poland*
[b] *Joint Institute for Nuclear Research, Dubna 141980, Russia*
[c] *Institute of Physics and Engineering, Obninsk 249033, Russia*
[d] *Institute for Energy Technology, 2007 Kjeller, Norway*

The quasi-elastic neutron scattering (QENS) spectra of durene and TCNB–durene complex were measured using the direct geometry spectrometer DIN-2PI, operating at the IBR-2 pulsed reactor of Joint Institute for Nuclear Research in Dubna, Russia. The initial neutron energy of 4.71 meV was used, the energy resolution was 0.14 meV (HWHM). The spectra were measured simultaneously for 18 scattering angles between 6º and 134º, corresponding to momentum transfer $Q < 2.8$ Å^{-1}. The spectra for durene were measured at temperatures T = 47 K, 100 K, 150 K, 200 K, 250 K and 290 K. For TCNB – durene complex the spectra were measured at T = 80 K, 150 K, 220 K and 290 K.

The measured spectra were corrected for the sample-holder scattering, the constant background of fast neutrons and for the inelastic scattering background. The multiple scattering corrections were applied as well. The instrumental resolution function was determined by measuring the spectra of vanadium. The resolution function was described by a slightly distorted Gaussian function.

For both substances no quasi-elastic broadening was observed for temperatures below 150 K (see Figures below). The spectra measured at temperatures from 150 K to 290 K could be described by the model of instantaneous 120º jumps of the CH_3 groups around the three-fold symmetry axis.

The fitted mean time between jumps τ changes from 40 ps at T = 150 K to 7 ps at room temperature for durene and from 20 ps at T = 150 K to 5 ps at room temperature for TCNB–durene complex. The temperature dependence of the best-fit time τ can be described by the Arrhenius formula. The fitted activation energy is 4.8 ± 1.3 kJ/mole for durene and 3.3 ± 1.2 kJ/mole for TCNB–durene complex.

The results of the QENS experiment for both substances are being published as a part of a larger paper containing also the results of other experimental methods in the journal Phase Transitions.

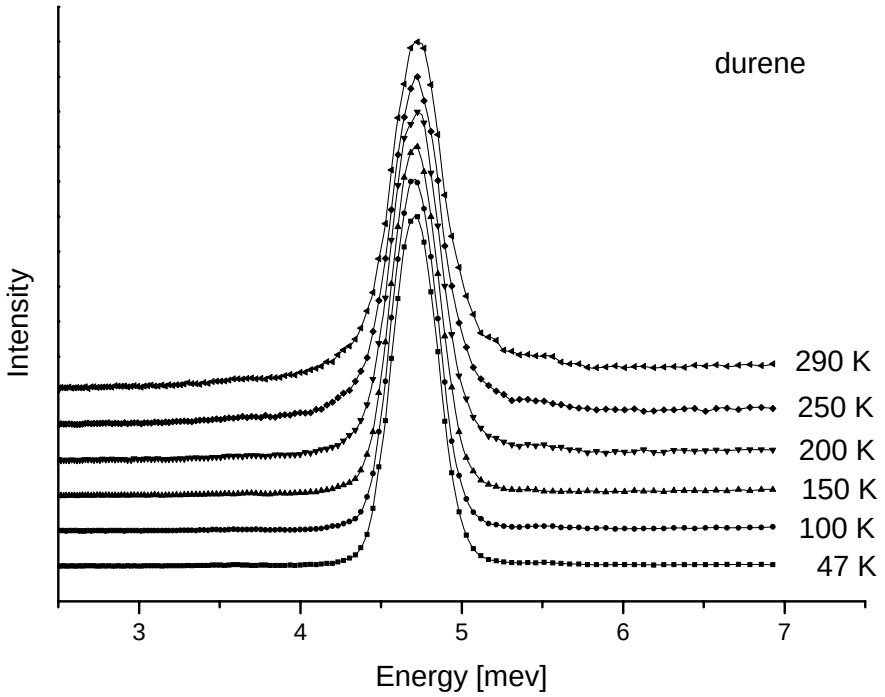
durene
Intensity
290 K
250 K
200 K
150 K
100 K
47 K
3
4
5
6
7
Energy [mev]

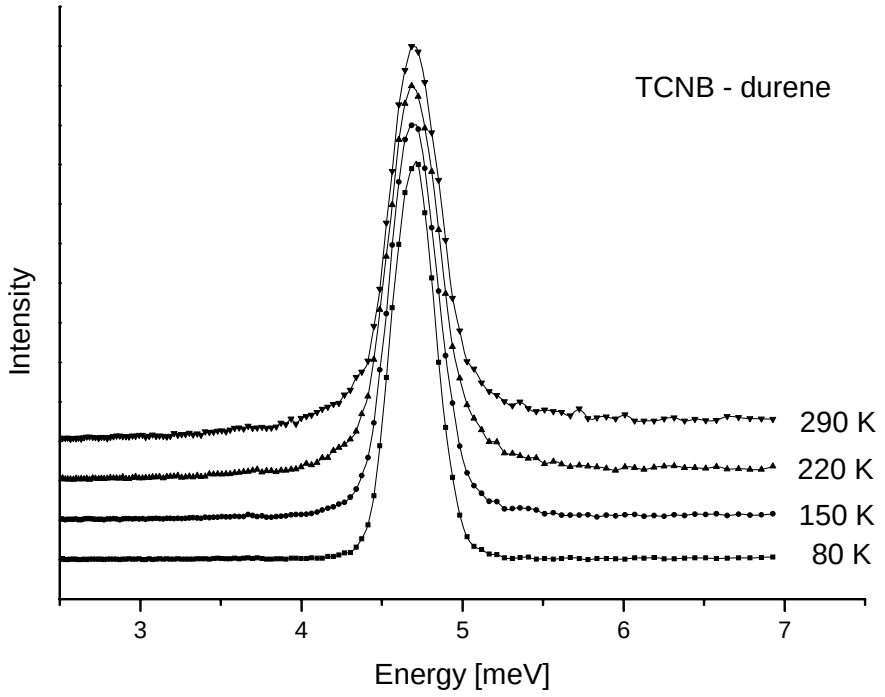
TCNB - durene
Intensity
290 K
220 K
150 K
80 K
3
4
5
6
7
Energy [meV]

INTERNAL DYNAMICS OF 17-α-METHYLTESTOSTERONE STUDIED BY ^{1}H NMR AND IINS

Krystyna Holderna-Natkaniec[2], Ireneusz Natkaniec[1,3], Dorota Nowak[1,2]

Joint Institute fon Nuclear Research, 141980 Dubna, Russia
Departament of Physics Adam Mickiewicz University,61-614 Poznan, Poland
H. Niewodniczanski Institute for Nuclear Physics Polish Academy of Sciences, 31-342 Krakow, Poland

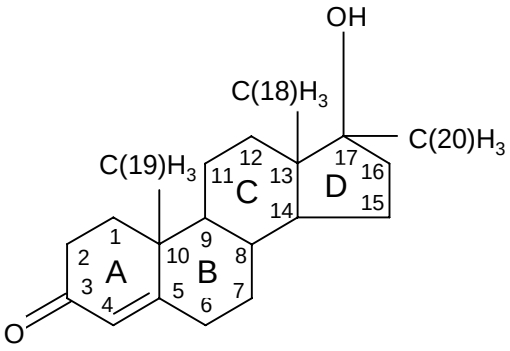

Fig.1. Structure of the methylotestosterone molecule and the

17-α-Methyltestosterone of the chemical formula $C_{20}H_{30}O_2$ ½ H_2O is built of a four-ring steroid carbon skeleton: three cyclohexane rings denoted henceforth as A, B and C, and a single cyclopentane ring denoted as D. In the 17-α-methyltestosterone molecules tree methyl groups denoted as C(19)H3, C(18)H3 and C(20)H3 are attached to the carbon atoms skeleton at C(10), C(13) and C(17), positions, respectively (Fig.1). Carbon atom C(17) is also substituted by a hydroxyl group. 17-α-Methyl-testosterone crystallizes in the tetragonal primary cell with the spatial group $P2_12_12_1$, Z=8.

The information on internal dynamics can be obtained from the temperature dependencies of: the slope line width and the second moment of ^{1}H NMR line as well as from analysis of the phonon density of state spectra and the assignment proposed on the basis of quantum mechanical calculations. The aim of our studies was analysis of the dynamics of methyl groups substituted at the steroid skeleton in different local arrangements.

Neutron scattering measurements were made on the inverted geometry time-of-flight NERA spectrometer operating at the pulsed reactor IBR-2 in Dubna. The quantum mechanical QC calculations were performed by the semi-empirical (as less time consuming) and the *ab initio* density functional theory methods. The DFT optimisation using Gaussian 03 set of programs was performed with the B3LYP hybrid functionals in conjugation with People basis set using all atoms coordinates from the crystals structure. The ^{1}H NMR measurements were carried out in the temperature range of 90-300 K on a home-made apparatus, with the continuous wave spectrometer operating in the double modulation system at 25 MHz .

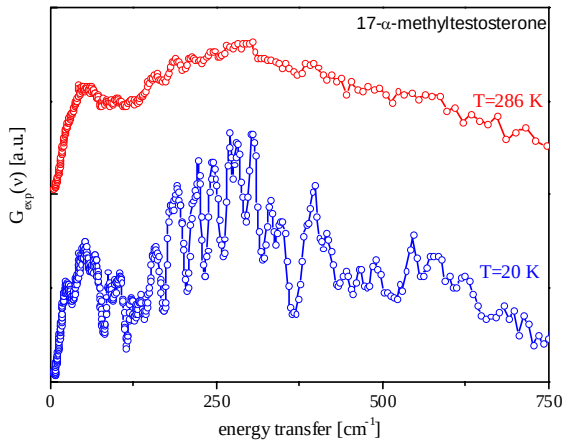

Fig.2. Phonon density of state spectra of 17-α-methyltestosterone at 287 and 20 K.

No phase transitions were observed in the temperature range studied. The tetragonal unit cell parameters are as follows: at 287K: a=6.38, b=12.63, c=44.13 and at 20 K: a=6.23, 12.74, c=42.51 in [A] . The IINS spectra were measured versus the incoming neutron wave-length from 0.7 to 6 A at 287 K and 20 K

The IINS spectra were transformed into the phonon density of state spectra G(ν) in one phonon scattering approximation, as shown in Fig.2. The $G_{exp}(\nu)$ spectra were compared with the ones calculated by PM3 and DFT/B3LYP/6-311G** methods, in Fig.3.

The quantum mechanical calculations permitted determination of the frequencies of internal normal modes and prediction of their assignment. In particular, according to PM3 calculations the torsional out-of-plane modes of the subsequent methyl groups $C(18)H_3$, $C(19)H_3$ $C(20)H_3$

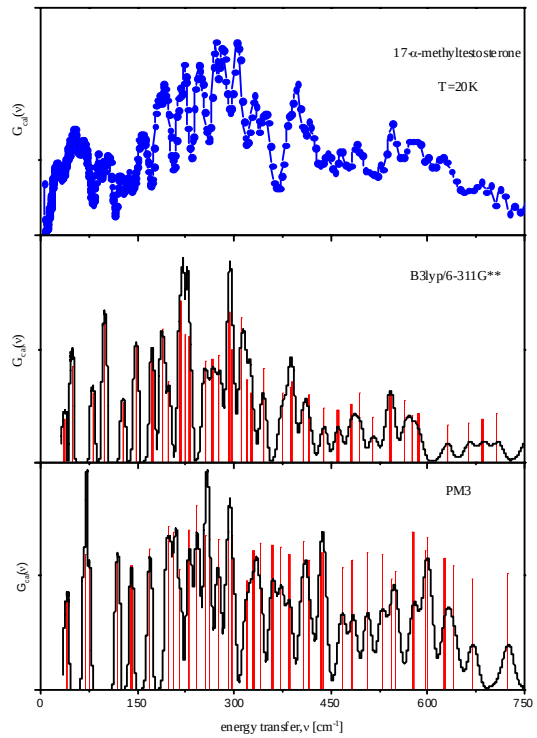

Fig.3. Comparison of experimental and simulated G() spectra in isolated molecule approximation by DFT and PM3 methods

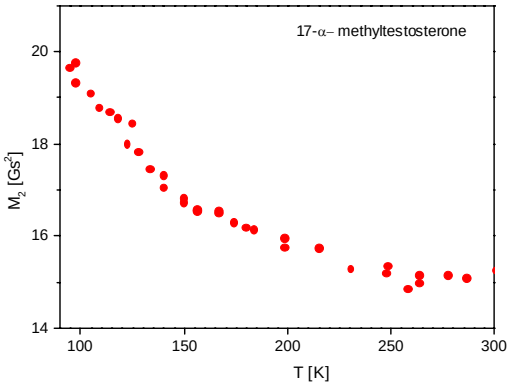

Fig.4. Temperature dependence of the second moment of ^{1}H NMR line.

should be at: (255.8; 275.2) cm^{-1} (196.8; 206.7; 230.6; 242.7; 290.1) cm^{-1} and (230.6; 242.7) cm^{-1}. The DFT calculations give that torsional out-of-plane modes of methyls at: (148,4; 174.7; 189.0; 200.3; 227.9; 233.4; 255.9; 267.8), (174.7; 189.0; 219.7; 227.9; 255.9; 267.8), (267.8; 278.4; 295.8) for C(18)H$_3$, C(19)H$_3$ and C(20)H$_3$, respectively (in sublattice A).In the IINS spectrum at 20 K the very intensive bands assigned to the methyl groups torsion are observed at (223.4; 271.1) cm^{-1}, at (157.1; 190.3; 216.2; 281.5) cm^{-1} and (190.3; 216.2) cm^{-1} for three methyl groups, respectively.

The internal dynamics of the methyl groups was determined by ^{1}H NMR. Fig.4 presents the temperature dependence of the second moment of ^{1}H NMR line. With increasing temperature the value of M_2 decreased continuously from 20 to 15 Gs^2. The experimental values are interpreted with respect to the value of M_2 calculated for the rigid lattice according to the van Vleck formula $M_2=358.081\ N_o^{-1}\Sigma r_{jk}^{-6}$, where N_o-the number of protons in the unit volume analysed, r_{jk}- the interproton distance. The reduction of M_2 may be attributed to subsequent onset of internal reorientation of methyl groups. The use of the hydrogen position of methyltestosterone from the X-Ray data [1] was assuming the steroid skeleton structure and the length of C-H bond as 1.09A and the CCH angles as tetrahedral leads to an unrealistic value of M_2.

The intramolecular part of the second moment for the rigid lattice was calculated as 21.6 Gs^2. Having taken into regard the subsequent onset of reorientations of one, two or three methyl groups around the three-fold symmetry axes, the value of M_2 was found as 17, 13 or 10 Gs^2. The intermolecular contribution to M_2 was 5 Gs^2. Taking into account the above values, the temperature dependence of M_2 can be interpreted as indicating a subsequent onset of the methyl groups reorientations. The calculations of the energy of the molecule *versus* methyl positions give different values of the barrier for subsequent methyl reorientation [2]. In conclusion, the methyl groups of 17-a-methyltestosterone are dynamically inequivalent.

Financial support under the grant of the Polish Plenipotentiary at JINR is gratefully acknowledged by the authors (KHN, IN).
The calculations have been performed at the PCSC in Poznan.

[1] Z.Galdecki ,P.Grochulski, Z.Wawrzek, J Cryst. Spectr.Res 19, 577, 1989.
[2] KHolderna-Natkaniec, I.Natkaniec, in preparation

VIBRATIONAL DENSITY OF STATES OF PHOTOSYNTHETIC PIGMENT-PROTEIN COMPLEXES

J. Pieper[1], I. Natkaniec[2], A. Skomorokhov[3], G. Renger[1]

[1]*Max-Volmer-Laboratories for Biophysical Chemistry, TU Berlin, Germany*
[2]*Frank laboratory of Neutron Physics, JINR, Dubna*
[3] *Institute for Physic and Power Engineering, Obninsk, Russia*

The light-harvesting complex of photosystem II (LHC II) is the major antenna complex of green plants (see e.g. [1] and references therein). In plant photosynthesis, antenna complexes like LHC II have a dual function: 1) increase of the spectral and spatial absorption cross section of the photosynthetic apparatus and 2) ultrafast excitation energy transfer (EET) to the photochemically active photosynthetic reaction centers. Time-resolved spectroscopic studies reveal that Chl b $\rightarrow$ Chl a EET in LHC II is ultrafast with kinetic components in the femtosecond - and picosecond range [2]. A detailed understanding of this rapid dynamics of EET requires –besides other aspects- quantitative information on the vibrational density of states, because the protein low-frequency vibrational modes mediate EET between energetically inequivalent electronic states via electron-phonon coupling [3].

So far, electron-phonon coupling has been preferentially studied by line-narrowing optical spectroscopy [4]. However, for technical reasons this approach is limited to temperatures as low as 5 – 30 K. Recently, we have used inelastic neutron scattering (INS) to directly characterize the vibrational dynamics of solubilized LHC II in the temperature range between 5 and 100 K [5]. The INS spectra are consistent with harmonic vibrational dynamics with a Boson peak observed at about 2.5 meV and thermal population of vibrational levels according to Bose-Einstein statistics (see Fig. 1). This effect is obviously more pronounced at higher energy transfers.

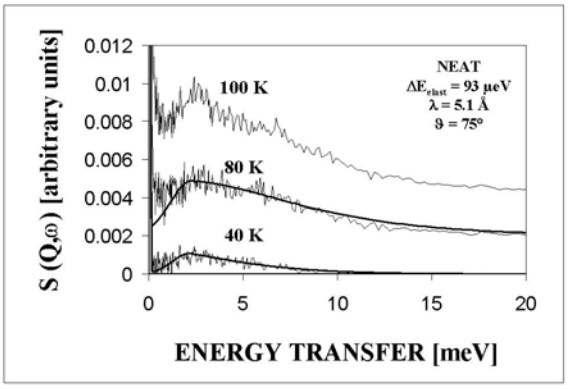

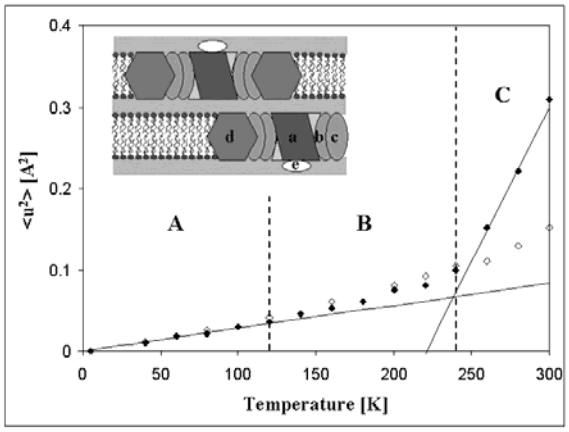

Figure 1:

INS spectra of solubilized LHC II (noisy lines) obtained with an incident neutron wavelength of 5.1 Å at different temperatures.

Figure 2:

Average atomic mean square displacement of hydrated (full diamonds) and dry PS II membrane fragments (open diamonds) as a function of temperature. The inset shows a schematic representation of the sample system with Photosystem II embedded into the thylakoid membrane. LHC II is labelled by "d".

The aim of the present experiment was to extend our inelastic measurements on photosynthetic pigment-protein complexes to higher and, especially, to physiologically relevant temperatures. As sample system we have chosen photosystem II (PS II) membrane fragments (see inset of Fig. 2), because of a) availability in higher quantities than isolated LHC II and b) the possibility of defined

hydration. Previous QENS studies of hydrated and dry PS II membrane fragments [6] revealed that the protein dynamics is characterized by harmonic vibrational motions below ~120 K (Range A in Fig. 2) and exhibits the onset of anharmonic motions at two distinct T-values of 120 and 240 K, respectively (Ranges B and C in Fig. 2). The dynamical transition at 240 K is widely suppressed in dry samples, which is in line with a plasticizing effect of water on proteins.

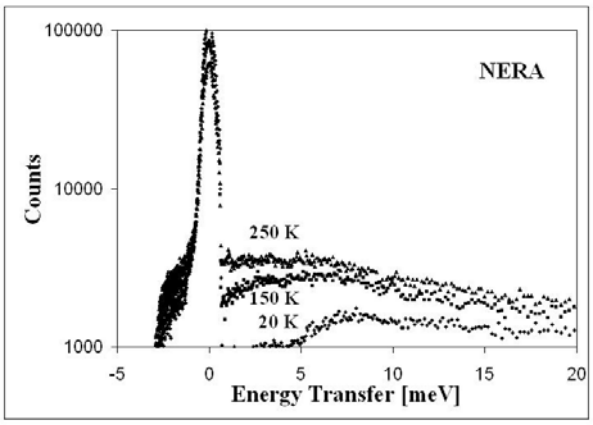

Figure 3:

INS spectra of PS II membrane fragments obtained using the spectrometer NERA at different temperatures.

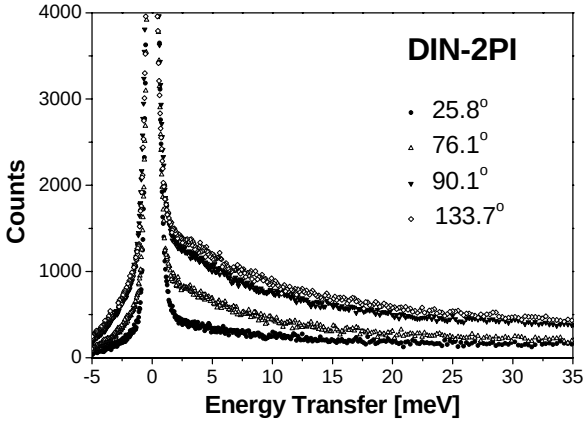

Figure 4:

INS spectra of PS II membrane fragments obtained using the spectrometer DIN-2PI at different scattering angles.

INS experiments on PS II membrane fragments hydrated in D_2O at 57 % r.h. were carried out as a function of temperature on the spectrometer NERA (Fig. 3) and as a function of scattering angle at room temperature at the spectrometer DIN-2PI (Fig. 4). At low-temperatures (20 K), the INS spectrum of PS II membrane fragments is qualitatively consistent with the results described above for LHC II. A Boson peak is observed at ~7.5 meV, which is well separated from the elastic line. At higher temperatures, however, the INS spectra are smeared out and exhibit a shift towards lower frequencies (see Figs. 3 and 4). This effect differs from that shown in Fig. 1 for LHC II, which is characteristic for harmonic vibrational motions below ~120 K (Range A in Fig. 2). Rather, the observed temperature dependence is consistent with a stronger damping of vibrational motions above a transition from the crystalline-like to the amorphous state of the protein (Ranges B and C in Fig. 2). A more detailed quantitative analysis of the data in terms of a damped harmonic oscillator model is currently in progress.

In terms of antenna functionality this means that the spectral overlap between different electronic states is significantly increased with increasing temperature, not only due to a larger thermal population of vibrational states, but also due to a broadening of the distribution of available vibrational frequencies. In consequence, higher transition propabilities and faster EET kinetics are observed at physiological temperatures. Thus, the data presented here from NERA and DIN-2PI measurements nicely demonstrate that INS is capable of providing valuable quantitative information on the vibrational dynamics of pigment-protein complexes not only at low, but also at physiological temperatures.

Acknowledgement:

Financial support from Deutsche Forschungsgemeinschaft (SFB 429, TP A1) and from JINR Dubna is gratefully acknowledged. We are also grateful to S. Kussin and M. Weß (TU Berlin) for their help in sample preparation, Dr. A.V. Puchkov for cooperation as well as to D. Nowak V.M. Morozov for assistance during the neutron scattering experiments.

References:

1. Renger, G. In Concepts in Photobiology and Photomorphogenesis; G. S. Singhal, G. Renger, K. Sopory, K.-D. Irrgang, Govindjee, Eds.; Narosa Publishing House, New Delhi, India, 1999; p. 52
2. Bittner, T.; Irrgang, K.-D.; Renger, G.; Wasilewski, M. R. J. Phys. Chem. 1994, 98, 11821.
3. Kühn, O.; Renger, T.; May, V.; Voigt, J.; Pullerits, T.; Sundström, V. Trends in Photochem. Photobiol. 1997, 4, 213.
4. Pieper, J.; Schödel, R.; Irrgang, K.-D.; Voigt, J.; Renger, G. J. Phys. Chem. B. 2001, 105, 7115.
5. Pieper, J.; Irrgang, K.-D.; Renger, G.; Lechner, R. E. J. Phys. Chem. B. 2004, 108, 10556.
6. Pieper, J.; T. Hauß, A. Buchsteiner, K. Baczyński, K. Adamiak.; Lechner, R. E.; Renger, G.; submitted to Biochemistry.

LATTICE VIBRATIONS IN AN α- AND β- AGCUS SUPERIONIC CONDUCTOR

A.N. Skomorokhov[1], D.M. Trots[2], S.G. Ovchinnikov[1], H. Fuess[2]

[1]*Institute for Physics and Power Engineering, Obninsk, Russia*
[2]*Insitute for Material Science, Darmstadt University of Technology, Germany*

A ternary compound of silver copper sulphide, AgCuS, has long been known to occur in nature with the mineral name stromeyerite [1]. At the beginning, the main interest in AgCuS was focused on its mineralogical occurrence. However, recently the high ionic conductivity and gradual disorder in sequential phase transitions of AgCuS has renewed the interest to this compound. Three structure modifications of AgCuS with different degree of disorder in crystal lattice are known now. The low temperature fully ordered γ-phase exist at temperature up to 250 K, β- AgCuS in the temperature range between 250 K and 366 K, and superionic α- AgCuS exist at temperature above 366 K. As is known, the lattice dynamics and diffusion in superionic conductors are closely related. In particular, it is assumed that diffusion in superionics can be considered as a process related to the low-energy optic (LEO) mode observed in the vibrational spectra of superionics [2]. However, the role and the origin of the LE-modes in superionic conductor is not clear [2].

In the present work we report the results of inelastic neutron scattering experiment on the powder α- and β- AgCuS superionic conductor performed on DIN-2PI spectrometer. The aim of the experiment consisted in studying the transformation of the lattice dynamics during phase transition, especially at low-energies.

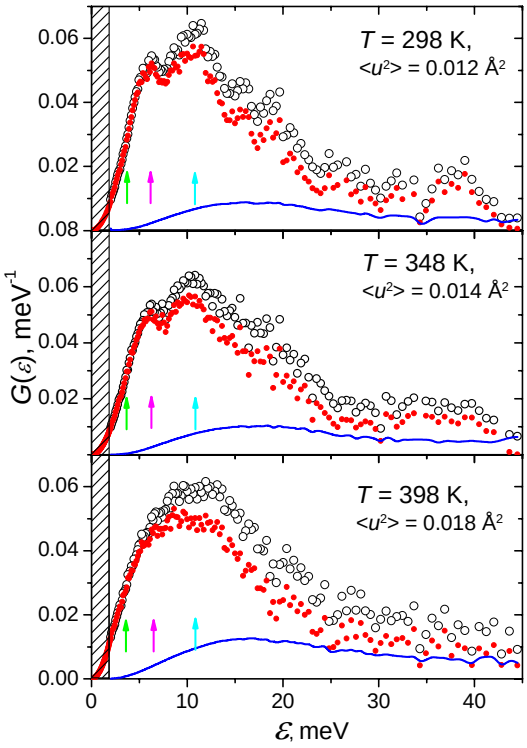

Figure 1. $G(\varepsilon)$ in α- and β- AgCuS with one-phonon and mutiphonon contributions. Dashed region corresponds to the energy range where $G(\varepsilon)$ was interpolated accordingly the Debye law.

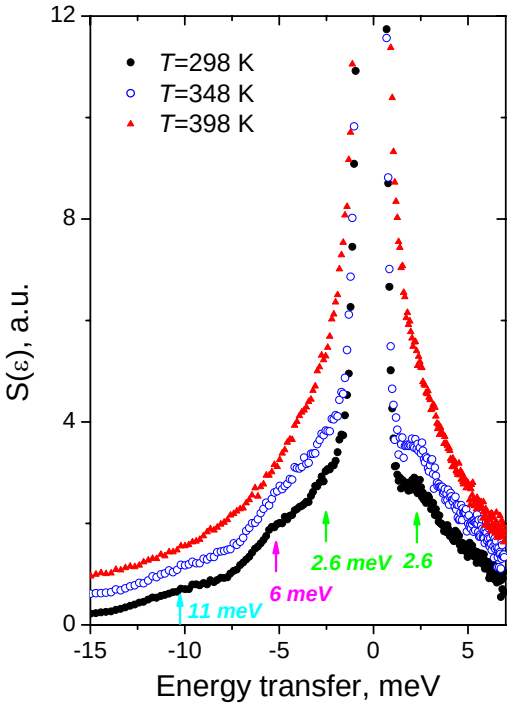

Figure 2. Dynamic structure factor of AgCuS averaged over all angles at 298, 348 and 398 K.

The neutron weighted phonon DOS in β- AgCuS consists of a broad distribution in the energy range between 0 and 25 meV with two main overlapped maxima at 6 and 10.5 meV and high-energy tail extended up to ~42 meV (figure 1). In booth phases, α- and β-, $G(\varepsilon)$ demonstrates the linear dependence on ε at the energy ε>2 meV, instead of the parabolic one, $G(\varepsilon) \sim \varepsilon^2$, typical of 3D solids. We can assume that linear dependence of $G(\varepsilon) \sim \varepsilon$ at low energy is connected with the presence of the lowest-energy mode observed in dynamic structure factor $S(Q,\varepsilon)$ at 2.6 meV. In β-phase, $S(Q,\varepsilon)$ changes with temperature according to Bose-

population factor; the resulting $G(\varepsilon)$ at 298 and 348 K fall together within statistical errors. Such type of $G(\varepsilon)$ and $S(Q,\varepsilon)$ temperature dependence of β- AgCuS suggests a harmonic behavior in this temperature range. On the other hand, At 398 K, $S(Q,\varepsilon)$ and $G(\varepsilon)$ spectra changes considerably. The low-energy part of $S(Q,\varepsilon)$ merges with the elastic peak to become an unified broad energy distribution centered at ~ 0 meV with long tails extended to 15-20 meV. Most probably, the changes in $S(Q,\varepsilon)$ at the β → α phase transition are caused by softening of the low energy modes accompanied by increase of the peak width. Phonon DOS at the β → α phase transition also changes considerably, there is increase intensity in low-energy modes bellow 4 meV, and the shape of $G(\varepsilon)$ is smeared out at the energy above 4 meV.

Some important lattice dynamics parameters were obtained from the phonon density of states (figure 3,4). The mean square displacements $\langle u^2 \rangle$ in β-phase demonstrates harmonic behavior, whereas α-β phase transition make the quasiharmonic approach to be inapplicable. In itself the harmonic behavior of β-AgCuS is surprising, because generally, the lattice dynamics of superionic conductor is characterized by high anharmonicity. We can suggest that anharmonic effects in lattice dynamics of AgCuS are connected with motion of Ag masked by its small weighting factor. A lattice specific heat $C_v(T)$ calculated on the basis of $G(\varepsilon)$ and experimental $C_p(T)$ shows low-temperature anomaly. This indicates the presence of low-energy mode in γ- as well in β- AgCuS. Calculated $\langle u^2 \rangle$ and $C_v(T)$ are in good agreement with experimental values obtained by powder diffraction and differential calorimetric methods correspondingly. Excess of $\langle u^2 \rangle$ obtained from diffraction experiment in comparison with $\langle u^2 \rangle$ derived from $G(\varepsilon)$ indicates that disorder in β-AgCuS has rather dynamic character than static one.

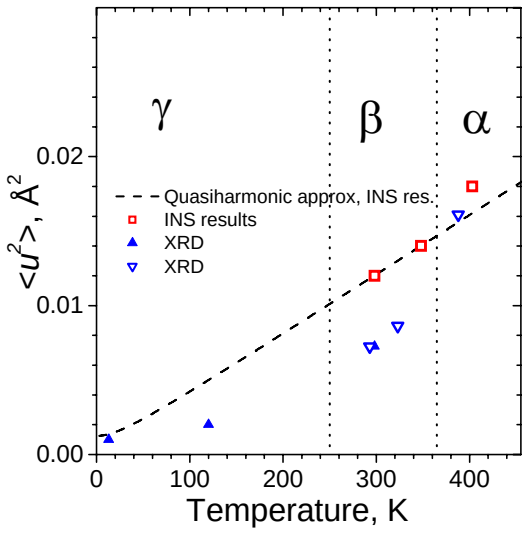

Figure 3. The neutron-weighted mean square displacement $\langle u^2 \rangle$ (AgCuS) derived from INS and XRD (U_{iso}) experiments.

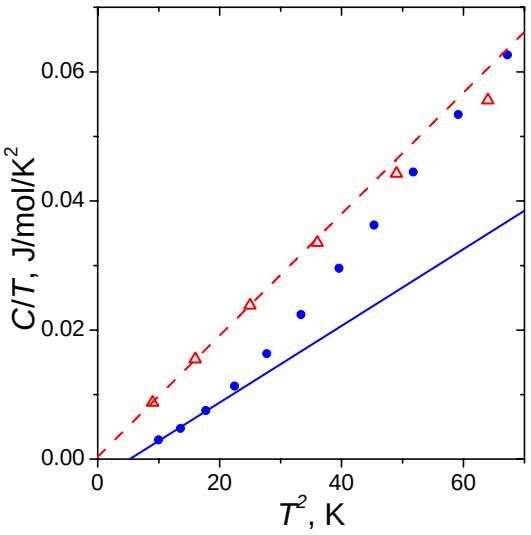

Figure 4. Total specific heat C/T of AgCuS (filled circles) and neutron weighted C_{vib}/T of β– (empty triangles) derived in quasiharmonic approximation. Linear interpolation is shown by lines.

Thermodynamic parameters C_V, $\langle \varepsilon \rangle$ and $\langle \varepsilon^2 \rangle$ derived from $G(\varepsilon)$ at 298, 348 and 398 K coincide within precision, whereas Debye temperature demonstrates considerable softening under β → α phase transition. Since C_V, $\langle \varepsilon \rangle$ and $\langle \varepsilon^2 \rangle$ are calculated by integration of $G(\varepsilon)$ over all the energy range of lattice vibrations and the Debye temperature was derived in the low-energy limit from $G(\varepsilon)$, we believe the most considerable changes in lattice dynamics take place at the β → α phase transition at the low-energy part of the spectra. However, for detailed studies of the low-energy dynamics in AgCuS, coherent INS experiment on single crystal as well numerical calculations are very required.

References

1. Schwartz G M 1935 *Econ. Geol*. **30** 128; Suhr N 1955 *Econ. Geol*. **50** 347; Frueh A J 1955 *Z. Kristallogr*. **106** 299; Djurle S 1958 *Acta Chem. Scand*. **12** 1427; Skinner B J 1966 *Econ. Geol*. **61** 1; Skarda C, Wuensch B J, Prince E 1981 *NBS Tech. Note* 1160 57
2. Wakamura K 1997 *Phys. Rev*. B **56** 11593; Wakamura K 1999 *Phys. Rev*. B **59** 3560; Boyer L L 1980 *Phys. Rev. Lett.* **45** 1858; Boyer L L 1981 *Solid State Ionics* **5** 581

INFLUENCE OF INTERCALATION ON PHONON SPECTRA OF TITANIUM DICHALCOGENIDES

A.N. Titov[1], A.N. Skomorokhov[2], A.A. Titov[3], S.G. Titova[3], V.A. Semenov[2]

[1] *Institute of Metal Physics, Ural Branch of Russian Acad. Sci., Ekaterinburg*
[2] *Institute for Physics and Power Engineering, Obninsk, Russia*
[3] *Institute of Metallurgy, Ural Branch of Russian Acad. Sci., Ekaterinburg*

The systematic study of inelastic neutron spectra (DIN-2PI spectrometer) for intercalation compounds based on titanium diselenide with a common formula M_xTiSe_2, M =Cr, Fe, Ni, Ag was performed. It is shown that intercaltion influence on phonon spectra of the material is determined mainly by host lattice modification due to formation of covalent Ti-M-Ti centers. It is established that in case when the impurity electron band is located in vicinity of Fermi level the significant lattice softness is possible.

Intercalation by metal M of titanium dichalcogenides leads to formation of covalent centers, which may be schematically written as Ti-M-Ti. Such centers act both as traps for free charge carriers and centers of lattice deformation. This fact gives a possibility to treat the electrons localized at Ti-M-Ti-centers as impurity polarons. An absence of dispersion for the impurity bands in spite their closeness to Fermi level (0.1-0.3 eV) [1,2] gives a support for such consideration. The temperature dependence of degree of localization for charge carriers trapped by Ti-M-Ti centers, in principal, coincides with theoretical prediction for polarons, demonstrating metallic-type conductivity for both high temperature range (above the limit of thermal stability for polarons) and low temperature range (so called heavy polaron regime) together with presence of intermediate temperature range with small conductivity of activation type (the regime of localized polarons). It was suggested that the change of regime occurs smoothly, while recently it was experimentally found that this change is accompanied by a first order phase transition [3]. This effect was explained as a sequence of relation between a degree of polaron localization and lattice elasticity, which is connected with an influence of density of states at Fermi level on dielectric constant of the material. Increase of density of states during enhancement of polaron localization may lead to enhancement of screening for interatomic repulsion by conducting electrons, and, as a result, to lattice softness. Moreover, as degree of polaron localization growths with lattice deformation, enhancement of localization makes its following increase easer.

The problem consists of an absence of experimental proof for infleunce of polaron localization degree on lattice elasticity. The inelastic neutron scattering is most direct method to find such an influence, because it gives direct density of phonon states $G(\omega)$. A comparison of $G(\omega)$ for an initial material $TiSe_2$ and intercalation compounds with different metals, forming the centers of localization with different bond energy, will give a possibility to establish a character of influence of polaron state for charge carrier on phonon spectra and, as a result, on elstic properties.

As objects of research the materials with general formula $M_{0,25}TiSe_2$, M = Cr, Fe, Ni, Ag have been chosen. Such interclant contents determines the limit at which the introduced atoms can be considered as independent: the increase of the intercalant content over x=0,25 results in its ordering [4] and essential modification of phonon spectrum of a material that complicates its comparison with data for initial $TiSe_2$.

Investigation of inelastic neutron scattering was performed with DIN-2PI spectrometer. The measurements were carried out with neutron energy 11.8 meV at room temperature. The energy resolution for an elastic line was equal to 0.8 meV. Scattering rate was registered by 15 ^3He-

detectors in 28°-134° an interval of angles. The measurements of a background and vanadium spectra for calibration of detectors were carried out in the same conditions. At spectra processing the contribution for multi-phonon scattering and absorption of neutrons was taken into account. Resulting spectra are shown in Fig. 1. It is well visible, that the form of phonon spectrum as a whole is kept, showing presence of three main well distinct peaks which position depends by intercalant nature.

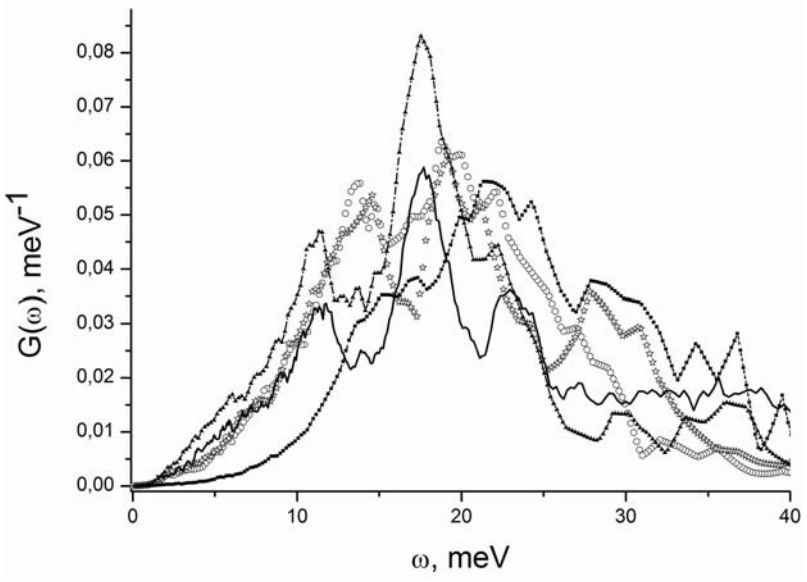

Fig. 1. Density of phonon states for фононных conditions $M_{0,25}TiSe_2$: $TiSe_2$ (line), M = Ag (triangles), Fe (open circles), Cr (asterisks), Ni (squares) calculated using inelastic neutron scattering spectra.

The typical temperature dependences of a heat capacity calculated from G(ω) data, are shown in a Fig. 2. These materials are chosen because there are experimental data of direct measurement of a heat capacity for these systems [5]. The experimental dependence of a heat capacity was approximated within the framework of Debye model. As well as at direct measurement, it is impossible to approach precisely the experimental data within the framework of this model with constant characteristic temperature Θ_D at T≥10 K. Apparently, Θ_D, obtained for T≤10 K should be considered as the parameter describing the general lattice elasticity.

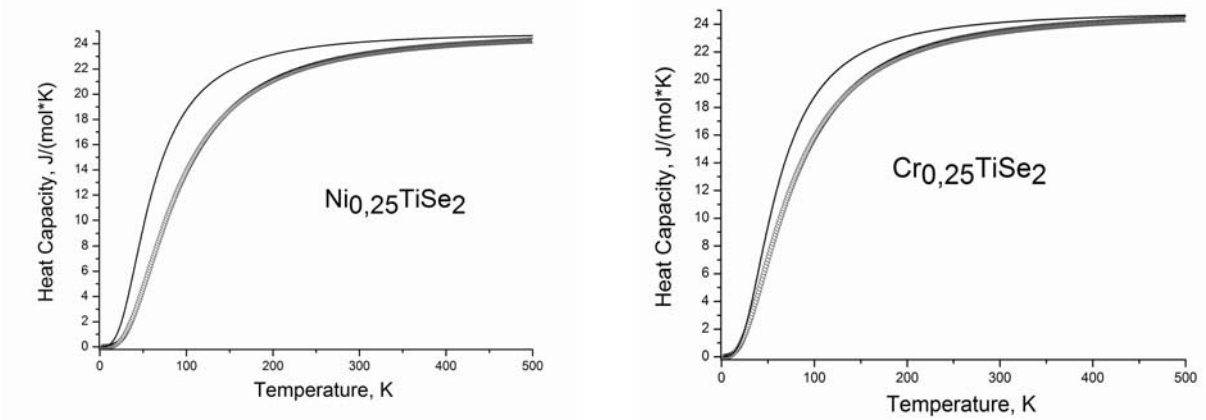

Fig. 2. The typical temperature dependences of a heat capacity obtained from density of phonon states data; symbols correspond to the experiment (data from [5]), the curve – to approximation using Debye model.

Apparently, a change of lattice elasticity during intercalation can be connected to the following: 1) weighting of a lattice because of additional atoms introduction; 2) described above the screening of inter-atomic repulsion by localized electrons; 3) general lattice deformation in form of volume compression, caused by formation of covalent links between host lattice and guest atoms. Qualitative representation about the nature of dominating effect can be visible after analysis of low-frequency edge of G(ω) in Fig.1 when the type of intercalant is varied. It is easy to see, that G(ω) data for $TiSe_2$, $Fe_{0,25}TiSe_2$ and $Cr_{0,25}TiSe_2$ practically coincide, despite of lattice weighting at

introduction of iron and chromium. On the other hand, the curve for $Ni_{0,25}TiSe_2$ lays essentially below, despite of closeness of weights of transition metals and their identical content in the material. It is obvious, that as the reason of difference in phonon spectra can be explained only by value of lattice deformation during intercalation, which is maximal for Ni_xTiSe_2.

As shown earlier [6], the size of lattice deformation in form of compression is determined by binding energy for impurity band which, in turn, depends on potential of ionization for intercalated impurity. Hence, the common change of lattice elasticity due to intercalation and the value of Θ_D as its quantitative measure should be a function of potential of intercalant ionization. Dependence of Θ_D on potential of ionization of an impurity is resulted in a Fig. 3 together with so called polaron shift – a change of electron energy at formation of impurity polarons, describing the work of lattice deformation such as compression.

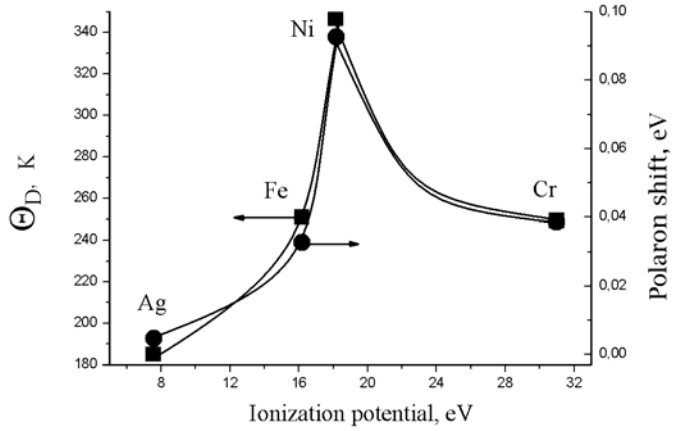

Fig. 3. The Debye temperature Дебая Θ_D, calculated using phonon density of states data and the value of polaron shift, determined as an energy of lattice deformation at formation of impurity polarons [6], both as functions of potential of ionization of intercalant atom.

Good agreement of Debye temperature and the value of polaron shift as functions of potential of ionization of impurity atom is visible. Hence, the basic contribution to change of lattice elasticity at intercalation is brought with lattice deformation at formation of the centers of charge carrier localization of polaron type. On the other hand, it is visible, that softest lattice occurs in case of silver intercalation when the value of polaron shift is close to zero. The low-frequency edge of $G(\omega)$ dependence passes even more to the low energy edge, rather than for initial $TiSe_2$, and the value of Θ_D makes 196 K for $Ag_{0,25}TiSe_2$ in comparison with 221 K for $TiSe_2$. Thus, intercalation of silver results in significant lattice softness. The reason may be as the big weight of silver in comparison with transition metals, and smallest binding energy of impurity band, providing its coincidence to Fermi level [7]. The last means, that lattice doftness may be a result of screening of interatomic repulsion by electrons belonging to impurity polaron band. That circumstance, that the effect of lattice weighting was not significant in case of other metals, forces to connect observable lattice softness with effect of screening.

Corresponded results clearly show that the effect of influence of increase in density of states at Fermi level at localization of charge carriers in form of polaron is suppressed by accompanying this process lattice deformation as compression. The effect of screening becomes distinct clear only in a case when deformation is weak what corresponds to small value of binding energy of impurity polaron band.

The work is supported by RFBR, grants № 06-03-32900 and 06-02-96307, and Programs of Ministry of Education and Science of RF « Development of scientific potential of the high school» (RNP.2.1.1.6945).

[1]. T.V.Kuznetsova, A.N.Titov, Yu.M.Yarmoshenko et al. //Phys. Rev. B. **72**, 085418 (2005).
[2]. X.Y. Cui, H. Negishi, S.G. Titova et al. // Phys. Rev. B. **73**, 085111 (2006).
[3]. A.N. Titov, Yu.M. Yarmoshenko, S.G. Titova, L.S. Krasavin, M. Neumann // Physica B **328**, 108 (2003).
[4]. Y.Arnaud, M.Chevreton, A.Ahouanjiou, M.Danot and J.Rouxel. J. Solid State Chem. **17,** 9 (1976).
[5]. N.V.Baranov, K.Inoue, V.I.Maksimov et al. // J. Phys.: Condens. Matter **16,** 9243 (2004).
[6]. A.N.Titov, A.V.Dolgoshein, I.K.Bdikin, S.G.Titova// Physics of the Solid State **42**, 1610 (2000)
[7]. A.N. Titov, A.V. Dolgoshein //Physics of The Solid State. **42**, 434 (2000).

STRUCTURE AND MAGNETIC CHANGES OF Co-BASED NANOCOMPOSITE AFTER PERCOLATION THRESHOLD

E.B. Dokukin[a], A.Kh. Islamov[a], A.I. Kuklin[a], M.E. Dokukin[b], E.A. Gan'shina[b], N.S. Perov[b], Yu.E. Kalinin[c] and A.V. Sitnikov[c]

[a] *Joint Institute For Nuclear Research, Frank Laboratory of Neutron Physics, 141980 Dubna, Russia*
[b] *Moscow State University, Faculty of Physics, 119992, Moscow, Russia*
[c] *Voronezh State Technical University, 394026, Voronezh, Russia*

Currently nanocomposites with typical size of elements no more than several nanometers are in focus. Composite granular systems exemplify such nanocomposites and can be interesting not only for fundamental investigations, but for industrial applications.

We investigate the composite nanostructures $(Co)_x(SiO_2)_{1-x}$, which are obtained by the method of ion-beam sputtering in the atmosphere of argon. Co concentration (x) is equal to 0.41-0.80. Samples consist of metal particles (2-7 nm), which are randomly distributed in a dielectric matrix. The size of granules decreases monotonically with increase of concentration of dielectric material [1]. The small-angle neutron scattering investigations of $(Co)_x(SiO_2)_{1-x}$ samples are carried out with the time-of-flight small-angle-scattering spectrometer YuMO [2] at the IBR-2 reactor in Dubna. The Q-range is chosen from 0.006Å^{-1} to 0.3Å^{-1}.

We find that magnetic properties of the samples are changed in the region of concentrations x=0.44–0.49 (below and above the percolation threshold) due to transition from superparamagnetic phase to ferromagnetic phase.

The small-angle neutron scattering is determined mainly by nuclear and magnetic density of Co particles (Fig. 1.). At Co concentration from x=0.41 to x=0.46 scattering intensity is increased

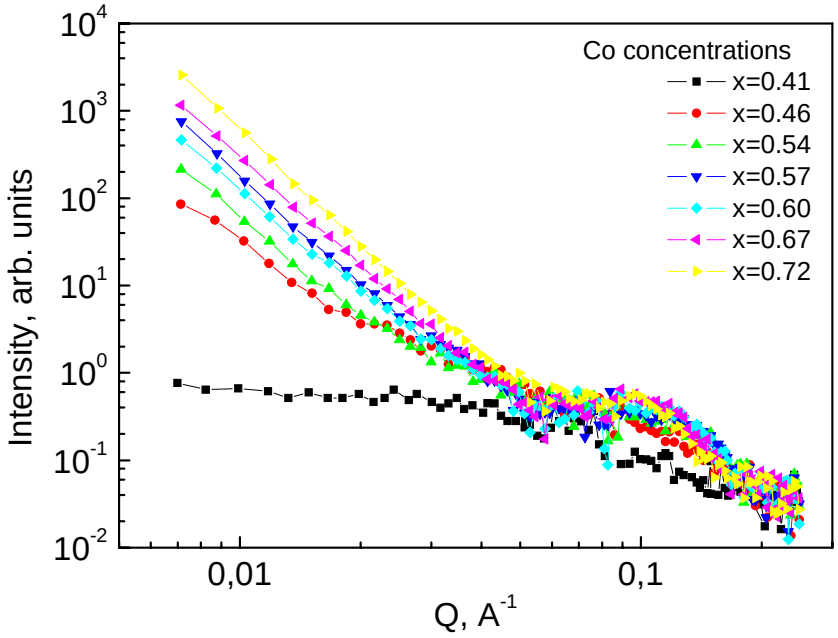

Fig. 1. Small-angle scattering curves of samples $(Co)_x(SiO_2)_{1-x}$ with x=0.41-0.72 .

by two order of magnitude, that can be explained by the self-organization of the magnetic structure. At Co concentration from x=0.46 to x=0.72 the scattering intensity as a function of momentum transfer Q is described by $I(Q) \sim Q^{-\alpha}$, were $\alpha = (2.3 \div 4.4) \pm 0.1$, over the range $Q = 0.006 \div 0.05$Å^{-1}.

Above the percolation threshold the structural size of granules are less than their magnetic size, it can be explained in the context of ferromagnetic exchange in composites. Thus, the experimental data is likely to show that the formation of magnetic clusters in the nanocomposite granular system at the percolation threshold are bringing to the changes in magnetic structure and the behavior of the neutron scattering.

This research are supported by President grant MK-7074.2006.2.

References:

1. Yu.E. Kalinin, A.T. Ponomarenko, A.V. Sitnikov, O.V. Stognej, Physics and chemistry of material handling **5** (2001) 14-20
2. A.I. Kuklin, A.Kh. Islamov and V.I. Gordeliy, Neutron News **16** (2005) 16

STRUCTURE OF FERROFLUIDS WITH EXCESS OF SURFACTANT BY SMALL-ANGLE NEUTRON SCATTERING

Viktor I. Petrenko[1, 2], Mikhail V. Avdeev[1], Leonid A. Bulavin[2], Viktor L. Aksenov[3, 1]

[1]*Frank Laboratory of Neutron Physics, Joint Institute for Nuclear Research, Dubna, Russia*
[2]*Physical Faculty, Kyiv Taras Shevchenko National University, Kyiv, Ukraine*
[3]*Russian Research Center "Kurchatov Institut", Moscow, Russia*

Small-angle neutron scattering (SANS) experiments were performed in the frame of the systematic and careful study of factors determining the stability of ferrofluids - fine liquid dispersions of magnetic nanoparticles coated with surfactant molecules. One of the factors, which determine the ferrofluid stability, is the excess of free surfactant molecules in the bulk liquid base of the ferrofluid. If the surfactant content is not enough for covering the entire free surface of magnetic nanoparticles, this results in worse stability of ferrofluids. The excess of free surfactant in the carrier also makes the stability worse. The reason for this effect is not completely understood at present. The problem is general for colloidal solutions [1, 2].

Classical ferrofluid magnetite/oleic acid/d-benzene was selected as the first system for structural investigations of the stability under surfactant excess. It is well known, that this type of ferrofluid is mostly stable when all surfactant is adsorbed on the surface of the magnetite (i.e. there is no free surfactants in the bulk). Samples for experiments were prepared by adding a certain quantity of oleic acid (up to 25% of volume fraction) to the initial high-stable ferrofluid with 1 % content of magnetite. The surfactant excess of more than 25 vol. % leads to the precipitation of magnetic particles from the liquid.

SANS experiments were carried out at the Frank Laboratory of Neutron Physics and Budapesr Neutron Center. Scattering curves were obtained in a q-range of 0.1-4 nm^{-1}. The core-shell model [5] was probed to describe the experimental data (Fig.1). The structural parameters of the colloidal particle were obtained by writing [5] the scattering intensity in terms of the polydiperse core-shell model:

$$I(q) = Io * \frac{\int_{R_{min}}^{R_{max}} Dn(R) * F(q,R) dR}{\int_{R_{min}}^{R_{max}} Dn(R) * (4/3\pi R^3 + \frac{\rho 1 - \rho s}{\rho - \rho 1}[4/3\pi(R+\delta)^3])^2 dR} + bkg$$

Here, R is the radius of magnetic core; $Dn(R)$ is the log-normal size distribution function for magnetic particles; $I0$ is the forward scattering intensity; q is the module of the scattering vector; δ is the thickness of surfactant shell; ρ, $\rho 1$ and ρs are the scattering length density of the core, shell and carrier, correspondingly and bkg is the background. The contribution of the magnetic scattering was neglected in the first approximation [5].

The preliminary treatment (example are given in Fig.2, 3) shows that the surfactant excess affects slightly the stabilizing shell, but does not result in observable aggregation of the particle. This means that the influence of the surfactant excess takes much time. It starts to be much faster only when approaching 25% of the surfactant.

The next step in understanding of conditions of the ferrofluid stability regarding the surfactant content is to realize how the surfactant behaves in pure carrier. SANS experiments were made for the solutions oleic acid/d-benzene with the volume fraction of the surfactant within interval of 5-35 %. The task was to reveal the visible volume of the surfactant molecules as a function of concentration and to conclude about the character of interaction in the system in a well-proven way [3, 4].

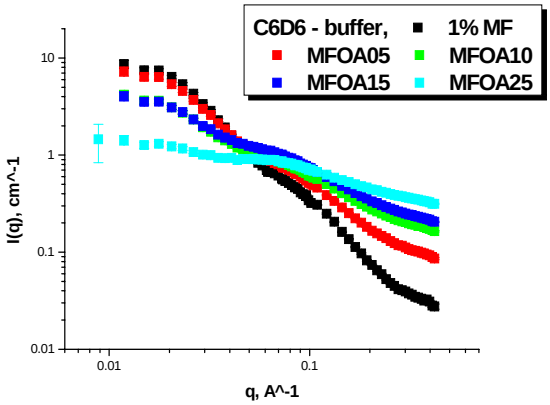

Fig.1. Experimental SANS curveы for magnetite/oleic acid/benzene ferrofluids with various volume fractions of surfactant (Oleic Acid).

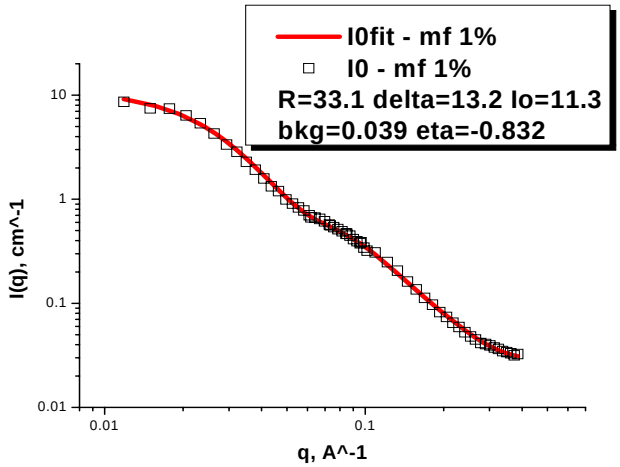

Fig.2. Results of fitting of the experimental curve for the ferrofluid without free surfactant. The concentration of magnetite in the system is 1.04%.

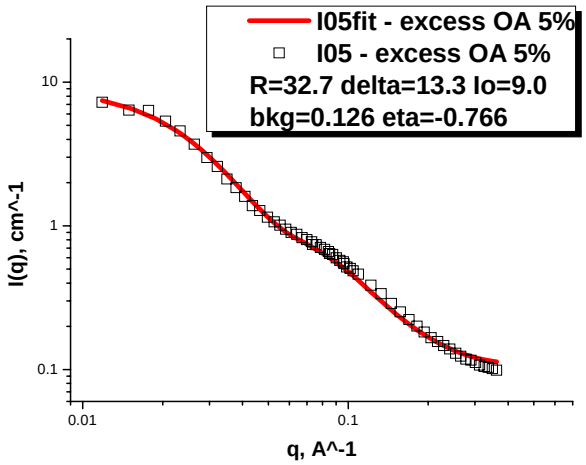

Fig.3. Results of fitting of the experimental curve for the ferrofluid with the 5% volume fraction of surfactant. The concentration of magnetite in the system is 1.04%.

The experimental SANS curve (Fig.4) in the Guinier approximation indicate the repulsion between the acid molecules. However, value of the second virial coefficient obtained from the data (Fig.5), B = -2.2, is lager than B = -8 for the case of hard spheres (purely repulsive system). This fact points out that in the pair potential describing the interaction between surfactant molecules, attractive component plays an important role. The volume of the molecule, V=657 Å^3, derived from the SANS data differs essentially from its Van der Waals volume, V_A=226 Å^3, and, at the same time, practically coincides with the partial volume of pure oleic acid in the liquid state, V_p=523 Å^3. The molecular dynamic simulations are in progress to explain the given observation. The negative slope (Fig.6) in the dependence of the radius of gyration on the concentration testifies also the repulsion between the surfactant molecules in the solution according to equation [3, 4]:

$$Rg^2 \approx Rg_0^{\,2} + \frac{\Phi * B * D_{\text{int}}^{\,2}}{1 + \Phi * B}.$$

Here, Rg is the radius of gyration at concentration Φ; Rg_0 is its value extrapolated to zero concentration; B is value of the second virial coefficient and D_{int} is a measure of the mean square distance at which the positions of two particles in the solutions are correlated.

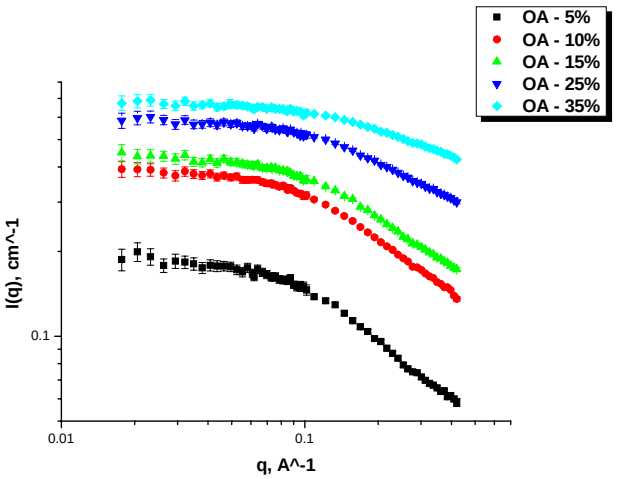

Fig.4. Experimental SANS curve for Oleic Acid in D-benzene solution with various volume fraction of OA.

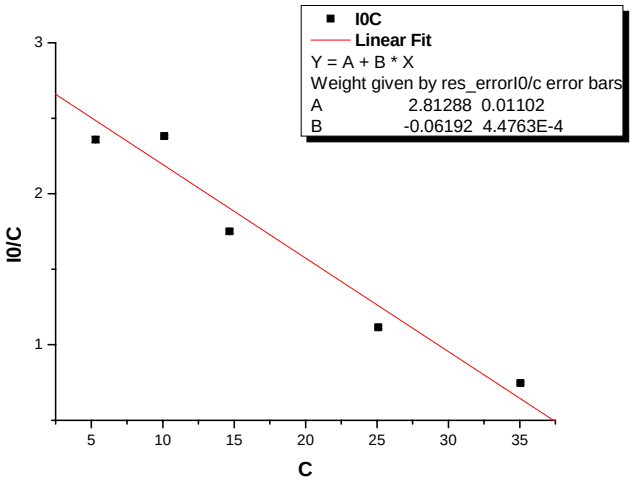

Fig.5. Forward scattering intensity (points) referred to one concentration vs. volume fraction of oleic acid (%). Fit to experimental data (solid line).

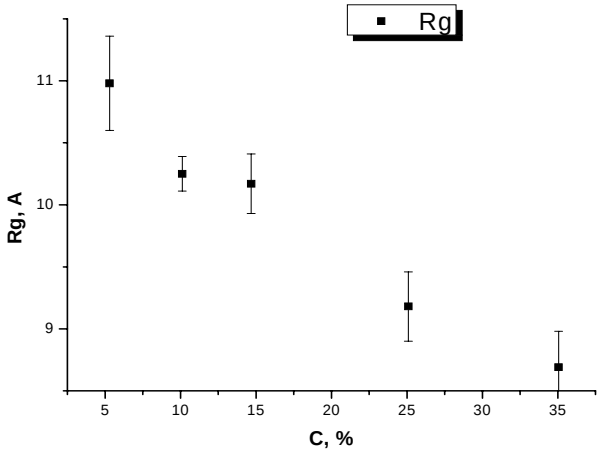

Fig.6. Obtained radius of gyration vs. volume concentration of Oleic Acid in D-benzene solution. The negative slope is testifying for repulsion of OA molecule in the solution.

References

[1] A.B.Jódar-Reyes, A.Martín-Rodríguez, J.L.Ortega-Vinuesa, *J. Coll. Interface Sci.* 298 (2006) 248–257.

[2] P.Izquierdo, et al, *Langmuir* 20 (2004) 6594 – 6598.

[3] L.Cser, T.Grosz , Y.M.Ostanevich, *Journal de Physique IV* 3 (1993) 229-232.

[4] L.Cser, B.Farago, T.Grosz, G.Jancso, Yu.M.Ostanevich, *Physica B: Condensed Matter* 180-181 (1992) 848-850.

[5] M.V.Avdeev, M.Balasoiu, V.L.Aksenov, V.M.Garamus, J.Kohlbrecher, D.Bica, L.Vekas, *J. Magn. Magn. Mater.* 270 (2004) 371-379.

Investigations of the non-locality effects in type I superconductor by means of the Polarized Neutron Reflectometry

V.L. Aksenov1,2, D.S. Drannikov2,3, Yu.N. Khaidukov2, V.F. Kozhevnikov4,
Yu.V. Nikitenko2, A.V. Petrenko2, V.V.Proglyado2,3 .

1 RRC Kurchatov Institute, 123182 ,Moscow, Russia
2 Frank Laboratory of Neutron Physics, JINR, 141980, Dubna, Russia
3 Dep. Of Physics, Moscow State University, Moscow, 119992, Russia
4 Laboratorium voor Vaste-stoffysica en Magnetisme, Katholieke Universiteit Leuven, B-3001 Leuven, Belgium

The first phenomenological theory describing electrodynamics of superconductors has been offered by F. and H. Londons in 1935 [1].The given theory is local and therefore applicable, if the sizes of superconducting carriers $\xi << \lambda L$ - penetration depth of magnetic field in a superconductor. In 1953 Pippard suggested the theory for case $\xi >> \lambda L$ (pippard superconductors), considering effects of non-locality [2]. According to this theory, the penetration depth of a magnetic field inside the pippard superconductor several times greater than inside a londons superconductor (fig. 1).

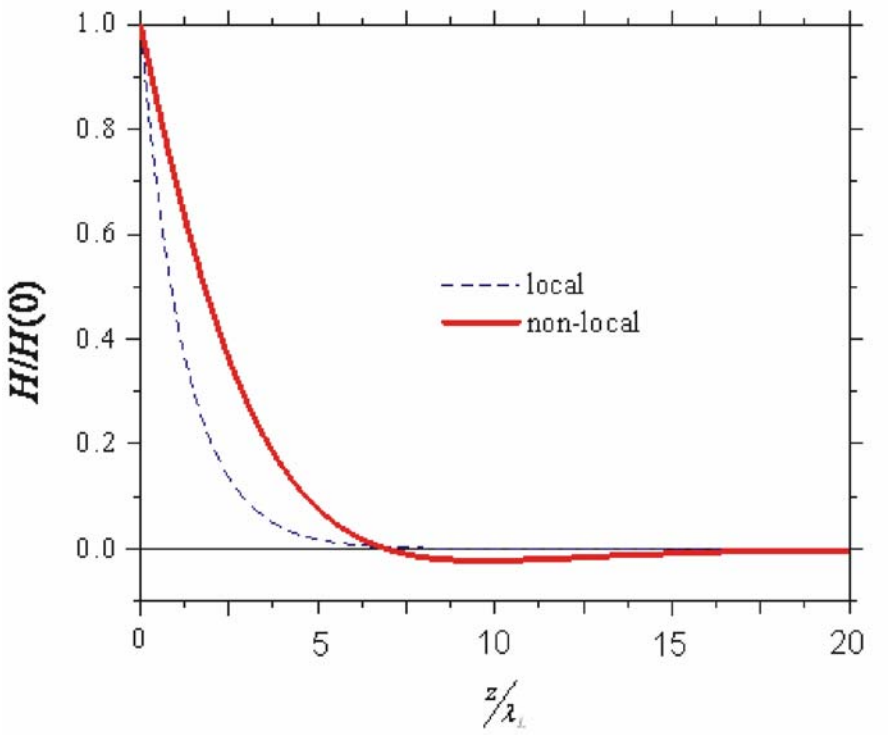

Fig. 1 The penetration depth of a magnetic field inside a superconductor with $\xi >> \lambda L$ in Londons' (blue) and Pippard's (red) theories.

The purpose of the given work was the definition of penetration depth of a magnetic field inside a type I superconductor by means of Polarized Neutron Reflectometry (PNR) to check the presence of non-locality effects. Similar measurements have been already done for Nb [3] and Pb [4, 5]. For studying of the non-locality effects the indium is the best candidate as it has the least parameter $\xi/\lambda L = 0.06$ [6]. Difficulty of PNR use for In is that it is a strong absorber of neutrons. Absorption cross-section for In has size 193.8 barn, that, for example, in one thousand times more than for Pb.
Structure In(2μm)/SiO2 has been prepared by vacuum sputtering at the university of Leuven (Belgium). Magnetometrical data and electric resistance measurements have shown that the given structure is a pure superconductor of the type I with critical temperature and a magnetic field of superconducting transition Tc = 3.4 K and Hc (0) = 280 Oe accordingly.

The PNR measurements have been done on spectrometers of polarized neutrons REMUR (JINR, Russia) and CRISP (ISIS, The Great Britain). Low temperature measurements in Dubna were done with the Orange cryostat at the temperature T=0.5 Tc and external magnetic fields
H = 0.68 Hc, 0.87 Hc, 0.97 Hc and 1.03 Hc. Here Hc = Hc(0.5 Tc)=200 Oe. Measurements were carried at the angle of reflection θ =2.4 mrad with angular divergence dθ/θ = 5 %. The R+ (Q) and R-(Q) reflectivities as a function of momentum transfer measured at T=0.5 Tc and H = 0.97 Hc are presented on fig. 2 a. On fig. 2 b spin asymmetry SA(Q) ≡ [R+(Q) - R-(Q)]/ [R+(Q) + R-(Q)] for the given parameters is presented.

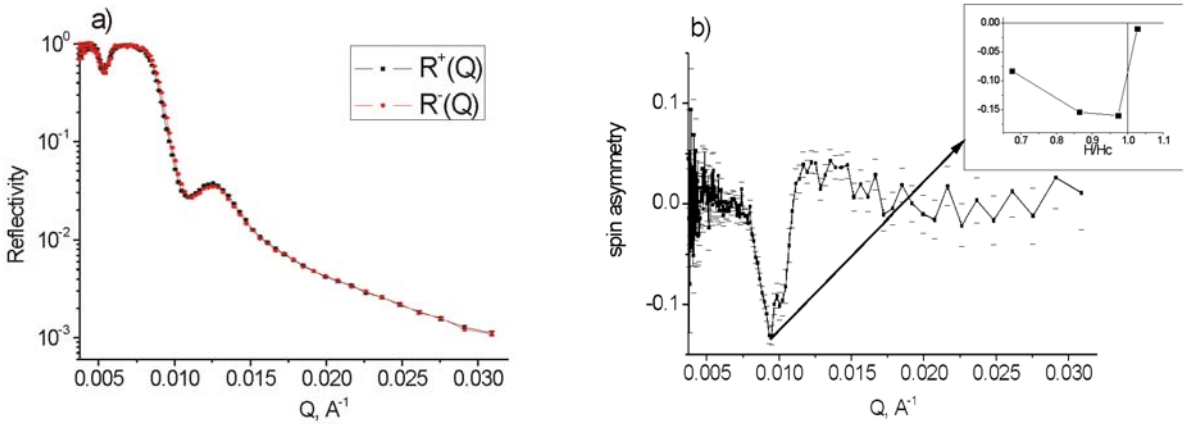

Fig. 2. R+(Q) and R-(Q) reflectivities (a) and spin asymmetry SA(Q) measured at T=0.5Tc and H=0.97Hc. Inset to b) is the behavior of minimum close Q=0.009A versus H/Hc.

Spin asymmetry for H < Hc is characterized by the strong minimum at Q = 0.009 Å-1 with width ΔQ = 0.002 Å -1. The size of spin asymmetry in the given minimum almost linearly depends on the diamagnetic moment in superconducting In and for the measured range made 10-15 %. Statistical uncertainty of the experiment in the given Q range made 1-2 %. The preliminary analysis shows, that the penetration depth in the investigated structure makes 2-3λL that speaks well for non-local theory of Pippard.
At H = 1.03 Hc depth of the minimum has decreased approximately in 20 times. Let's assume that the value of minimum proportionally depends on product of the diamagnetic moment of the superconducting layer on its thickness. Then the thickness of overcritical superconducting layer can be estimated as 103 Å. For exact extraction of parameters of the given layer it is necessary to essentially increase time of measurement.
To sum up we can say that the high resolution and precise measurements of quite small diamagnetic moment of superconducting indium film has been done at the spectrometer REMUR. Obtained data pointed on presence of non-locality effects in superconducting indium.

References:
F. London and H.London, Proc. Roy. Soc. (Lond.) A 149 (1935) 71,
A.B. Pippard, Proc. R. Soc. London. Ser.A 216, 547 (1953),
V. Lauter-Pasyk, H.J. Lauter, V.L. Aksenov et al., Physica B (1998), p166,
M.P. Nutley, A.T. Boothroyd, C.R. Staddon et al., PRB V. 49, #2, p. 15790 (1994),
K.E. Gray, G.P. Felcher, R.T. Kampwirth and R. Hilleke, PRB. V. 42, #7. p 3971 (1990),
F. W. Smith, A. Baratoff, and M. Cardona, Phys. Kon-dens. Materie 12, 145 (1970).

"Zero" experiment in the measurement of the P-odd asymmetry in the reaction $^{6}Li(n,\alpha)^{3}H$.

Vesna V. A.[1], Gledenov Yu. M.[2], Nesvizhevsky V. V.[3], Petukhov A. K.[3],
Sedyshev P. V.[2], Soldner T.[3], Shulgina E. V.[1], Zimmer O.[4]

[1]*Petersburg Nuclear Physics Institute of RAS, Gatchina, Russia.*
[2]*Frank Laboratory of Neutron Physics, JINR, Dubna, Russia.*
[3]*Institut Laue-Langevin, Grenoble, France.*
[4]*Technische Universität, München, Germany*

The P-odd asymmetry coefficient in the reaction $^{6}Li(n,\alpha)^{3}H$ has been measured to be equal to $\alpha_{PN} = -(8.6 \pm 2.0)\cdot10^{-8}$. This measurement has been carried out at the PNPI RAS and at the ILL [1]. This result allows us to estimate the neutral current constant following the theoretical model [2] with the value of $h_\rho = -11.4\cdot10^{-7}$. Our estimation $f_\pi = (0.4 \pm 0.4)\cdot10^{-7}$ is smaller than the widely-used value of $f_\pi = 2\cdot10^{-7}$.

In order to prove reliability of the obtained result, one has to consider a possible admixture of the P-odd effects in various accompanying reactions of neutrons with the elements of the ionization chamber, with emitting of charged particles and γ-quanta following decays of radioactive nucleus.

The most suspicious impurity is the admixture of ^{7}Li in the target material (LiF). Neutron capture on ^{7}Li gives unstable ^{8}Li isotope with a half-life of $T_{1/2} = 0.89$ s, which decays with the beta rays emission. The amount of ^{7}Li in the target [3] is ~10%. The average energy of beta particles is equal to E ~ 13 MeV. A particle with this energy passes through the sensitive volume of the ionization chambers assembly [4], deposing small portion of energy; moreover it deposes energy both in the chambers, in which the effect of tritons asymmetry is positive as well as in the chambers, in which the effect of tritons asymmetry is negative. The upper constrain for this admixture of the P-odd effect due to beta particles from ^{8}Li is $3\cdot10^{-9}$ for an in-use chamber. This value is so small due to the smallness of the cross-section of the reaction of neutrons with ^{7}Li, as compared to the cross-section of the reaction with ^{6}Li, as well as due to small absorption of the beta particles in the chamber.

Fluoro-plastic is used in the ionization chambers assembly. The half-life for ^{20}F $T_{1/2} = 11.56$ s, the energy of beta particles is E ~ 5.4 MeV. Reliable estimation of this P-odd effect admixture contribution (with beta particles) to the studied effect is not an easy task, because the mass of fluoro-plastic and the flux of scattered neutrons in the fluoro-plastic are not known.

Besides, some P-odd effects with gamma-quanta emission are possible in different construction materials of the ionization chamber.

Because of these uncertainties in the reliable estimation of the mentioned effects, we had to carry out experimental check of any possible contributions of some false asymmetry to the measured effect.

In order to do that, we closed all 24 targets in the ionization chamber by aluminum foils with the thickness of 20 μm. Thus the total thickness of the foils in the pass of tritons and alpha particles was equal to 34 μm. This thickness ensures complete absorption of the alpha particles and tritons. On the other hand, gamma-quanta and beta particles from construction materials and targets pass through the foils with little absorption. This experiment was a "zero"-test, as it allowed us to detect any P-odd effects emitted from all admixtures in the pass of neutrons. The result of this experiment has to be compared to the result of the main experiment (without additional aluminum foils). In order to do that, the result of this "zero"-test is normalized to the amplification factor of the detector

signal and to the constant component of the signal in the main experiment. Such estimation corresponds to the admixture of any P-odd parasite effect to the main result.

The "zero" experiment for the P-odd asymmetry (measured in the chamber, in which the targets were closed by foils absorbing the products of the reaction $^{6}Li(n,\alpha)^{3}H$ has been carried out at the PF1B instrument at the ILL; the following result was obtained:

$$\alpha_{0\text{-}test} = -(0.0 \pm 0.5)\ 10^{-8}.$$

This value was normalized to the constant component of the signal in the main experiment and corrected to the neutron polarization and the average cosine of the tritons emission from the target (taking into account a difference in the amplification factors of the "zero" experiment and the main one).

The result of the main experiment at the ILL:

$$\alpha_{PN} = -(9.0 \pm 2.1)\cdot 10^{-8}\ [1].$$

Comparison of these two results shows that the effect of the P-odd asymmetry in the main experiment is really due to the studied reaction

1. Vesna V.A. et al, JETP Letters 82(8) (2005) 463.
2. Nesterov M.M., Okunev I.S., JETP Letters 48(1) (1988) 573.
3. Y.G. Abov et al. Physics Nuclear 34, (1962) 505.
4. Yu.M.Gledenov et al. NIM A350 (1994) 517.

Ramsey Resonance for a Pulsed Beam

Yasuhiro Masuda[1*], Vadim Skoy[2], Takashi Ino[1], Sun-Chang Jeong [1], Yutaka Watanabe[1]

[1]High Energy Accelerator Research Organization, Oho 1-1, Tsukuba, Ibaraki 305-0801 Japan
[2]Joint Institute for Nuclear Research, 14980 Dubna Moscow Region, Russia

I. Introduction

We discuss here the Ramsey resonance for a pulsed beam, for example a pulsed neutron beam. From a pulsed neutron source, higher energy neutrons come to the oscillatory fields earlier than lower energy neutrons. In the present method, oscillatory fields for NMR are synchronized with these neutron motions. The oscillatory fields are applied to neutron spins in a time interval, which corresponds to the TOF of some particular neutron energies, by use of the start timing of the neutron pulse for triggering oscillatory field generation. The amplitudes of the oscillatory fields are modulated as a function of the neutron TOF so that the condition of $\pi/2$ spin rotation is satisfied for all of the neutrons in this energy region. In addition, the phase of the second oscillatory field is modulated. The result of the Ramsey resonance is observed as a neutron-beam intensity modulation as a function of the neutron TOF. A square-wave phase modulation was tried before for the frequency stabilization of an atomic clock. The present method is different from this. The phase is modulated as a function of the neutron TOF by use of the start timing of the neutron pulse. The neutron velocity can be measured by beam intensity modulation.

By using the present method, neutron spin can be precisely manipulated as a function of the neutron TOF. In a measurement of the *T*-violating correlation, $\vec{s}\cdot(\vec{k}\times\vec{I})$, the neutron spin, $\vec{s}$, should be perpendicular to the nuclear spin, $\vec{I}$, as well as to the neutron momentum, $\vec{k}$. A large enhancement in the *T*-violation effect is expected at a p-wave resonance. The neutron spin and the nuclear spin are aligned with magnetic fields upon polarization. When we place a polarized nuclear target between the two oscillatory fields, the neutron spin can be rotated by $\pi/2$ from the parallel to perpendicular directions to the magnetic field in some particular neutron energy region so that a *T*-violating correlation is formed in the p-wave resonance. The neutron spin rotates about the magnetic field as well as the pseudomagnetic field, which arises from a spin-dependent neutron nucleus interaction. The two neutron spin rotations can be controlled so as to keep the *T*-violating correlation during transmission through the polarized nuclear target. The result of the spin manipulation can be observed in neutron-beam intensity modulation, and then precision neutron spin control becomes possible.

The pseudomagnetic field was measured by means of the usual Ramsey resonance for a monochromatic neutron beam from a nuclear reactor. In the present method, the field strength can be measured via a neutron-beam intensity modulation as a function of the neutron TOF, which arises

from the neutron velocity dependent of the pseudomagnetic precession.

II. Experimental principle

The experimental apparatus comprises a ^{3}He neutron spin polarizer, a first radio frequency (RF) coil for $\pi/2$ rotation, a Larmor precession path, a second RF coil for $\pi/2$ rotation and a ^{3}He neutron spin analyzer, which are placed in a static magnetic field of solenoids, as shown in Fig. 1. The apparatus is placed in a neutron beam line at the KEK pulsed neutron source, KENS. Neutrons from the pulsed neutron source are longitudinally polarized upon passing through the ^{3}He neutron spin polarizer. After polarization, the neutrons enter the first RF coil. An oscillatory field is switched on when neutrons of higher energy, E_h, arrive at the RF coil, and is then switched off when neutrons of lower energy, E_l, leave from the RF coil. When the frequency of the oscillatory field, ω, is at the Larmor frequency, $\omega_0 = \gamma H_0$, namely at the resonance, neutron spins rotate about a rotating field, H_1, which is produced by the oscillatory field. H_0 denotes the strength of the static magnetic field and γ the gyro magnetic ratio. The rotation axis of H_1 is in the direction of H_0. The neutron spin rotation angle in the RF coil becomes $\gamma H_1 t_r$. The parameter t_r is the neutron TOF in the RF coil, which is represented in terms of the RF coil length, $l_{\pi/2,}$ and the neutron velocity, v, as $l_{\pi/2}/v$. The amplitude of the rotating field, H_1, is modulated as a function of the neutron TOF so that all of the neutron spins in the energy region from E_l to E_h rotate by $\pi/2$, and then become perpendicular to H_0. After the first RF coil, the neutron spins rotate about H_0 with a Larmor frequency of ω_0. After Lamor precession, the neutrons enter the second RF coil, and then another oscillatory filed is switched on and off in the same way as in the first RF coil. The neutron spins are always perpendicular to the first rotating field before entering the second RF coil. When the phase of the second oscillatory field is the same as the first one, the neutron spins continue to rotate about the second rotating field, H_1, by $\pi/2$ in exactly the same way as in the first RF coil, as if there is no space between the two RF coils. As a result, the neutron spins rotate by π. If the phase of the second oscillatory field is shifted by θ, this phase shift is transformed to the projection angle of the neutron spin on the direction of H_0 after the second RF coil and is then detected by means of the ^{3}He neutron spin analyzer. If the oscillatory field frequency is deviated from the resonance frequency, any phase difference, $(\omega-\omega_0)t$, is transformed to the projection angle of the neutron spin on the static magnetic field after the second RF coil. The variable t denotes the neutron TOF between the two RF coils.

Neutron transmission can be analyzed by means of the density matrix formalism. The neutron transmission becomes $T_{on} = T_1 T_2 \left(1 + \alpha(E) P_{n1} P_{n2}\right)$, when the oscillatory fields are switched on. Here, T_1 and T_2 are the neutron transmissions of the polarized ^{3}He neutron spin polarizer and analyzer, which are represented as $T_1 = \exp(-n_1\sigma_0 d_1)\cosh(P_1 n_1 \sigma_0 d_1)$ and $T_2 = \exp(-n_2\sigma_0 d_2)\cdot\cosh(P_2 n_2 \sigma_0 d_2)$, respectively. P_1 and P_2 are ^{3}He polarizations, n_1 and n_2 the ^{3}He number densities, and d_1 and d_2 the ^{3}He thicknesses. The parameter σ_0 is the neutron total cross section of ^{3}He. In terms of σ_0, the

neutron cross section of polarized ^{3}He is represented as $\sigma_{\pm} = \sigma_0(1 \mp P_{He})$ for parallel and antiparallel neutron spin states to ^{3}He polarization, respectively. P_{n1} and P_{n2} are the polarizing and analyzing powers of the polarizer and analyzer, which are represented as $P_{n1} = \tanh(P_1 n_1 \sigma_0 d_1)$ and $P_{n2} = \tanh(P_2 n_2 \sigma_0 d_2)$, respectively. The effect of the neutron spin rotation during transmission through the first $\pi/2$ coil, the static field and the second $\pi/2$ coil is represented as $\alpha(E)$, which is the projection component of the neutron polarization on the static field. Here, E is the neutron energy. When the oscillatory fields are switched off, $\alpha(E)$ becomes 1, then the neutron transmission becomes $T_{on} = T_1 T_2(1 + P_{n1}P_{n2})$.

III. Experimental result

The ^{3}He polarizations and thicknesses of the neutron spin polarizer and analyzer were measured by means of neutron transmission. The results of the polarizations were P_1 = 31% and P_2 = 51%, respectively. The two ^{3}He polarizations were in the longitudinal direction. The ^{3}He gas pressures were 2.32 atm and 2.13 atm at 195^{o}C, respectively. The length of the ^{3}He gas in the neutron beam direction was 5 cm for both the polarizer and the analyzer. The neutron energies, E_h and E_l , were set at 80 meV and 23.6 meV, respectively. We counted the neutrons that passed through the apparatus shown in Fig. 1 as a function of the neutron TOF.

We changed the frequency of the oscillatory fields around the resonance frequency. When we switched on the oscillatory field, the neutron counts were greatly changed at neutron energies from 23.6 to 80 meV. No effect was observed at other neutron energies. For normalization of the incident neutron spectrum, we calculated the neutron transmission ratio, which was defined as $R = T_{on}/T_{off} - 1$. In the transmission ratio the transmission factors, T_1 and T_2, were also removed, since it is described as $R = (1 + \alpha(E)P_{n1}P_{n2})/(1 + P_{n1}P_{n2}) - 1$. The experimental result of the transmission ratio at the resonance is shown in Fig. 2a. The solid curve is the theoretical curve that fit the experimental result. At the resonance, the neutron spin rotates by π after the two separated oscillatory fields including the static field. As a result, the neutron polarization becomes anti-parallel to the analyzer ^{3}He polarization, and then the neutron transmission has the minimum value, which is represented as $R_{res} = (1 - P_{n1}P_{n2})/(1 + P_{n1}P_{n2}) - 1$.

We modulated the phase of the second oscillatory field proportionally to the neutron TOF, t, between the two RF coils from 0 to 2π for the energy region from E_h to E_l. The transmission ratio with the phase modulation becomes $R_{mod} = [1 + \cos(\pi + \theta)\cdot P_{n1}P_{n2})]/[1 + P_{n1}P_{n2}] - 1$. Here, $\theta = 2\pi(t(E_l) - t)/(t(E_l) - t(E_h))$. The parameters $t(E_l)$ and $t(E_h)$ are the neutron TOF at neutron energies of E_l and E_h, respectively. We set these energies at 23.6 meV, 80 meV.

We placed a small additional solenoid of H_s = 30 G, and then measured the transmission ratio as a function of the neutron TOF. The result is shown in Fig. 2b. The effect of the additional field is found in the sinusoidal beam intensity modulation, which arises from an additional phase, $\gamma H_s t_s$.

The parameter t_s is the neutron TOF in the additional coil, which is represented in terms of an additional field length, x, as x/v. In the least square fitting of Fig. 2b, we assume that the magnetic field strength of the small coil has a constant value of H_s in the length x.

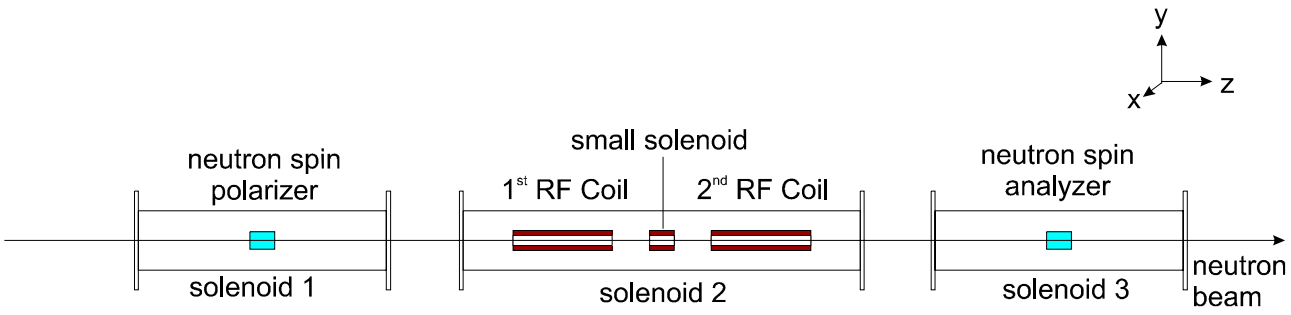

Fig.1. Installation is based on a pulsed Ramsey's method. All scales are in mm.

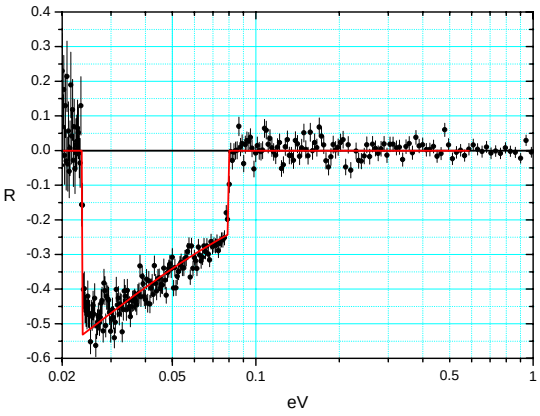

Fig.2a. Quantity R at an oscillatory field resonance frequency of 60.37 kHz.

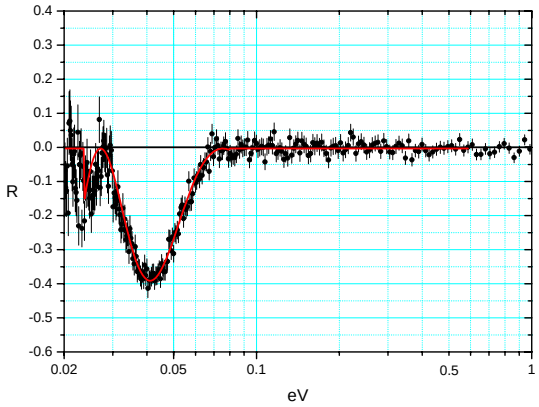

Fig.2b. Neutron transmission with an additional field. The oscillatory field frequency was set at the resonance, and then a small solenoid of 33.4 G was placed between the two RF coils. This value was obtained from the neutron TOF dependence of the ratio R.

Thus, we developed the method of measurement of magnetic field, which can be applied for determination of pseudomagnetism in polarized targets, namely ^{139}La in $LaAlO_3$, and magnetic characteristics of ferro- and paramagnetic substances as well. The procedure will be exactly the same as described above but the small solenoid will be replaced with La target. The measurements with unpolarized and polarized La nuclei will allow us to determine pseudomagnetic field for particular nuclear polarization.

1. Y. Masuda, *et al*, "A pulsed neutron Ramsey's method", Physica B 356 (2005), 182-186.

2. Y. Masuda, *et al*, "Ramsey resonance for a pulsed beam", Phys. Lett. A 364 (2007), 87-92.

Temperature dependence of neutron scattering on He-4 gas

V. Ignatovich
Frank Laboratory of Neutron Physics of Joint Institute for Nuclear Research, 141980, Dubna
Moscow region, Russia

Abstract

A suggestion [**?**] that temperature dependence of the total neutron-^{4}He cross section can be proportional to $T^{3/2}$ is checked. The experiment is described. The temperature dependence was found to be $T^{1/2}$ in agreement with the standard scattering theory (SST). The consequence of this result for the scattering theory is discussed.

1 Introduction

Experiments on storage of ultracold neutrons (UCN) reveal [1] anomalously high loss coefficient at a single collision of neutrons with material walls of storage vessels. After many unsuccessful attempts to explain this anomaly, a hypothesis was spoken out [2] that the cause of high losses is related to wave packet form of the free neutron wave function. It was supposed (there are also other arguments that lead to the same hypothesis [3]) that the wave packet can be of the de Broglie singular form [4]:

$$\psi_{dB}(\boldsymbol{r},t)=\sqrt{\frac{s}{2\pi}}\exp(i\boldsymbol{v}\boldsymbol{r}-i\omega t)\frac{\exp(-s|\boldsymbol{r}-\boldsymbol{v}t|}{|\boldsymbol{r}-\boldsymbol{v}t|}, \tag{1}$$

where $\omega=[v^2-s^2]/2$, s determines the packet width, and $\boldsymbol{v}$ is wave packet velocity, which in our units $m=\hbar=1$ coincides with the wave vector $\boldsymbol{k}$.

The wave packet can be representable in Fourier expansion form. Because of its width s a particle incident on a mirror surface at grazing angles θ less than critical θ_c can go through the mirror with probability $w\propto s\lambda_c$, where λ_c is critical wavelength of the mirror substance. A problem, which arises here is: what is the parameter s? Is it a fundamental constant or some function, which depends on neutron energy? At first sight it should be proportional to the neutron speed v. However in such a case the transmission probability at subcritical incidence angles should increase with the neutron energy. Experiments searching for such a transmission [5] did not reveal a dependence on energy, and it was concluded that parameter s is some fundamental constant.

However, if s does not depend on speed, then neutron transmission through gases would decrease with the gas temperature proportionally to $T^{3/2}$. So, it was necessary to check this temperature dependence. Experiments of such type were performed long ago [6]. However that time it was measured not the temperature dependence but dependence of cross section on energy of incident neutrons, and temperature dependence was deduced from it.

It was possible to make direct measurement of the temperature dependence of neutron transmission through ^{4}He gas, and thanks to kind permission and help of P.Geltenbort and T. Brenner these measurements were done. Below we describe the experiment, its results and discuss the consequences of the obtained temperature dependence.

2 Description of the experiment and its results

The experiment, scheme of which is shown in fig. 1, was performed at the PF2/TEST beam port. Ultra-cold neutrons (UCN) pass through an electropolished stainless steel tube of length

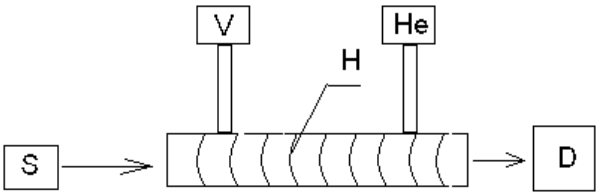

Figure 1: Scheme of the experiment. S — source of the neutrons, D — detector, V — system for vacuum, He — helium tank, H — heating wire.

$d = 0.5$ m, which has at both ends stainless steel or Al windows of 0.1 mm thickness. Therefore, either only neutrons with energies above the limiting energy of stainless steel or only those with energies above the limiting energy of Al are transmitted. When the tube was evacuated and kept at room temperature the average neutron count rate was 6700 n/s for stainless steel windows and 34000 n/s with Al windows. For the detector we used a strip ^{3}He counter. Without any special shielding the background count rate (exit shutter of PF2/TES closed) was 2.3 n/s for both window types.

When the stainless steel tube is filled with ^{4}He gas the neutron count rate of the detectors decreases. For small He pressures the decrease of count rate is proportional to $\Delta J = JN\sigma d$, where N is the density of the He gas, J is the count rate for the evacuated bottle, d is the length of the tube and σ is the total neutron scattering cross section in He. At pressures P up to 1000 mbar the count rate decreased linearly: $\Delta J \propto P$. When the tube was filled with 1000 mbar of He at room temperature, the count rate was only 20% less than for evacuated tube.

The main idea of the experiment was to check the dependence of ΔJ on P when P increased not because of amount of He, but because of the gas temperature increase, which was achieved with the heating wire H shown in fig. 1.

The results of measurements for Al windows (the results for stainless steel windows were the same) are demonstrated in fig. 2. Curve 1 shows the dependence of $\Delta J = JN\sigma d$ on P at room temperature, when the He pressure is increased by pumping He into the tube. The branch 2 of the curve 1 shows the same dependence, when the pressure is increased by heating the stainless steel tube with fixed amount of He. In this case $JN\sigma d$ increases not because of increase of the density N of the He gas, but due to increase of the total cross section σ. The graph shows that the increase of σ with P is about two times slower than the increase of N with P. Such a behavior is predicted by the standard scattering theory where $\sigma \propto T^{1/2} \propto P^{1/2}$.

We were not able to measure whether the power of T is really 1/2, because we had no monitor, and the decrease of count rate with increase of temperature by $\approx 60^\circ$ C, was only several %, while reactor intensity[1] was fluctuating at the level 1.5%. Nevertheless, since the fluctuations were sufficiently slow, we could find an interval of time where the measurements were reproducible, and they show that the temperature dependence is below the linear one and not above it. This dependence testifies in favor of $T^{1/2}$ and against $T^{3/2}$.

3 Conclusion

This experiment definitely shows that the packet width s is proportional to the relative speed v of the neutron with respect to scattering nucleus, and we now must resolve the contradiction, which arises between this work and the results of the experiment [5] on subcritical transmission.

[1]It was reported by reactor staff.

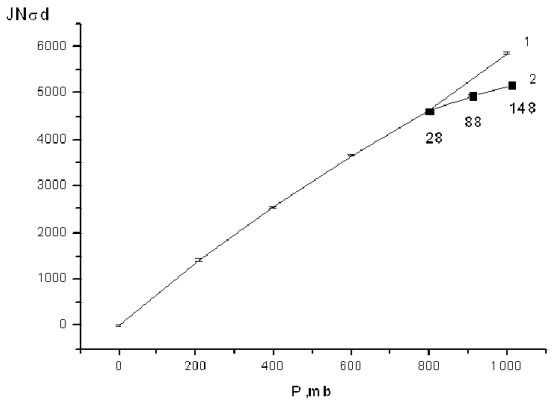

Figure 2: Dependence of $JN\sigma d$ on the pressure P of ^{4}He-gas in stainless steel tube with Al windows: 1 - at room temperature (28^{o}C); 2- for a constant number N of atoms, but different temperatures. The numbers indicate the gas temperature in °C. All the other points correspond to room temperature.

We think that the experiment [5] should be repeated with more careful search of the transmitted neutrons, when grazing angle of incident beam is below the critical one.

Acknowledgement

The author is very grateful to P.Geltenbort and T. Brenner of ILL staff for their help and excellent preparation of the experiment, to Prof. J-F. Bloch of IFPG (Grenoble), and Dr. E.P.Shabalin of JINR (Dubna) for their interest and support.

References

[1] V.K.Ignatovich. The Physics of Ultracold Neutrons. Oxford Clarendon Press. 1990.

[2] V.K. Ignatovich, M. Utsuro, Phys. Lett. **A225**, 195-202 (1997.)

[3] V.K. Ignatovich, Concepts of Physics, **1**, 51 (2004).

[4] L. de Broglie, *Non-Linear Wave Mechanics: A Causal Interpretation*, (Elsevier, Amsterdam, 1960.)

[5] M. Utsuro, V. Ignatovich, P. Geltenbort, Th. Brenner, J. Butterworth, M. Hino, K. Okumura, M. Sugimoto, *Proceedings of VII International Seminar on Interaction of Neutrons with Nuclei: Neutron Spectroscopy, Nuclear Structure, Related Topics, Dubna, May 25-28, 1999*, **E3-98-212**, 110, JINR, Dubna, 1999.

[6] R. Genin, H. Beil, C. Signarbieux a. o., Le Journal de physique et le radium **24** 21 (1963).

JINR CONTRIBUTION TO THE EUROPEAN PROGRAMME «ATMOSPHERIC HEAVY METAL DEPOSITION»: FROM 1995 TO 2005/2006 MOSS SURVEYS

M.V. FRONTASYEVA

Department of Neutron Activation Analysis, Frank Laboratory of Neutron Physics, Joint Institute for Nuclear Research, 141980 Dubna, Moscow Region, Russia
E-mail:Marina@nf.jinr.ru

Increased concern in air pollution by toxic heavy metals in industrialized countries has lead to establishing the international programme «Atmospheric Heavy Metal Deposition in Europe: – *estimations based on moss analysis*». Since 1995 JINR is contributing to this programme reporting results to the European Atlas from moss surveys 1995/1996 and 2000/2001, and 2005/2006. In 2000 the JINR project on air pollution studies in some industrial areas of Russia, Poland, Romania, Czech Republic, Bulgaria and Slovakia was supported by grants of the Plenipotentiaries of these JINR member-states, and by two IAEA grants (for Russia and Romania). Pilot studies were carried out in Central Russia, Western Ukraine, northern Serbia, Bosnia, Macedonia, European part of Turkey (Thrace Region), and Croatia. The experience in applying epithermal neutron activation analysis at IBR-2 reactor, FLNP JINR, to these studies is reviewed.

1. Introduction

Air pollution by toxic heavy metals is of great concern in industrialized countries. A comprehensive survey of their emission into the atmosphere shows their potential risks on the environment and human health. In many European countries, increased efforts to establish heavy metal monitoring have lead to the international programme «Atmospheric Heavy Metal Deposition in Europe: - *Estimations Based on Moss Analysis*» [1]. The heavy metals in mosses project is coordinated by the Coordination Centre of the International Cooperative Programme on Effects of Air Pollution on Natural Vegetation and Crops (ICP Vegetation) [2].

The data from the regular surveys for heavy metal concentrations in mosses are an invaluable resource for international negotiations on heavy metal pollution. These data allow both spatial and temporal trends in heavy metal concentration/deposition to be examined, and the areas where there is high deposition of heavy metals from long-range transport to be identified. The Task Force on Heavy Metals was established by the United Nations Economic Commission for Europe Convention on Long-Range Transboundary Air Pollution (UNECE - CLRTAP) as a response to the concern over the accumulation of heavy metals in ecosystems, and their impacts on the environment and human health. In 1998, the first Protocol (Aarhus Protocol) for the control of emissions of heavy metals was adopted and signed by 36 Parties to the Convention. One of the objectives of the ICP Vegetation is to provide information for review of the Aarhus Protocol on heavy metals, planned for 2005.

The moss survey objectives are to characterize qualitatively and quantitatively the regional atmospheric deposition pattern of heavy metals in Europe, to indicate the location of important heavy metal pollution sources and to allow retrospective comparison with similar studies repeated every 5 years.

Content of heavy metals in moss is closely correlated to atmospheric deposition, and conversion to absolute deposition rates by calibration against metal content in the bulk precipitation data is rather straightforward [3].

Since 1995 Department of NAA FLNP JINR is involved in the European programme reporting results to the European Atlas from the moss survey 1995/1996 [4] on the Eastern Carpatians of Romania [5].

In 2000 the project «Atmospheric deposition of heavy metals in some industrial areas of Russia, Poland, Romania, Czech Republic, Bulgaria and Slovakia studies by the moss biomonitoring technique and employing nuclear and related analytical techniques and GIS technology» (REGATA) was accepted by the JINR Theme Plan. It was also supported by several grants of Plenipotentiaries of JINR and resulted in the following publications with specialists from Poland [6, 7], Bulgaria [8, 9], Czech Republic, and Slovakia [10, 11], and Romania [12–14]. IAEA provided grants for biomonitoring studies in the South Urals [15–17]. Pilot studies were initiated in Central Russia [18–20], Western Ukraine [21], Northern Serbia and Bosnia [22, 23] and during the summer 2002 and 2005 in Macedonia [24, 25]. More than 2000 moss samples were analyzed in Dubna using epithermal neutron activation analysis (ENAA) for the European Atlas 2000/2001 [26]. The results on moss survey in 2002 in the Thrace region of Turkey [27] stimulated further activity in biomonitoring studies in Turkey in moss survey 2005.

In addition to the above-mentioned countries, in the moss survey 2005/2006 Croatia [28] and jointed our studies, providing collection of 100 moss samples from the entire territory of this country. Belarus [29] contributed to this survey with a collection of samples from Minsk and Grodno regions. The results on biomonitoring atmospheric deposition by means of NAA were reviewed [30] at the 20th Task Force Meetings UNECE ICP Vegetation hold in Dubna in March 2007. This report contained also the new data on the Republic of Udmurtia [31].

Similar local biomonitoring projects were undertaken in our Department together with scientists from China [32, 33] and South Korea [34], and later on with Mongolia [35] and Vietnam [36].

2. Experimental

The moss survey used a combination of instrumental ENAA in Dubna and AAS (atomic absorption spectrometry carried out at Geological Institute of RAS, Moscow, for Russia and in relevant participating member-states) provide data for concentrations of about 40 chemical elements (Al, **As**, Au, Ba, Br, Ca, **Cd**, Ce, Cl, Co, **Cr**, Cs, **Cu**, Dy, Eu, **Fe**, Hf, **Hg**, I, In, La, Lu, Mg, Mn, Na, Nd, **Ni**, **Pb**, Rb, Sb, Sc, Se, Sm, Ta, Tb, Th, **V**, W, Yb, **Zn**) that substantially exceeded the requested number of elements (marked as bold) normally presented in the European Atlas. The analytical peculiarities are described elsewhere in the above-cited papers.

Not all the above trace elements are strictly relevant as air pollutants, but they come from the multi-elemental analyses with insignificant extra cost, and most of them can be used as air-mass tracers.

3. Data interpretation

By applying multivariate statistical analysis to the data sets, it is possible to uncover the character and the origin of pollution sources within an area under investigation, as well as those sources affecting this area through long-range atmospheric transport.

4. Mapping

Most advanced Russian developments of GIS (geographical information system) technologies for the purposes of environmental monitoring are widely used for interpretation of the distribution of heavy metals over examined territories. The program GRINVIEW from the geographical information system software package GIS-INTEGRO with raster and vector graphics was used to generate raster-based pollution contour maps for the elements of interest for the entire studied area. This system is supplied with interfaces for all international standard GIS: ARC-Info, MAP-Info, etc. Our “home-made” Atlases are produced in addition to mapping provided by the UNECE ICP. Examples of maps constructed using GRINVIEW are given in Fig. 1.

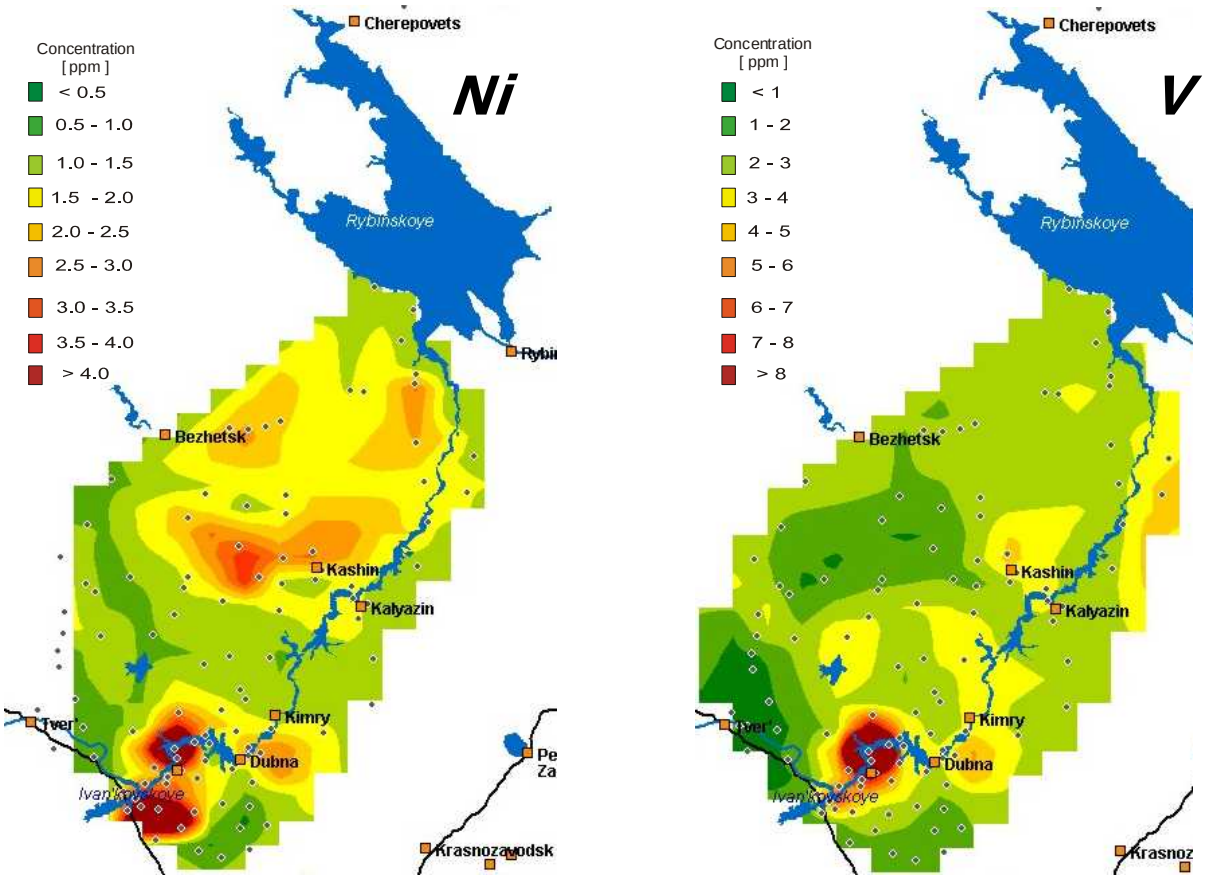

Fig. 1. *Distribution maps of nickel and vanadium in Central Russia [16].*

The Department of NAA FLNP educates and trains young specialists from many countries in nuclear analytical technique to study environmental pollution as part of the framework for current international projects.

5. Acknowledgement

The international Dubna team appreciates the scientific guidance and supervision of Prof. **E. Steinnes** (NUNT, Norway) to whom we are obliged for our achievements in biomonitoring studies using nuclear and related techniques.

References

[1] Å. Rühling. Atmospheric Heavy Metal Deposition in Europe - estimations based on moss analysis. Nordic Council of Ministers, Copenhagen, Nord, 1994:9.

[2] http://icpvegetation.ceh.ac.uk

[3] T. Berg and E. Steinnes. Use of mosses (*Hylocomium splendens* and *Pleurozium schreberi*) as biomonitors of heavy metal deposition: from relative to absolute deposition values. Environmental Pollution, Vol. 98, No. 1 (1997) p. 61-71.

[4] Å. Rühling and E. Steinnes Atmospheric Heavy Metal Deposition in Europe 1995-1996. NORD Environment, NORD 1998:15 (1998).

[5] A. Lucaciu, M.V Frontasyeva, E. Steinnes, Ye.N. Cheremisina, C. Oprea, T.B. Progulova, S. Spiridon, L. Staicu, L. Timofte, Atmospheric Deposition of Heavy Metals in Romania Studied by the Moss Biomonitoring Technique Employing Nuclear and Related Analytical Techniques and GIS Technology, J. Radioanal. Nucl. Chem., Vol. 240, No. 2, 457-458, 1999.

[6] K. Grodzinska, M. Frontasyeva, G. Szarek-Lukaszewska, M. Klich, A. Kucharska-Fabis, T. Ostrovnaya, S.F. Gundorina. Trace element contamination in industrial regions of Poland studied by moss monitoring. Environmental Monitoring and Assessment. Vol. 87, No. 3, 255-270, 2003.

[7] K. Grodzinska, G. Szarek-Lukaszewska, M. Frontasyeva, S.S. Pavlov, S.F. Gudorina. Multielement concentration in mosses in the forest influenced by industrial emissions (Niepolomice Forest, South Poland) at the end of 20th century. *Polish Journal of Environmental Studies*, Vol. 14, No. 2, 2005, p. 171-178.

[8] J. Stamenov, M. Iovchev, B. Vachev, E. Gueleva, L. Yurukova, A. Ganeva, M. Mitrikov, A. Antonov, A. Strentz, Z. Varbanov, I. Batov, K. Damov, E. Marinova, M.V. Frontasyeva, S.S. Pavlov, L.P. Strelkova. New results from air pollution studies in Bulgaria (Moss Survey 2000-2001). Preprint JINR, E14-2002-204, Dubna, 2002 (Submitted to International Journal "Balkan Ecology").

[9] S.G. Marinova, M.V. Frontasyeva, L.D. Yurukova, L.P. Strelkova, A.T. Marinov. Air pollution studies in South Bulgaria using the moss biomonitoring technique and neutron activation analysis. Book of Abstracts. 6th International Conference of the Balkan Physical Union, Istanbul, Turkey, August 22-26, 2006, p. 1004; Submitted to- Proceedings to be published in the *Journal of American Institute of Physics* (AIP), 2007.

[10] M. Florek, M.V. Frontasyeva, B. Mankovska, K. Oprea, S.S. Pavlov, E. Steinnes, I. Sykora. Air pollution with heavy metals and radionuclides in Slovakia studies by the moss biomonitoring technique. JINR preprint, E3-2001-155, Dubna, 2001. Proceedings of the 9the Int. Seminar on Interaction of Neutrons with Nucleai (ISINN-9), May 23-26, 2001, Dubna, Russia.

[11] B. Mankovska, M. Florek, M.V. Frontasyeva, E. Ermakova, C. Oprea, S.S. Pavlov. Atmospheric deposition of heavy metals in Slovakia studied by the moss biomonitoring technique, neutron activation analysis and flame atomic absorption spectrometry. *Ekologia,* Bratislava, Vol. 22, Supplement 1/2003, 2003, p. 157-162.

[12] O.A.Culicov, M.V.Frontasyeva, E. Steinnes, O.S. Okina, Zs. Santa, R. Todoran. Atmospheric deposition of heavy metals around the lead and copper-zinc smelters in Baia Mare, Romania, studied by the moss biomonitoring technique, neutron activation analysis and flame atomic absorption spectrometry. J. Radioanal. Nucl. Chem., Vol. 254, No. 1, 2002, 109-115.

[13] A. Lucaciu, L. Timofte, O. Culicov, M.V Frontasyeva, C. Oprea, S. Cucu-Man, R. Mocanu, E. Steinnes. Atmospheric deposition of trace elements in Romania studied by the moss biomonitoring technique. *Journal of Atmospheric Chemistry*, Vol. 49, 2004, p. 533-548.

[14] S. Cucu-Man, R.Mocanu, O. Culicov, E. Steinnes, M.V. Frontasyeva. Atmospheric deposition of metals in Romania studied by biomonitoring using the epiphytic moss *Hypnum cupressiforme*. *International Journal of Environmental Analytical Chemistry*, Vol. 84, No. 11, 2004, p. 845-854.

[15] M.V. Frontasyeva, E. Steinnes, S.M. Lyapunov, V.D. Cherchintsev, I.L. Smirnov, Biomonitoring of Heavy Metal Deposition in the South Ural Region: Some preliminary results obtained by nuclear and related techniques, *J. Radioanal. Nucl. Chem.*, Vol. 245, No. 2, 2000, 415-420.

[16] M.V. Frontasyeva, L.I .Smirnov, E. Steinnes, S.M. Lyapunov, V.D. Cherchintsev. Heavy metal atmospheric deposition study in the South Ural Mountains. *J. Radioanal. Nucl. Chem.*, Vol. 259, No. 1, 2004, p. 19-26.

[17] L.I. Smirnov, M.V. Frontasyeva, E. Steinnes. Multivariate statistical analysis of heavy metal and radionuclide concentrations in moss and soil of the South Urals. *Atomic Energy*, Vol. 97, No. 1, 2004, p. 68-74 (in Russian).

[18] E.V.Ermakova, M.V. Frontasyeva, E. Steinnes. Investigation of atmospheric deposition of heavy metals and other elements in the territory of Tula Region by means of moss biomonitors. *JINR Preprint*, P-14-2002-15, 2002, Dubna (submitted to the *Russian Journal of Ecology*, Yekaterinburg) (in Russian).

[19] E.V. Ermakova, M.V. Frontasyeva, S.S.Pavlov, E.A. Povtoreiko, E. Steinnes. Air pollution studies in Central Russia Using the moss biomonitoring technique and Neutron Activation Analysis. Proceedings of BioMAP-3, 21-25 September, 2003, Bled, Slovenia (in press).

[20] K.N. Vergel', E.V. Ermakova, M.V. Frontasyeva, S.S. Pavlov. Air pollution studies in Central part of Russia using the moss-biomonitoring technique: moss-surveys 2000 and 2005. Book of Abstracts 20th Task Force Meeting of the ICP Vegetation (Dubna, March, 5-9, 2007), p. 41.

[21] O.Blum, O.A.Culicov, M.V.Frontasyeva. Heavy meatal deposition in Ukrainian Carpathians (Zakarpattia and Chernivtsi regions): regional biomonitoring, Proceedings of the EuroBionet 2002, 2-6 November 2002, Stuttgart.

[22] M.V Frontasyeva., T.Ye. Galinskaya, M. Krmar, M. Matavuly, S.S. Pavlov, D. Radnovich, E. Steinnes. Atmospheric deposition of heavy metals in Serbia studies by moss biomonitoring, neutron activation analysis and GIS technology. Preprint JINR, E18-2002-144, Dubna, 2002 (Submitted to Journal of Radioanalytical and Nuclear Chemistry).

[23] M. Krmar, D. Radnovic , M.V. Frontasyeva, S.S. Pavlov, Yu.S. Pankratova. Comparison of moss surveys 2000 and 2005 in Northern Serbia. Book of Abstracts 20th Task Force Meeting of the ICP Vegetation (Dubna, March, 5-9, 2007), p. 60.

[24] L. Barandovski, M. Cekova, M.V. Frontasyeva, S.S. Pavlov, T. Stafilov, E. Steinnes, V. Urumov. Air pollution studies in Macedonia sing the moss biomonitoring technique, NAA, AAS and GIS technology. *JINR Preprint*, E18-2006-160, Dubna 2006 (submitted to *Environmental Monitoring and Assessment*.

[25] L. Barandovski, M. Cekova, M.V. Frontasyeva, S.S. Pavlov, V. Urumov. Air pollution in the Republic of Macedonia: moss biomonitoring stuidy–2005. Book of Abstracts 20th Task Force Meeting of the ICP Vegetation (Dubna, March, 5-9, 2007), p. 49.

[26] Heavy Metals in European mosses: 2000/2001 survey, UNECE ICP Vegetation. Editors: A.Buse, D. Norris, H. Harmens, P. Buker, T. Ashenden and G. Mills. Centre for Ecology&Hydrology, Universoty of Walse Bangor, United Kingdom, March 2003, pp.45.

[27] Mahmut Coşkun, M.V. Frontasyeva, E. Steinnes, A.Y. Çotuk, S.S. Pavlov, Münevver Coşkun, A.S. Sazonov, A. Çayır, M. Belivermis. Atmospheric deposition of heavy metals in Thrace Region studied by analysis of moss (*Hypnum cupressiforme). Bulletin of Environmental Contamination and Toxicology*, Vol. 74, No. 1, 2005, p. 201-209.

[28] Z. Spiric, V. Kusan, Z. Mesic, M.V. Frontasyeva, S.F. Gundorina, T.M. Ostrovnaya. The moss survey 2006 in the Republic of Croatia. Book of Abstracts 20th Task Force Meeting of the ICP Vegetation (Dubna, March, 5-9, 2007), p. 68.

[29] Yu. Aleksiayenak, M.V. Frontasyeva, T.M. Ostrovnaya. Trace element atmospheric deposition in the Republic of Belarus: Minsk and Grodno case study. Book of Abstracts 20th Task Force Meeting of the ICP Vegetation (Dubna, March, 5-9, 2007), p. 46.

[30] M.V. Frontasyeva. JINR contribution to trace elements atmospheric deposition study in some selected coun tries of Europe and Asia based on moss analysis. Book of Abstracts 20th Task Force Meeting of the ICP Vegetation (Dubna, March, 5-9, 2007), p. 21.

[31] Yu.S. Pankratova, M.V. Frontasyeva, N.I. Zelnitchenko, S.S. Pavlov. Atmonspheric deposition of heavy metals and other elements in the Republic of Udmurtia, Russian Federation, studied by

the moss biomonitoring, NAA and GIS technology. . Book of Abstracts 20th Task Force Meeting of the ICP Vegetation (Dubna, March, 5-9, 2007), p. 32.

[32] J. Shao, Z. Zhang, Z. Chai, X. Mao, Y. Lu, O. Stan, M.V. Frontasyeva, P. Wu. Study of concentration of heavy metals deposited from atmosphere by mosses. *Journal of Nuclear and Radiochemistry*, Vol. 24, No. 1, 2002, p. 6-11 (in Chinese).

[33] Z. Zhang, O. Stan. Study of epiphytic mosses using as biomonitors of heavy metal atmospheric deposition by INAA. Workshop of 4th National Instrumental Analysis and Sample Preparation, May 19-25, Chengdu, Sichuan Province, P. R. China, 2000; *Modern Instruments Application & Maintenance,* No. 2, May 2000, p. 25-31.

[34] Y.S. Kang, K.Guinyun, M.V. Frontasyeva, S.S.Pavlov. Biomonitoring in South Korea using moss, lichens and tree bark. In Proceedings, Workshop on Nuclear Data Production and Evaluation. , August 25-25, 2001, Pohang, Korea, p.35.

[35] G.Gandbol, Sh. Gerbish, S.F. Gundorina, M.V. Frontasyeva, T.M. Ostovnaya, S.S. Pavlov, Ts. Tsenddeekhuu. Atmospheric deposition of trace elements around Ulan-Bator city studied by moss and lichen biomonitoring technique and INAA. *JINR Preprint*, E18-2005-113, Dubna, 2005, cc.17.

[36] My T.T, Trinh, M.V. Frontasyeva, Nguyen Hong Nhung. Leaves of *Tamarindus Indica* used to monitor metal contamination in Hochiminh City, Vietnam. Book of Abstracts 20th Task Force Meeting of the ICP Vegetation (Dubna, March, 5-9, 2007), p. 72.

5. PUBLICATIONS

CONDENSED MATTER PHYSICS

Diffraction

1. Antonov V.E., Beskrovny A.I., Fedotov V.K., Ivanov A.S., Khasanov S.S., Kolesnikov A.I., Sakharov M.K., Sashin I.L., Tkacz M. Crystal structure and lattice dynamics of chromium hydrides, submitted in J. Alloys and Compounds, 2006.
2. Babushkina N.A., Chistotina E.A., Balagurov A.M., Pomjakushin V.Yu. , Gorbenko O.Yu., Kaul A.R., Kartavtseva M.S. "Isotope effect and cation disorder in manganites" JMMM, 2006, v. 300 (1), pp. e114-e117.
3. Balagurov A.M., Bobrikov I.A., Pomjakushin V.Yu., Sheptyakov D.V., Babushkina N.A., Gorbenko O.Yu., Kaul A.R. "Structural origin of the giant oxygen isotope effect in $Re_{0.5}Sr_{0.5}MnO_3$ perovskites". Physica B, 2006, v. 385-386, pp. 94-96.
4. Balagurov A.M., Pomjakushin V.Yu. "Structural aspects of the giant oxygen isotope effect in perovskite manganese oxides". Crystallography Reports, 2006, v. 51(5), pp. 828-839.
5. Belushkin A.V., Kozlenko D.P., Golosova N.O., Zettersröm P., Savenko B.N. "A study of disorder effects at ferroelectric phase transition in BaTiO3", Physica B, v.385-386, pp. 85-57 (2006).
6. Beskrovny A., Guskos N., Typek J., Ryabova N.Yu., Blonska-Tabero A., Kurzawa M., and Zolnierkiewicz G. «Crystal structure of $Mg_3Fe_4V_6O_{24}$ studied by neutron diffraction». Rev. Adv. Mat. Sci. 11, 166, 2006.
7. Bikkulova N.N., Skomorokhov A.N., Beskrovny A.I., Yadrovsky E.L., Stepanov Yu.M., Mikolaichuk A.N., Sagdatkireeva M.B., Karimov L.Z. "Lattice dynamics and ion transfer in structural-disordered copper and silver chalcogenides". Submitted to "Crystallography Reports".
8. Bushmeleva S.N., Pomjakushin V.Yu., Pomjakushina E.V., Sheptyakov D.V., Balagurov A.M. "Neutron diffraction evidence for band ferromagnetism in $SrRuO_3$". JMMM, 2006, v.305(2), pp. 491-496.
9. Chichev A.V., Dlouha M., Vratislav S., Knizek K., Hejtmanek J., Marysko M., Veverka M., Jirak Z., Golosova N.O., Kozlenko D.P.and Savenko B.N."Structural, Magnetic and Transport Properties of Single-Layered Perovskites $La_{2-x}Sr_xCoO_4$ (x=1.0-1.4)", Phys. Rev. B, v. 74, pp. 134414 (2006).
10. Efimchenko V.S., Antonov V.E., Barkalov O.I., Beskrovny A.I., Fedotov V.K., Klyamkin S.N.. Phase transitions and equilibrium hydrogen content of phases in the water-hydrogen system at pressures to 1.8 kbar, High Pressure Research, Vol. 26, No. 4, 2006.
11. Golosova N.O., Kozlenko D.P., Sikolenko V.V., Sazonov A.P., Troyanchuk I.O., Savenko B.N., Glazkov V.P. "High pressure effects on the crystal and magnetic structure of $Nd_{0.78}Ba_{0.22}CoO_3$ cobaltite". Journal of Experimental and Theoretical Physics Letters, v.84, pp. 16-20 (2006).
12. Golosova N.O., Kozlenko D.P., Voronin V.I., Glazkov V.P.and Savenko B.N."The influence of high pressure on the crystal and magnetic structures of the $La_{0.7}Sr_{0.3}CoO_3$ cobaltite", Physics of the Solid State, v. 48, pp. 96-101 (2006).
13. Itkis D.M., Goodilin E.A., Balagurov A.M., Bobrikov I.A., Sinitskii A.S., Tretyakov Y.D. "Preparation-dependent properties of $Ca(Cu,Mn)_7O_{12}$ CMR materials" Solid State Communications, 2006, v.139(7), pp.380-385.
14. Kiselev M.A., Ryabova N.Yu., Balagurov A.M., Otto D., Dante S., Hauss T., Wartewig S., Neubert R. "Effect of ceramide 6 on the structure and hydration of the membrane of dipalmitoylphosphatidylcholine", Poverkhnost', No.6, 30-37, 2006. (in Russian).
15. Kozlenko D.P., Kichanov S.E., Lee S., Park J.-G., Glazkov V.P.and Savenko B.N. "High Pressure Effect on the Crystal and Magnetic Structure of $LuMnO_3$: Correlation between the Distortion of the Triangular Lattice and the Symmetry of the Magnetic State in Hexagonal Frustrated Manganites". Journal of Experimental and Theoretical Physics Letters, v. 83, pp. 346-350 (2006).
16. Kozlenko D.P.and Savenko B.N. "High-Pressure Effects on the Crystal and Magnetic Structure of Manganites", Physics of Particles and Nuclei, 2006, Vol. 37, Suppl. 1, pp. S1–S12 (2006).
17. Nietz V.V., Osipov A.A. "Ball solitons and kinetics of the first order magnetic phase transition". Submitted to the Journal of Magnetism and Magnetic Materials.
18. Nietz V.V., Osipov A.A. "Ball solitons in kinetics of the first order magnetic phase transitions (New mechanism of phase transformation". Submitted to "Crystallography Reports". Reduced version.
19. Nietz V.V., Stavisskiy Yu.Ya. "Prospects for neutron research of magnetism with a pulsed magnetic field at powerful pulsed neutron sources". Admitted in Journal of Neutron Research.

20. Pomjakushin V.Yu., Balagurov A.M., Conder K., Pomjakushina E.V., Sheptyakov D.V. “Effect of oxygen isotope substitution and crystal micro-structure on magnetic ordering and phase separation in $(La_{1-y}Pr_y)_{0.7}Ca_{0.3}MnO_3$”. Submitted to Phys. Rev. B, November-2006.
21. Sazonov A.P., Troyanchuk I.O., Kozlenko D.P., Balagurov A.M.and Sikolenko V.V. “Magnetic Ordering in the Nd_2CoMnO_{6+d} Perovskite System”. Journal of Magnetism and Magnetic Materials, v. 302, pp. 443-447 (2006).
22. Vasilovskiy S.G., Sikolenko V.V., Beskrovnyi A.I., Belushkin A.V., Flerov I.N., Tressaud A., Balagurov A.M. Neutron diffraction studies of temperature induced phase transitions in Rb_2KFeF_6 elpasolite. Z. Kristallorg. Suppl. 23, pp.467-472 (2006).
23. Zvezdin A.K., Nietz V.V., Stavisskiy Yu.Ya. Powerful pulsed neutron sources for investigations with a pulsed magnetic field. Submitted to “Crystallography Reports”.

Texture and stresses

1. Balagurov A.M., Vasin R.N., Lokajicek T., Nikitin A.N., Papushkin I.V., Pros Z., Subbotin A.V., Sumin V.V. Anisotropy, texture and residual stress of reactor graphite to be after exploitation. Proceedings of Tula State University, Seria Fizika, 2006, vol.6, pp. 96-111.
2. Frischbutter A., Janssen Ch., Scheffzük Ch., Walther K, Ullemeyer K., Behrmann J. H., Nikitin A. N., Ivankina T. I., Kern H., Leiss B. Strain and texture measurements on geological samples using neutron diffraction at IBR-2, Joint Institute for Nuclear Research Dubna (Russia).
3. Levin D.M., Nikitin A.N. Study of physical and mechanical properties of polycrystalline calcite at high temperatures and pressures to development of safety criteria for waste disposal at large depths. Proceedings of Tula State University, Seria Fizika, 2006, vol.6, pp. 88-95.
4. Nikitin A.N., Ermakova E.V. Sludge waste of thermoelectric power stations - pollution sources of ambient air and potential resources of mineral. Proceedings of Tula State University, Seria Fizika, 2006, vol.6, pp. 75-87.
5. Nikitin A.N., Ermakova E.V. Sludge waste of thermoelectric power stations - pollution sources of ambient air and potential resources of mineral. Proceedings of Tula State University, Seria Fizika, 2006, vol.6, pp. 75-87.
6. Nikitin A.N., Markova G.V., Balagurov A.M., Vasin R.N. Alekseeva O.V. An investigation of structure and properties of quartz at the interval of α-β transition by neutron diffraction and mechanical spectroscopy. Crystallography. 2007 (accepted).
7. Nikitin A.N., Vasin R.N., Balagurov A.M., Sobolev G.A., Ponomarev A.V. An investigation of thermal and deformation properties of quartzite at the temperature interval of polymorphic α-β transition by neutron diffraction and acoustic emission. Particles and Nuclei. Letters, 2006, vol.3, № 1(130), pp. 76-91.
8. Priesmeyer H.-G. and Bokuchava G. “Positron annihilation as an additional source of information about plastic deformation in structural materials”. Materials Science and Engineering A, v. 437, pp. 54-59, 2006.
9. Prokoshkin S.D., Korotitskiy A.V., Tamonov A.V., Khmelevskaya I.Yu., Brailovski V.and Turenne S. “Comparative X-ray and time-of-flight neutron diffraction studies of martensite crystal lattice in stressed and unstressed binary Ti–Ni alloys”. Materials Science and Engineering A, v. 438-440, pp. 549-552, 2006.
10. Taran Yu.V., Daymond M.R., Schreiber J. “Study of martensitic transformation in fatigued stainless steel by neutron diffraction stress analysis”. Zeitschrift fur Kristallographie, Supplement Issue no. 23, pp.345-350, 2006.
11. Taran Yu.V., Schreiber J., Daymond M.R., Oliver E.C. “Fatigue degradation and martensitic transformation of austenitic stainless steel AISI 321: new results and prospects”. Materials Science Forum, v. 524-25, pp. 899-904, 2006.
12. Taran Yu.V., Schreiber J., Stuhr U., Kockelmann H., Balagurov A.M., Zlokazov V.B. “Residual stresses in a composite steel tube measured by neutron diffraction”. Communication of JINR, E18-2006-66, Dubna, 2006.
13. Vasin R.N., Nikitin A.N., Lokajicek T., Rudaev V. Acoustic emission of quasi-isotropic rock samples initiated by temperature gradients. Fizika Zemli, 2006, № 10, pp.26-35.
14. Vasin R.N., Nikitin A.N., Plotnikova E.M., Ullemeyer K. Quartz crystallographic textures of monophase and multiphase rocks measured by neutron diffraction. Proceedings of Tula State University, Seria Fizika, 2006, vol.6, pp. 126-151.
15. Vasin R.N., Nikitin A.N., Plotnikova E.M., Ullemeyer K. Quartz crystallographic textures of monophase and multiphase rocks measured by neutron diffraction. Proceedings of Tula State University, Seria Fizika, 2006, vol.6, pp. 126-151.

Inelastic neutron scattering

1. Antonov V.E., Bashkin I.O., Fedotov V.K., Khasanov S.S., Hansen T., Ivanov A.S., Natkaniec I., “Crystal structure and lattice dynamics of high-pressure scandium trihydride”, Phys. Rev. B 73 (2006) 054107-1-6.
2. Antonov V.E., Beskrovnyy A.I., Fedotov V.K., Ivanov A.S., Khasanov S.S., Kolesnikov A.I., Sakharov M.K., Sashin I.L. and Tkacz M., “Crystal structure and lattice dynamics of chromium hydrides” Journal of Alloys and

Compounds, In Press, Corrected Proof, Available online 12 June 2006.

3. Bikkulova N.N., Skomorokhov A.N., Beskrovny A.I., Yadrovsky E.L., Stepanov Yu.M., Mikolaichuk A.N., Sagdatkireeva M.B., Karimov L.Z. “Lattice dynamics and ion transfer in structural-disordered copper and silver chalcogenides”. Submitted to “Crystallography Reports”.

4. Blagoveshchenskii N.M., Morozov V.A., Novikov A.G., Pashnev M.A., Savostin V.V., Shimkevich A.L. “Study of microdynamics of liquid lithium by neutron scattering”. “Crystallography Reports“ (in print).

5. Blagoveshchenskii N.M., Morozov V.A., Novikov A.G., Savostin V.V., Savostin D.V., Shimkevich A.L. “Microstructure of liquid two-component alloys studied by neutron diffraction”. Poverkhnost’, 2006, № 6, p. 5 – 9. (in Russian).

6. Blagoveshchenskii N.M., Morozov V.A., Novikov A.G., Savostin V.V., Savostin D.V., Shimkevich A.L. “Study of the microstructure melt “lithium-nitrogen” by neutron diffraction”. “Crystallography Reports“ (in print).

7. Blagoveshchenskii N.M., Morozov V.A., Novikov A.G., Savostin V.V., Shimkevich A.L. “Study of the spectrum of elementary excitations of liquid lead”. Poverkhnost’, 2006, № 6, p. 10-17. (in Russian).

8. Blagoveshchenskii N.M., Morozov V.A., Novikov A.G., Savostin V.V., Shimkevich A.L. “Studies of the lead melt and liquid-metal compostitions on the basis of lead by neutron scattering ”. Submitted to “Nuclear power engineering”. (in Russian).

9. Bogoyavlenskii I.V., Kalinin I.V., Puchkov A.V., Skomorokhov A.N. “Experimental investigation of peculiarities of the excitation spectrum of superfluid helium” Proceedings of the regional competition of scientific projects in the field of natural sciences, № 9, 2006, p.118-129. (in Russian).

10. Dubovskiy O.A., Orlov A.V. “Non-linear high-amplitude soliton oscillations in crystalline materials with atom-atom potential of the Lenard-Jones interaction”. Preprint IPPE-3074, 2006, 17 p. (in Russian).

11. Dubovskiy O.A., Orlov A.V. “Supersonic soliton compression waves in crystalline materials with the Lenard-Jones interatomic potential”. Preprint IPPE-3081, 2006, 20 p. Submitted to “Crystallography Reports“, 18.10.06.

12. Dubovsky O.A., Orlov A.V., "Supersonic soliton and selflocalized waves in crystal materials with Lennard-Jones potential of atomic interaction, p. 17, Submitted to “Physics Letters” A.

13. Fedotov V.K., Antonov V.E., Bashkin I.O., Hansen T., Natkaniec I., “Displacive ordering in the hydrogen sublattice of yttrium trihydride”, J. Phys. Condens. Matter, 18 (2006) 1593-1599.

14. Holderna-Natkaniec K., Natkaniec I., Jurga K., Nowak D., Szyczewski A., „Internal dynamics of norethisterone by NMR, IINS and QC methods”, Solid State Phenomena, Vol. 112 (2006) 93-100.

15. Holderna-Natkaniec K., Natkaniec I., Kasperkowiak W., Sciesinska E., Sciesinski J., Mikuli E., „The IINS, IR and DFT studies of hydrogen bonds in 6-Furfuryl and 6-Benzyl-aminopurines”, J. Molec. Struct., **790** (2006) 94-113.

16. Ibberson R.M., Parsons S., Natkaniec I., Holderna-Natkaniec K., “Structure determination and phase transition behaviour of mesitylene”, Zeitschrift fur Kristallographie, 2006 (in print).

17. Juszynska E., Massalska-Arodz M., Mayer J., Natkaniec I., Krawczyk J., Tracz P., „Neutron scattering in 3,3-dimethyl-2-butanol and 2,3-dimethyl-2-butanol”, Solid State Phenomena, Vol 112 (2006) 89-92.

18. Kalinin I., Lauter H., Puchkov A., “Experimental study of zero sound and single-particle excitations in ^{4}He”, Physica B 44 (2006), in press.

19. Kalinin I.V., Lauter H., Koza M., Lauter-Pasyuk V.V., Puchkov A.V. “Surface excitations in nanofilms of liquid helium”, “Crystallography Reports“, 2006 (in print).

20. Kalinin I.V., Lauter H., Puchkov A.V. “Investigation of peculiarities of the excitation spectrum of superfluid helium by inelastic neutron scattering”, Bulletin of the Russian Academy of Sciences. Physics, 2006 (in print).

21. Kalinin I.V., Lauter-Pasyuk V.V., Puchkov A.V. “ Surface excitations in nanofilms of liquid helium”, Proceedings of the regional competition of scientific projects in the field of natural sciences, Publishing house "Polygraph-Inform", Kaluga, 2006, (in print). (in Russian).

22. Kazarnikov V.V., Morozov S.I., Ivanov A.S., Kalinin I.V., Primakov N.G., Rudenko V.A., Sashin I.L., Shovkun D.V. "Neutronoscopic investigation of dynamics of interstitial atoms in bulk-centered lattices of transition metals in the modes with "heating" and "cooling" of neutrons", Proceedings of the regional competition of scientific

projects in the field of natural sciences, Publishing house "Polygraph-Inform", Kaluga, 2006, (in print). (in Russian).

23. Kazimirov V.Yu., Guerlou-Demourgues L., Servant L., Smirnov M.B., Balagurov A.M., Natkaniec I., Khasanova N.R., Antipov E.V. "Lattice dynamics and crystal structure of Ni-hydroxides" JINR Communications, Dubna, December 2006.

24. Loose A., Melnyk G., Zink N., Wozniak K., Dominiak P., Smirnov L.S., Pawlukojc A., Shuvalov L.A., "Refinement of Hydrogen Positions in $(NH_4)_2SeO_4$", submitted to Poverkhnost'.

25. Loose A., Smirnov L.S., Dolbinina V.V., Yakovleva L.M., Grebenev V.V., "The refinement of hydrogen positions in phase II of β-$LiNH_4SO_4$" submitted to Poverkhnost'.

26. Loose A., Wozniak K., Dominiak P.M., Smirnov L.S., Natkaniec I., Frontasjeva M.V., Pomjakushina E.V., Baranov A.I., Dolbinina V.V., "X-ray and neutron single crystal diffraction on $[Rb_x(NH_4)_{1-x}]_3H(SO_4)_2$. I. Refinement of crystal structure of phase II with x=0.11 at 300 K", Preprint JINR, E14-2006-59, Dubna, 2006, 23p.

27. Majerz I., Natkaniec I., "Experimental and theoretical IR, R and INS spectra of 2,2,4,4-tetramethyl-3-t-butyl-pentane-3-ol", J. Mol. Struct.,788/1-3 (2006) 93-101.

28. Mayer J., Krawczyk A., Massalska-Arodz M., Natkaniec I., Janik J.A., Steinsvoll O., „Neutron Scattering study of low-energy excitations in some organic glass formers", Physica B, **371** (2006) 249-256.

29. Mikuli E., Natkaniec I., "Niespójne kwasielastyczne i nieelastyczne rozpraszanie neutronów", in: Komplementarne Metody Badań Przemian Fazowych, Ed. Migdał-Mikuli A. and Mikuli E., Wydawnictwo UJ, Kraków 2006, Wyd. I. p. 121-142. (in Polish).

30. Morozov S.I. "Investigation of dynamics of oxigen atoms in the Ta-O interstitial system". FTT (Physics of the Solid State), 2006, vol.48, № 4, p.578-582.

31. Morozov S.I., Kazarnikov V.V., Ivanov A.S. "Sidebands of the oscillation spectrum of interstitial elements in a metal lattice". JETP Letters, 2006, vol.83, №11, p.588-591.

32. Natkaniec I., Holderna-Natkaniec K., Nowak D., "Neutron scattering studies of molecular dynamics in solid phases of neohexane and diisopropyl", Materials Research Society, Proceedings QENS2006 Conf., Bloomington, 14-17 June 2006. (in print).

33. Natkaniec I., Holderna-Natkaniec K., Nowak D., Majerz I., Prager M., "Molecular dynamics in crystalline and glassy state of 2,4,6-trimethyl-piridine", Materials Research Society, Proceedings QENS2006 Conf., Bloomington, 14-17 June 2006. (in print).

34. Natkaniec I., Shabalin E., Kulikov S., Holderna-Natkaniec K., „Comparative studies of neutron scattering and radiation properties of methane, methanol, mesitylene and water at low temperature", Proc. ICANS-XVII, April 25-29, 2005, Santa Fe, New Mexico USA, Ed. Russell G.J., Rhyne J.J. and Maes B.V., LA-UR-06-3904, Vol. II, p. 519-529.

35. Pawlukojć A., Natkaniec I., Bator G., Sobczyk L., Grech E., Nowicka-Scheibe J., "Low frequency internal modes of 1,2,4,5-tetramethylbenzene, tetramethylpyrazine and tetramethyl-1,4-benzoquinone. INS, Raman, IR and theoretical DFT studies". Spectrochimica Acta Part A, 63 (2006) 766-773.

36. Pawlukojć A., Sawka-Dobrowolska W., Bator G., Sobczyk L., Grech E., Nowicka-Scheibe J., "X-ray diffraction, inelastic neutron scattering (INS) and infrared (IR) studies on 2:1 hexamethylbenzene (HMB)- tetracyanoethylene (TCNE) complex." Chem. Phys. 327 (2006) 311-318.

37. Pawlukojć A., Starosta W., Leciejewicz J., Natkaniec I., Nowak D. "The molecular structure and dynamics of 2-aminopyridine-3-carboxilic acid by X-ray diffraction at 100K, inelastic neutron scattering, infrared, Raman spectroscopy and from *first principles* calculation", submitted to Chem. Phys. Lett. (2006).

38. Prager M., Sawka-Dobrowolska W., Sobczyk L., Pawlukojć A., Grech E., Wischniewski A., Zamponi M., "X-ray diffraction and inelastic neutron scattering study of 2,,6-dimethylopyrazine (DMP) – chloranilic acid (CLA) complex" Chem. Phys. (2006) in print.

39. Prager M., Zamponi M., Wischniewski A., Pietraszko A., Sobczyk L., Pawlukojć A., Grech E., Seydal T., "X-ray diffraction and inelastic scattering (INS) studies of tetramethylpyrazine-chloranilic acid complex: temperature, isotope and pressure effects" J. Chem. Phys. (2006) in print.

40. Reehuis M., Wozniak K., Dominiak P., Smirnov L.S., Natkaniec I., Baranov A.I., Dolbinina V.V., "X-ray and neutron single crystal diffraction on $(NH_4)_3H(SO_4)_2$. II. Refinement of crystal structure of phase II at room temperature", Preprint JINR, E14-2006-111, Dubna, 2006, 17 p.

41. Sawka – Dobrowolska W., Bator G., Czernik – Matusewicz B., Sobczyk L., Pawlukojć A., Grech E., Nowicka –

Scheibe J., Rundlöf H., "X-ray and neutron diffraction, IR and INS spectroscopic and DFT theoretical studies on the tetramethylpyrazine-1,2,4,5,-tetracyanobenzene complex." Chem. Phys. 327 (2006) 237-242.

42. Semenov V.A., Kozlov Zh.A., Kraechun I., Matiesku G., Morozov V.M., Oprea A., Oprea K., Padureanu I., Puchkov A.V. "Inelastic scattering of slow neutrons by vanadium at the temperatures of 293-1773K", Preprint IPPE-3085, 2006, 17 p. (in Russian).

43. Skomorokhov A.N., Titov A.N., Titova S.G., Semenov V.A., Ovchinnikov S.G. "Dynamics of the crystalline lattice in materials with strong electron-phonon interaction", Proceedings of the regional competition of scientific projects in the field of natural sciences, Publishing house "Polygraph-Inform", Kaluga, 2006, (in print), (in Russian).

44. Skomorokhov A.N., Trots D.M., Knapp M., Bickulova N.N. and Fuess H., "Structural behaviour of β-$Cu_{2-\delta}Se$ (δ = 0, 0.15, 0.25) in dependence on temperature studied by synchrotron powder diffraction", Journal of Alloys and Compounds, v. 421. 2006, p. 64.

45. Skomorokhov A.N., Trots D.M., Sashin I.L., Fuess H., Yadrovskii E.L., Ovchinnikov S.G. "Density of phonon states in γ-, β- and α-AgCuS". Submitted to FTT (Physics of the Solid State).

46. Skomorokhov A.N., Trots D.M., Semenov V.A., Bickulova N.N., Yadrovskii E.L., Stepanov Yu.M., Knapp M., Fuess H. "Investigations of superionic conductor AgCuSe by inelastic neutron scattering", Poverkhnost', № 6, 2006. p. 18. (in Russian).

47. Smirnov L.S., Natkaniec I., Johnson M.R., Ivanov A.S., Troyanov S.I., "Neutron scattering study and computer modeling of hydrogen vibrational modes in $NH_4H_5(PO_4)_2$", Preprint JINR, E14-2006-114, Dubna, 2006, 11 p.

48. Smirnov L.S., Natkaniec I., Loose A., Wozniak K., Dominiak P. M., Zink N., Melnyk G., Pawlukojc A., Martinez Sarrion M.L., Mestres L., Nowak D., "Structure and dynamics of $K_{2-x}(NH_4)_xSeO_4$ mixed crystals studied by X-ray and neutron scattering", Preprint JINR, E14-2006-31, Dubna, 2006, 18 p.

49. Trots D.M., Skomorokhov A.N., Knapp M. and Fuess H., "High-temperature behavior of average structure and vibrational density of states in the ternary superionic compound AgCuSe", The European Physical Journal B - Condensed Matter, v. 51. 2006, p. 507.

Reflectometry, polarized neutron

1. Aksenov V.L., Ignatovich V.I., Nikitenko Yu.V. Neutron reflection from helical system, JETP Letters, vol. 84, N 9, page 563-569, 2006.
2. Aksenov V.L., Ignatovich V.I., Nikitenko Yu.V. Neutron reflection from helical system. Poverkhnost', accepted.
3. Aksenov V.L., Ignatovich V.I., Nikitenko Yu.V. Neutron Standing Waves in Layered Systems. Crystallography Reports, 2006. Vol 51, No. 5, pp. 734-753.
4. Aksenov V.L., Nikitenko Yu.V. Nano-spin-echo neutron spectrometer based on magnetic nanostructures. Crystallography Reports, accepted.
5. Aksenov V.L., Nikitenko Yu.V. Neutron polarization reflectometry at the IBR-2 pulsed reactor. Crystallography Reports, accepted.
6. Aksenov V.L., Nikitenko Yu.V., Petrenko A.V., Uzdin V.M., Khaidukov Yu.N., Tsabel H. Study of magnetic state of the lamellar structure V(39nm)/20[V(3nm)/Fe(3nm)] using polarized neutrons, Crystallography Reports, accepted.
7. Nikitenko Yu.V., Ul'yanov V.A., Pusenkov V.M. et al. Fan analyzer of neutron beam polarization on REMUR spectrometer at the IBR-2 pulsed reactor. NIM A 564 (2006) 395-399.

Small-angle neutron scattering

1. Aksenov V.L., Avdeev M.V., Kizima E.A., Rosta L., Korobov M.V. Effect of ageing of solution C_{60}/N-methyl-2-pyrrolidone on cluster structure in the system C_{60}/N-methyl-2- pyrrolidone/water as revealed by small-angle neutron scattering. Crystallography Reports, (2006) accepted.
2. Aksenov V.L., Avdeev M.V., Tropin T.V., Korobov M.V., Kozhemyakina N.N., Avramenko N.V., Rosta L. Formation of fullerene clusters in the system C60-NMP-water, Physica B (2006), in press.

3. Aksenov V.L., Avdeev M.V., Tropin T.V., Priezzhev V.B., Schmelzer J.W.P. Cluster growth and dissolution of fullerenes in non-polar solvents. J. Mol. Liq. 127 (2006) 142-144.

4. Avdeev M.V. Contrast Variation in Small-Angle Scattering Experiments on Polydisperse and Superparamagnetic Systems: Basic Functions Approach, J. Appl. Cryst. (2006), accepted.

5. Avdeev M.V., Aksenov V.L., Balasoiu M., Garamus V.M., Schreyer A., Török Gy., Rosta L., Bica D., Vékás L. Comparative analysis of the structure of sterically stabilized ferrofluids on polar carriers by small-angle neutron scattering. J. Col. Interface Sci. 295 (2006) 100–107.

6. Avdeev M.V., Bica D., Vékás L., Marinica O., Balasoiu M., Aksenov V.L., Rosta L., Garamus V.M., Schreyer A. On the possibility to use short chain length mono-carboxylic acids for stabilization of magnetic fluids. J. Mag. Mag. Mater. (2006), accepted.

7. Avdeev M.V., Tropin T.V., Aksenov V.L., Rosta L., Garamus V.M., Rozhkova N.N. Pore structures in shungites as revealed by small-angle neutron scattering, *Carbon* 44 (2006) 954–961.

8. Balasoiu M., Avdeev M.V., Aksenov V.L. Investigation of clusters in aqueous magnetic fluids by small-angle neutron scattering, "Crystallography Reports", accepted (2006).

9. Balasoiu M., Avdeev M.V., Aksenov V.L., Hasegan D., Garamus V.M., Schreyer A., Bica D., L.Vékás. Structural organization of water-based ferrofluids with sterical stabilization as revealed by SANS. J. Mag. Mag. Mater. 300 (2006) e225–e228.

10. Balasoiu M., Avdeev M.V., Kuklin A.I., Aksenov V.L., Ghenescu V., Hasegan D., Garamus V., Schreyer A., Bica D., Vékás L., Almasan V. Nuclear and magnetic structures of non-polar ferrofluids by small-angle neutron scattering, Preprint JINR E14-2005-1, Dubna, 2005.

11. Balasoiu M., Avdeev M.V., Kuklin A.I., Aksenov V.L., Hasegan D., Garamus V., Schreyer A., Bica D., Vékás L., Almasan V. Nuclear and magnetic structures of non-polar ferrofluids by small-angle neutron scattering. Romanian Reports in Physics 58 (2006) 305–311.

12. Bica D., Vékás L., Avdeev M.V., Marinică O., Socoliuc V., Bălăsoiu M., Garamus V.M. Sterically stabilized water based magnetic nanofluids, synthesis, structure and properties, J. Mag. Mag. Mater. (2006), accepted.

13. Efremov R., Gordeliy V.I., Heberle J. and Büldt G. (2006) Time-resolved microspectroscopy on a single crystal of bacteriorhodopsin reveals lattice induced differences in the photocycle kinetics. Biophys. J. 91, 1441-1451.

14. Fedotov G.N., Tret'yakov Yu.D., Pakhomov E.I., Kuklin A.I., Islamov A.Kh., Pochatkova T.N. Effect of the Soil Water Content on the Fractal Properties of Soil Colloids, Doklady Akademii Nauk, 2006, Vol. 409, No. 2, pp. 199–201. Eng.: ISSN 0012-5008, Doklady Chemistry, 2006, Vol. 409, Part 1, pp. 117–119.

15. Fedotov G.N., Tret'yakov Yu.D., Pakhomov E.I., Kuklin A.I., Islamov A.Kh. Temperature Effect on the Evolution of Soil Gels, Doklady Akademii Nauk, 2006, Vol. 407, No. 6, pp. 782–784. Eng.: ISSN 0012-5008, Doklady Chemistry, 2006, Vol. 407, Part 2, pp. 51–53.

16. Fedotov G.N., Tret'yakov Yu.D., Pakhomov E.I., Kuklin A.I., Islamov A.Kh. Inhomogeneity of Soil Gels, Doklady Akademii Nauk, 2006, Vol. 408, No. 2, pp. 207–210. Eng.:ISSN 0012-5008, Doklady Chemistry, 2006, Vol. 408, Part 1, pp. 73–75.

17. Haramagatti C.R. , Islamov A., Gibhardt H., Gorski N., Kuklin A.and Eckold G. Pressure induced phase transitions of TTAB-micellar solutions studied by SANS and Raman spectroscopy. Phys.Chem.Phys., 2006, 8, 994-1000.

18. Ion I., Bondar A.M., Kovalev Yu., Banciu C., Pasuk I., Kuklin A.. The influence of nanocarbon-coated iron on the mesophase. Poverhnost'. 2006, №6, p.84-88.

19. Islamov A., Haramagatti C.R., Gibhardt H., Kuklin A., Eckold G. Pressure-induced phase transitions in micellar solutions, Physica B 385–386 (2006) 791–794.

20. Khokhryakov A.O., Avdeev M.V., Aksenov V.L., Bulavin L.A. Structural organization of colloidal solution of fullerene C_{60} in water by data of small angle neutron scattering, J. Mol. Liq. 127 (2006) 73-78.

21. Khokhryakov A.O., Avdeev M.V., Kizima O.A., Len A., Aksenov V.L., Bulavin L.A. Structure and stabilization mechanism of non-modified fullerene water solutions. Kiev University bulletin (2006), accepted.

22. Khokhryakov A.A., Avdeev M.V., Kizima O.A., Len A., Aksenov V.L., Bulavin L.A. Structure and stabilization mechanism of non-modified fullerene water solutions. "Crystallography Reports", accepted (2006).

23. Kiselev M.A. Combined application of neutron and synchrotron radiation to study the influence of dimethyl sulfoxide on the structure and properties of vesicles from dipalmitoylphosphatidylcholine. Submitted to "Crystallography Reports" (2006).

24. Kiselev M.A. Conformation of ceramide 6 molecules and chain-flip transitions in lipid matrix of the upper layer of skin - Stratum Corneum. Submitted to “Crystallography Reports” (2006).

25. Kiselev M.A., Kiselev A.M., Borbely S., Lesieur P. Investigations of ethanol penetration through model biological membrane by small-angle neutron scattering. Poverkhnost’, 2006, v. 6, pp. 67-73. (in Russian).

26. Kiselev M.A., Zemlyanaya E.V., Aswal V.K., Neubert R.H.H. What can we learn about the lipid vesicle structure from the small angle neutron scattering experiment? European Biophys. J., 2006, v. 35, pp 477-493.

27. Kuklin A.I, Islamov A.Kh., Kovalev Yu.S., Utrobin P.K., Goredeliy V.I. Optimization of two- detector system of small-angle neutron spectrometer for study of nanoobjects. Poverhnost’. 2006, №6, p.74-83 (in Russian).

28. Molchanov V.S., Philippova O.E., Khokhlov A.R., Kovalev Y.A. and Kuklin A.I. Self-Assembled Networks Highly Responsive to Hydrocarbons, Langmuir G, (in press).

29. Moukhametzianov R.E., Klare J.P., Efremov R.G., Baeken C., Göppner A., Labahn J., Engelhard M., Büldt G. and Gordeliy V.I. (2006) Development of the signal in sensory rhodopsin and its transfer to the related transducer**.** *Nature* 440, 115-119.

30. Murugova T.N., Gordeliy V.I., Islamov A.Kh., Kovalev Yu.S., Kuklin A.I., Vinogradov A.D., Yaguzhinsky L.S. Structure of membrane of submitochondrial particles studied by small angle neutron scattering, Materials structure in Chemistry, Biology, Physics and Technology, Czech and Slovak Crystallographic Association. Materials Structure, vol.13, no 2 (2006).

31. Murugova T.N., Gordeliy V.I., Islamov A.Kh., Kuklin A.I., Solodovnikova I.M., Yaguzhinsky L.S. Detection of new type of membrane structure in mitochondria under low-amplitude swelling by small angle neutron scattering, Biochim. Biophys. Acta, 2006. V.14. P. 524-525.

32. Murugova T.N., Gordeliy V.I., Kuklin A.I., Kovalev Yu.S., Yurkov V.I., Nuernberg A., Islamov A.Kh., Yaguzhinsky L.S. "Detection of new double-membrane structures in native mitochondria by small angle neutron scattering", Biofizika, 2006 (in press) (in Russian).

33. Ozerin A.N., Svergun D.I., Volkov V.V., Kuklin A.I., Gordeliy V.I., Islamov A.Kh., Ozerina L.A. and Zavorotnyuk D.S. The spatial structure of dendritic macromolecules, J. Appl. Cryst. (2005). 38, 996–1003.

34. Petukhov M., Lebedev D., Shalguev V., Islamov A., Kuklin A., Lanzov V., and Isaev-Ivanov V.. Conformational Flexibility of RecA Protein Filament: Transitions between Compressed and Stretched States. PROTEINS: Structure, Function, and Bioinformatics 65:296–304 (2006).

35. Serdyuk I.N. Structured proteins and proteins with internal disorder, Molecular Biology (2006), accepted.

36. Serdyuk I.N., Evseeva O.N. New possibilities of analytical ultracentrifugation to analyze hydrodynamic properties of proteins, Uspekhi biologicheskoi khimii (2006), accepted (in Russian).

37. Török Gy., Lebedev V.T., Bica D., Vékás L., Avdeev M.V., Concentration and temperature effect in microstructure of ferrofluids, *J. Mag. Mag. Mater.* 300 (2006) e221-e224.

38. Török Gy., Len A., Rosta L., Balasoiu M., Avdeev M.V., Aksenov V.L., Ghenescu I., Hasegan D., Bica D., Vékás L. Interaction effects in non-polar and polar ferrofluids by small-angle neutron scattering. Romanian Reports in Physics 58 (2006) 293–298.

39. Tropin T.V., Avdeev M.V., Aksenov V.L. Fullerene clusters in non-polar solutions by small-angle neutron scattering data. “Crystallography Reports”, accepted (2006).

40. Tropin T.V., Avdeev M.V., Priezzhev V.B., Aksenov V.L. Nonmonotonic behaviour of concentration in the kinetics of dissolution of fullerenes, JETP Letters 83 (2006) 467-472.

41. Zemlyanaya E.V., Kiselev M.A., Zbytovska J., Almasy L., Gutberlet T., Strunz P., Wartewig S., Neubert R.H.H. Numerical analyses of structure of unilamellar vesicles from the small angle neutron experiments. Crystallography reports, 2006, v51 suppl. 1, pp. s22-s26.

Conferenses

1. Kuklin A.I. , Islamov A.Kh., Gordeliy V.I. YuMO –spectrometer for small-angle neutron scattering with wild range of transmitted pulses. Book of Abstracts. XIX Workshop on Neutron Scattering Application in Condensed Matter Investigations (RNIKS-2006), Obninsk, Russia, September 12-15, 2006, p. 101.

2. Aksenov V.L., Tropin T.V., Avdeev M.V., Priezzhev V.B., Schmelzer J.W.P. “Kinetics of fullerene dissolution in non-polar solvent”, XX IWEPNM: Molecular Nanostructures, March 12-20, 2006, Kirchberg Tirol, Austria.

3. Avdeev M.V. “Contrast Variation in Small-Angle Scattering Experiments on Polydisperse and Superparamagnetic Systems: Basic Functions Approach”, International Small-Angle Scattering Workshop, October 5 – 7, 2006, Dubna, Russia.
4. Avdeev M.V. “What we can learn about structure of ferrofluids from small-angle neutron scattering”, COST Action P17 Meeting, July 22-25, 2006, Timisoara, Romania.
5. Avdeev M.V. Diagnostics of nanomagnetic fluids using small-angle neutron scattering, X Scientific Conference of JINR young scientists and specialists, February 6 – 11, 2006, Dubna, Russia.
6. Avdeev M.V. Introduction to the small-angle neutron scattering, Summer School-Seminar «Studies of nanosystems and materials using nuclear physical methods», SINP MSU, July 2-9, 2006, Dubna, Russia. (in Russian).
7. Avdeev M.V. Neutron investigations of nanosystems in FLNP, PAC Meeting on Condensed Matter Research in JINR, April 2006, Dubna, Russia.
8. Avdeev M.V., Aksenov V.L. «Use of small-angle neutron scattering in study of nanocarbon and its liquid dispersions», Combined International Symposium on Nanodiamond-Nanocarbon-2006, September 11-15, 2006, St-Petersburg, Russia.
9. Avdeev M.V., Aksenov V.L., Bulavin L.A., Kizima O.A., Korobov M.V., Tropin T.V. Formation of fullerene clusters in the system C_{60}-NMP-H_2O, XIX Workshop on Neutron Scattering Application in Condensed Matter Investigations (RNIKS-2006), September 11-15, 2006, Obninsk. (in Russian).
10. Avdeev M.V., Balasoiu M., Aksenov V.L., Török Gy., Rosta L., Garamus V.M., Schreyer A., Bica D., Vékás L. “Interaction effect in ferrofluids by small-angle neutron scattering”, Euromech Colloquium 470 «Physical Research of Magnetic Fluids”, February 27 – March 1, 2006, Dresden, Germany.
11. Avdeev M.V., Bica D., Vékás L., Marinica O., Balasoiu M., Aksenov V.L., Rosta L.,.Garamus V.M, Schreyer A. “On the possibility to use short chain length mono-carboxylic acids for stabilization of magnetic fluids”, 6th International Conference on the Scientific and Clinical Applications of Magnetic Carriers, May 17 – 20, 2006, Krems, Austria.
12. Avdeev M.V., Tropin T.V., Priezzhev V.B., Aksenov V.L. “Nonmonotonic Behaviour of Concentration in the Kinetics of Dissolution of Fullerenes”, 2nd International Workshop MSSMBS'06 "Molecular Simulation Studies in Material and Biological Sciences", September 18-21, 2006, JINR, Dubna, Russia.
13. Baeva M., Beskrovny A.I., Boianova A. and Shelkova I. Investigation of renal stones by X-ray and neutron diffraction, Proc. of 6-th International Conference of Balcan Physical Union, 22-26 August 2006, Istambul, Turkey.
14. Baeva M., Beskrovnyi A.I., Yadrowskii E.L., “Phase Composition of the Four-Component Nitrified Steels at Increasing Manganese Concentration”, Six International Conference of Balkan Physical Union, 22-26 August 2006, Istanbul, Turkey.
15. Balagurov A.M. “A programme of spectrometer development at the IBR-2 reactor in 2007 - 2010”. XIX Workshop on Neutron Scattering Application in Condensed Matter Studies (RNIKS-2006), Obninsk, Russia, September 12-15, 2006.
16. Balagurov A.M. “Equilibrated magneto-structural inhomogeneous states in mixed oxides”. IV Russian Crystal-Chemistry Conference, Chernogolovka, 26-30 June 2006.
17. Balagurov A.M., Papushkin I.V., Popa N.C., Sumin V.V., Nikitin A.N. Study of the residual strain-stress in anisotropic cold-rolled Zr-alloy by neutron diffraction. Proc. of the Workshop on Investigations at the IBR-2 Pulsed Reactor. June 14-17, 2006, Dubna, Russia, p.71.
18. Balagurov A.M., Papushkin I.V., Sumin V.V., Tamonov A.V. “Residual stress studies in reactor materials by neutron diffraction”. XIX Workshop on Neutron Scattering Application in Condensed Matter Studies (RNIKS-2006), Obninsk, Russia, September 12-15, 2006.
19. Balagurov A.M. “High-resolution Fourier-diffractometry”. Workshop on Investigations at the IBR-2 Pulsed Reactor. June 14-17, 2006, Dubna, Russia.
20. Beskrovnyy A.I., Guskos N., Typek J., Ryabova N., Blonka-Tabero A., Zolnierkiewicz G. Crystal structure nonstechiometric of $Co_{2.616}Fe_{4.256}V_6O_{24}$ compound studied by neutron diffraction, Workshop on Functional Materials FMA’2006 Athens, Greece, 17-23 September, 2006, p.52.
21. Beskrovnyy A.I., N. Guskos, J. Typek, N. Ryabova, M. Bosacka, G. Zolnierkiewicz, A. Worsztynowicz, Crystal structure of $M_2CrV_3O_{11-\delta}$ (M=Mg, Zn) studied by neutron diffraction, Workshop on Functional Materials FMA’2006 Athens, Greece, 17-23 September, 2006, p.29.
22. Bikkulova N.N., Skomorokhov A.N., Beskrovny A.I., Yadrovsky E.L., Stepanov Yu.M., Mikolaichuk A.N., Sagdatkireeva M.B., Ishmuratov T. “Lattice dynamics and ion transfer in structural-disordered copper and silver

chalcogenides". Proc. of the Workshop on Investigations at the IBR-2 Pulsed Reactor, Dubna, June 14-17, 2006, p.18.

23. Blagoveshchenskii N.M., Loginov N.I., Morozov V.A., Novikov A.G., Puchkov A.V., Savostin V.V., Shimkevich A.L., Shimkevich I.Yu. Study of structural-dynamic properties of liquid-metal systems by neutron scattering, Book of Abstracts of the XIX Workshop on Neutron Scattering Application in Condensed Matter Investigations (RNIKS-2006), Obninsk, Russia, September 12-15, 2006, p.86.
24. Blagoveshchenskii N.M., Morozov V.A., Novikov A.G., Pashnev M.A., Savostin V.V. Study of microdynamics of liquid lithium and Li-H melt by inelastic neutron scattering, Book of Abstracts of the XIX Workshop on Neutron Scattering Application in Condensed Matter Investigations (RNIKS-2006), Obninsk, Russia, September 12-15, 2006, p.86.
25. Blagoveshchenskii N.M., Morozov V.A., Novikov A.G., Pashnev M.A., Savostin V.V., Shimkevich A.L. Study of microdynamics of liquid lithium by neutron scattering. V Workshop on Investigations at the IBR-2 Pulsed Reactor, Book of Abstracts, p. 59.
26. Blagoveshchenskii N.M., Morozov V.A., Novikov A.G., Savostin V.V., Savostin D.D., Shimkevich A.L. Study of the microstructure melt "lithium-nitrogen" by neutron diffraction. V Workshop on Investigations at the IBR-2 Pulsed Reactor, Book of Abstracts, p. 66.
27. Blagoveshchenskii N.M., Morozov V.A., Novikov A.G., Savostin V.V., Savostin D.D., Shimkevich A.L. Studies of metal melts on the basis of lead by neutron scattering. Book of Abstracts. XIX Workshop on Neutron Scattering Application in Condensed Matter Investigations (RNIKS-2006), Obninsk, Russia, September 12-15, 2006, p.88.
28. Blagoveshchenskii N.M., Novikov A.G., Pashnev M.A., Savostin V.V. Interatomic power characterisics of liquid lithium. V Workshop on the investigations at the IBR-2 pulsed reactor, Book of Abstracts, p.20.
29. Blagoveshchenskii N.M., Novikov A.G., Pashnev M.A., Savostin V.V. Interatomic power characterisics of liquid lithium. Book of Abstracts. XIX Workshop on Neutron Scattering Application in Condensed Matter Investigations (RNIKS-2006), Obninsk, Russia, September 12-15, 2006, p.89.
30. Clementyev E.C., Sashin I.L., Boni P. and Shirane G. "Mapping of magnetic excitations in single-domain and multi-domain chromium", V workshop on investigation at the IBR-2 pulsed reactor, Book of Abstracts, p.69.
31. Dubovsky O.A., Orlov A.V. Amplitude-spectral characteristics of high-amplitude supersonic soliton compression waves in crystalline materials. Book of Abstracts. XIX Workshop on Neutron Scattering Application in Condensed Matter Investigations (RNIKS-2006), Obninsk, Russia, September 12-15, 2006, p.40.
32. Efimchenko V.S., Antonov V.E., Barkalov O.I., Beskrovnyi A.I., Fedotov V.K. and Klyamkin S.N. TRANSFORMATIONS OF THE HIGH-PRESSURE HYDROGEN CLATHRATE HYDRATE, International Workshop on Crystallography at High Pressure, 28 September – 1 October 2006, Dubna, Russia, Book of Abstracts, p. 52. Erhan R.V., Balasoiu M., Barna E., Kuklin A. Investigation of polymeric rubber by SANS. V Workshop on investigations at the IBR-2 pulsed reactor, 14-17 June 2006. Book of Abstracts. Dubna: JINR, 2006. p.27.
34. Gulevich T.A., Avdeev M.V. Evaluation of experimental accuracy on small-angle neutron scattering on magnetic fluids with organic non-polar bases. XIX Workshop on Neutron Scattering Application in Condensed Matter Investigations (RNIKS-2006), Obninsk, Russia, September 12-15, 2006 (in Russian).
35. Holderna-Natkaniec K., Natkaniec I., Jakubas R., Grech E., „ IINS/QC studies of aminopyridine cation with different acid radicals", 3rd American Conference on Neutron Scattering, ACNS2006, June 18-22, 2006, St. Charles, Illinois, Book of Abstracts, WP12, p.126.
36. Holderna-Natkaniec K., Natkaniec I., Swiergiel J., Jakubas R., Nowak D., „IINS/QC studies of $(C_3N_2H_5)_5Bi_2Cl_{11}$", 3rd American Conference on Neutron Scattering, ACNS2006, June 18-22, 2006, St. Charles, Illinois, Book of Abstracts, MP54, p.71.
37. Ion I., Kovalev Y., Bara A., Kuklin A. Study of the structural modification induced on the coal tar pitch by addition of single, multiwalled carbon nanotubes and nanocarbon fibers. V Workshop on investigations at the IBR-2 pulsed reactor, 14-17 June 2006. Book of Abstracts. Dubna: JINR, 2006. – 29 p (in Russian).
38. Ion I., Kovalev Y.S., Kuklin A.I. Study of the structural modification induced on the coal tar pitch by addition of single, multiwalled carbon nanotubes and nanocarbon fibers. Book of Abstracts. XIX Workshop on Neutron Scattering Application in Condensed Matter Investigations (RNIKS-2006), Obninsk, Russia, September 12-15, 2006, p. 85.
39. Ivankina T.I., Kern H.M., Klima K., Locajicek T., Nikitin A.N. and Pros Z. Application of neutron diffraction and ultrasonic methods at high pressures to study geological samples. Proc. of International Workshop "Crystallography at high pressure – 2006". Dubna, Russia, September 28 - October 1, 2006, p. 28.

40. Ivankina T.I., Kern H.M., Nikitin A.N. Correlation of elastic properties of rocks from the Outokumpu hole (Finland) with their texture-microstructure characteristics. Proc. of the Workshop on Investigations at the IBR- 2 Pulsed Reactor. June 14-17, 2006. Dubna. Russia, p.28. (in Russian).

41. Ivankina T.I., Kern H.M., Klima K.,.Locajicek T, Nikitin A.N. and Pros Z. Study of geological samples of deep crustal levels and upper mantle by neutron diffraction and ultrasonic methods at high pressures. Proceedings of the VII Conference "Physical-chemical and petrophysical researches in Earth's sciences". September, 2006, Borok, Russia, p.92.

42. Juszynska E., Natkaniec I., Sciesinski J., Sciesinska E., Holderna-Natkaniec K., Nowak D., Massalska-Arodz M., "Vibrational dynamics in methyl butanol glass formers studied by IINS and IR", XVIIIth International School on Physics and Chemistry of Condensed Matter, Spectroscopy of Modern Materials, Białowieża, 1-8 July, 2006, P3.

43. Kalinin I.V., Lauter H., Koza M., Lauter-Pasyuk V.V., Puchkov A.V. Search for superfluid transition in ^{4}He films of atomic thickness, report on 34 Workshop on the low temperature physics, Sochi, 2006. (in Russian).

44. Kalinin I.V., Lauter H., Puchkov A.V. Dynamic structural factor of liquid helium and model of damping harmonic oscillator. Book of Abstracts. XIX Workshop on Neutron Scattering Application in Condensed Matter Investigations (RNIKS-2006), Obninsk, Russia, September 12-15, 2006, p.87.

45. Kalinin I.V., Lauter H., Puchkov A.V. Investigation of peculiarities of the excitation spectrum of superfluid helium by inelastic neutron scattering. Report at the 34th Workshop on Low Temperature Physics, Sochi, 2006.

46. Kalinin I.V., Lauter H., Puchkov A.V. Surface excitations in nanofilms of liquid helium, Book of Abstracts. XIX Workshop on Neutron Scattering Application in Condensed Matter Investigations (RNIKS-2006), Obninsk, Russia, September 12-15, 2006, p.89.

47. Kalinin I.V., Lauter H., Puchkov A.V. Temperature dependence of the scattering law of liquid helium in phonon-maxon region. Book of Abstracts. Workshop on Investigations at the IBR-2 Pulsed Reactor, Dubna, p.31, 2006.

48. Karelov D.V. , Lebedev D.V., Suslov A.V., Shalguev V.I., Islamov A.Kh., Lanzov V.A., Isaev-Ivanov V.V. SANS investigation of the structure of REcA protein from Deinococcus radiodurance on YuMO spectrometer. V Workshop on investigations at the IBR-2 pulsed reactor, 14-17 June 2006 г. Book of Abstracts. Dubna: JINR, 2006, p.41.

49. Kazarnikov V.V., Kalinin I.V., Morozov S.I., Primakov N.G., Rudenko V.A., Sashin I.L., Shovkun D.V. Temperature dependence of hydrogen localization in interstitial phases of $Nb_2(N,C)H_xV$, V Workshop on investigations at the IBR-2 pulsed reactor, 14-17 June 2006. Book of Abstracts. Dubna, JINR, 2006, p.48.

50. Kazarnikov V.V., Morozov S.I., Primakov N.G., Rudenko V.A., Shovkun D.V. The nature of low-energy excitations of light admixtures in lattices of metals, Book of Abstracts. XIX Workshop on Neutron Scattering Application in Condensed Matter Investigations (RNIKS-2006), Obninsk, Russia, September 12-15, 2006, p.23.

51. Kazarnikov V.V., Morozov S.I., Shovkun D.V., Sashin I.L., Primakov N.G., Rudenko V.A. Local structure and dynamics of hydrogen in interstitial phases with hexagonal lattice of metal matrix. Book of Abstracts. XIX Workshop on Neutron Scattering Application in Condensed Matter Investigations (RNIKS-2006), Obninsk, Russia, September 12-15, 2006, p.31.

52. Khaidukov Yu.N. Neutronography of magnetic lamellar systems. X Symposium "Nanophysics and nanoelectronics ", March 13-17, 2006, Nizni Novgorod. (in Russian).

53. Khaidukov Yu.N. Study of influence of superconductivity on ferromagnetism in lamellar structure V(39nm)/20[V(3nm)/Fe(3nm)]. V Workshop on Investigations at the IBR-2 Pulsed Reactor, June 14-17, 2006, Dubna, Russia.

54. Khaidukov Yu.N. Study of influence of superconductivity on ferromagnetism in lamellar structure V(39nm)/20[V(3nm)/Fe(3nm)]. XIX Workshop on Neutron Scattering Application in Condensed Matter Investigations (RNIKS-2006), Obninsk, Russia, September 12-15, 2006.

55. Khokhryakov A.A. , Avdeev M.V., Kyzyma O.A., Len A., Bulavin L.A., Aksenov V.L. "Structure and stabilization mechanism of non-modified fullerene water solutions", V Workshop on Investigations at the IBR-2 Pulsed Reactor, June 14-17, 2006, Dubna, Russia.

56. Kichanov S.E. "The phase diagram of pyridinium perrhenate study by neutron diffraction", V Workshop on Investigations at the IBR-2 Pulsed Reactor, June 14-17, 2006, Dubna, Russia.

57. Kichanov S.E. , Kozlenko D.P., Savenko B.N., Voronin V.I., Proskurina N.V., Kiseleva E.A. "The pressure induced changes in magnetic structure of the $La_{0.75}Ca_{0.25}MnO$ manganite", International Workshop on Crystallography at High Pressure, 28 September – 1 October 2006, Dubna, Russia.

58. Kichanov S.E., Kozlenko D.P., Wasicki J., Nawrocik W., Czarnecki P., Savenko B.N., Glazkov V.P. and Lathe C. "The structure and dynamic study of the pyridinium salts $PyHNO_3$ и $PyReO_4$" XIX Workshop on Neutron Scattering Application in Condensed Matter Investigations (RNIKS-2006), Obninsk, Russia, September 12-15, 2006.

59. Kichanov S.E., Kozlenko D.P., Wasicki J., Nawrocik W., Czarnecki P., Savenko B.N., Glazkov V.P. and Lathe C. "Investigation of structural phase transition in the pyridinium perrhenate at low temperatures and high pressure" International Workshop on Crystallography at High Pressure, 28 September – 1 October 2006, Dubna, Russia.

60. Knotko A.V., Garshev A.V., Putlyaev V.I., Kuklin A.I. Small angle neutron scattering study of the oxidation process in the ceramic oxide solid solutions. Book of Abstracts. XIX Workshop on Neutron Scattering Application in Condensed Matter Investigations (RNIKS-2006), Obninsk, Russia, September 12-15, 2006, p. 33.

61. Knotko A.V., Garshev A.V., Putlyaev V.I., Morozov S.I. Inelastic neutron scattering by cation- substituted solid solutions based on $Bi_2Sr_2CaCu_2O_8$", Book of Abstracts. XIX Workshop on Neutron Scattering Application in Condensed Matter Investigations (RNIKS-2006), Obninsk, Russia, September 12-15, 2006, p.34.

62. Knotko A.V., Garshev A.V., Putlyaev V.I.and Kuklin A.I. Small angle neutron scattering study of the oxidation process in the Pb – substituted $SrFe_{12}O_{19}$. V Workshop on investigations at the IBR-2 pulsed reactor, 14-17 June 2006. Book of Abstracts. Dubna: JINR, 2006, p.35.

63. Kovalev Yu.S., Apel P.Yu., Levkovich N.V., Islamov A.Kh., Kuklin A.I. Investigation of solutions of nonionic surfactants by small angle neutron scattering. Book of Abstracts. XIX Workshop on Neutron Scattering Application in Condensed Matter Investigations (RNIKS-2006), Obninsk, Russia, September 12-15, 2006, p. 89.

64. Kovalev Yu.S., Apel P.Yu., Levkovich N.V., Islamov A.Kh., Kuklin A.I. Investigation of solutions of nonionic surfactants by small angle neutron scattering. V Workshop on investigations at the IBR-2 pulsed reactor, 14-17 June 2006. Book of Abstracts. Dubna: JINR, 2006. p.36.

65. Kozhevnikov S.V. Enhanced Off-Specular Scattering in Magnetic Neutron Wave-Guides. PNCMI 2006. Berlin, 25-28 September.

66. Kozhevnikov S.V. Workshop under FP6 contract of Polarized Neutron Technology collaboration, 18-19 May 2006, Vienna, Austria.

67. Kozlenko D.P., Golosova N.O., Jirak Z., Dubrovinski L., Savenko B.N., Voronin V.I., Taker M.G., Le Godec Y. "High Pressure Effects on the Spin State, Crystal and Magnetic Structure of Cobaltites $La_{1-x}Sr_xCoO_3$ (x=0, 0.3)", 44th EHPRG International Conference, September 4-8 2006, Prague, Czech Republic.

68. Kozlenko D.P., Golosova N.O., Jirak Z., L.Dubrovinski, B.N.Savenko, V.I.Voronin, M.G.Taker, Y. Le Godec. "The spin phase transition in $LaCoO_3$" XIX Workshop on Neutron Scattering Application in Condensed Matter Investigations (RNIKS-2006), Obninsk, Russia, September 12-15, 2006.

69. Kozlenko D.P., Golosova N.O., Jirak Z., Dubrovinski L., Savenko B.N., Voronin V.I., Taker M.G., Le Godec Y. "Temperature and pressure driven spin state transition in $LaCoO_3$" International Workshop on Crystallography at High Pressure, 28 September – 1 October 2006, Dubna, Russia.

70. Kozlenko D.P., Jirak Z., Kichanov S.E., Glazkov V.P.and Savenko B.N. "Pressure induced magnetic phase transition in $Pr_{1-x}Sr_xMnO_3$(x=0.3-0.9), International Workshop on Crystallography at High Pressure, 28 September – 1 October 2006, Dubna, Russia.

71. Kozlenko D.P., Kichanov S.E., Savenko B.N., Glazkov V.P. and Somenkov V.A. "DN-6 diffractometer for investigation of microsamples at IBR-2M", V Workshop on Investigations at the IBR-2 Pulsed Reactor, June 14-17, 2006, Dubna, Russia.

72. Kozlenko D.P., Kichanov S.E., Savenko B.N., Glazkov V.P., Lee S., Park J.-G. "Hexagonal manganites under high pressure: suppression of antiferromagnetism and generalized magnetic phase diagram", V Workshop on Investigations at the IBR-2 Pulsed Reactor, June 14-17, 2006, Dubna, Russia.

73. Kozlenko D.P., Kichanov S.E., Savenko B.N., Glazkov V.P., Lee S., Park J.-G. "Hexagonal manganites under high pressure: suppression of antiferromagnetism and generalized magnetic phase diagram" XIX Workshop on Neutron Scattering Application in Condensed Matter Investigations (RNIKS-2006), Obninsk, Russia, September 12-15, 2006.

74. Kuklin A.I., Cherniy A.Yu., Ozerin A.N., Rogatchev A.V., Islamov A.Kh. The spherical cone model for small angle neutron scattering dendrimers curves data treatment. V Workshop on investigations at the IBR-2 pulsed reactor, 14-17 June 2006 г. Book of Abstracts. Dubna: JINR, 2006, p. 63.

75. Kuklin A.I., Cherniy A.Yu., Ozerin A.N., Rogatchev A.V., Islamov A.Kh. The spherical cone model for small angle neutron scattering dendrimers curves data treatment. Book of Abstracts. XIX Workshop on Neutron

Scattering Application in Condensed Matter Investigations (RNIKS-2006), Obninsk, Russia, September 12-15, 2006, p. 75.

76. Kuklin A.I., Islamov A.Kh. and Gordeliy V.I. Small-angle neutron spectrometer MURN-C. V Workshop on investigations at the IBR-2 pulsed reactor, 14-17 June 2006 г. Book of Abstracts. Dubna: JINR, 2006, p. 38.
77. Kuklin A.I., Islamov A.Kh. and Gordeliy V.I. YuMO – spectrometer for small-angle neutron scattering with wild range of transmitted pulses. V Workshop on investigations at the IBR-2 pulsed reactor, 14-17 June 2006 г. Book of Abstracts. Dubna: JINR, 2006. p.39.
78. Kuklin A.I., Kutuzov S.A., Gabriel A., Utrobin P.K., Bogdzel A.A., Islamov A.Kh., Koskas G., Eckold G., Gordeliy V.I. New type of position sensitive detector for two-detector system of small-angle YuMO spectrometer. Book of Abstracts. XIX Workshop on Neutron Scattering Application in Condensed Matter Investigations (RNIKS-2006), Obninsk, Russia, September 12-15, 2006, p. 108.
79. Kuklin A.I., Kutuzov S.A., Gabriel A., Utrobin P.K., Smirnov A.A., Bogdzel A.A., Islamov A.Kh., Kompara V., Koskas G., Eckold G., Gordeliy V.I. Position-sensitive detector with central hole for small angle scattering and diffraction back geometry. V Workshop on investigations at the IBR-2 pulsed reactor, 14-17 June 2006 г. Book of Abstracts. Dubna: JINR, 2006. p. 40.
80. Lebedev D.V., Filatov M.V., Kuklin A.I., Islamov A.Kh., Kentzinger E., Lauter H., Pantina R.A.,.Topoverg B.P, Isaev-Ivanov V.V. Organization of chromatin in interphase cell nuclei of eurokaryotes by SANS. V Workshop on investigations at the IBR-2 pulsed reactor, 14-17 June 2006. Book of Abstracts. Dubna: JINR, 2006. – 30 p (in Russian).
81. Lisichkin Yu.V., Sakharova L.A., Tumanov A.A. Molecular-dynamic characteristics of netlike polymeric ionites by inelastic neutron scattering. Book of Abstracts. XIX Workshop on Neutron Scattering Application in Condensed Matter Investigations (RNIKS-2006), Obninsk, Russia, September 12-15, 2006, p.74.
82. Lisichkin Yu.V., Situkha N.V., Novikov A.G., Savostin V.V. Computer simulation of experiments on inelastic neutron scattering by liquid lithium, V workshop on investigation at the IBR-2 pulsed reactor, Book of Abstracts, p. 68.
83. Lokajíček T., Rudajev V., Vilhelm J., Vasin R., Ivankina T.I., Nikitin A.N., Acoustic emission induced by thermal heating of rocks, XXXI General Assembly of European Geophysical Union. Austria. Vienna. 2-7 April 2006. Geophysical Research Abstracts, 2006, Vol. 8.
84. Lukin E.V., Kozlenko D.P., Kichanov S.E., Savenko B.N., Truhanov S.V., Troyanchuk I.O. "High pressure and oxygen deficiency effects on the crystal and magnetic structure of $La_{0.7}Sr_{0.3}MnO_{3-d}$ manganites", International Workshop on Crystallography at High Pressure, 28 September – 1 October 2006, Dubna, Russia.
85. M.V.Avdeev, Neutron investigations of nanosystems in FLNP, HAS-JINR introductory course and training, FLNP JINR, October 1-8, 2006, Dubna, Russia.
86. Morozov S.I., Kazarnikov V.V., Ivanov A.S., Shovkun D.V. Dynamics of interstitial impurities in lattice of Ta and V, ISCMP Scientific conference "Investigations in the field of condensed matter physics, nanosystems and superconductivity. Book of Abstracts. Moscow, April 11-13, 2006, p. 72.
87. Morozov S.I., Kazarnikov V.V., Ivanov A.S., Shovkun D.V. Structure of spectra of localized states of atoms of oxygen and hydrogen in tantalum lattice. V Workshop on Investigations at the IBR-2 Pulsed Reactor. June 14-17, 2006. JINR, Dubna. Russia, Book of Abstracts. p.49.
88. Morozov V. Neutron scattering technique in investigations of structural and dynamic characteristics of impurity atoms in metals. Book of Abstracts. XIX Workshop on Neutron Scattering Application in Condensed Matter Investigations (RNIKS-2006), Obninsk, Russia, September 12-15, 2006, p. 22.
89. Murugova T.N., Gordeliy V.I., Islamov A.Kh., Kuklin A.I., Solodovnikova I.M., Yaguzhinsky L.S. Study of structure of rat heart mitochondria by small-angle neutron scattering. Book of Abstracts. XIX Workshop on Neutron Scattering Application in Condensed Matter Investigations (RNIKS-2006), Obninsk, Russia, September 12-15, 2006. P. 75.
90. Natkaniec I., Holderna-Natkaniec K., Nowak D. Neutron investigations and quantum-chemical modelling of structure and dynamics of dimethylbutane isomers. Book of Abstracts. XIX Workshop on Neutron Scattering Application in Condensed Matter Investigations (RNIKS-2006), Obninsk, Russia, September 12-15, 2006, p.78.
91. Natkaniec I., Holderna-Natkaniec K., Nowak D., „Neutron scattering studies of molecular dynamics in solid phases of neohexane and diisopropyl", 8th International Conference on Quasi-Elastic Neutron Scattering, QENS2006, 14-17 June, 2006, Bloomington, Book of Abstracts, p.15.

92. Natkaniec I., Holderna-Natkaniec K., Nowak D., „Neutron scattering investigations and DFT modeling of molecular structure and dynamics of neohexane and diisopropyl", 3rd American Conference on Neutron Scattering, ACNS2006, June 18-22, 2006, St. Charles, Illinois, Book of Abstracts, TP51, p.95.

93. Natkaniec I., Holderna-Natkaniec K., Nowak D., Majerz I., Prager M., „Molecular dynamics in crystalline and glassy state of 2,4,6-trimethyl-pyridine. 8th International Conference on Quasi-Elastic Neutron Scattering, QENS2006, 14-17 June, 2006, Bloomington, Book of Abstracts, p.25.

94. Natkaniec I., Holderna-Natkaniec K., Nowak D., Majerz I., Prager M., Molecular dynamics of crystalline and glassy collidine. Book of Abstracts. XIX Workshop on Neutron Scattering Application in Condensed Matter Investigations (RNIKS-2006), Obninsk, Russia, September 12-15, 2006, p.78.

95. Natkaniec I., Prager M., Grimm H., Holderna-Natkaniec K., „Rotational tunneling and librations of methyl groups in solid phases of 1,3,5-trimethyl-benzene. JCNS Symposium and EU User Meeting, 16-17 February 2006, Jülich.

96. Nikitenko Yu.V. Neutron polarization reflectometry at the IBR-2 Reactor. Plenary report at the XIX Workshop on Neutron Scattering Application in Condensed Matter Investigations (RNIKS-2006), Obninsk, Russia, September 12-15, 2006.

97. Nikitenko Yu.V. Neutron reflectometry with atomic resolution and at supersmall momentum transfers. Plenary report at V Workshop on Investigations at the IBR-2 Pulsed Reactor, June 14-17, 2006, Dubna, Russia.

98. Nikitin A.N., Markova G.V., Balagurov A.M., Vasin R.N., Alekseeva O.V. Investigation of structure and properties of quartz in the region of phase transition by neutron diffraction and mechanical spectroscopy. 7 International conference "Physicochemical and petrophysical investigations in Earth sciences". September, 2006, Borok, Russia. p. 52.

99. Nikitin A.N., Rodkin M.V., Jurchenko O.A., Ivankina T.I., Vasin R.N. The problem of burial of high-level radioactive wastes –new approaches and restrictions. Proc. of the Workshop on Investigations at the IBR- 2 Pulsed Reactor. June 14-17, 2006. Dubna. Russia, p.52.

100. Nikitin A.N., Rodkin M.V., Jurchenko O.A., Ivankina T.I., Vasin R.N. On ecological safety of deposits of high-level radioactive wastes. Proceedings of the VII Conference "Physical-chemical and petrophysical researches in Earth's sciences". September, 2006, Borok, Russia, p.53-55.

101. Nowak D., Holderna-Natkaniec K., Natkaniec I., Jurga K., "Internal dynamics of 17-α-methylotestosterone studied by NMR and IINS", XVIIIth International School on Physics and Chemistry of Condensed Matter, Spectroscopy of Modern Materials, Białowieża, 1-8 July, 2006, P4.

102. Nowak D., Holderna-Natkaniec K., Natkaniec I., Jurga K., Szyczewski A., "Internal dynamics study of testosterone and norethisterone by IINS, QC and ^{1}H NMR methods", V workshop on investigation at the IBR-2 pulsed reactor, Book of Abstracts, p.54.

103. Orlova V.A., Bortsova E.V., Koryttseva A.K., Beskrovnyi A.I., Orlova A.I., Nagornova S.V. New phosphates of lanthanides with structure of langbeinite mineral. Synthesis, crystal chemistry, properties.// Book of Abstracts of 15-th Radiochemical Conference. Marianske Lazne. Czech Republic. 23-28 April, 2006. P. 257.

104. Orlova V.A., Koryttseva A.K., Nagornova S.V., Bortsova E.V., Beskrovnyi A.I., Orlova M.P., Orlova A.I. Waterless lanthanide phosphates with the structure of langbeinite mineral. Crystal chemical modeling, synthesis and investigation of new compounds. Book of Abstracts of the 5 Russian Conference on Radio-chemistry. Dubna. 2006. p.60. (in Russian).

105. Osipov A.A. Spin-echo neutron spectrometer at the IBR-2 Reactor. V Workshop on Investigations at the IBR-2 Pulsed Reactor, June 14-17, 2006, Dubna, Russia. (in Russian).

106. Osipov A.A. Spin-echo neutron spectrometer at the IBR-2 Reactor. XIX Workshop on Neutron Scattering Application in Condensed Matter Investigations (RNIKS-2006), Obninsk, Russia, September 12-15, 2006.

107. Ozerin A.N., Kuklin A.I., Islamov A.Kh., Rogatchev A.V. SANS study of the polymer-colloid complexes. V Workshop on investigations at the IBR-2 pulsed reactor, 14-17 June 2006. Book of Abstracts. Dubna: JINR, 2006, p. 55.

108. Pawlukojć A., Starosta W., Leciejewicz J., Natkaniec I., Nowak D., "The molecular structure and dynamics of 2-aminopyridine-3-carboxilic acid by X-ray diffraction, inelastic neutron scattering, infrared, Raman spectroscopy and from *first principles* calculation", V workshop on investigation at the IBR-2 pulsed reactor, Book of Abstracts, p.58.

109. Petrenko V.I, Avdeev M.V., Aksenov V.L., Bulavin L.A. Structure of magnetic fluids in excess of surfactants by small-angle neutron scattering. XIX Workshop on Neutron Scattering Application in Condensed Matter Investigations (RNIKS-2006), Obninsk, Russia, September 12-15, 2006.

110. Popa N.C., Papushkin I.V., Sumin V.V., Nikitin A.N., Balagurov A.M. "A new method for residual stress investigation in strongly textured samples". XIX Workshop on Neutron Scattering Application in Condensed Matter Studies (RNIKS-2006), Obninsk, Russia, September 12-15, 2006.

111. Puchkov A.V. "The project of the modernization and the development for the DIN-2PI spectrometer". Book of Abstracts of IV Workshop on Investigations at the IBR-2 Pulsed Reactor, Dubna, p.61, 2006.

112. Ryabova N.Yu., Beskrovnyi A.I., Kiselev M.A., Balagurov A.M., Aksenov V.L. Influence of cholesterol on the hydration of the membrane of dipalmitoylphosphatidylcholine. Proc. of XIX Workshop on Neutron Scattering Application in Condensed Matter Investigations (RNIKS-2006), Obninsk, Russia, September 12-15, 2006.

113. Ryabova N.Yu., Kiselev M.A., Balagurov A.M., Aksenov V.L., Neubert R.H.H., «Investigation of structure and hydration of Stratum Corneum lipid model membrane by neutron diffraction», Proc. of «New concepts in lipidology: from lipidomics to disease», Noordwijkerhout, The Netherlands, October 21-26, 2006.

114. Ryabova N.Yu., Vassilovsky S.G., Beskrovny A.I., Kiselev M.A., Balagurov A.M., Aksenov V.L. Investigation of structure and hydration of mixed lipid membranes by Fourier-analysis in the real-time mode, Proc. of «V Workshop on the investigations at the IBR-2 pulsed reactor», Dubna, June 14-17, 2006, p. 64.

115. Sawka-Dobrowolska W., Nowicka-Scheibe J., Bator G., Prager M., Pawlukojc A., Grech E., Sobczyk L., „Strukturalne i spektroskopowe badania kompleksów molekularnych tetrametylopirazyny". Materialy XV Ogolnopolskiej Konferencji KRYSZTAŁY MOLEKULARNE 2006, Łódź, 19-23.09.2006, Poland, p 60-61.

116. Sazonov A.P., Golosova N.O., Kozlenko D.P., Sikolenko V.V., Troyanchuk I.O., Savenko B.N. "Suppression of magnetic order in $Nd_{0.22}Ba_{0.78}CoO_3$ by high pressure" 44th EHPRG International Conference, September 4-8 2006, Prague, Czech Republic.

117. Skomorokhov A.N., Titov A.N., Titova S.G., Semenov A.V., "Inelastic Neutron Scattering Study of $Fe_{0.25}TiSe_2$ Intercalate Compound", V workshop on investigation at the IBR-2 pulsed reactor, Book of Abstracts, p.69.

118. Skomorokhov A.N., Titov A.N., Titova S.G., Semenov V.A., Ovchinnikov S.G. A.H., Investigation of intercalated compounds Me_xTiSe_2 (Me = Fe, Ni, Cr, Ag) by inelastic neutron scattering. Book of Abstracts. XIX Workshop on Neutron Scattering Application in Condensed Matter Investigations (RNIKS-2006), Obninsk, Russia, September 12-15, 2006, p. 39.

119. Skomorokhov A.N., Trots D.M., Sashin I.L., Ovchinnikov S.G., Jadrovski E.L., Fuess H., "Inelastic Neutron Scattering Study of AgCuS Superionic Compound", V workshop on investigation at the IBR-2 pulsed reactor, Book of Abstracts, p.70.

120. Skomorokhov A.N., Trots D.M., Sashin I.L., Ovchinnikov S.G., Yadrovskii E.L., Fuess H. Investigation of triple superionic coductor AgCuS by inelastic neutron scattering. Book of Abstracts. XIX Workshop on Neutron Scattering Application in Condensed Matter Investigations (RNIKS-2006), Obninsk, Russia, September 12-15, 2006, p. 39.

121. Smirnov L.S., Natkaniec I., Johnson M., Ivanov A.S., Troyanov S.I., "Neutron scattering study and computer modeling of hydrogen vibrational modes in $NH_4H_5(PO_4)_2$", V Workshop on Investigations at the IBR-2 Pulsed Reactor, June 14 – 17, 2006, Dubna, Russia.

122. Sumin V.V., Papushkin I.V., Bannykh O.A., Blinov V.M., Lukas P. "Investigation of 0X16H4АБ martensitic steel under applied load by neutron diffraction". XIX Workshop on Neutron Scattering Application in Condensed Matter Studies (RNIKS-2006), Obninsk, Russia, September 12-15, 2006.

123. Sumin V.V., Simkin V.G., Sheverev S.G. "Investigation of heat-resistant 12% chromium steel with rapid activity decay using thermal neutron scattering". XIX Workshop on Neutron Scattering Application in Condensed Matter Studies (RNIKS-2006), Obninsk, Russia, September 12-15, 2006.

124. Svanidze A.V., Lushnikov S.G., Sashin I.L. Study of influence of isotopic exchange of hydrogen on deuterium in oscillating spectrum of lysozyme by inelastic neutron scattering. V Workshop on Investigations at the IBR-2 Pulsed Reactor. June 14-17, 2006. JINR, Dubna. Russia, Book of Abstracts. p. 43.

125. Taran Yu.V., Schreiber J., Balagurov A.M., Stuhr U., Kockelmann H., Zlokazov V.B. "Triaxial residual stresses in composite tube from austenitic stainless steel with welded ferritic steel cladding", The 10th European Powder Diffraction Conference, Geneva, Switzerland, 1-4 September 2006.

126. Taran Yu.V., Schreiber J., Daymond M.R., Oliver E.C. "Fatigue degradation and martensitic transformation of austenitic stainless steel AISI 321: new results and prospects", The 7th European Conference on Residual Stresses, Berlin, Germany, 13-15 September 2006.

127. Tropin T.V. «Study of clusters in non-polar solvents by small-angle neutron scattering», V Summer School on Condensed Matter Research, August 20-26, 2006, Zuoz, Switzerland.

128. Tropin T.V., Avdeev M.V., Aksenov V.L. “Cluster formation in non-polar solvents”, V Workshop on Investigations at the IBR-2 Pulsed Reactor, June 14-17, 2006, Dubna, Russia.

129. Tropin T.V., Avdeev M.V., Aksenov V.L. Formation and kinetics of cluster growth in fullerene solutions. XIX Workshop on Neutron Scattering Application in Condensed Matter Investigations (RNIKS-2006), Obninsk, Russia, September 12-15, 2006.

130. Trukhanov S.V., Troyanchuk I.O., Bobrikov I.A., Simkin V.G., Balagurov A.M., Vassilovsky S.G., Beskrovny A.I. Structural investigation of anion-deficit manganites La0.75Sr0.3MnO3-δ, Proc. of «V Workshop on the investigations at the IBR-2 pulsed reactor», Dubna, June 14-17, 2006, p.75.

131. Vasin R.N. Acoustic emission in samples of rocks induced by thermal gradients. X Scientific conference of JINR young scientists and specialists. Book of Abstracts, Dubna, 2006.

132. Vassilovsky S.G., Beskrovny A.I., Balagurov A.M., Flerov I.N., Aleksandrov K.S. Investigation of Rb_2KGaF_6 crystalline structure, Proc. of «V Workshop on the investigations at the IBR-2 pulsed reactor», Dubna, June 14-17, 2006, p. 21.

133. Voronin V.I., Skripov A.V., Buzlukov A.L., Berger I.F., Sashin I.L., “Hydrogen in Ti_3Al: N- and X-ray diffraction and inelastic neutron scattering studies”, V workshop on investigation at the IBR-2 pulsed reactor, Book of Abstracts, p.22.

NEUTRON NUCLEAR PHYSICS

Experimental Investigations

1. Frank A.I., Geltenbort P., Kulin G.V., Kustov D.V., Nosov V.G., Strepetov A.N. Interaction of neutrons with accelerating substance. JINR Communications. P2-2006-113. (in Russian).
2. Frank A.I., Geltenbort P., Kulin G.V., Kustov D.V., Nosov V.G., Strepetov A.N. Effect of accelerating medium in neutron optics. JETP Letters, v. 84 (2006) 485-489. (in Russian).
3. Frank A.I., Geltenbort P., Kulin G.V., Kustov D.V., Nosov V.G., Strepetov A.N. Effect of accelerating medium in neutron optics. JETP Letters, v. 84 (2006) 435-439. (in Russian).
4. Frank A.I., Geltenbort P., Kulin G.V., Strepetov A.N. Experimental verification of the validity of the 1/v law for the UCN absorption cross section in natural gadolinium. JETP Letters, v.84, (2006) p. 131-135.
5. Gericke M.T., Bowman J.D., Carlini R.D., Chupp T.E., Coulter K.P., Dabaghyan M., Dawkins M., Desai D., Freedman S.J., Gentile T.R., Gillis R.C., Greene G.L., Hersman F.W., Ino T., Jones G.L., Kandes M., Lauss B., Leuschner M., Lozowski W.R., Mahurin R., Mason M., Masuda Y., Mitchell G.S., Muto S., Nann H., Page S. A., Penttila S.I., Ramsay W.D., Santra S., Seo P.-N., Sharapov E.I., Smith T.B., Snow W.M., Wilburn W.S., Yuan V., and Zhu H. «Upper bounds on parity violating gamma-ray asymmetries in compound nuclei from polarized cold neutron capture,» Phys. Rev. C. 74, no. 6 (2006).
6. Gould C.R., Sharapov E.I., Lamoreaux S.K., «Time variability of alpha from realistic models of Oklo reactors» Phys. Rev. C. 74, 024607 (2006).
7. Gundorin N.A., Zhdanova K.V., Zhuchko V.E., Pikelner L.B., Rebrova N.V., Salamatin I.M., Smirnov V.I., Furman V.I., “Measurement of delayed neutron yield at thermal neutron fission of ^{237}Np”, Nuclear Physics (2006), accepted.
8. Guohui Zhang, Rongtai Cao, Jinxiang Chen, Guoyou Tang, Gledenov Yu.M., Sedysheva M.V., Khuukhenkhuu G. Differential and Angle–Integrated Cross-Section Measurement for the $^6Li(n,t)^4He$ Reaction at E_n=1.05, 1.54, and 2.25 MeV. Nuclear Science and Engineering. Vol. 153, p. 41-45 (2006).
9. Kartashov D.G., Lychagin Ye.V., Muzychka A.Yu. Nesvizhevsky V.V., Nekhaev G.V., Strelkov A.V., “Study of the nature of changes in UCN energy by $\sim 10^{-7}$ eV at the interaction with surface”, JINR Communications P3-2006-29.
10. Maczka D., Latuszynski A., Kobzev A.P., Yushkevich Yu.V., Vaganov Yu.A., Drozdziel A. “Calculation of work parameters for plasma ion source” JINR Communication, Dubna, 2006, E13-2006-146.
11. Magli R., Mitsyna L.V., Nikolenko V.G., Parzhitski S.S., Popov A.B., Samosvat G.S. Neutron-Electron Scattering Length Deduced from Neutron Diffraction Experiment on Noble Gas ^{36}Ar. ISINN-14 (in press), submitted to Eur. Phys. J. C.
12. Magli R., Mitsyna L.V., Nikolenko V.G., Parzhitski S.S., Popov A.B., Samosvat G.S. Neutron-Electron Scattering Length Extracted from Neutron Diffraction on Liquid Krypton. E3-2006-139 (in press).

13. Masuda Y., Skoy V., Ino T., Jeong S., and Watanabe Y. " Ramsey Resonance for a Pulsed Beam ", Phys. Lett. (accepted).
14. Pokotilovski Yu.N. Phys. Lett., B639 (2006) 214-217.
15. Pokotilovski Yu.N., Novopoltsev M.I., Geltenbort P. „Small energy transfer at the ultracold neutron reflection from solid surfaces“, Phys. Lett., A353 (2006) 236-240.
16. Semenov V.A., Kozlov Zh.A., Krechun L., Matiesku G., Morozov V.M., Oprea I.A., Oprea K., Padureanu I., Puchkov A.V., “Inelastic scattering of slow neutrons by vanadium at temperatures of 293-1773K”, Preprint IPPE-3085. Obninsk, 2006. UDK 539.2, p.17..
17. Sukhovoj A.M., Khitrov V.A. Partial level density of n-quasiparticle excitations, radiative strength functions and new experimental information about nuclear structure changing dynamics in the Bn range. Physics of Paricl. and Nuclei, 2006 37(6) p. 899-922.
18. Sukhovoj A.M., Khitrov V.A., “Partial level density of n-quasiparticle excitations, radiation strength functions and new experimental data on dynamics in changing the nuclear structure in the Bn range”, PEPAN, 2006, 37(6), p. 1705-1743.
19. Ťapajna M., Hušeková K., Machajdik D., Kobzev A.P., Schram T., Lupták R., Harmatha L., Frőhlich K. “Electrical properties and thermal stabilities of MOCVD grown Ru gate electrodes for edvanced CMOS technology”. Microelectronic Engineering 83, 2006, p.2412.
20. Vesna V.A., Gledenov Yu.M., Nesvizhevski V.V., Petukhov A.K., Sedyshev P.V., Soldner T., Zimmer O., Shulgina Ye.V., “Zero experiment in the study of P-odd asymmetry of triton escape in the reaction $^{6}Li(n,\alpha)^{3}H$ ”, PNPI Preprint, №2697, 2006, p. 17. (in Russian).

Theoretical investigations

1. Aksenov V.L., Ignatovich V.K., Nikitenko Yu.V., “Neutron standing waves in layered media”, Crystallography Reports, v.51, № 5, pp. 23-43, 2006..
2. Aksenov V.L., Ignatovich V.K., Nikitenko Yu.V., “Reflection of neutrons from helicoidal systems”, JETP Letters, v.84, N 9, p.563-569, 2006.
3. Aksenov V.L., Ignatovich V.K., Nikitenko Yu.V., “Reflection of neutrons from helicoidal systems”, JINR Communications P4-2008-137, Dubna, 2006.
4. Ignatovich V. K. Comments on: "Uncoupling which-way information from interference: A novel interference experiment using a super-focussed laser beam." Concepts of Physics, V.III p. 243-247, 2006.
5. Ignatovich V.K. "On uncertainty relations and interference in quantum and classical mechanics" -Concepts of Physics, V.III p. 11, 2006.
6. Ignatovich V.K. “Neutron optics”, M. Fizmatlit, 2006.
7. Ignatovich V.K., “Temperature dependence of neutron transmission by ^{4}He gas.”
8. Ignatovich V.K.: “Neutrostriction in neutron stars.” – arXiv: astro-ph/0311471.--- 2006.
9. Petrascu M., Constantinescu A., Lyuboshitz V.L., Lyuboshitz V.V. “Neutron-neutron correlation approach for ^{11}Li halo structure investigation”. NP v. 69 (7), 2006, pp. 1291 – 1296.
10. Petrascu M., Constantinescu A., Lyuboshitz V.L., Lyuboshitz V.V., K. Ieki . “Target screening effect on the pre-emission of neutrons from ^{11}Li halo nuclei”. Phys. Rev. C, v. 73 (5), 2006, 057601 (4 pages).

Applied Research

1. Aničić M., Frontasyeva M.V., Tomašević M., Popović A. Assessment of atmospheric deposition of heavy metals and other elements in Belgrade using the moss biomonitoring technique and neutron activation analysis. JINR Preprint, E18-2006-22, Dubna, 2006 (Accepted By Environment Monitoring And Assessment).
2. Badot P.-M., Bernard N., Crini N., Gilbert D., Frontasyeva M.V., Nguyen-Viet H., Trinh Thu M. Atmospheric heavy metal deposition in Northern Vietnam: Hanoi and Thai Nguyen case study using the moss biomonitoring technique, INAA and AAS. (Submitted to Environmental Ecotoxicology and Safety), 2007.

3. Barandovski L., Cekova M., Frontasyeva M.V., Pavlov S.S., Stafilov T., Steinnes E., Urumov V. Air pollution studies in Macedonia using the moss biomonitoring technique, NAA, AAS and GIS Technology. JINR Preprint, E18-2006-160, Dubna, 2006 (Submitted To Environmental Monitoring And Assessment).
4. Barandovski L., Frontasyeva M.V., Pavlov S.S., Stafilov T., Urumov V. NlAA and AAS for air pollution study in Macedonia. FLNP JINR Annual Report-2005 (CD version), 2006.
5. Culicov O.A., Yurukova L. Comparison of element accumulation of different moss- and lichen-bags, exposed in the city of Sofia (Bulgaria). J. Atmos. Chem., No. 55, 2006, p. 1-12.
6. Frontasyeva M.V. Neutron activation analysis at the IBR-2 reactor in Dubna for Life Sciences. Ecological Chemistry and Engineering. Vol. 13, No. 5, 2006, p. 373-381.
7. Frontasyeva M.V., Kirkesali E.I., Aksenova N.G., Mosulishvili L.M., Belokobylsky A.I., Khizanishvili A.I. Neutron activation analysis for development of mercury sorbent based on blue-green alga Spirulina platensis. Journal of Neutron Research, Vol. 14, No. 2, 2006, p. 131-138.
8. Frontasyeva M.V., Pavlov S.S., Aksenova N.G., Kirkesali E.I., Mosulishvili L.M., Khizanishvili A.I., Rcheulishvili A.N. Interaction of microalgae Spirulina platensis with metals studied by NAA and AAS. FLNP JINR Annual Report-2005 (CD version), 2006.
9. Gandbol G., Frontasyeva M.V., Ostrovnaya T.M., Pavlov S.S., Gerbish Sh., Baljinnyam N. Assessment of hazardous impact of non-ferrous industry in the town of Erdenet, Mongolia, on the pasture animals. JINR Communications, Dubna, 2007 (in press).
10. Gorbunov A.V., Lyapunov S.M., Okina O.I., Frontasyeva M.V., Gundorina S.F. Assessment of human organism's intake of trace elements from foodstuffs in central regions of Russia. Journal of Environmental Chemistry, St.Petersburg, v. 15, N 1, 2006, p .47-59.
11. Loose A., Wozniak K., Dominiak P., Smirnov L.S., Natkaniec I., Frontasyeva M.V., Pomjakushina E.V., Baranov A.I., Dolbinina V.V. X-Ray and neutron single-crystal diffraction on $[Rb_x(NH_4)_{1-x}]_3H(SO_4)_2$. Part I. Refinement of crystal structure of phase II with x=0.11 at 3000 K. JINR Preprint, E14-2006-59, Dubna, 2006. Submitted to "Crystallography Reports".
12. Mahmut Coskun, Steinnes E., Frontasyeva M.V., Cotuk Y., Munevver Coskun, Sjobakk T.E., Dyomkina S.V. Heavy metal pollution of surface soil in Thrace Region, Turkey. Environmental Monitoring and Assessmen, No. 119, 2006, p. 545-556.
13. Mosulishvili L.M., Belokobylsky A.I., Kirkesali E.I., Frontasyeva M.V., Pavlov S.S. and Aksenova N.G. Neutron activation analysis for studying Cr uptake in the blue-green microalga Spirulina platensis. Accepted by Journal of Neutron Research, No. 2, 2007.
14. Pacheco A.M.G., Freitas M.C., Ventura M.G., Dionísio I., Ermakova E. Chemical elements in common vegetable components of Portuguese diets, determined by K0-INAA. Nuclear Instruments and Methods in Physics Research, A, Vol. 564, 2006, 721-728.
15. Szczepaniak K., Sarbu C., Astel A., Rainska E., Buziuk M., Culicov O., Frontasyeva M.V., Bode P. Assessment of the impact of a phosphatic fertilizer plant on the adjacent environment using fuzzy logic. Central European Journal of Chemistry, Vol. 4, No. 1, 2006, P. 29-55.
16. Tsibakhashvili N.Ya., Frontasyeva M.V., Kirkesali E.I., Aksenova N.G., Kalabegishvili T.L., Murusidze I.G., Mosulishvili L.M., Holman H.-Y.N. Epithermal Neutron activation analysis of Cr(Vi)-reducer basalt-inhabiting bacteria. Analytical Chemistry, USA, Vol. 78, 2006; P. 6285-6290
17. Tyutyunova F.I., Frontasyeva M.V., Schipakina I.G. Anthropogenic Dispersion of Anionogenic Toxicants in Groundwater in the European Russia. Water Resources, №. 3, 2006.
18. Zlatko Pančevski, Trajče Stafilov and Frontasyeva M.V. Copper in surface soil of Veles Region, Macedonia. Geologica Macedonia, No. 2, 2006, p. 3-10.

Conferences and Meetings

1. Anicic M., Frontasyeva M.V., Tomasevic M., Popovic A. Assessment of trace element atmospheric deposition in Belgrade and source apporionment using moss and INAA. Proceedings of the 8th International Conference on Fundamental and Applied Aspects of Physical Chemistry (September 2006, Belgrade, Vol. II, 2006, pp. 627- 629).
2. Aničić M., Frontasyeva M.V., Tomašević M., Rajšić S., Tasić M., Steinnes E. Aactive biomonitoring with wet and dry moss: Belgrade urban area case study. In the Book of abstract of the Seventh European Meeting on Environmental Chemistry, EMEC7 (December 6-9, 2006, Brno, Czech Republic), pp.169.
3. Astakhova N.V., Bordyugov L.G., Gerasimov A.V., Dikusar N.D., Eremin G.I., Ivanov A.I., Kryukov Yu.S., Maznyj N.G., Ryabchun O.V., Salamatin I.M. "Distributed wireless system with the synchronization of data flows", JINR Communications, P13-2006-41, Dubna, 2006.

4. Bancuta A., Stihi C., Popescu I.V., Frontasyeva M.V., Culicov O., Busuioc G., Cimpoca V., Constantinescu O., Gugiu M. INAA and PIXE methods applied to environmental biomonitoring. ISINN-14, International Seminar on Interaction of Neutrons with Nucei (Dubna, Russia, 24–27 May, 2006).

5. Bondarenko V.A., Honzatko J., Khitrov V.A., Sukhovoj A.M., Tomandl I. Parameters of the 125Te Compound State Cascade gamma-Decay, In: XIII International Seminar on Interaction of Neutrons with Nuclei, Dubna, May 2005, E3-2006-7, Dubna, 2006, pp. 13-35.

6. Bystritsky V.M., Bystritskii Vit.M., Enik T.L., Filipowicz M., Gerasimov V.V., Grebenyuk V.M., Kobzev A.P., Kublikov R.V., Nesvizhevskii V.V., Parzhitskii S.S., Pavlov V.N., Popov N.P., Salamatin A.V., Shvetsov V.N., Slepnev V.M., Strelkov A.V., Wozniak J., Zamyatin N.I. Experimental Research of the Radiative Capture of Thermal Neutrons in 3He. JINR Preprint D15 – 2006 – 23 (254, 355).

7. Bystritsky V.M., Krylov A.R., Pikelner L.B., Kobzev A.P., Kozyrev A. Litvak M., Mitrofanov I., Timoshenko G.N., Tretyakov V., Shvetsov V.N. Calibration of the HEND Neutron Counters Mounted on BOARD of Mars Odyssey 2001 Spececraft. In Proc. N48 of the ISINN – 13 (Dubna, May 25-28, 2005) – Dubna, JINR, 2006, p.172.

8. Bystritsky V.M., Zamyatin N.I., Kobzev A.P., Rogov Yu.N., Sapozhnikov M.G., Slepnev V.M., Chepurchenko I.A., "Source of labeled neutrons on the basis of electrostatic generator", XVI International Conference on Electrostatic Accelerators and Beam Technologies. Russia, Obninsk, 6-8 June 2006.

9. Culicov O., Frontasyeva M.V., Yurukova L., Mocanu R., Sarbu C. Identification of a new pollution source in the town of Baia Mare by discriminant analysis applied to data obtained analyzing transplanted moss bags. ISINN-14, International Seminar on Interaction of Neutrons with Nuclei (Dubna, Russia, 24–27 May, 2006).

10. Culicov O., Yurukova L., Mocanu R., Frontasyeva M.V., Sarbu C. Active moss biomonitoring applied to an industrial area in Romania: variation of element contents with the height of exposure site. 2nd Environmental Physics Conference (Alexandria, Egypt, February 18-22, 2006).

11. Ermakova E., Freitas M.C., Ventura M.G. Re-evaluation of the detector and the reactor parameters for the new k0-IAEA software and determination of the chemical elements in common vegetable components of Portuguese diets by k0-INAA. ISINN-14, International Seminar on Interaction of Neutrons with Nucei (Dubna, Russia, 24–27 May, 2006).

12. Florek M., Holy K., Mankovska B., Mereshova J., Frontasyeva M.V., Ermakova E.V., Pavlov S.S. Application of NAA and AAS in Environmental Research in Slovakia. 2nd Environmental Physics Conference (Alexandria, Egypt, February 18-22, 2006).

13. Florek M., Holy K., Meresova J., Sykora I., Frontasyeva M.V., Ermakova E.E., Pavlov S.S. INAA and FAAS in environmental studies in Slovakia. ISINN-14, International Seminar on Interaction of Neutrons with Nucei (Dubna, Russia, 24–27 May, 2006).

14. Frontasyeva M. Life Sciences Research at JINR, Dubna, Russia. 2nd Environmental Physics Conference (Alexandria, Egypt, February 18-22, 2006).

15. Frontasyeva M.V. "Atmospheric deposition of heavy metals in some regions of Russia and Europe according to the analysis of moss-biomonitors", Book of Abstracts. II All-Russian Conference "Scientific aspects of Russian ecological problems", (Moscow, May 29-31, 2006).

16. Frontasyeva M.V. Atmospheric deposition of trace elements in some selected countries of Europe and Asia – estimations based on moss analysis. Book of Abstracts of the 15th annual Central European Conference on Chemical substances in the Environment, ECOpole '06 (19-21 October, 2006, Opole, Poland).

17. Frontasyeva M.V. Neutron activation analysis at FLNP JINR: ten years of experience from collaboration with the IAEA (Vienna, Austria). ISINN-14, International Seminar on Interaction of Neutrons with Nuclei (Dubna, Russia, 24–27 May, 2006).

18. Frontasyeva M.V., Barandovski L., Stafilov T., Urumov V. Air pollution studies in Macedonia using the moss biomonitoring technique, NAA, AAS and GIS technology. The 19th Task Force Meeting of UNECE ICP Vegetation on Long Range Atmospheric Transport of Pollutants (30th January-2nd February, 2006, Caernarfon, Wales, UK)

19. Ganbold G., Frontasyeva M.V., Ostrovnaya T.M., Pavlov S.S., Gerbish Sh., Baljinnyam N. Assessment of hazardous impact on the pasture animals of non-ferrous industry in the town of Erdenet, Mongolia. ISINN-14, International Seminar on Interaction of Neutrons with Nucei (Dubna, Russia, 24–27 May, 2006).

20. Gledenov Yu.M. P-even and P-odd angular correlations in the reactions induced by thermal and resonance neutrons with charged particle escape. In: Proc. of Intern. School on Contemporary Physics-III, August 08-15, 2005, Ulaanbaatar, Mongolia, p.124-131.

21. Gledenov Yu.M., Sedysheva M.V., Guohui Zhang, Jinxiang Chen, Guoyou Tang, Khuukhenkhuu G. Measurement of Differential Cross-Section of the ^{6}Li(n,t)^{4}He Reaction. In: Proc. of the 13 International Seminar on Interaction of Neutron with Nuclei (ISINN-13), Dubna, 2006, p. 217-221.

22. Gledenov Yu.M., Sedysheva M.V., Rongtai Cao, Guohui Zhang, Jinxiang Chen, Guoyou Tang, G.Khuukhenkhuu. Measurement of Differential and Angle-Integrated Cross-Sections of the ^{64}Zn(n,α)^{61}Ni Reaction at 5.03 and 5.95 MeV. In: "Neutron Spectroscopy, Nuclear Structure, Related Topics". XIV International Seminar on Interaction of Neutrons with Nuclei, 2006, Dubna, p.37.

23. Gundorin N. A., Furman V.I., Pikelner L.B., Rebrova N.V., Salamatin I.M., Smirnov V.I., Zhdanova K.V., Zhuchko V.E. «Measurement of delayed neutron yields from thermal neutron induced fission of 237Np», Proc. of ISINN-14 (2006).

24. Kadmensky S. G., Lyuboshitz V.V., Tchuvil'sky Yu. M."Self-consistent weak P-odd nucleon potential for various sets of weak meson-nucleon constants within the generalized Fermi-liquid theory". Proceedings of the XVI International School on Nuclear Physics, Neutron Physics and Nuclear Energy (Varna-2005, Varna, Bulgaria, September 19-26, 2005), Transactions of the Bulgarian Nuclear Society, v. 10, No. 2, 2005, pp. 184 – 193

25. Kadmensky S.G., Lyuboshitz V.V., Tchuvil'sky Yu.M."Self-consistent weak P-odd nucleon potential within the generalized Fermi-liquid theory". Abstracts of the NSRT-2006 Conference, JINR E4-2006-65, Dubna, 2006, p. 43.

26. Kadmensky S.G., Lyuboshitz V.V., Tchuvil'sky Yu.M."Self-consistent weak P-odd nucleon potential for various sets of weak meson-nucleon constants within the generalized Fermi-liquid theory". Poster presentation at the 18-th International IUPAP Conference on Few-Body Problems in Physics – FB18 (Santos, Sao Paulo, Brazil, August 21 - 26, 2006), Book of Abstracts of FB18, Sao Paulo, 2006, p.160.

27. Khitrov V.A., Sukhovoj A.M., Model-Free Determination of Level Density, Radiative Strength Functions and General Tendency Nuclear Structure Changing Below Bn, In: XIII International Seminar on Interaction of Neutrons with Nuclei, Dubna, May 2006, E3-2006-7, Dubna, 2006, pp. 36-40.

28. Khitrov V.A., Sukhovoj A.M., Pham Dinh Khang, Vuong Huu Tan, Nguyen Xuan Hai. Level Density and Radiative Strength Functions of Dipole gamma-Transitions in 139Ba and 165Dy In: XIII International Seminar on Interaction of Neutrons with Nuclei, Dubna, May 2006, E3-2006-7, Dubna, 2006, pp. 41-47.

29. Khuukhenkhuu G., Gledenov Yu.M., Bayarbadrakh B., Odsuren M., Sedysheva M.V. 14 MeV Neutron Induced (n,p) Reaction Cross Section Analysis. In: Proc. of the 13 International Seminar on Interaction of Neutron with Nuclei (ISINN-13), Dubna, 2006, p. 229-232.

30. Khuukhenkhuu G., Gledenov Yu.M., Bayarbadrakh B., Odsuren M., Sedysheva M.V. Statistical Model Analysis for Isotopic Effect in (n,p) Cross Sections. In: "Neutron Spectroscopy, Nuclear Structure, Related Topics". XIV International Seminar on Interaction of Neutrons with Nuclei, 2006, Dubna, p.47.

31. Kobzev A.P., Maczka D. and Reutov V.F. Investigation of hydrogen depth profiles in subsurface layers of silicon. VI International Conference "Ion Implantation and other Application of Ions and Electrons", Kazimierz Dolny, Poland, June 26-29, 2006, Abstract book, p. 88.

32. Kulik M., Kobzev A.P., Jaworska D., Zuk J. and Filiks J. Investigation of indium diffusion process and optical effects in In+ implanted GaAs. VI International Conference "Ion Implantation and other Application of Ions and Electrons", Kazimierz Dolny, Poland, June 26-29, 2006, Abstract book, p. 97.

33. Lyuboshitz V. L., Lyuboshitz V.V. "On the coherent inelastic processes in collisions of hadrons and γ-quanta with nuclei at ultrarelativistic energies". Talk at the IX International Conference on Nucleus-Nucleus Collisions – NN2006 (Rio de Janeiro, Brazil, August 28 – September 1, 2006), will be allocated on the NN2006 website http://www.nn2006.com.br ; Book of Abstracts of NN2006, Rio de Janeiro, 2006, p. 42.

34. Lyuboshitz V. L., Lyuboshitz V.V. "Spectrum of relative momenta of the neutron and proton at deuteron peripherical breakup in the limit of very low momentum transfer". Talk at the International School on Few-Body Problems in Physics – FBS2006 (Dubna, August 7 - 17, 2006); will be allocated on the FBS2006 website

35. Lyuboshitz V.L., Lyuboshitz V.V. "Correlations of polarizations of two photons". Proceedings of the Bogolyubov-2004 Conference (Moscow – Dubna, September 2 – 6, 2004), Physics of Particles and Nuclei (EChAYa), v. 36, Suppl. 2, 2005, pp. S198 – S202.

36. Lyuboshitz V.L., Lyuboshitz V.V. "On the coherent inelastic processes in collisions of elementary particles with nuclei at ultrarelativistic energies". Proceedings of the 18-th International Conference on Ultrarelativistic Nucleus-Nucleus Collisions – Quark Matter 2005 (Budapest, Hungary, August 4–9, 2005), Heavy Ion Physics – Acta Physica Hunga-rica A , v. A27/2-3, 2006, pp. 347 - 350 .

37. Lyuboshitz V.L., Lyuboshitz V.V. "On the coherent inelastic processes in the interaction of hadrons and γ-quanta with nuclei at ultrarelativistic energies" Poster presentation at the IV International Conference on Quarks and

Nuclear Physics – QNP06 (Madrid, Spain, June 5 - 10, 2006), allocated on the QNP06 website (address: accepted for publication in Proceedings of the QNP06 Confe-rence (2007).

38. Lyuboshitz V.L., Lyuboshitz V.V. "On the coherent inelastic processes in collisions of hadrons and γ-quanta with nuclei at ultrarelativistic energies". Talk at the Helmholtz International School & Workshop "Calculations for Modern and Future Colliders" – CALC-2006 (Dubna, July 15 - 25, 2006); allocated on the CALC-2006 website (address: http://theor.jinr.ru/~calc2006/Talks/lyuboshitz_calc06.pdf).

39. Lyuboshitz V.L., Lyuboshitz V.V. "On the correlations of polarizations in the system of two photons". Proceedings of the XI Advanced Research Workshop on High Energy Spin Physics – DUBNA-SPIN-05 (Dubna, September 27 – October 1, 2005), JINR E1,2-2006-105 , Dubna, 2006, pp. 92 - 98.

40. Lyuboshitz V.L., Lyuboshitz V.V. "On the correlations of polarizations in the system of two photons". Poster presentation at the 17-th International Spin Physics Symposium – SPIN2006 (Kyoto, Japan, October 2 – 7, 2006); Book of Abstracts of SPIN2006, Kyoto, 2006, p. 42; accepted for publication in Proceedings of SPIN2006 (2007).

41. Lyuboshitz V.L., Lyuboshitz V.V. "On the Coulomb dissociation of relativistic nuclei and hypernuclei with small binding energies". Proceedings of the XVIII International Workshop on High Energy Physics and Quantum Field Theory –QFTHEP'2004 (Saint-Petersburg, Peterhof, Russia, June 17 – 23, 2004), Max Press, Moscow, 2005, pp. 425-431 (appeared in fact in 2006)

42. Lyuboshitz V.L., Lyuboshitz V.V. "On the process of Coulomb dissociation of weakly bound relativistic nuclei and hypernuclei". Talk at the 18-th International IUPAP Conference on Few-Body Problems in Physics – FB18 (Santos, Sao Paulo, Brazil, August 21 - 26, 2006), allocated on the FB18 website Book of Abstracts of FB18, Sao Paulo, 2006, p. 69; accepted for publication in Proceedings of the FB18 Conference – Nuclear Physics A (2007).

43. Lyuboshitz V.L., Lyuboshitz V.V. "Pair correlations of neutrons produced in nuclear fission". Poster presentation at the IX International Conference on Nucleus-Nucleus Collisions – NN2006 (Rio de Janeiro, Brazil, August 28 – September 1, 2006); Book of Abstracts of NN2006, Rio de Janeiro, 2006, p. 76.

44. Lyuboshitz V.L., Lyuboshitz V.V. "Role of spin effects in the "forward" nucleon charge-exchange reaction n + p $\rightarrow$ p + n". Talk at the XIV International Seminar on Interaction of Neutrons with Nuclei – ISINN-14 (Dubna, May 24 – 27, 2006); ISINN-14 Abstracts, JINR E3-2006-53, Dubna, 2006, p. 49; Proceedings of ISINN-14, Dubna, 2007 (in press).

45. Lyuboshitz V.L., Lyuboshitz V.V. "Role of spin effects in the nucleon charge-exchange process n + p $\rightarrow$ p + n at zero angle". Poster presentation at the XI International Seminar on Electromagnetic Interactions of Nuclei – EMIN-2006 (Moscow, September 21 – 24, 2006); accepted for publication in Proceedings of EMIN-2006 (Moscow, 2007).

46. Lyuboshitz V.L., Lyuboshitz V.V. "Spin structure of the charge-exchange process n + p $\rightarrow$ p + n at zero angle". Talk at the 17-th International Spin Physics Symposium – SPIN2006 (Kyoto, Japan, October 2 – 7, 2006), allocated on the SPIN2006 website (address:http://www-nh.scphys.kyoto-u.ac.jp/SPIN2006/SciPro/pres/session6.7/ ValeryVLyuboshitz.pdf) ; Book of Abstracts of SPIN2006, Kyoto, 2006, p.175; accepted for publication in Proceedings of SPIN2006 (2007) .

47. Lyuboshitz V.L., Lyuboshitz V.V. "Strangeness conservation and pair correlations of neutral kaons with close momenta in inclusive processes". Proceedings of the 18-th International Conference on Ultrarelativistic Nucleus-Nucleus Collisions – Quark Matter 2005 (Budapest, Hungary, August 4–9, 2005) , Nukleonika , v. 51, Suppl. 3, 2006, pp. S69 - S72 .

48. Lyuboshitz V.L., Lyuboshitz V.V. "Strangeness conservation and pair correlations of neutral kaons with close momenta produced in inclusive multiparticle processes". Proceedings of the VI International Workshop on Very High Multiplicity Physics – VHMP'05 (Dubna, April 16-17, 2005) – Pis'ma v EChAYa (Particles and Nuclei. Letters), Dubna, 2007 (in press); finally accepted for publication in 2006.

49. Lyuboshitz V.L., Lyuboshitz V.V. "Strangeness conservation and pair correlations of neutral kaons with close momenta produced in inclusive multiparticle processes". Talk at the XI Frascati Spring School on Nuclear, Subnuclear and Astroparticle Physics – "Physics in the LHC era" (LNFSS'06, Frascati, Italy, May 15-19, 2006), allocated on the LNFSS'06 website (address: http://www.lnf.infn.it/conference/lnfss/06/Talks/valery.lyuboshitz.pdf).

50. Lyuboshitz V.L., Lyuboshitz V.V. "Strangeness conservation and pair correlations of neutral kaons with low relative momenta produced in inclusive multiparticle processes" .Talk at the IV International Conference on Quarks and Nuclear Physics – QNP06 (Madrid, Spain, June 5 - 10, 2006), allocated on the QNP06 website; accepted for publication in Proceedings of the QNP06 Conference (2007) .

51. Lyuboshitz V.L., Lyuboshitz V.V. "Strangeness conservation and pair correlations of neutral kaons with close momenta produced in inclusive multiparticle processes". Poster presentation at the IX International Conference on

Nucleus-Nucleus Collisions – NN2006 (Rio de Janeiro, Brazil, August 28 – September 1, 2006); Book of Abstracts of NN2006, Rio de Janeiro, 2006, p.43 .

52. Lyuboshitz V.L., Lyuboshitz V.V. "Strangeness conservation and structure of pair correlations of neutral kaons with low relative momenta in inclusive processes". Pro-ceedings of the XVII International Baldin Seminar on High Energy Physics Problems – ISHEPP-17 (Dubna, September 27 – October 2, 2004), JINR E1,2-2005-103, vol. I, Dubna, 2005, pp. 361 - 365 (appeared in fact in 2006) .
53. Lyuboshitz V.L., Lyuboshitz V.V. "The coherent inelastic processes on nuclei at ultrarelativistic energies". Proceedings of the NPD2005 Conference (ITEP, Moscow, December 5-9, 2005) – Yadernaya Fizika, 2007 (in press).
54. Lyuboshitz V.L., Lyuboshitz V.V. "The coherent inelastic processes on nuclei at ultrarelativistic energies" .Talk at the XVIII International Baldin Seminar on High Energy Physics Problems – ISHEPP-18 (Dubna, September 25 – 30, 2006); Abstracts of ISHEPP-18, JINR E1,2-2006-129, Dubna, 2006, p.58; accepted for publication in Proceedings of ISHEPP-18 (Dubna, 2007).
55. Lyuboshitz V.L., Lyuboshitz V.V. "The nucleon charge transfer reaction $n + p \rightarrow p + n$ at zero angle and the role of spin effects". Proceedings of the XI International Con-ference on Elastic and Diffractive Scattering – XVII Rencontres de Blois (Blois, France, May 15–20, 2005): "Elastic and Diffactive Scattering: Towards High Energy Frontiers", Gioi Publishers (Vietnam), 2006, pp. 223 - 227 .
56. Lyuboshitz V.L., Lyuboshitz V.V. "The process of Coulomb dissociation of weakly bound relativistic nuclei and hypernuclei within the two-cluster model". Proceedings of the VIII International Workshop "Relativistic Nuclear Physics – from Hundreds of MeV to TeV"– RNP-2005 (Dubna, May 23–28, 2005), JINR E1,2-2006-30 , Dubna, 2006, pp. 79 – 86.
57. Lyuboshitz V.L., Lyuboshitz V.V. "The process of Coulomb dissociation of weakly bound relativistic nuclei and hypernuclei within the two-cluster model". Talk at the International Conference "Nuclear Structure and Related Topics" – NSRT-2006 (Dubna, June 13 - 17, 2006); Abstracts of NSRT-2006 , JINR E4-2006-65 , Dubna, 2006, p. 52; Proceedings of the NSRT-2006 Conference – Yadernaya Fizika, v.70, 2007 (in press).
58. Lyuboshitz V.L., Lyuboshitz V.V. "The process of Coulomb dissociation of weakly bound relativistic nuclei and hypernuclei within the two-cluster model". Talk at the International School on Few-Body Problems in Physics – FBS2006 (Dubna, August 7 - 17, 2006); will be allocated on the FBS2006 website.
59. Lyuboshitz V.L., Lyuboshitz V.V. "The process of Coulomb dissociation of weakly bound relativistic nuclei and hypernuclei within the two-cluster model". Poster presentation at the IX International Conference on Nucleus-Nucleus Collisions – NN2006 (Rio de Janeiro, Brazil, August 28 – September 1, 2006); Book of Abstracts of NN2006, Rio de Janeiro, 2006, p.44 .
60. Lyuboshitz V.L., Lyuboshitz V.V. "The process of Coulomb dissociation of weakly bound relativistic nuclei and hypernuclei within the two-cluster model". Talk at the XI Interna-tional Seminar on Electromagnetic Interactions of Nuclei – EMIN-2006 (Moscow, September 21 – 24, 2006); accepted for publication in Proceedings of EMIN-2006 (Moscow, 2007).
61. Machajdik D., Kobzev A.P., Hušeková K., Ťapajna M., Frőhlich K. and Schram T. "Thermal stability of advanced gate stacks consisting of a Ru electrode and Hf-based gate dielectrics for CMOS technology." VI International Conference "Ion Implantation and other Application of Ions and Electrons", Kazimierz Dolny, Poland, June 26-29, 2006, Abstract book, p. 37.
62. Marinova S.G., Frontasyeva M.V., Yurukova L.D., Strelkova L.P., Marinov A.T. Atmospheric deposition of heavy metals in the Rhodope Mountaines studied by the moss biomonitoring and neutron activation analysis. ISINN-14, International Seminar on Interaction of Neutrons with Nucei (Dubna, Russia, 24–27 May, 2006).
63. Marinova S.G., Frontasyeva M.V., Yurukova L.D., Strelkova L.P., Marinov A. T. Air pollution studies in South Bulgaria using the moss biomonitoring technique and neutron activation analysis. Book of Abstracts. 6th International Conference of the Balkan Physical Union, Istanbul, Turkey, August 22-26, 2006, p. 1004; Submitted to Journal of American Institute of Physics (AIP), 2007.
64. Mutterer M., Kopatch Yu.N., Yamaletdinov S., Lyapin V., von Kalben J., Khlebnikov S., Sillanpää M, Tjurin G., Trzaska W.H. "Precise Measurement of the Energy Distribution of Ternary alpha Particles Emitted in 252Cf(sf)", in Proc. 14th Int. Seminar on the Interaction of Neutrons with Nuclei, ISINN14, Dubna, Russia, May 24-27 2006.
65. Mutterer M., Kopatch Yu.N., Yamaletdinov S., Lyapin V., von Kalben J., Khlebnikov S., Sillanpää M, Tjurin G., Trzaska W.H. "Energy Distribution of Ternary α-Particles in 252Cf(sf)", in Proc. 6th International Conference Dynamical Aspects of Nuclear Fission DANF-2006, October 2 - 6, 2006, Smolenice Castle, Slovak Republic.
66. My Trinh T. T., Frontasyeva M.V., Gustova M.V., Nguyen Hong Nhung. Elemental content of potential terrestrial and aquatic biomonitors of trace element contamination in Vietnam studied by INAA and XRF. ISINN-14, International Seminar on Interaction of Neutrons with Nuclei (Dubna, Russia, 24–27 May, 2006).

67. Olteanu C., Culicov O., Frontasyeva M.V., Toma M., Duliu O.G., Oaie G. ENAA studies of profound Black Sea sediments pollution. 10th International Symposium on Radiation Physics (17-22 September, 2006, Coimbra, Portugal).

68. Oprea A.I., Oprea C., Gledenov Yu.M., Sedyshev P.V. Recent Results in the Study of Asymmetries in Neutron p-Resonances of ^{14}N at Neutron Energy 1 MeV. In: "Neutron Spectroscopy, Nuclear Structure, Related Topics". XIV International Seminar on Interaction of Neutrons with Nuclei, 2006, Dubna, p.58.

69. Oprea A.I., Oprea C., Gledenov Yu.M., Sedyshev P.V., Szalanski P.J. Calculation of angular correlations in the $^{14}N(n, p)^{14}C$ reaction up to 1 MeV neutron energy region. In: Proc. of the 13 International Seminar on Interaction of Neutron with Nuclei (ISINN-13), Dubna, 2006, p. 153-159.

70. Oprea C., Cernenko L.P. Ornamental lawn as passive biomonitor of atmospheric pollution in urban areas. XXXVI Annual Meeting of European Society for New Methods In Agricultural Research, 10 – 14 September 2006, Iasi, Romania, 10p.

71. Oprea C., Cupsa D., Tentis M., Oprea I. A., Tomulescu I., Teusdea A., Radoviciu E., Cadar D., Candea D., Gergely I., Ortan F., Corund M. Effectiveness of environmental protection management system in Water Crisuri Basin. ISINN-14, May 24-27, Dubna, RF, 2006, 8p.

72. Oprea C., Kobzev A.P., Codescu M., Szalansky P.I., Curuia M. PIXE and RBS analysis of Fe - Cu nanoalloy. Vacuum, VAC-081, 2006 (accepted, in press), 4p.

73. Oprea C., Kobzev A.P., Oprea I. A., Buzguta V., Szodorai F., Tomulescu I., Cadar D., Ozunu A., Candea D. Concentration measurements of micro- and macro- matrix constituents in human dental enamel by IBA techniques. ISINN-14, May 24-27, Dubna, RF, 2006, p. 57, 8p.

74. Oprea C., Kobzev A.P., Oprea I.A., Szalanski P.J., Buzguta V. PIXE detection limits for dental enamel from some human teeth by excitation with protons and $^{4}He^{2+}$ ions from a 3 MeV Van der Graaff accelerator. Vacuum, VAC-080, 2006 (accepted, in press), 5p.

75. Oprea C., Mateescu Gh., Curuia M., Oprea I.A., Craciun L., Mihai I., Padureanu I., Rapeanu S., Kozlov Zh., Semenov V. The vacuum system of the Thermostat TS-3000 K. The Conference of "Progrese in criogenie si separarea izotopilor", Oct. 25-27, Caciulata, Valcea, Romania, 2006, (accepted, in press), 5p.

76. Oprea C., Oprea I. A., Cadar D. Comparative study for optimization of different measurement techniques. ISINN-14, May 24-27, Dubna, RF, 2006, 8p.

77. Oprea C., Oprea I.A., Buzguta V. Fluorine determination in human healthy and carious teeth using the RBS technique. The Conference of "Progrese in criogenie si separarea izotopilor", Oct. 25-27, Caciulata, Valcea, Romania, 2006, (accepted, in press), 5p.

78. Oprea C., Kobzev A.P., Buzguta V., Oprea A., Szodorai F., Cadar D. Determination of Trace Heavy Metals in Human Teeth Using PIXE. In Proc. N48 of the ISINN – 13 (Dubna, May 25-28, 2005) – Dubna, JINR, 2006, p.285.

79. Pankratova Yu.S., Frontasyeva M.V., Zelnitchenko N.I. Atmospheric deposition of heavy metals and other elements in the Republic of Udmurtia, Russian Federation, studied by the miss biomonitoring, NAA and GIS technology. ISINN-14, International Seminar on Interaction of Neutrons with Nucei (Dubna, Russia, 24–27 May, 2006).

80. Panteleev Ts., Oprea C.D., Oprea A.I. New experimental method to determine the averaged squared radius of the nuclei in the process of the direct and isomer fission. ISINN-14, May 24-27, Dubna, RF, 2006, p 60.

81. Povtoreyko E.A., Pavlov S.S. The designing and development of new spectrometry software. ISINN-14, International Seminar on Interaction of Neutrons with Nucei (Dubna, Russia, 24–27 May, 2006).

82. Pyatkov Yu., Trzaska W., Mutterer M., Yamaletdinov S., Tjukavkin A., Bolgov D., Kamanin D., Khlebnikov S., Kopach Yu., Kuznetsova E., Lavrova J., Lyapin V., Sillanpää M., Tishchenko V., Tyurin G. "Searching for rare decay modes in the reaction 238U+4He (40 MeV)", in Proc. Int. Symp. On Exotic Nuclei EXON-2006, Khanty-Mansiysk, 17-22 July 2006.

83. Pyatkov Yu., Trzaska W., Mutterer M., Yamaletdinov S., Tjukavkin A., Bolgov D., Kamanin D., Khlebnikov S., Kopach Yu., Kuznetsova E., Lavrova J., Lyapin V., Sillanpää M., Tishchenko V., Tyurin G. "Multicluster Decay of 242Pu* from the Reaction 238U+4He (40 MeV)", in Proc. 14th Int. Seminar on the Interaction of Neutrons with Nuclei, ISINN14, Dubna, Russia, May 24-27 2006.

84. Samosvat G.S., Oprea C., Nikolenko V.G., Kozlov Zh.A., Oprea I. A., Popov A.V., Parzhitsky S.S., Semionov V.A., Puchkov A.V., Morozov V.M., Mateescu G., Craciun L. Proposal for the Investigation of the neutron-electron scattering length in liquid 208Pb and Bi by the TS-3000K thermostat at IBR-2 reactor. ISINN-14, May 24-27, Dubna, RF, 2006, p. 64, 8p.

85. Sashina I.I., Frontasyeva M.V., Sudnitsin I.I., Gundorina S.F., Pavlov S.S. NAA for assessment of heavy metal and other trace element contamination in roadside surface soil. ISINN-14, International Seminar on Interaction of Neutrons with Nucei (Dubna, Russia, 24–27 May, 2006).

86. Sharapov E.I., Furman W.I., Lychagin E.V., Muzichka A.Yu, Nekhaev G.V., Strelkov A.V., Shvetsov V.N., Chernukhin Yu.I., Kandiev Ya.Z., Levakov B.G., Litvin V.I., Lyzhin A.E., Mitchell G.E., Crawford B.E., Stephenson S.L., Howell C.R. and Tornow W. «An approach to the spatial-temporal analysis of the n-n collision rate in the YAGUAR experiment.» XIII International Seminar on Interactions of Neutrons with Nuclei, ISINN-XIII, E3-2006-7, p.130, Joint Institute for Nuclear Research, Dubna, 2006.

87. Sharapov E.I., Furman W.I., Lychagin E.V., Muzhychka A.Yu., Nekhaev G.V., Strelkov A.V., Shvetsov V.N., Chernukhin Yu.I., Kandiev Ya.Z., Levakov B.G., Litvin V.I., Lyzhin A.E., Mitchel G.E., Crawford B.E., Stephenson S.L., Howell C.R., Tornow W. "An Appoach to the Spatial-Temporal Analysis of the n-n Collision Rate in the YAGUAR Experiment"// Neutron Spectroscopy, Nuclear Structure, Related Topics; ISINN-13 Dubna May25-28, 2005, JINR Report E3-2006-7, pp. 130-13.

88. Stamenov J., Yurukova L., Spirič Z., Šmit Z., Papastefanou C., Saitanis C., Boev B., Stafilov T., Urumov V., Revenco M., Steinnes E., Wolterbeek H. Th., Mocanu R., Cucu-man S., Culicov O., Ivanov V.V., Kadyshevsky V.G., Lyapunov S.M., Frontasyeva M.V., Bek-Uzarov G.N., Krmnar M., Tasič M., Popovič A., Šajn R., Coşkun M. Impact of endemic geochemical peculiarities of the Balkans on population health studied through soil, water and air analysis. Proceedings of the International Conference on Regional Environmental Issues - Cooperation Avenues (Turkey, Izmir, October19-21, 2006).

89. Sukhovoj A.M., Khitrov V.A., Li Chol, Pham Dinh Khang, Nguyen Xuan Hai, Vuong Huu Tan. Some Problems in Determinining Level Density and Radiative Strength Functions in Light and Near-Magic Nuclei, In: XIII International Seminar on Interaction of Neutrons with Nuclei, Dubna, May 2006, E3-2006-7, Dubna, 2006, pp. 56-63.

90. Sukhovoj A.M., Khitrov V.A., Li Chol, Pham Dinh Khang, Vuong Huu Tan, Nguyen Xuan Hai. The Probable Level Densities and Radiative Strength Functions of Dipole Gamma-Transitions in ^{57}Fe Compound Nucleus, In: XIII International Seminar on Interaction of Neutrons with Nuclei, Dubna, May 2006, E3-2006-7, Dubna, 2006, pp. 72-82.

91. Sukhovoj A.M., Khitrov V.A., Pham Dinh Khang, Vuong Huu Tan, Nguyen Xuan Hai. Level Density and Radiative Strength Functions in Light Nuclei: 60Co as an Example of Method for Determination and Their Reliability Verification, In: XIII International Seminar on Interaction of Neutrons with Nuclei, Dubna, May 2006, E3-2006-7, Dubna, 2006, pp. 64-71.

92. Telezhnikov S.A., Granja C., Honzatko J., Pospisil S., Tomandl I. «A precise determination of the ^{64}Cu binding energy», Proc. of ISINN-14 (2006).

93. Tsibakhashvili N.Ya., Kalabegishvili T.L., Kirkesali E.I., Mosulishvili L.M., Frontasyeva M.V., Pavlov S.S., Aksenova N.G., Holman H.-Y.N. Study of Cr(VI) detoxification by basalt-inhabiting bacteria using NAA and ESR methods. 2nd Environmental Physics Conference (Alexandria, Egypt, February 18-22, 2006).

94. Vergel K.N., Frontasyeva M.V., Zelnitchenko N.I. Atmospheric deposition of heavy metals and other elements around Lake Seliger, Tver Rigion, Russia, studied by the moss biomonitoring, NAA, and GIS technology. ISINN-14, International Seminar on Interaction of Neutrons with Nuclei (Dubna, Russia, 24–27 May, 2006).

95. Vesna V.A., Gledenov Yu.M., Nesvizhevsky V.V., Petukhov A.K., Sedyshev P.V., Soldner T., Shulgina E.V., Zimmer O. Observation of the P-odd Asymmetry of Triton Emission in the ^{6}Li(n,α)^{3}H Reaction with Cold Polarized Neutrons. In: "Neutron Spectroscopy, Nuclear Structure, Related Topics". XIV International Seminar on Interaction of Neutrons with Nuclei, 2006, Dubna, p.75.

NEUTRON SOURCES

1. Karamian S.A., Carroll J.J., Adam J., Kulagin E.N., Shabalin E.P. Production of long-lived hafnium isomers in reactor irradiations. High Energy Density Physics**,** 2, p.48-56, 2006.
2. Kulikov S., Shabalin E. Complex of neutron moderators for the IBR-2M reactor. In Proc. of 17th Meeting of the International Collaboration on Advanced Neutron Sources, ICANS-XVII. April 25-29, 2005, Santa Fe, New Mexico, LA-UR-06-3904, Vol. II, p.341-345, June 2006.
3. Natkaniec I., Shabalin E. Kulikov S., Holderna-Natkaniec K. Comparison of Neutron Scattering and Radiation Properties of Methane and Water Ices with Methyl Derivatives of Benzene at Low Temperatures. In Proc. of 17th Meeting of the International Collaboration on Advanced Neutron Sources, ICANS-XVII, April 25-29, 2005, Santa Fe, New Mexico, LA-UR-06-3904, Vol. II, p.519-529, June 2006.

4. Neuninghoff K., Pohl Ch., Bollini V., Bubak A., Kulikov S., et al. Investigation of neutron performance of methane hydrate moderator. In Proc. of 17th Meeting of the International Collaboration on Advanced Neutron Sources, ICANS-XVII. April 25-29, 2005, Santa Fe, New Mexico, LA-UR-06-3904, Vol. II, p.530-535, June 2006.
5. Pepelyshev Yu.N., Melnikov V.N., Chistozvonov A.S. Application of the probability method to analyze operation failures. JINR Communications, P13-2006-49, Dubna, 2006.
6. Pepelyshev Yu.N., Popov A.K. Estimation of parameters of power feedback and the IBR-2 reactor operation stability at various mean power levels. JINR Communications, P13-2006 101, Dubna, 2006.
7. Pepelyshev Yu.N., Popov A.K. Influence of nearest environment of core on the power pulse dynamics in the IBR-2 reactor. Annals of Nuclear Energy, 2006, v. 33, pp. 813-819.
8. Pepelyshev Yu.N., Popov A.K. Investigation of dynamical reactivity effects of IBR-2 moving reflectors. Atomic Energy, 2006, v.101, N2, pp.98-103.
9. Pepelyshev Yu.N., Smirnov V.S., Measurement of mean lifetime of generation of neutrons in the IBR-2 reactor. JINR Communications, P13-2006-115, Dubna, 2006.
10. Shabalin E.P., Ignatovich V.K. Neutron Albedo. JINR Preprint, P4-2005-107,Dubna, 2005 (in Russian). «Nuclear Physics», 2, 2007.
11. Shabalin E.P., Petruski I. Unknown additional delayed neutron source in the IBR-2 reactor. JINR Communications, E3-2006-46, Dubna, 2006.

DEVELOPMENT AND CREATION OF ELEMENTS OF NEUTRON SPECTROMETERS FOR CONDENSED MATTER INVESTIGATIONS

1. Belushkin A.V. et al. One-dimensional Position-sensitive Detector of Thermal Neutrons. Preprint JINR P-13-2006 -152, Dubna, 2006. Submitted to PTE.
2. Belushkin A.V. et al. Two-dimensional Monitor Position-sensitive Detector of Thermal Neutrons. Preprint JINR P-13-2006-124, Dubna, 2006. Submitted to "Journal of Technical Physics"
3. Kirilov A.S. The approach to incorporate the Python scripting language into an instrument control software. Report on the Conference NOBUGS 2006, October 2-4, 2006, LBNL, Berkeley USA (to be published in Conf. Proc.)
4. Levchanovsky F.V., Litvinenko E.I., Nikiforov A.S., Gebauer B., Schulz Ch., Wilpert Th. ”Software Modules of DAQ PCI board (DeLiDAQ) for Positive-Sensitive MWPC Detectors with Delay Line Readout”, NIM A569 (2006), pp 900-904.
5. Petukhova T.B., Kirilov A.S. Creation of Visual Studio.Net Wizard for Development of Modules of Management by Devices for Software Complex Sonix+. JINR communications P10-2006-27, Dubna, 2006.

6. PRIZES

JINR Prizes:

Physics Instruments and Methods:

Second Prize:

A.Frischbutter, Ch.Janssen, Ch.Scheffzuek, K.Walther, K.Ullemeyer, D.Nikolaev, A.Nikitin, T.Ivankina. "Neutron Diffraction Study of the Physical Properties of Rock Samples of the Upper Part of Lithosphere"

Applied Physics Research*:*

Second Prize:

E.Lychagin, A.Muzychka, G.Nekhaev, A.Strelkov. "Observation and Investigation of Weak Heating of Ultracold Neutrons"

***FLNP Prizes*:**

In Nuclear Physics:

First Prize:

Yu.M.Gledenov, P.V.Sedyshev, et al. "Measurement of p-odd asymmetry of triton emission in the reaction $^{6}Li(n\alpha)^{3}H$ with cold polarized neutrons"

Second Prize:

A.I.Frank, G.V.Kulin, D.V.Kustov, et al. "Effect of accelerating matter in neutron optics"

Third Prize:

R.Gaehler, V.K.Ignatovich. "Neutron holography without reference beam"

In Condensed Matter Physics:

First Prize:

A.M.Balagurov, V.B.Zlokazov, Yu.V.Taran. "Study of spatial distribution of residual stresses in a composite steel tube by neutron diffraction"

Second Prize:

A.M.Balagurov, R.N.Vasin, N.I.Ivankina, A.N.Nikitin. "Properties of quartz and quartziferous rocks at high pressures and temperatures by neutron diffraction and acoustic emission"

Encouraging Prizes:

D.P.Kozlenko, C.E.Kichanov, B.N.Savenko. "High Pressure Effect on the Crystal and Magnetic Structure of $LuMnO_3$: Correlation between the Distortion of the Triangular Lattice and the Symmetry of the Magnetic State in Hexagonal Frustrated Manganites"

M.A.Kiselev. "Structure of unilamellar Dimyristoylphosphatidilholine vesicles. Method of separated form-factors"

In Applied and Methodical Physics:

First Prize:

V.K.Ignatovich, E.P.Shabalin. "Neutron albedo"

Second Prize:

L.Barandovski, M.Cekova, M.V.Frontasyeva, S.S.Pavlov, T.Stafilov, E.Steinnes, V.Urumov. "Air pollution studies in Macedonia using the moss biomonitoring technique, NAA, AAS and GIS-Technologies".

Encouraging Prize:

G.Gandbol, et al. "Assessment of hazardous impact of ore-mining and processing plant in the town of Erdenet, Mongolia, on pastured animals"

I.M.Frank Stipend:

In Nuclear Physics:
O.A.Culicov

In Condensed Matter Physics:
D.P.Kozlenko

In Methodical Investigations:
R.N.Vasin

F.L.Shapiro Stipend:

E.V.Lychagin
Yu.N.Khaidukov

7. SEMINARS

Date	Authors	Title
26.01.06	B.G.Yerozolimsky (Harvard Univ., USA)	Proposed experiment to measure the electron-antineutrino correlation in neutron decay
03.02.06	N.N.Salashchenko (Institute for Physics of Microstructures RAS, Nizhny Novgorod)	Modern problems in multilayer X-ray optics
31.03.06		Seminar in commemoration of D.A.Korneev
05.10.06	Laszlo Cser (RISP HAS, KFKI, Hungary)	How and why to do neutron holography
20.10.06	Sow-Hsin Chen (MIT, USA)	Observation of fragile-to-strong dynamic crossover in protein and DNA hydration water and its relation to the glass transition of biopolymers
26.10.06	N.K.Cherezov (Scientific Manufacture Enterprise V.G.Khlopin Radium Institute (St.Petersburg)	Construction of highly efficient portable nuclear and radiation safety control equipment

8.1. STRUCTURE OF LABORATORY AND SCIENTIFIC DEPARTMENTS

Directorate:
Director:
A.V.Belushkin
Deputy Directors:
N.Popa
V.N.Shvetsov
Scientific Secretary:
V.A.Khitrov

Reactor and Technical Departments
Chief engineer: V.D.Ananiev
IBR-2 reactor
Chief engineer: A.V.Vinogradov
Department of IREN
Head: V.G.Pyataev
Mechanical maintenance division
Head: A.A.Belyakov
Electrical engineering department
Head: A.A.Yakovlev
Design bureau
Head: A.A.Kustov
Experimental workshops
Head: A.N.Kuznetsov

Scientific Departments and Sectors
Condensed matter department
Head: A.M.Balagurov
Nuclear physics department
Head: Yu.N.Kopatch
Department of IBR-2 spectrometers complex
Head: A.V.Belushkin

Administrative Services
Deputy Director: S.V.Kozenkov
Secretariat
Finances
Personnel

Scientific Secretary Group
Translation
Graphics
Photography
Artwork

NEUTRON SCATTERING STUDIES OF CONDENSED MATTER

Sub-Division	Title	Head
Sector 1: Neutron Diffraction. Head: A.M.Balagurov		
Group No.1	HRFD	V.Yu.Pomjakushin
Group No.2	DN-2	A.I.Beskrovnyi
Group No.3	DN-12	B.N.Savenko
Group No.4	Geomaterials	A.N.Nikitin
Group No.5	SCAT	Ch.Scheffzük
Sector 2: Neutron Optics. Head: V.L.Aksenov		
Group No.1	Surfaces	Yu.V.Nikitenko
Group No.2	Nanostructures	M.V.Avdeev
Small angle scattering group. Head: V.I.Gordeliy		
Inelastic scattering group. Head: I.Natkaniec		

NUCLEAR PHYSICS DEPARTMENT

Sub-Division	Title	Head
Sector 1. Correlation γ-spectroscopy and development of experimental installations.		**Head: N.A.Gundorin**
Sector 2. Polarized neutrons and nuclei.		**Head: V.R.Skoy**
Group No.1	Polarized nuclear targets	V.R.Skoy
Group No.2	Thermal polarized neutrons	M.I.Tsulaya
Sector 3. Neutron activation analysis.		**Head: M.V.Frontasyeva**
Group No.1	Analytical	M.V.Frontasyeva
Group No.2	Experimental	S.S.Pavlov
Group No.2	**Neutron spectroscopy**	**Yu.N.Kopatch**
Group No.5	**Proton and α-decay**	**Yu.M.Gledenov**
Group No.6	**Properties of γ-quanta**	**A.M.Sukhovoy**
Group No.7	**Neutron structure**	**V.G.Nikolenko**
Group No.8	**Ultra-cold neutrons**	**E.V.Lychagin**
Group No.9	**Neutron optics**	**A.I.Frank**
Group No.11	**Theory**	**V.K.Ignatovich**
Group No.12	**Electrostatic generator-5**	**A.P.Kobzev**

DEPARTMENT OF IBR-2 SPECTROMETERS COMPLEX

Sub-Division	Title	Head
Group No.1	Scintillation detectors	E.S.Kuzmin
Group No.2	Gaseous detectors	Ts.Panteleev
Sector No.1	**Electronics**	**V.I.Prikhodko**
Group No.1	Analog electronics	A.A.Bogdzel
Group No.2	Digital electronics	V.F.Levchanovsky
Group No.3	Software	A.S.Kirilov
Group No.4	Local network	G.A.Sukhomlinov
Sector No.2	**Spectrometers**	**A.P.Sirotin**
Group No.1	Development of spectrometer elements	A.P.Sirotin
Group No.2	Sample environment	A.N.Chernikov

8.2. USER POLICY

In 2006 the experimental activity at the IBR-2 spectrometers strictly followed the users' program adopted in 2004 (see Laboratory web site http:/nfdfn.jinr.ru/ibr-2/index.html) only in the first half of the year. For the second half of 2006 some points of the program like proposals review and the meeting of the expert commission were suspended because of the reactor shutdown for refurbishment to be started in January, 2007. A number of 156 experiments were performed as follows: 50 experiments (32%) by external users from 13 countries, 36 experiments (23%) with fast access and 70 experiments (45%) by the Laboratory staff. A summary diagram is given below.

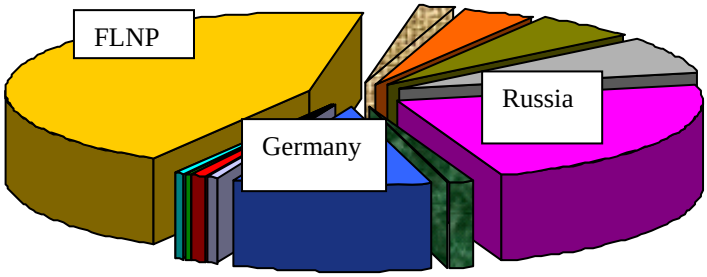

8.3. MEETINGS AND CONFERENCES

In 2006, FLNP organized the following meetings:

1.	XIV International Seminar on Interaction of Neutrons with Nuclei ISINN-14	May 24-27	Dubna
2.	V Workshop on Investigations at the IBR-2 Pulsed Reactor	June 15-17	Dubna
3.	Crystallography at High Pressures	September 28-October 1	Dubna
4.	IV Workshop on Investigations at the IBR-2 Pulsed Reactor	June 15-17	Dubna
5.	International Small-Angle Scattering Workshop	October 5-8	Dubna

In 2007, FLNP will organize the following meetings:

1.	XV International Seminar on Interaction of Neutrons with Nuclei (ISINN-15)	May 16-19	Dubna

8.4. EDUCATION

The objective of the FLNP educational program is the training of specialists in the field of neutron methods for condensed matter and nuclear physics research. The students of the Neutron Diffraction Department of MSU, of the Interfaculty Center «Structure of Matter and New Materials» and of the Electronics and Automatics Department of MIREA (Moscow State Institute of Radioengineering, Electronics and Automatics) perform their term and diploma works in FLNP. At the University Centre of JINR the students from Tula State University, Belgorod State University, Tver State University and other universities of Russia and JINR Member States write their term papers and do summer practical work in FLNP.

On June 2-10, 2006 the Seminar-School "Studying Nanosystems and Materials with Nuclear Physics methods" was held.

On June 2-22, 2006 the practical work for the students of the University Centre of JINR was organized.

8.5. PERSONNEL

Distribution of the Personnel per Department as of 01.01.2007

Theme	Departments	Main staff
-1036-	Nuclear Physics Department	55
-1031-	Condensed Matter Physics Department	45
-1052-	IBR-2 Spectrometers Complex Department	43
-0993-	IREN Department	8
-0851-	IBR-2 Department	47
	Mechanical and Technical Department	45
	Electric and Technical Department	28
	Central Experimental Workshops	38
	Nuclear Safety Group	3.5
	Cold Moderator Group	8
	Design Bureau	7
	FLNP infrastructure:	
	Directorate	9.5
	Services and Management Department	22
	Scientific Secretary Group	5
	Supplies Group	3
Total		**367**

Personnel of the Directorate as of 01.01.2007

Country	People
Armenia	1
Bulgaria	1
Vietnam	1
Germany	1
Georgia	2
KPDR	5
Kazakstan	1
Mongolia	3
Poland	5
Romania	6
Russia	29
Ukraine	6
TOTAL	**61**

8.6. FINANCE

Financing of the FLNP Scientific Research Plan in 2006 (th. USD)

No.	Theme	Financing plan, $ th.	Expenditures for 9 months, $ th.	In % of FLNP budget
I	Condensed matter physics -1031- -0851- -1052-	4567.7 2667.9 1168.4 731.4	3827.2 2046.7 1135.3 645.2	83.8 76.7 97.2 88.2
II	Neutron nuclear physics -1036- -0993-	1208.0 872.1 335.9	1281.6 1009.2 272.4	106.1 115.7 81.1
III	Elementary particle physics -1007-	4.4	4.9	111.4
IV	**TOTAL:**	**5780.1**	**5113.7**	**88.5**

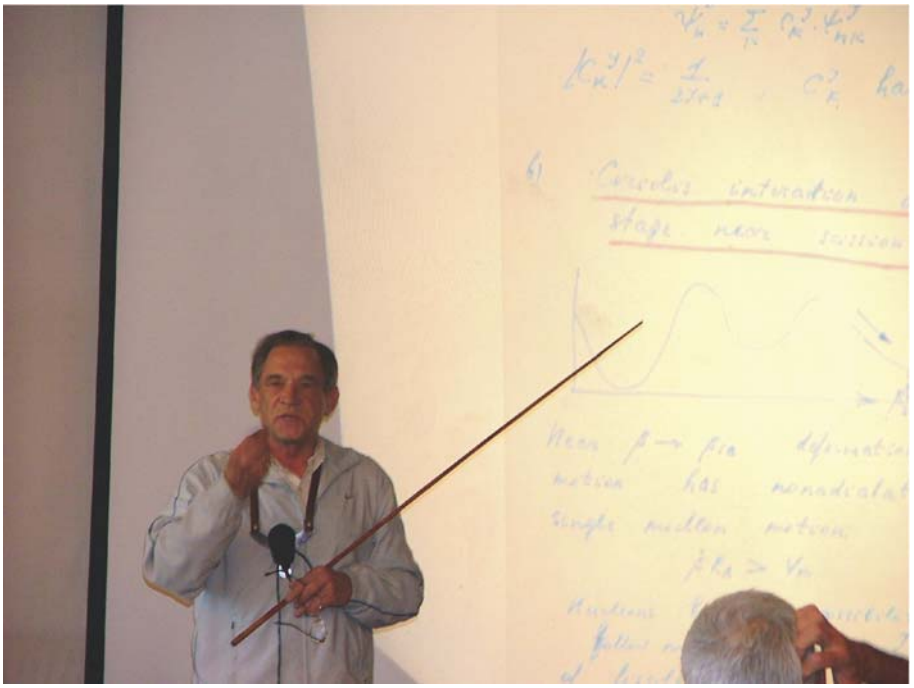

Fig.1. S.G.Kadmensky (Voronezh University) presenting his report.

Fig.2. V.V.Bunakov (right) and V.V.Nesvizhevsky (left) discussing the experiment on levels of neutrons in a gravitational field.

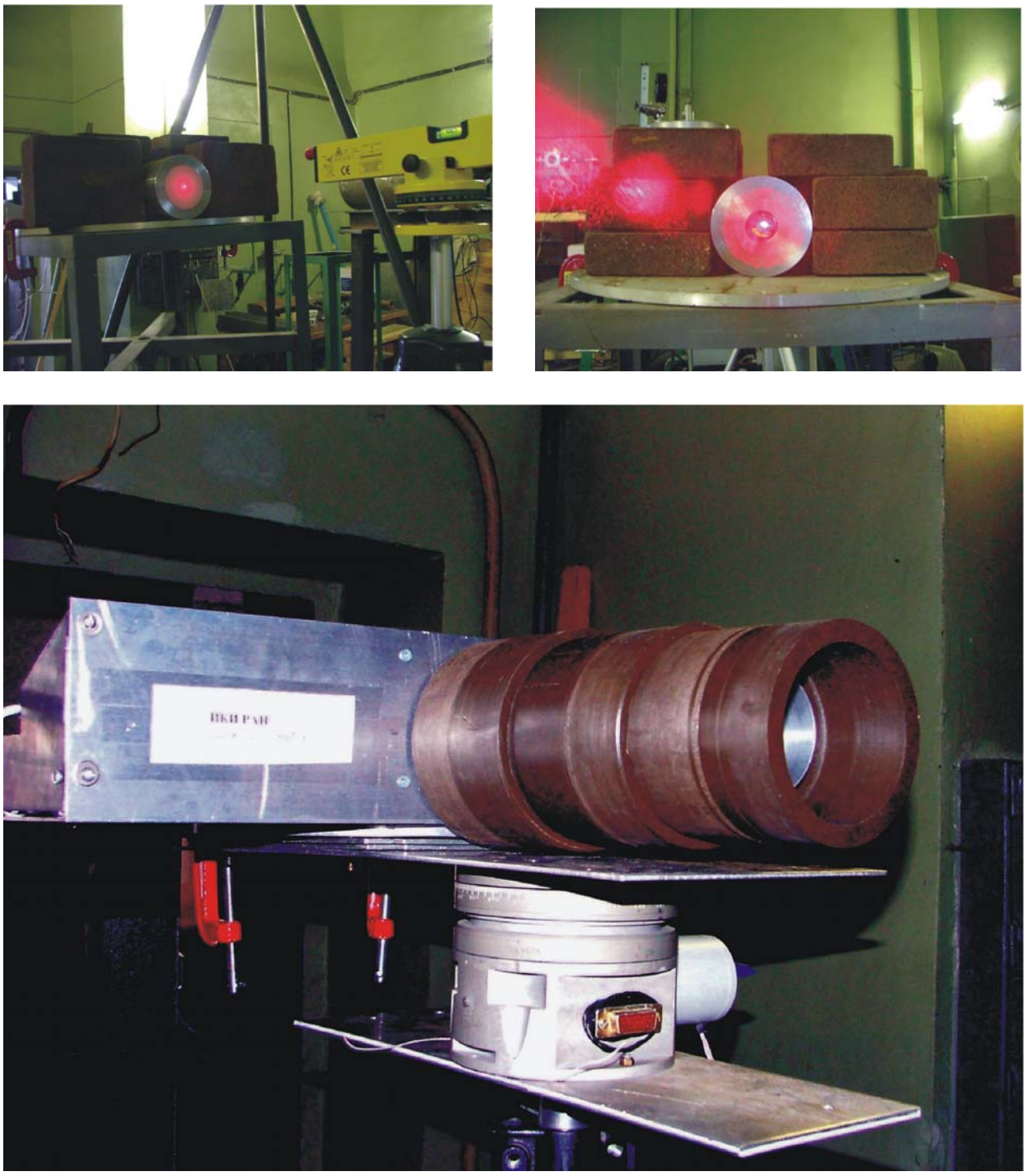

Fig.3. Calibration of the laboratory prototype of the LEND instrument for the NASA orbital vehicle Lunar Reconnaissance Orbiter 2008.

Assembling of IREN equipment

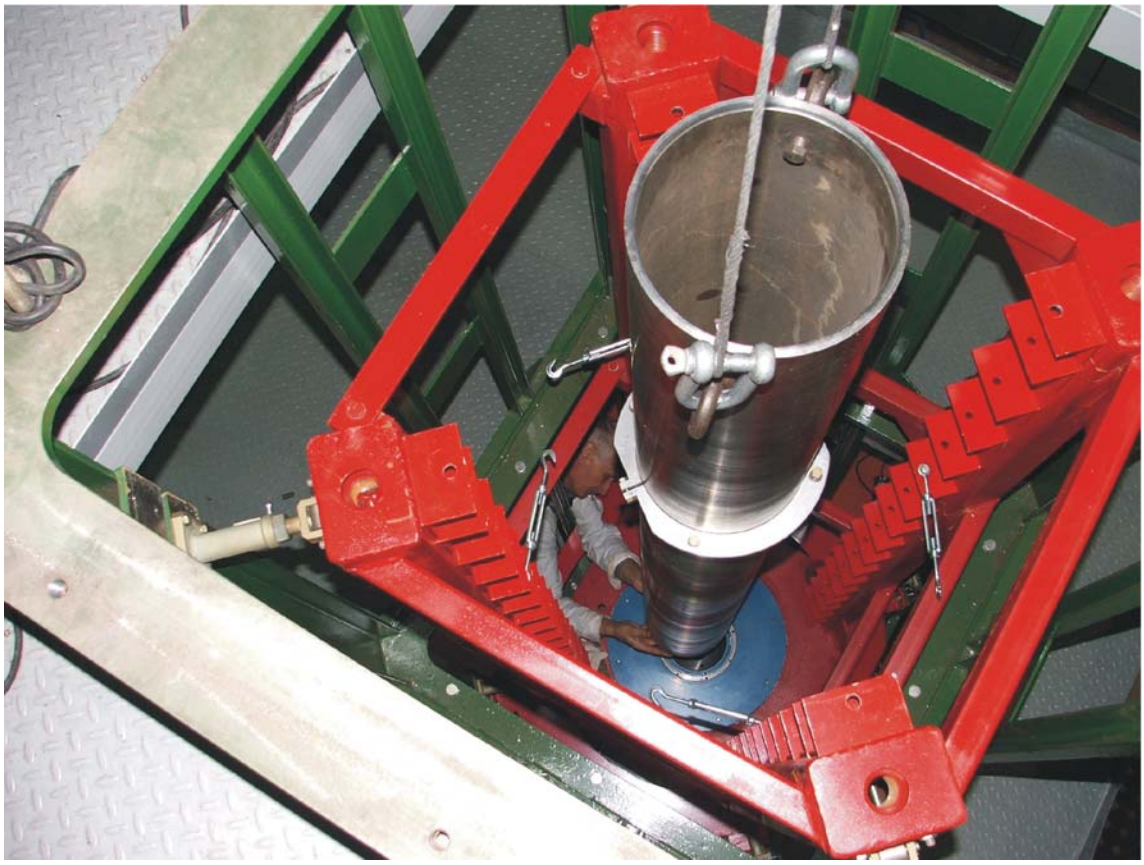

Fig.4. Assembling of the focusing solenoid.

Fig.5. Assembling of the electron gun.

Fig. 6. V.G.Simkin during preparations for tests of 1D position-sensitive detector at HRFD.

18 December 2006:
The IBR-2 completed its operation for physics experiments

1984 – 2006:
200 runs with the total operation time for experiments – 49121 hrs, more than 100 scientific papers each year

Fig.7. The IBR-2 reactor shutdown.

IBR-2 → IBR-2M: modernization of the reactor until 2010

Fig.8. Assembling of fuel elements into fuel assemblies for the IBR-2M reactor.